Politecnico di Milano

Department of Chemistry, Materials and Chemical Engineering “Giulio Natta”

PhD Industrial Chemistry and Chemical Engineering

Doctoral Thesis

Synthesis of biologically active molecules by continuous flow biocatalysis

Cadidate:
Francesca Tentori

Supervisor:
Prof. Maria Elisabetta Brenna

Doctoral Cycle XXXIII 2017-2021

"[…] un po' Tiresia mi sentivo, e non solo per la duplice esperienza: in tempi lontani anch'io mi ero imbattuto negli dèi in lite fra loro; anch'io avevo incontrato i serpenti sulla mia strada, e quell'incontro mi aveva fatto mutare condizione donandomi uno strano potere di parola: ma da allora, essendo un chimico per l'occhio del mondo, e sentendomi invece sangue di scrittore nelle vene, mi pareva di avere in corpo due anime, che sono troppe."

(Primo Levi, *La chiave a stella*)

"[...] I really did feel a bit like Tiresias, and not only because of my double experience. In distant times I, too, had got involved with gods quarreling among themselves; I, too, had encountered snakes in my path, and that encounter had change my condition, giving me a strange power of speech. But since then, being a chemist in the world's eyes, and felling, on the contrary, a writer's blood in my veins, I felt as if I had two souls in my body, and that's too many."

(Primo Levi, *The wrench*, transl. by William Weaver)

Table of contents

Table of contents 5

Preface 7

Abstract 11

Sommario 13

Introduction 17

Chapter 1 63

Biocatalytic approach to chiral β-nitroalcohols by enantioselective alcohol dehydrogenase-mediated reduction of α-nitroketones

Chapter 2 81

Immobilization of Old Yellow Enzymes via covalent or coordination bonds

Chapter 3 97

Continuous-flow biocatalytic process for the synthesis of the best stereoisomers of the commercial fragrances leather cyclohexanol (4-isopropylcyclohexanol) and woody acetate (4-(*tert*-butyl)cyclohexyl acetate)

Chapter 4 113

Chemo-enzymatic oxidative cleavage of isosafrole for the synthesis of piperonal

Chapter 5 137

Multi-step chemo-enzymatic synthesis of azelaic and pelargonic acids from the soapstock of high-oleic sunflower oil refinement

Appendix 157

Preface

The term “biocatalysis” refers to the use of biological systems like microorganisms or enzymes to perform chemical reactions, exploiting the high chemo-, regio- and stereoselectivity typical of living organisms and their mild and environmental benign conditions. Although efficient, large scale applicability of biocatalytic reactions is often limited by several issues like low efficiency, low productivity and low stability of such catalysts. To address those issues, implementation of enzyme immobilization and enabling technologies like flow chemistry are rated as important means to spread biocatalysis applicability, as it will be widely discussed later.

During my PhD program at Department of Chemistry, Materials and Chemical Engineering (Politecnico di Milano), I took part in a research group (BiocatLab) with a long-standing experience in biocatalysis for synthetic scopes, often applied to preparation of chiral flavors and fragrances. When I started my internship as a chemical engineer graduate, I was more familiar with large, bulky chemical production and oil-based processes. During my training, I could gain information on biocatalysis end enzymatic reactions and I could contribute to my research group’s knowledge with my engineering skills to implement chemo-enzymatic continuous-flow systems and working on the issues that still limit biocatalysis applicability at larger scales. The aim of my PhD work was then the increment of the knowledge concerning biocatalysis applicability to the synthesis of various fine chemical products, as a tool that could possibly lead, in future, to a wider and more feasible application of enzymatic reactions to industry. So, after acquiring knowledge concerning traditional biocatalysis methodologies, I worked also on enzyme immobilization which is often a critical aspect for continuous-flow reactions implementation.

This PhD thesis reflects my research path in these past four years: starting from acquiring basic biocatalysis to development of continuous-flow processes, through enzyme immobilization. The structure of this elaborate aims to represent this course and, after an introduction for the presentation of the main topics relevant to my work (with a special attention to examples of industrial applications), the published papers or, when yet unpublished, the manuscripts produced are presented as separate chapters.

List of the papers included in this thesis:

- **Paper 1.** Tentori, F.; Brenna, E.; Colombo, D.; Crotti, M.; Gatti, F.G.; Ghezzi, M.C.; Pedrocchi-Fantoni, G. Biocatalytic approach to chiral β-nitroalcohols by enantioselective alcohol dehydrogenase-mediated reduction of α-nitroketones. *Catalysts* **2018**, *8*, 308.
- **Paper 2.** Tentori, F.; Bavaro, T.; Brenna, E.; Colombo, D.; Monti, D.; Semproli, R.; Ubiali, D. Immobilization of old yellow enzymes via covalent or coordination bonds. *Catalysts* **2020**, *10*, 260.
- **Paper 3.** Tentori, F.; Brenna, E.; Crotti, M.; Pedrocchi-Fantoni, G.; Ghezzi, M.C.; Tessaro, D. Continuous-flow biocatalytic process for the synthesis of the best stereoisomers of the commercial fragrances leather cyclohexanol (4-isopropylcyclohexanol) and woody acetate (4-(*tert*-butyl)cyclohexyl acetate). *Catalysts* **2020**, *10*, 102.
- **Paper 4.** Tentori, F.; Brenna, E.; Ferrari, C.; Gatti, F.G.; Ghezzi, M.C.; Parmeggiani, F. Chemo-enzymatic oxidative cleavage of isosafrole for the synthesis of piperonal. *React. Chem. Eng.* **2021**, *6*, 1591-1600.
- **Paper 5.** Tentori, F.; Brenna, E.; Casali, B.; Parmeggiani, F.; Tessaro, D. Multi-step chemo-enzymatic synthesis of azelaic and pelargonic acids from the soapstock of high-oleic sunflower oil refinement (manuscript in preparation).

Contribution of the authors

The advisor of this thesis is Prof. Elisabetta Brenna from Politecnico di Milano.

This is an experimental work that required the cooperation of different competences concerning synthetic chemistry, biotechnology and chemical engineering from different research groups, in particular:

- The conception and design of the experimental setting is entirely due to the authors of this thesis, together with and under the supervision of Prof. Elisabetta Brenna, as well as the writing of all the papers.
- The realization of the experimental setting is mainly due to the author of the thesis. For the synthesis and characterization of the substrates, the author was assisted by Maria Chiara Ghezzi, Beatrice Casali and Chiara Ferrari from Politecnico di Milano.
- Enzyme preparation and enzyme screening was carried out by Dr. Michele Crotti and Danilo Colombo from Politecnico di Milano under the supervision of Dr. Daniela Monti from C.N.R. (Istituto di Chimica del Riconoscimento Molecolare, Milano).

- For immobilization experiments the author was supported by Riccardo Semproli, Dr. Teodora Bovaro and Prof. Daniela Ubiali from Università di Pavia.
- Feedbacks on papers and on potential directions of the work have been provided by Dr. Davide Tessaro, Dr. Fabio Parmeggiani and Prof. Francesco G. Gatti from Politecnico di Milano.

Abstract

Biocatalysis is a deeply investigated field, whose importance lies in the broad range of highly stereo- and enantioselective reactions under low environmental impact conditions it offers to organic chemists. Still, some issues like low productivity and low long-term stability of the biocatalysts can sometimes hinder larger-scale industrial applications. Enzyme immobilization is a widely exploited tool to overcome some of such limitations by increasing biocatalyst durability and affording its reusability. Moreover, the immobilization favors enzyme exploitation in small-sized reactors, working under continuous-flow conditions, according to the "flow chemistry" approach. Integration between enzyme-catalyzed reactions and in-line work-up or among other enzymatic or synthetic steps is considered one of the main advantages ascribed to flow biocatalysis, along with significantly easier scalability.

Starting from conventional, aqueous-based enzymatic reactions, the main goal of this project was the development of continuous-flow enzymatic-mediated reactions for the preparation of compounds of industrial interest such as flavors, fragrances or pharmaceutical intermediates. The work has been carried out in collaboration with the *Dipartimento di Scienze del Farmaco*, of the University of Pavia (Pavia, Italy) and with the *Istituto di Chimica del Riconoscimento Molecolare*, of the C. N. R. (Milano, Italy). To better represent the technological upgrade involving biocatalysis, this work is divided into three parts: first, "traditional" biocatalysis was addressed; then, enzyme immobilization was concerned and finally continuous-flow enzymatic and chemo-enzymatic reactions were approached as possible final development for enzymatic mediated processes.

In the first part, enzymatic reduction of aliphatic and aromatic α-nitroketones to β-nitroalcohols using commercial alcohol dehydrogenases (ADHs) is described. High conversions and enantioselectivity values could be achieved with two specific ADHs, affording either the (*S*) or the (*R*)-enantiomer of the corresponding nitroalcohols.

In the second part, immobilization of OYE3, an ene-reductase particularly active for stereoselective reduction of activated C=C bonds, was investigated. Glyoxyl agarose (for covalent immobilization) and EziGTM Opal (a commercial Fe^{3+} glass support for metal coordination) were selected as suitable carriers. After some experiments for testing immobilized derivatives stability and reusability, the

former appeared superior to the latter in terms of reusability, suggesting that glyoxyl agarose could be a more suitable support for OYE3 immobilization.

The last part concerns the application of flow conditions to enzymatic and chemo-enzymatic reactions. Moving from immobilization to implementation of continuous-flow biocatalytic reactions, the first process studied in this work was the continuous-flow preparation of two commercial fragrances, leather cyclohexanol and woody acetate that are sold as mixture of cis- and trans-isomers. The two compounds were prepared with high diastereoisomeric excess (*de*>90%) to the cis-isomer (more valuable for its olfactory characteristics but less thermodynamically favored) by ADHs-reduction, followed by lipase-mediated acetylation for woody acetate synthesis. The implementation of the two processes under continuous-flow conditions was made possible by using a membrane reactor (CSTR) for ADH-mediated reduction and a column reactor (PFR) for lipase-mediated acetylation, coupled with in-line extraction and work-up. The last two studied processes were based on lipase-mediated in situ formation of peroxycarboxylic acids for alkene epoxidation. In both cases, epoxidation was meant as the first step of C=C oxidative cleavage, as an alternative chemo-enzymatic route to ozonolysis or chromic acid oxidation. In one example, perhydrolysis of ethyl acetate was exploited for peroxyacetic acid formation to obtain epoxidation of isosafrole, followed by chemical epoxide opening to the diol and its MnO_2-based oxidative cleavage to piperonal. In the other work, lipase promoted oleic acid self-epoxidation in presence of H_2O_2 for oleic acid diol preparation, followed by oxidation with NaClO to azelaic and pelargonic acid. Continuously-stirred tank reactor was chosen as best reactor configuration for enzymatic epoxidation, while for the second synthetic step a plug-flow configuration was developed.

The introduction of biocatalyzed continuous-flow reactions offers the benefits of increasing the automation degree of the process, with a gain in productivity and yields. Beyond that, when coupled with enzyme immobilization, stability and reusability of the biocatalyst can be an additional benefit. For these reasons, flow biocatalysis with immobilized enzymes is becoming a well-established practice receiving an ever-increasing interest from academia and industry. In summary, this work contributed to expand the range of the possible applications of continuous-flow biocatalysis, as a further proof of the advantages of its exploitation, demonstrating its efficiency for the enzymatic and chemo-enzymatic reactions involved.

Sommario

La biocatalisi è un campo scientifico di grande interesse la cui importanza risiede soprattutto nell'offerta di un'ampia gamma di reazioni altamente selettive e a basso impatto ambientale, utilizzabili nell'ambito della chimica organica. Tuttavia, l'applicazione su scala industriale di reazioni biocatalitiche è spesso limitata da una bassa produttività e dalla ridotta stabilità a lungo termine dei catalizzatori. Tali limitazioni possono essere parzialmente superate dall'immobilizzazione degli enzimi coinvolti, aumentandone la stabilità e favorendone il riutilizzo per più reazioni consecutive. Un altro aspetto vantaggioso è la possibilità di utilizzare enzimi immobilizzati all'interno di reattori miniaturizzati operanti in condizioni di flusso continuo, secondo l'approccio della "chimica in flusso". I principali vantaggi attribuiti a tale approccio sono la possibilità di combinare più reazioni (enzimatiche o sintetiche) e di abbinarle ai rispettivi passaggi di work-up senza dover intervenire nell'isolamento dell'intermedio e a una più semplice scalabilità del processo.

Partendo da reazioni enzimatiche convenzionalmente condotte in acqua, questo lavoro di tesi ha come obiettivo lo sviluppo di reazioni enzimatiche in condizioni di flusso continuo per la preparazione di composti di interesse industriale come aromi, fragranze e intermedi farmaceutici. Il lavoro è stato condotto in collaborazione con il *Dipartimento di Scienze del Farmaco* dell'Università di Pavia e con l'*Istituto di Chimica del Riconoscimento Molecolare* del C.N.R. di Milano. Seguendo il percorso di incremento tecnologico che ha coinvolto la biocatalisi, gli argomenti trattati all'interno della tesi sono suddivisibili in tre gruppi principali: la prima parte del lavoro riguarda la biocatalisi "convenzionale" che utilizza soluzioni acquose ed enzimi in soluzione, nella seconda parte viene trattata l'immobilizzazione di un enzima mentre nella terza viene presentato lo sviluppo di reazioni enzimatiche e chemo-enzimatiche in condizioni di flusso continuo come possibile punto d'arrivo nello sviluppo di processi enzimatici.

Nella prima parte è descritta la riduzione enzimatica di α-nitrochetoni, sia alifatici che aromatici, ai corrispondenti β-nitroalcoli utilizzando alcol deidrogenasi (ADH) commerciali. Alti valori di conversione ed enantioselettività sono stati ottenuti con due degli enzimi utilizzati, attraverso i quali sono stati isolati entrambi gli enantiomeri (*S*) ed (*R*) di tutti i nitroalcoli analizzati.

Nella seconda parte, l'immobilizzazione di OYE3, una ene-reduttasi particolarmente attiva nella riduzione stereoselettiva di doppi legami C=C attivati, viene descritta per la prima volta. Il gliossil-agarosio e il supporto commerciale EziG^{TM} Opal contenete ione Fe^{3+} sono stati selezionati come possibili supporti per, rispettivamente, l'immobilizzazione di tipo covalente e per coordinazione a metalli di transizione. Dati diversi esperimenti volti a testare la stabilità e il potenziale riutilizzo dei derivati immobilizzati, il gliossil-agarosio mostra una più alta efficacia in termini di riusabilità del derivato.

Per quanto riguarda i processi enzimatici o chemo-enzimatici in flusso continuo, il primo lavoro qui presentato tratta della preparazione in continuo di due fragranze commerciali, il "leather cyclohexanol" e il "woody acetate", vendute come miscele di isomeri *cis*- e *trans*-. Utilizzando delle alcol deidrogenasi commerciali, i due composti sono stati preparati per riduzione selettiva dei corrispondenti chetoni, favorendo l'isomero *cis*- (cui corrispondono migliori caratteristiche olfattive, ma che è più difficile da ottenere dell'isomero trans- per ragioni termodinamiche) con un elevato eccesso diasteromerico (*de*>90%). La sintesi enzimatica del woody acetate è stata completata acetilando l'alcol ottenuto in precedenza per mezzo di una lipasi. L'implementazione dei due processi in condizioni di flusso continuo è stata resa possibile dall'utilizzo di un reattore a membrana (CSTR) per la riduzione con le alcol deidrogenasi e da un reattore a colonna (PFR) per l'acetilazione con lipasi, combinati tra loro da un'estrazione con solvente e separazione delle due fasi liquide in continuo. Gli altri due processi studiati riguardano l'epossidazione di alcheni mediata da acidi percarbossilici preparati *in situ* utilizzando delle lipasi come catalizzatori. In entrambi i casi, l'epossidazione rappresenta il primo passaggio della scissione ossidativa del doppio legame C=C, come possibile alternativa chemo-enzimatica all'ozonolisi o all'ossidazione con acido cromico. Nel primo esempio, la peridrolisi di acetato di etile è stata utilizzata per la formazione di acido peracetico per l'epossidazione dell'isosafrolo, seguito dall'apertura chimica dell'epossido a diolo e dalla scissione ossidativa dello stesso a piperonale utilizzando MnO_2 come ossidante. Nel secondo lavoro, la lipasi promuove l'auto-epossidazione dell'acido oleico in presenza di H_2O_2 per la preparazione del diolo dell'acido oleico, seguito dall'ossidazione con NaClO ad acido azelaico e acido pelargonico. Un reattore continuo di tipo CSTR è stato scelto come migliore configurazione per l'epossidazione enzimatica, mentre per il secondo stadio sintetico il reattore utilizzato è di tipo PFR.

L'introduzione di reazioni biocatalitiche in flusso continuo offre i benefici di aumentare il grado di automazione del processo, con conseguente aumento di produttività e rese. Oltre a ciò, quando

accoppiato con l'immobilizzazione enzimatica, la stabilità e la riusabilità del biocatalizzatore possono essere ulteriori vantaggi. Per queste ragioni, la biocatalisi in flusso continuo con enzimi immobilizzati sta diventando una pratica consolidata, ricevendo un interesse sempre crescente sia dal mondo accademico che da quello industriale. Questo lavoro cerca perciò di contribuire ad espandere la gamma di possibili applicazioni di reazioni biocatalitiche in flusso continuo, come ulteriore prova dei vantaggi del suo utilizzo, dimostrandone l'efficacia quando reazioni enzimatiche e chemo-enzimatiche sono coinvolte.

Introduction

Biocatalysis

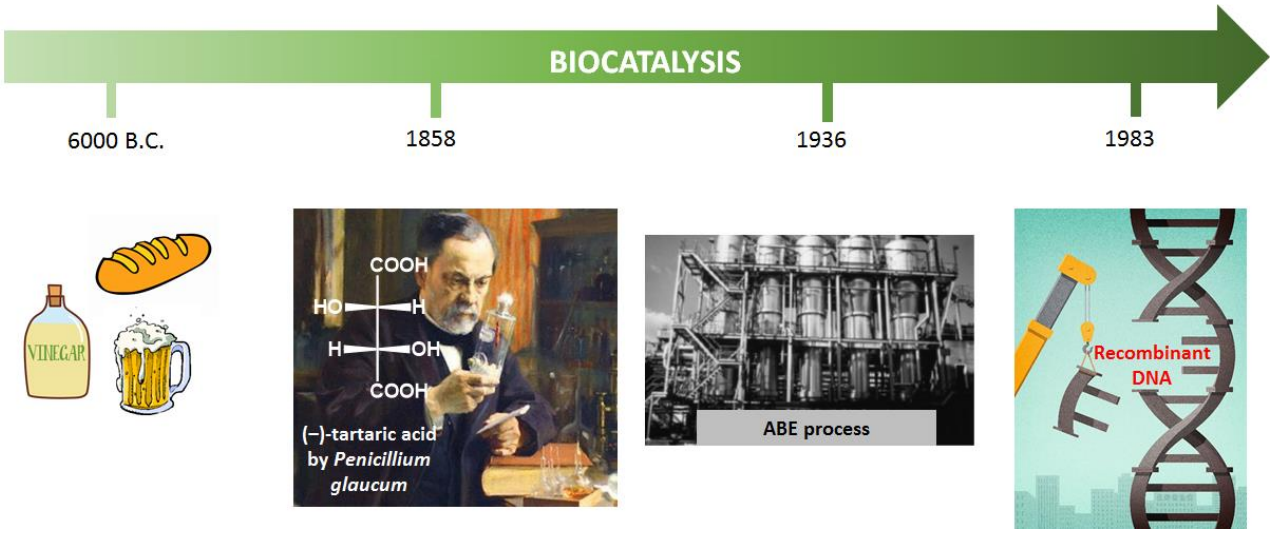

In the history of mankind, biocatalysts have been used for millennia with little awarness: bread leavening, beer brewing, milk curdling, grapes fermentation to vine and vinegar, practiced by humans for at least 6000 years, are all enzyme-mediated reactions for the preparation of daily food [1]. Only starting from the late 1700s, enzymes were gradually identified as biological catalysts: the first enzymatic process to be discovered was the digestion of meat by stomach secretions when in 1783 Lazzaro Spallanzani, an Italian biologist known as the first to discredit the theory of spontaneous generation, performed the first *in vitro* digestion of meat by animal gastric juice [2]. Later, in 1833, the French chemists Anselme Payen and Jean-François Persoz, employees at a sugar factory, discovered the first enzyme from a malt solution. They actually observed that during heating of beer mash, when the starch in the barley seeds is converted by the enzyme in soluble sugars, the husk was separated from the rest of the seed. They called this extract "diastase" (from the Greek word "διάστασις" meaning a parting or a separation") after this phenomenon [3]. Few decades later, Louis Pasteur brought a major contribution to enzymes understanding with two main experiments: first (1858) he subdued the ammonium salt of racemic tartaric acid to *Penicillium glaucum* fermentation, obtaining (–)-tartaric acid (by metabolic degradation of (+)-tartaric acid), thus performing the first biocatalytic enantiomeric resolution of a racemate [4]. Later (1862), reflecting on fermentation phenomena, he theorized that sugar conversion into alcohol was caused by the presence of a "vital

force" inside yeast cells that he named "ferments", thus correlating fermentation to living microorganisms [5]. A step forward was taken by the German physiologist Wilhelm Kühne (1876): he achieved sugar conversion into alcohol by means of dead yeast cells ground with sand. To explain the conversion, he coined the term "enzyme" from the ancient Greek "ἔνζυμον", meaning "in yeast" [6]. The newly coined word gained popularity and was used for other non-living substances (like pepsin), while "ferment" was used to refer to chemical activity produced by living organisms. Kühne's experiments with cell extract are considered the begin of enzyme-catalyzed reactions, overcoming fermentation as the only way to achieve bio-mediated chemical activity. While the discovery of new enzymes was being acknowledged and enzymes start to be commercialized for industrial scopes, the nature of enzymes and the involved reaction mechanisms were still poorly known. Although it became clear that their catalytic action was connected to some proteins, it was still uncertain whether enzymes were to be considered proteins or just needed proteins as carriers. Only in 1926, the American chemist James B. Sumner could crystallize the enzyme urease, demonstrating the protein nature of enzymes [7]. In the meantime, investigations about the mechanisms were carried on. The most significant theories were developed by Emil Fischer that suggested the "lock-and-key" theory to explain substrate specificity of the enzymes [8] and then, in 1913, Michaelis and Menten published their considerations about enzymatic mechanism that led to the formulation of the famous Michaelis-Menten equation to describe enzymatic kinetics [9]. During the 20th century, enzyme investigations were flanked by development of industrial fermentation processes. First of all, at the beginning of the century, improvements in beer production, especially in Germany, drove the rise of fermentation as an industrial field, that produced a better understanding of malting, mashing and yeast fermentation process. Moreover, the Great War determined a call for several bulk chemicals whose supply could not be addressed because of the dramatic geopolitical conditions of the time. The need of acetone for explosive manufacture stimulated the development of the first non-food fermentation for large scale production by ABE fermentation (acetone-butanol-ethanol) by cereal fermentation promoted by *Clostridium acetobutylicum*. War purposes drove also the production of glycerol (used as starting material for nitroglycerine production) by yeast fermentation of sugars with a production scale of 1000 ton per month [10]. Other fermentative processes developed during the 1950s were production of citric acid (fermentation of *Aspergillus niger*) [11], vitamin B_{12} (predominantly utilizing *Pseudomonas denitrificans*, *Propionibacterium shermanii*, or *Sinorhizobium meliloti*) [12] and penicillin G (*Penicillium* spp.) [13]. By the late 1950s many enzymes had been discovered and their reaction mechanisms clarified. An unexpected push to

enzymology came from the DNA-related discoveries that monopolized the scientific scene in the same decade. First, Alfred Hershey and Martha Chase in 1952 correlated the genetic information to DNA (already known to biologists since 1869 [14]), as the only responsible for holding the genetic code of heredity [15]. Second, the discovery of DNA chemical composition and its structure in 1953, due X-ray diffraction images of DNA by James Watson, Francis Crick and Rosalind Franklin [16]. The progresses in DNA knowledge paved the way, twenty years later, to the exploration of DNA manipulation: after Paul Berg's work on recombinant DNA [17] it was possible to introduce an external piece of DNA from any organism into a new organism (cloning), causing an impressive leap in engineered and tailor-made enzymes production. The last huge steps from that moment on, from the development of the polymerase chain reaction (PCR) in the 1980s by Kary Mullis [18] to Frances Arnold's studies in the early 1990s [19] that applied direct evolution, enabled the creation of large libraries of mutants to be screened to identify specific enzymatic activities. All the achievements of enzyme engineering have been supporting an increased interest in biocatalytic application to industrial scale, demonstrated that it is possible to obtain tailor-made enzymes with improved characteristics in terms of activity and stability over a wide range of non-natural compounds that could be transformed by enzymatic synthesis, broadening the suitable operative conditions of the reactions.

Nowadays, biocatalysis is an established multidisciplinary field between molecular biology, organic chemistry and chemical engineering which have been carving out an important role in the manufacture of pharmaceutical intermediates and fine chemicals according to the 12 principles [20] of green chemistry. Compared to traditional metal-based catalysts, biocatalysis provides their inherently high stereo- and enantioselectivity transformations with safe and low environmental impact conditions. Despite the many benefits displayed in these years, a wider implementation of enzymatic reactions is often an issue. Significant drawbacks may hamper larger scale applications: most of the time enzymes require buffered aqueous solutions as reaction medium, implicating low solubility of hydrophobic substrates and low productivity. Moreover, the complex structure of proteins easily misfolds, causing low long-term stability and a limited tolerance to non-optimal temperature and pH conditions. To partially overcome some of these disadvantages, immobilization techniques have been developed to increase long-term stability and facilitating enzyme recovery and reuse. Moreover, investigation on enzyme immobilization have been promoting development of flow chemistry systems applied also to biocatalytic reactions. According to many biocatalysis specialists, flow chemistry could really provide an effective strategy in designing industrially appealing

processes, especially in an industrial contest that is aiming to implement more and more automatic processes and interconnected systems.

Enzymes

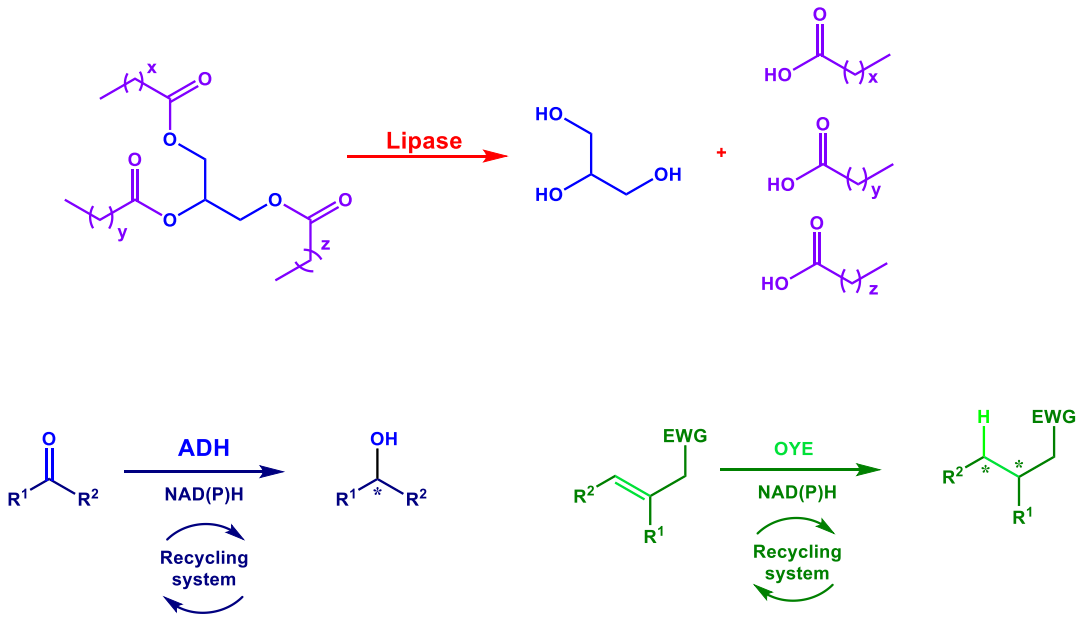

Enzymatic classes studied for synthetic applications are several and this number is steadily increasing. In this place, an extensive description of all of them would be neither feasible nor useful for the scope. Therefore, the enzyme classes that can be found in this work are described briefly in the following paragraph, by highlighting also their main applications in industrial processes.

Lipases

Lipases (triacylglycerol acylhydrolase, E.C. 3.1.1.3) are part of the family of hydrolases that act on carboxylic ester bonds. Lipases are ubiquitous enzymes with the biological function of hydrolyzing triglycerides into diglycerides, monoglycerides, fatty acids, and glycerol. They can also act on non-natural substrates catalyzing esterification, interesterification, and transesterification reactions in nonaqueous media, often displaying a wide range of regio-, enantio- and stereoselectivity. They are probably the most exploited and studied type of enzymes, for many reasons: they can be produced in significant amount and with little effort (especially when harvested from fungi and bacteria), they are easy to use because they do not require any cofactor or co-substrate, they are active at a wide range of pH and temperature values and can be generally used in organic solvents [21]. All these characteristics make them valuable candidates for different industrial applications and among the first to be developed: synthesis of chiral compounds for APIs (*i.e.* preparation of single enantiomers through resolution of racemic mixtures), processing of meat, fish and dairy products, industrial

treating of textile and paper products, biodiesel production by enzyme-catalyzed transesterification and used as additives in laundry products [22-27]. Moreover, many lipases are commercial enzymes which makes them available for rapid development of industrial processes [28]. The relevance of lipases in industrial uses is testified by the impressive number of patents published. Within 2015, 671 patents on lipase-mediated kinetic resolution were filed, 456 on production of detergents and 544 on food applications. Many other patents certify lipase employment for biodiesel production (165), beyond several examples of implementation of lipase-mediated biodiesel production from vegetable oil sources [29].

Alcohol dehydrogenases

Alcohol dehydrogenases (ADHs) (E.C. 1.1.1.1) are enzymes belonging to the oxidoreductase class (redox enzymes). They can reduce aldehydes and ketones by transferring electrons from an electron donor to the substrate. In humans and other animals, they participate to the metabolism of toxin molecules (like alcohols) but they take also part in the biosynthesis of various metabolites. Used as biocatalysts for synthetic applications, they serve as a powerful tool for the desymmetrization of prochiral carbonyl compounds. Nonetheless, unfortunately, their employment at large scale is often hindered by the requirement of cofactors, typically nicotinamide adenine nucleotide (NADH) or its phosphate analog (NADPH) [30]. Beyond the cofactor itself, a regeneration system for reducing the oxidized cofactor ($NAD(P)^+$) has to be implemented, due to cofactors high costs. Cofactor recycling is usually performed by coupling the ADH with a second enzyme like formate dehydrogenase (FDH) from *Candida boidinii* or glucose dehydrogenase (GDH) from *Bacillus megaterium* with the aim of transferring electrons from the oxidized cofactor to a sacrificial compound (respectively formate and glucose). Although their role in the chemical industry is less acknowledged than lipases', several patents show great interest for ADHs employment for stereoselective reduction of carbonyl compounds. For instance, Zeneca Limited, in 1996, patented a process for the stereoselective preparation of 4(*S*)-hydroxy-6(*S*)-methylthienopyran derivatives by reduction of the corresponding ketones by a NAD^+ dependant ADH from *Neurospora crassa* [31], providing high yields (>85%), and high enantiomeric excesses (>98%). More recently, a noteworthy example is found in a process by F.I.S. Fabbrica Italiana Sintetici that in 2010 patented the use of a recombinant murine hydroxysteroid dehydrogenase to testosterone by chemo- and stereoselective reduction of 4-androstene-3,17-dione [32].

Ene-reductases

Ene-reductases (E.C. 1.6.99.1) are redox enzymes and represent a powerful tool for stereoselective reduction of carbon-carbon double bonds activated by a suitable electron-withdrawing group (like as α,β-unsaturated carbonyl compounds or nitroolefins, and maleimides). As for ADHs, they require NAD(P)H as cofactor and a cofactor recycling system, generally GDH/glucose [33]. Although their physiological function is still not clear, these enzymes have been commonly found and isolated from many different organisms like fungi, bacteria, and plants. The vast majority of ene-reductases can be reconducted to the family of old yellow enzymes (OYEs), whose name is due to the presence of flavin mononucleotide ($FMNH_2$) prosthetic group that confers their characteristic color. OYE1-3 were isolated from yeasts (OYE1 from *Saccharomyces pastorianus* while OYE2/OYE3 from *Saccharomyces cerevisiae*) and their first synthetic applications are referred to the employment of baker's yeast fermentation. Although their stereoselective C=C reduction activity is a very desirable tool for synthetic chemistry and their synthetic potential has been deeply studied in the academic field, their industrial application is at a very early stage. After an early multikilogram scale implementation of an ene-reductase-mediated reaction in 1976 [34] where 13 kg of ketoisophorone was converted into the (*R*)-enantiomer of the reduced form with 97% *ee* by fermentative reduction of baker's yeast, only few patents for possible effective industrial applications of ene-reductases can be found, all of them published in the past few years. Two of them made use of recombinant microorganisms with microorganisms overproducing ene-reductases to enable the production of citronellal/citronellol [35] and a sigle stereoisomer of menthol [36]. Only one patent by F.I.S. Fabbrica Italiana Sintetici [37] exploited an ene-reductase as isolated enzyme for synthetic purposes for the preparation of (*R*)-β-angelica lactone.

Enzyme immobilization

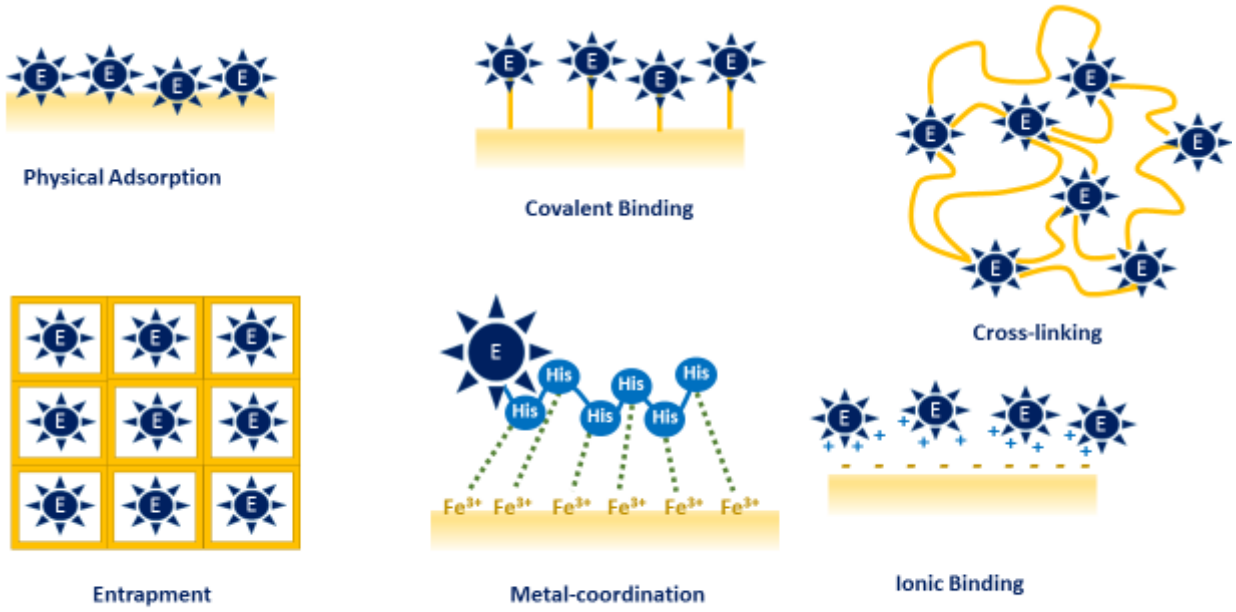

Enzyme (but also whole-cell biocatalyst) immobilization is often rated as one of the main key point for the development of sustainable biocatalyzed processes [38-40]. Immobilization is the tool to enable transition from homogeneous to heterogeneous catalysis as well. This change provides *per se* advantages and drawbacks in common to heterogeneous and homogeneous metal-based catalysis: from one side, solid catalysts can be easily removed from a liquid/gaseous environment without energy consumption, from the other side heterogeneous reactions can suffer from diffusion limitations that reduce the overall reaction rate. Some other issues concern specifically immobilization of enzymes: due to the complex enzymatic structure, securing enzymes to a solid support can often determine an increase in stability during time and an enhanced robustness to more severe reaction conditions, thus broadening the reaction conditions range, also beyond the optimal conditions. Moreover, immobilization avoids protein contamination in the product, allows catalyst reusability and facilitates the downstream procedures of separation and purification of the products. Furthermore, work-up can be sensibly bettered, avoiding emulsions that easily occur during organic solvent extraction of the substrate (especially in case of whole-cell mediated reactions). Although enzyme immobilization is often rated as a powerful tool in enzymatic reactions implementation at industrial scale, in practice it is not often considered economically feasible. First, immobilization often requires

conditions that can lead to significant activity loss and a balance between the reduced activity and the increased stability has to be carefully evaluated. Then, from an economical point of view, the implementation of immobilized enzyme reactions at large scales suffers from the cost of the support, the chemicals and from the long time required for immobilization procedure. The overall costs of support and chemicals are not often counterbalanced by an increase in enzyme stability or the diminishing of downstream process costs. Beyond that, when approaching to immobilization of a new enzyme, it is still mainly an empirical process that, although a good knowledge of enzyme structure and mechanism is essential for a good evaluation of which procedure is more suitable, often proceeds through a trial-and-error approach without any methodology that can be universally applied to all the given enzymes. Actually, many techniques have been developed during years, together with a broad range of supports and carriers of different nature [41-43].

In order to evaluate the effectiveness of an immobilization procedure on an enzyme, there are two main terms that are generally defined to determine the success of enzyme immobilization [44]:

immobilization yield, for indicating the percentage of the starting enzyme that is immobilized on the support:

$$Immobilization\ Yield\ (\%) = 100\ \times \frac{immobilized\ protein}{starting\ protein}$$

and activity recovery that conveys an idea of the total success of immobilization process and it is defined as the percentage of the starting activity observed in the immobilized derivative:

$$Activity\ recovery\ (\%) = 100\ \times \frac{observed\ activity}{starting\ activity}$$

After definig the terms for immobilized derivative description, a brief introduction to the main immobilization techniques will be illustrated and the most interesting cases of large-scale applications.

Cross-linking

A first immobilization possibility consists in enzyme precipitation as molecular aggregates by adding salts, organic solvents or acids to promote precipitation and a cross-linking agent like glutaraldehyde to promote irreversible binding among enzyme molecules. The aggregates thus prepared, named CLEAs (cross-linked enzyme aggregates) are usually carrierless particles. This immobilization

technique has the main advantage of zeroing the cost of the carrier, with a generally low-cost procedure. Unfortunately, these aggregates generally lack mechanical stability and are often affected by mass transfer limitations due to their particle size. Moreover, a significant part of the added enzyme is not available to the substrate, resulting in a "dilution of activity" that decreases the space-time yield of the enzymatic reaction. In order to reduce the thickness of "non active" layers, a single layer of enzyme molecule is adsorbed on the surface of a carrier. Cross-linking aggregates adsorbed onto a solid support was the key formulation of the commercial enzymatic-based process for the production of HFCS (high-fructose corn syrup), a sweetener made from corn starch and obtained by D-glucose/xylose isomerase that converts the starch-derived glucose into fructose. The enzyme aggregates are obtained employing glutaraldehyde as cross-linking agent [45] and adsorbed onto an inexpensive inorganic carrier such as bentonite clay or diatomaceous earth, mechanically extruded and dried. This enzymatic formulation is extremely stable and can be used up to two years in a packed-bed reactor at 60°C. The operative characteristics of this xylose isomerase immobilized derivative makes the HFCS biocatalyzed process the largest process based on immobilized enzyme with 500 tons of immobilized xylose isomerase consumed every year for the production of 10 million tons of HFCS [45].

Entrapment

Biocatalyst entrapment consists in the physical retainment of the enzyme or the cell inside the matrix of a polymer that can be organic (like alginate-gelatins, chitosan, polyacrylamide among the most used) or inorganic (like silica sol-gel or membrane devices such as hollow fiber or microcapsule). Since immobilization conditions are often very mild, immobilized derivatives do not suffer severe loss of activity. Lack of covalent binding determines reversible procedures that allow the recycling and reuse of the carrier after the useful enzyme lifetime. The natural negative consequence is enzymatic structure lack of rigidity that can cause leaching and denaturation during the process. For all these reasons, the procedure is more successfully accomplished with whole cells catalysts. A major example of this case was applied to the production of a bulk chemical like acrylamide, mediated by an immobilized whole cell catalyst.

Acrylamide is a commodity chemical largely produced as a monomer for the polymer industry. Traditionally, acrylamide production relied on a copper-based process for acrylonitrile hydration with water. Actually, the high temperature required for catalyst activation could easily result in undesired

acrylamide polymerization but, at the same time, corresponded to low conversion and productivity and the need of downstream units for product purification from the unreacted nitrile. Nitto Chemical Industry developed in 1985 a process based on a nitrile hydratase produced by *Rhodococcus rhodochrous* J1, immobilized as whole-cell catalyst in a polyacrylamide gel. The reaction achieved complete hydration of the starting nitrile at 10°C, replacing the copper-based process. In 2000 Nitto could produce about 6000 tons of acrylamide per year exploiting *R. rhodochrous* J1 that became the first example of successful implementation of biocatalytic process of a bulk chemical [45]. A second important application of entrapped enzymes is the production of lactose-free milk developed by SNAMprogetti in Centrale del Latte (Milan, Italy) in 1970 exploiting an immobilized galactosidase from the yeast *Saccharomyces lactis* entrapped in cellulose triacetate fibers. The process was run in a rotary horizontal column reactor and could process up to 10 tons milk per day, while the enzymatic derivative could be used for 50 cycles without any significant loss of activity, allowing the production of a high-quality milk at reduced costs [45].

Physical adsorption

Physical adsorption is a reversible immobilization technique that exploits reversible bonds like hydrophobic, van der Waals and hydrogen bonding interactions between the enzyme and the carrier. The generally mild immobilization conditions maintain high level of starting activity and permit carrier recovery once the enzyme activity is reduced to zero. On the other hand, possible protein leaching and low enzyme stability are issues to be faced. A multitude of different possible carriers have been studied, including cellulose fiber, molecular sieves, kaolin and micro and mesoporous materials. At larger scale, the most common material used as carrier for physical adsorption is methacrylate which was found to be a robust support with high resistance to flow conditions to organic solvents. Commercially available formulations of immobilized enzymes by physical adsorption concern mainly lipase immobilization because of the partial hydrophobicity of their surface which makes them suitable to this kind of immobilization. Moreover, by physical adsorption, lipases can be submitted to one-pot purification and immobilization procedure, which is particularly convenient also for lipase commercialization. The most successful immobilized lipase is by far Novozym® 435, a commercial immobilized derivative of *Candida antarctica* lipase B on a macroporous acrylic polymer resin commercialized by Novozymes® which have known during years an impressive popularity among academics, demonstrating also applicability on industrial scale.

Novozym® 435 has been mainly studied as catalyst in biofuel production for methanol/ethanol esterification or transesterification of starting acylglycerols or free fatty acids derived from the vegetable oil refining industry. For its robustness and versatility, it has been studied for large scale processing and few examples of pilot plants have been operated. For instance, a mixture of low-value oil was employed in 2006 for Novozym 435®-mediated production of biodiesel in a plant in Hunan Province (China), developed by Hainabaichuan Co. Ltd.. Novozym 435® was chosen as catalyst for the conversion of a high acidic oil coming from palm oil and edible oil waste to into biodiesel, with a capacity of 40,000 tons per year [46].

Ionic binding

The immobilization by ionic binding is often classified as a special kind of adsorption immobilization. Basically, it involves the ionic and electrostatic interaction between protein ions and opposite ions on the carrier and takes usually advantages of ion exchange resins for the purpose. Unfortunately, also for ionic binding, a simple and low stressing immobilization procedure is counterbalanced by possible protein leaching in conditions of non-optimal temperature, pH or ionic strength. Ion exchange resins like DEAE-Sephadex derivatives have been industrially exploited since early 1970s. One of the earliest industrial application of immobilized enzymes was developed by the Tanabe Seiyaku Co. of Japan that exploited a mold aminoacylase to perform racemic resolution for the production of several L-amino acids. In order to overcome the limitations of the batch process with soluble enzymes, they found immobilization of aminoacylase on DAEA-Sephadex the best choice after a comparison of several immobilization protocols and they found that continuous-flow process with immobilized enzymes determined a significant saving in terms of energy and time consumption [47].

Metal coordination

Another reversible immobilization protocol suitable to those engineered enzymes endowed with peptide tags (*i.e.* His-tag) is based on the coordination of the tag with a metal ion on a solid support. The tag is added to the end of a protein by genetic modification to allow its purification through the same mechanism, entailing that purification and immobilization can occur in only one step. As other types of “affinity immobilization” not based on covalent binding (like ionic on physical adsorption), metal-coordination represents a reversible immobilization protocol. Furthermore, even if this support is often expensive, the binding reversibility allows a complete and efficient recovery of the carrier

when the enzymatic activity has been lost or considerably decreased. In contrast to other non-covalent binding protocols, metal-coordination is still a little established technique at larger scale, and it has mainly dragged attention in the academic field. However, in the past years attention is increasing and a company, EnginZyme AB®, Sweden, has successfully developed a general matrix for His-tagged enzyme immobilization consisting of a controlled porosity glass carrier with dispersed Fe(III) ion that coordinate the histidine tail of the enzyme. These carriers have been exploited extensively in recent years in both academic and industrial settings and several papers have been published concerning immobilization of different classes of enzymes [48-50].

Covalent binding

The strongest binding between enzyme and carrier that can ensure the highest enzyme structure fixation and least leaching grade is provided by covalent bond formation between the amino acid residues onto enzyme surface and a differently activated carrier. Usually, the amino acid functional groups involved in covalent binding are amino (NH_2), carboxyl (COOH), hydroxyl (OH), and sulphydryl (SH) groups. A broad range of carriers have been studied for covalent binding: synthetic resins, biopolymers such as polysaccharides (usually activated to provide a desired functional group), or inorganic solids such as (mesoporous) silicas or zeolites are the most desirable. Covalent binding is often appreciated for the improvement of enzyme lifetime, an increase in stability and low leaching phenomenon, which makes this immobilization technique most suitable to plug-flow reactor applications. The main drawbacks displayed by the technique lies in immobilization conditions that can be harsh and could compromise enzyme structure resulting in low recovery activity. A covalent binding protocol has to be carefully evaluated for each enzyme and can be often not the best practice. Moreover, being covalent binding an irreversible immobilization, recyclability of the carrier is compromised, significantly increasing the costs of the process. The cost of the carrier, its non-reusability and the cost of the immobilization protocol are significant limitations of covalently immobilized derivatives at larger scale, and their occurrence in industrial processes is rare. Instead, covalent binding has been extensively studied and discussed in academia and many valuable carriers for covalent immobilization have been selected to address the challenges of developing covalent immobilization protocols that can be easily and less costly applied to higher scale. Among these carriers, agarose has been found of particular interest so far. Agarose is a natural polysaccharide, generally extracted by the seaweed Rhodophyta, and is generally appreciated for various reasons like

its renewable source, high porosity, high mechanical resistance, and high hydrophilicity. Moreover, agarose can be differently activated [51] to implement enzyme immobilization. In particular, the aldehyde-activated agarose (glyoxyl agarose) is considered highly suitable to continuous-flow applications [52-54].

Flow chemistry

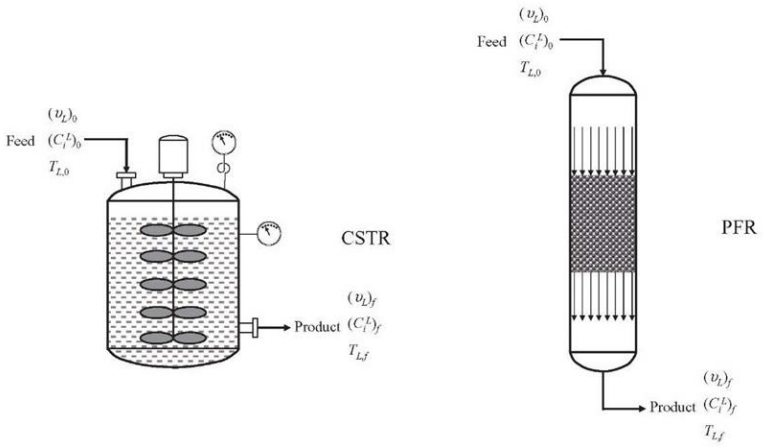

Continuous production is an intrinsic characteristic of modern industry. The first examples of continuous-process date back to the end of XVIII century, when Richard Arkwright designed the Cromford mill in 1769 [55] (the first continuous process where a finished product was prepared from raw material by different continuous steps) and when Oliver Evans patented his flourmill in 1785 which worked under fully automatic [56] conditions. Concerning the chemical industry, the first attempts to implement a continuous chemical process refer to oil refining, converted to continuous operation at the end of XIX century, after the improvements reached with remote control systems [57].

The beginning of XX century witnessed the raising of the modern continuous industry. 1913 is the key year for the continuous manufacturing with the development and theorization of the assembly line by Henry Ford for Ford Model T production [58], but it is also the year in which continuous ammonia production on industrial scale was developed by Carl Bosch from a small-scale process previously designed by Fritz Haber, reaching a production rate of 20 tons per day the following year [59]. The so-called Haber-Bosch process, which is still used for ammonia production, became the first continuous-large scale process for a bulky chemical production. The initial process configuration was more or less the same used a century later and it is based on continuous reactors and continuous downstream purification units. Nowadays, bulk chemistry is still conducted in continuous-flow processes, that are based on continuous reactors, modelled according to two ideal behaviors represented by a continuous stirred-tank reactor (CSTR) and a plug-flow reactor (PFR).

A reactor following a CSTR-behavior is constituted by a stirred tank where, hypothesizing an ideal mixing, reagents are instantaneously and uniformly mixed throughout the reactor. Consequently, the

output composition is identical to the composition inside the reactor, which is a function of residence time and reaction rate. It is normally operated at steady state meaning that there is no time dependence of the temperature, concentration, or reaction rate [60]. CSTR-like reactors are usually employed for industrial applications requiring liquid-phase reactions like environmental applications (for example industrial wastewater treatment), fermentations or productive processes based on homogeneous catalysis like production of acetic acid (Cativa or Monsanto process), acetaldehyde (Wacker process) or slurry production of polypropylene.

A PFR, instead, can be modelled as a tubular reactor constituted of a series of infinitely thin layers, each one with a uniform composition, moving in the axial direction (the "plug" direction) of the reactor. As a consequence, it can be assumed that the fluid is perfectly mixed in the radial direction while conversion, composition and temperature vary constantly in the axial direction of the reactor. Also PFR reactors are run at stationary state with no time dependence and are usually employed for large scale reactions in gas phase catalyzed by solid, metal-based catalysts [60]. These reactors find place in oil-refining units like catalytic cracking and gas reforming, production of inorganic bulk chemicals (nitric and sulfuric acid, ammonia), organic bulk chemicals (methanol, formaldehyde, ethylene oxide) and environmental applications (NO_x abatement in dedicated selective catalytic reduction units). For several of these abovementioned processes continuous reactors are run with a capacity of few tons per day.

Downstream requires other continuous unit operations for product purification like distillation operations, absorption, liquid-liquid extraction and so on. Due to the significant dimensions, process design and operative conditions must be carefully controlled and sophisticated plant control systems are mandatory. Shutdowns and startup of the plant are long and complex. Shutdowns of complicated processes may take weeks or months of planning, involving multiple considerations and decisions regarding maintenance, engineering, safety and operating units. While startup requires running a process under non-steady state conditions and can require days to reach regime conditions. For all these reasons, bulk chemical engineering is quite conservative and little disposed to structural changes and improvements, due to the high costs of plant stopping and technical intervention or equipment replacements, especially considering that all the profits are limited to the amount of sold products for the low price of bulk chemicals. Instead, the fine chemical industry is founded on completely different bases. Fine chemical industry is driven by product and formulation research for the high added value of products. Although the high profits on the products and the high level of research connected to this

industry, little research is conducted on the process itself: small quantities and often seasonal production make exploitation of batch reactors convenient, designed as vessels of different dimensions equipped with a stirrer and heat exchanging systems. Although simple vessels are extremely inexpensive reactors, safety is a concern for batch-based processes. Actually, batch productions rely on efficiency of heat and mass transfer and, therefore, on mixing efficiency. But, although efficient, vessels are often subjected to dead zones or stagnant regions that are exposed to not optimal conditions: these dead zones can determine, in the best cases, a loss in selectivity causing increase of purification costs and diminishing of the amount of valuable product to sell. In the worst cases, dangerous parasite exothermic reactions expose the system to extremely dangerous situations like reactor runaway and explosions.

These risks are not remote possibilities. The probably most notorious event in Europe took place in Seveso (Italy) in 1976, where dead zones in the vessel activated the formation of dioxine-like compounds and, in the end, the opening of the relief valve with the release of approximately 2 kg of chemicals over a residential area of 2.8 km^2 [61,62]. A semi-batch runaway occurred also in a Hoechst A.G. plant in Griesheim (Germany) in 1993 where a 10 tons of reaction mixture containing a significant concentration of azo and azoxy derivatives were released to the environment. The probable cause of the disaster was agitator failing [62]. This kind of risks, fifty years later, are no longer considered acceptable. Beyond safety, environmental sustainability, minimizing consumption of resources like energy and raw materials are compelling topics that are encouraging development of new safer and more sustainable processes to be applied to smaller scale for the preparation of high value products like pharmaceuticals, cosmetics, food additives, flavors and fragrances. A possible approach has been inspired by continuous processes, by scaling down reactor dimensions, both to suite the low product demand and, especially, to reduce mass and thermal inertia of the typical batch scale for fine chemistry. This approach was named “flow chemistry” and it is based on the use of miniaturized reactors connected to a pumping system to move reagents and products in and out the reactive parts of the system. Flow chemistry aims to take advantages of both small reaction dimensions (characterized by increased heat and mass transfer resulting in an increase of safety and selectivity) and the continuous-flow conditions (affording higher productivity and easier scale-up by numbering-up of single units). The reactors are bench-size and can be applied both in academia field and for industrial purposes. During the last twenty years, the state-of-art related to flow chemistry has reached important achievements both in terms of devices and equipment to perform the reactions and examples of syntheses developed under continuous-flow conditions.

Concerning the tools now available for continuous-reaction implementations, research interests have been focused on: 1) the reactor itself and the correlated pump systems, 2) downstream units for in-line work-up and product isolation and purification, and 3) machine-assisted systems for remote control and automated optimization.

Reactors and pumping systems

Reactors employed for flow applications are usually classified according to their scale. In fact, they are divided into two main classes: microreactors and mesoreactors. The smaller ones (called "microreactors") correspond to a hydraulic diameter scale of 10-500 μm and they can be configured either as a chip-type (corresponding to a bankcard with external dimensions of few centimeters at most) or microtube devices [63-65]. They can be customized by 3D-printing using different materials like glass, silicon, ceramics, steel or advanced composites to obtain faster heat transfer [64,66]. Mesoreactors (also referred as mini-/millireactors) are larger-scale reactors (corresponding to a hydraulic diameter within a range of 500 μm to several mm) suitable for production that can vary from g/h to tons/year. They can represent scaled-up versions of chip-type microreactors (*i.e.* millichannelled reactors) or single tubular reactors [67,68], moreover they can be easily combined to fixed-bed components for implementation of solid-based reactions. The pumping systems connected to micro- and mesoreactors are usually based on either HPLC or peristaltic pumps, depending on the required flowrate, operative duration, the presence of gas bubbles or particles and to what extent solvents and reagents can be detrimental. In general, since flow systems are meant to work under steady-state conditions, the amount of product is defined by process duration, processed volumes and flowrates. Along with the intense experimental research to broad the range of available equipment for continuous-flow reactions, model-based reactor design has been increasing in popularity as an important supporting tool. By exploiting engineering approaches like characteristic times and scale analysis [69,70] or computational fluid dynamics (CFD) simulation [71-73] it is possible to gain more process knowledge concerning the dynamic phenomena of the process, facilitating reactor characteristic optimization.

Downstream units

The easiest downstream units to implement in continuous-flow systems are liquid-liquid extraction and phase separation systems [74-76]. The latter can be gravity-driven [77] or, much more commonly,

membrane based-separators exploiting surface tension differences between the aqueous and organic phases, which are the most efficient devices employed for phase separation in continuous multistep syntheses [78-80]. Some solvent-switch systems have also been developed [81], or continuous solvent removal like falling film evaporators [82], distillation on chip [83] and miniaturized distillation columns [84]. Product isolation can be achieved with the use of scavengers or catch and release systems, generally based on interaction between the products and a solid support like polymer-supported acids or ion-exchange resins [85]. An issue that is still difficult to overcome is solid handling, especially concerning purification *via* crystallization but, still, some solutions have been proposed like a miniaturized version of CSTRs similar to the ones already employed in pharmaceutical industry for continuous crystallization [86] or gas-liquid flows have been reported to be employed to convey slurries [87].

Machine-assisted automation

Flow chemistry, for its modularity and the intrinsic interconnection among the different process units, could take great advantage of Internet-based software platforms which facilitate the monitoring and control of chemical reactions. These systems often combine in-line reaction parameters monitoring, feedback control and self-optimization modules, especially by facilitating the adoption of new optimization algorithms. Several examples have been reported so far where the automation degree could lead to significant process enhancement in terms of reaction optimization [88] and an easier unit interconnection and merge between chemical steps and downstream units [78]. Moreover, this approach has been achieving significant goals concerning the collection of reaction data to determination of kinetics [89] and the discovery of new APIs by automatically switching different modules for the synthesis of different compound libraries [90]. In general, the development of a machine-assisted flow process should lead to a significant reduction of process costs, eliminating also some of the downstream operations and, thus, reducing the distances between a lab-bench synthesis to industrial kilogram-scale production.

Concerning the examples of successful implementation of synthesis under flow-mode, some of the most relevant exploitations of this technique are here reported, to better illustrate the advances of this technology.

Prof. Ley's group in Cambridge is acknowledged for its pioneering work in the continuous-flow synthesis of natural products and for the solutions found during years to overcome the challenges

related to downstream processing. One of the most cited paper is the continuous synthesis of (±)-oxomaritidine [91] (Scheme 1), a cytotoxic alkaloid of the Amaryllidaceae family, accomplished through a multi-step synthesis for a total of seven synthetic steps. These steps were implemented through various packed columns containing immobilized reagents, catalysts, scavengers or catch and release agents, allowing also in-line product isolation. The process showed significant benefits in reducing the overall costs and increasing the yields, avoiding batch purification procedures and intermediates isolation. Moreover, the low grade of manual handling allowed a rapid optimization and made operative conditions easily and efficiently controlled.

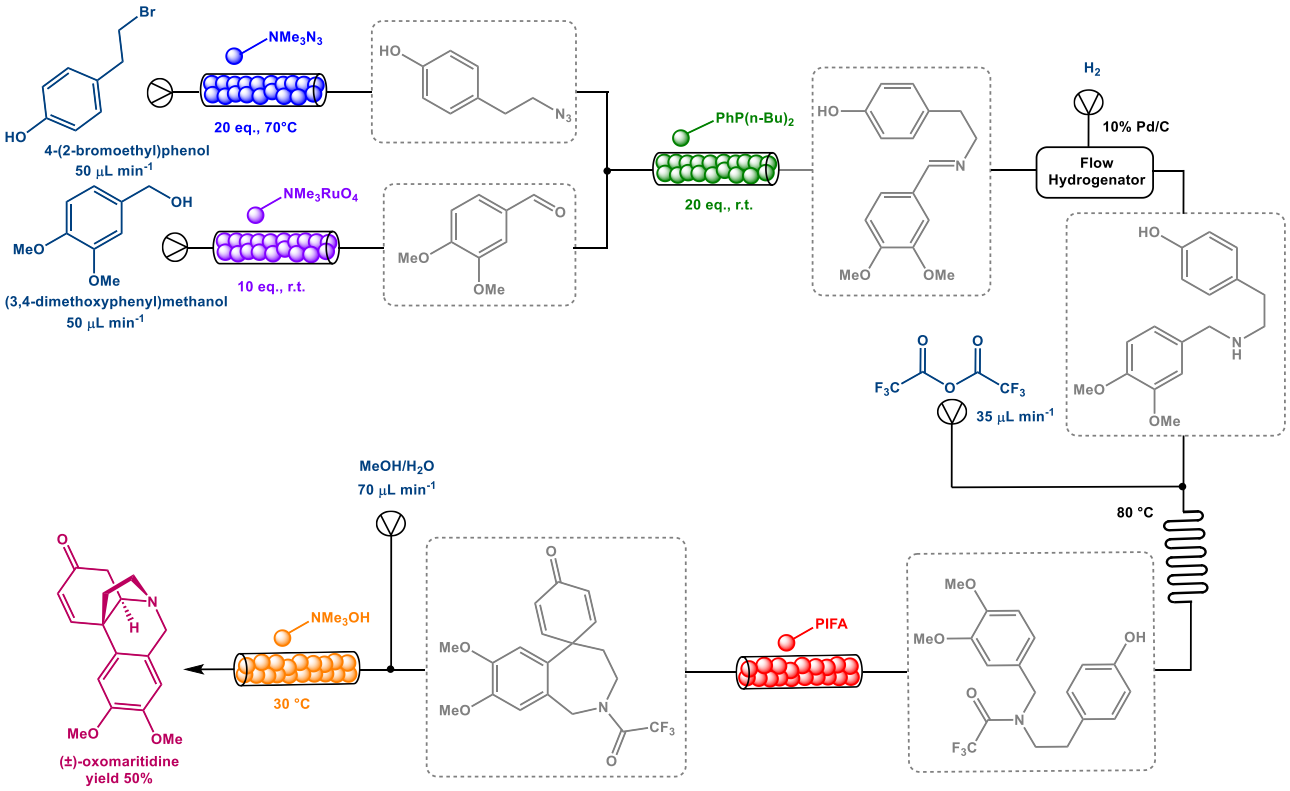

Scheme 1. Continuous-flow synthesis of (±)-oxomaritidine [91].

The advantages of flow technology were well displayed by Fuse *et al.* [92] exploiting a highly toxic gas such as phosgene in flow processes. Phosgene, although potentially highly useful in organic synthesis is troublesome in industrial chemistry due to its extreme toxicity. The authors obtained phosgene preparation *in situ* from triphosgene in a microflow device to a safe handling of the gas. Immediately after its formation, phosgene was consumed by the following reaction, eliminating the problems of storage or dispersion. In the paper, phosgene was employed as chlorination reagent for

the preparation of an acyl chloride that was continuously converted into the corresponding amide. The procedure did not require any heating or cooling systems (was conducted at 20 °C) and provided high yields (about 98%) with a very low residence time (1.5 s) (Scheme 2).

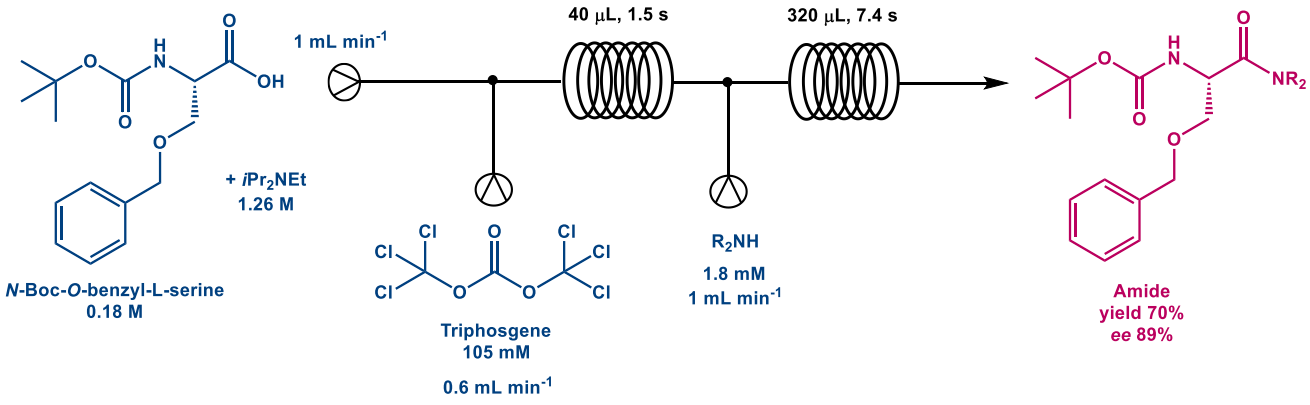

Scheme 2. *In situ* generation of phosgene and continuous-flow synthesis of amides from carboxylic acids [92].

A major example of the importance of microdevices for synthetic applications was provided by prof. Yoshida's group in 2008 [93] and in 2010 [94]. Both papers deal with application of organolithium compounds for a Br/Li exchange reaction in presence of ester or nitrile groups that are highly reactive to organolithium compounds. Instead, prof. Yoshida's work is based on the concept of "flash chemistry" which means that using a microflow system and keeping the residence time very low (<1 s) it is possible to generate a reactive intermediate and rapidly use it in a following reaction before decomposition takes place. In Nagaki *et al.* (2008) [93] (Scheme 3) the Br/Li exchange reaction of alkyl *o*-bromobenzoates was achieved with a 61% yield while later, in Nagaki *et al.* (2010) [94], a set of bromobenzonitriles were submitted to lithium exchange with a yield range of 60-80% (Scheme 4). These impressive examples show how flow chemistry could enable reactions that are impossible to carry out in batch conditions, displaying all the potential of this technique.

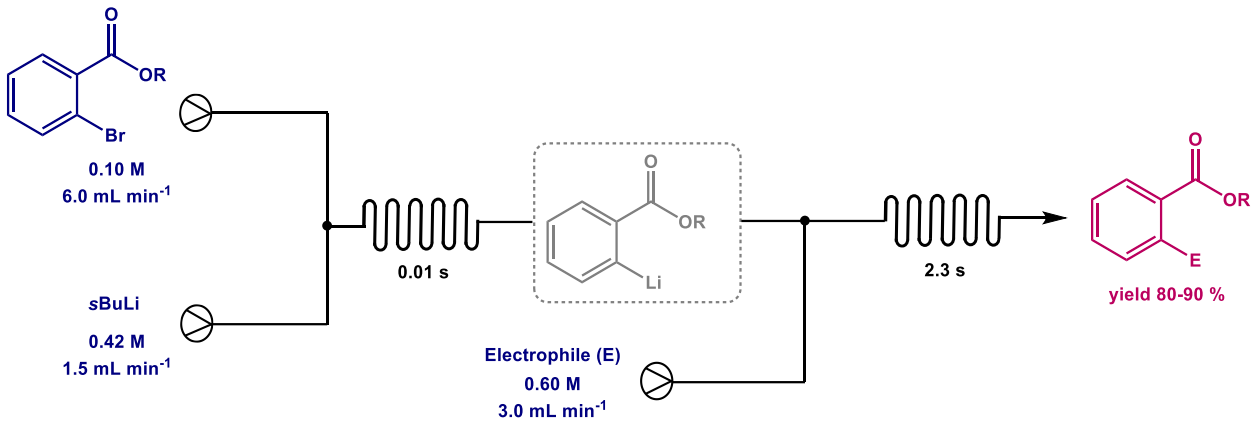

Scheme 3. Microflow system for Br/Li exchange reactions with alkyl *o*-bromobenzoates followed by reaction with electrophiles [93].

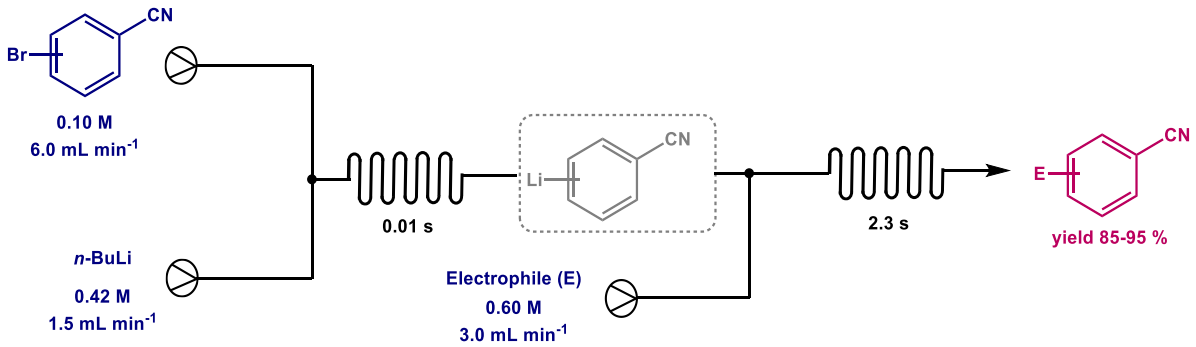

Scheme 4. Microflow system for Br-Li exchange reactions with bromobenzonitriles followed by reaction with electrophiles [94].

Although the available devices have reached a certain level of sophistication and the process state-of-art shows the advantages that could be obtained in an industrial setting, flow chemistry is still little developed for industrial production. Economic reasons are usually addressed as the main responsible, due to the equipment costs, but, actually, several examples of economic analysis highlight the cost benefits concerning continuous-flow production, compared to the batch processes, especially when industrial scales are involved and the equipment seems to be a smaller issue in the total process costs [95-97]. Causes have to be found elsewhere. For instance, it has been highlighted that more "human" factors, related to industrial culture aspects, could be determinant. Pashkova *et al.* [98] expressed an interesting consideration about small and medium enterprises in the chemical field that still, due to lack of knowledge and experience about continuous processes, perceive investing in the technology as too risky, compared to big companies whose investments in the development of continuous processes implementation is significantly increasing.

A viewpoint embraced by the experts points out that the gap is mainly of a cultural matter, and it could be filled by integrating education of graduate and undergraduate chemists with some engineering knowledge together with a higher sensibilization on safety and sustainability issues. At the same time, it would be necessary involving chemical plants employees to work in a multi-disciplinary team, integrating chemistry to chemical engineering to computer science [99]. It is interesting to note that transition from batch to flow started in China and India before the rest of industrialized world: nowadays, most part of industrial-scale flow processes are placed in China, and still few are located in Europe. The main reason could be ascribed to the industrial growth connected to the development of new chemical plants that China and India are facing: building a new plant is probably less risky for testing a new technology rather than changing already existing assets as the long-dated plants in Europe [100]. Perhaps the most publicized example of newly implemented continuous-flow process is actually located in China, in the city of Shaoxing, and was designed by Ehrfeld Mikrotechnik for the company Shaoxing Eastlake Biochemical. In the plant, a highly exothermic alkoxylation reaction is run in millireactors from Ehrfeld with a production capacity of up to 10,000 tonnes $year^{-1}$. The system has been running in continuous since 2016.

Although batch systems are still by far the most exploited reactor configurations, many pharmaceutical companies, like AstraZeneca, Novartis, Lonza and Eli Lilly are increasing their participation to various flow chemistry symposia and conferences presenting their achievements on continuous processes. Significant improvements have been reached in the last ten years, in terms of both device availability and industrial interest into the subject. Many aspects are encouraging a cultural change: regulatory pushes together with the need for more eco-efficient processes are driving implementation of flow production. A positive and optimistic climate is spreading, and expectations try to foresee new significant results in the next ten years [99]. As for any technological improvement, research has the mandatory scope of pushing the boundaries of knowledge and skills, to make them more and more available also to a factual technological upgrade for the chemical industry. A field in which flow chemistry is a very hot topic and that is trying to gain significant improvements in terms of scalability and applicability is certainly biocatalysis, as it will be illustrated later.

Continuous-flow Biocatalysis

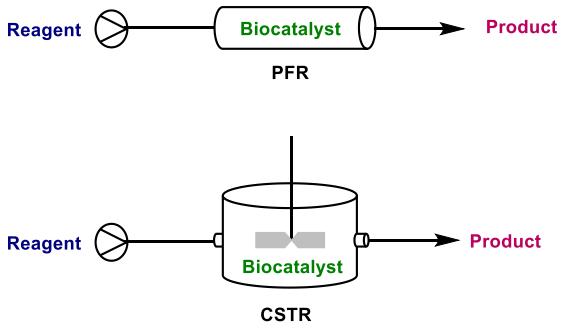

The popularity that flow chemistry has gained among biocatalysis experts relies on the desire of overcoming some of the main issues that hinder biocatalysis applications at larger scale. The appeal of continuous-flow approach to biocatalysis can be attributed to three main characteristics considered the key to this enabling technology for a larger-scale biocatalysis development:

Improvement of yield

Many continuous-flow biocatalysis works highlight an enhancement of the enzymatic reaction space-time yield, which is always rated as one of the main benefits for any type of reaction run in flow-mode. The main reasons can be ascribed to a higher homogeneity of temperature and concentration in the system (due to mass and heat transfer improvement) while the small dimension and the high enzyme concentration in a small chamber promote a local significant increase of enzyme concentration speeding the reaction rate. Furthermore, the intrinsic combination of continuous reaction and filtration in flow-mode entails a more efficient reutilization of enzyme until its deactivation, increasing flow-mode productivity over the batch per unit of enzyme.

A definition for yield, which is generally adopted for comparison between flow and batch, takes into account the amount of product formed per unit of time and volume, and it is called “space-time yield” (STY) [101]:

$$STY = \frac{amount\ of\ product\ generated}{Volume \cdot unit\ of\ time}$$

Another common definition of yield can be expressed over the amount of biocatalyst employed for the reaction, in this case the definition is sometimes referred as “biocatalyst productivity” [102,103]:

$$biocatalyst\ productivity = \frac{amount\ of\ product\ generated}{biocatalyst\ mass \cdot unit\ of\ time}$$

Another term to define the stability of the biocatalyst over all its lifetime is the total turnover number (TTN), which is calculated as the amount of the product generated during biocatalyst usuful lifetime (until its inactivation) over the amount of the biocatalyst employed [101]:

$$TTN = \frac{amount\ of\ product\ generated}{amount\ of\ biocatalyst}$$

Comparison of performances between batch and flow reactions are easy to find in the literature. For instance, Woodcock *et al.* (2008) [104] compared batch and flow for the synthesis of a series alkyl esters promoted by Novozym® 435. In order to compare the two systems, the authors run the batch and flow reactions under the same conditions, observing that in 10 min of batch operations only 3% conversion was reached while flow-mode afforded in a few minutes 93% conversion (Scheme 5). Moreover, at the end of batch reaction a maximum of 70% conversion could be reached while the stationary state in flow mode afforded 94% for 8 h.

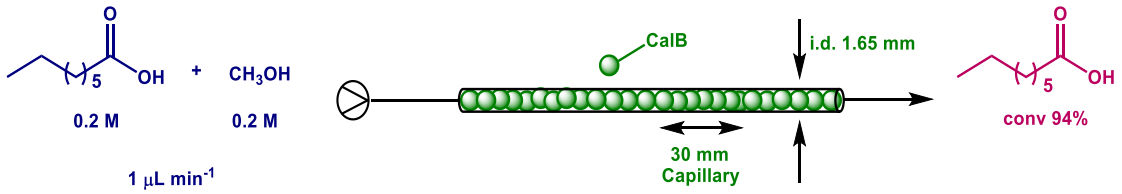

Scheme 5. Continuous-flow esterification of octanoic acid in a capillary tube packed with Novozym® 435 [104].

A reaction acceleration was observed also by Wang *et al.* (2014) [105] in using flow biocatalysis for the preparation of caffeic acid phenyl ester (CAPE) by Novozym® 435 in a packed-bed microreactor using ionic liquids as reaction medium (Scheme 6). The authors observed that, under optimum conditions, in flow-mode a 93.21% of yield CAPE was achieved in 2.5 h while the same yield required 24 h in a batch reactor.

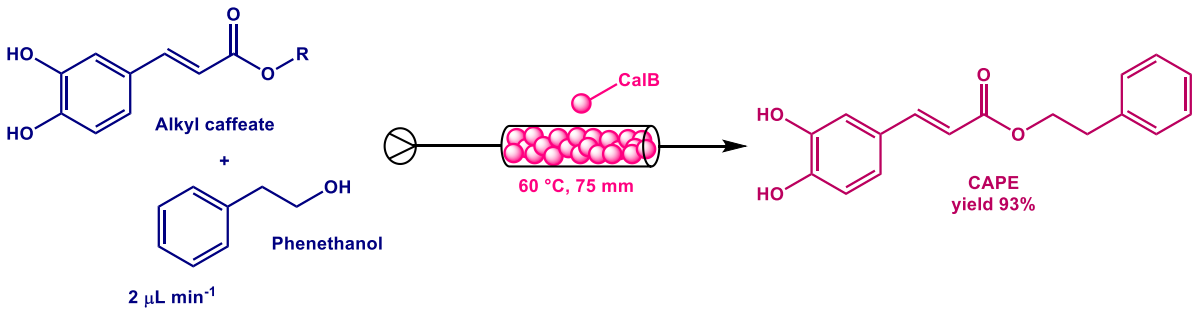

Scheme 6. Continuous-flow biocatalyzed synthesis of caffeic acid phenethyl ester (CAPE) by Novozym® 435-mediated transesterification of alkyl caffeate [105].

Hugentobler *et al.* (2016) [106] published a whole paper dedicated to comparison between batch and flow in biocatalytic applications. The paper deals with the enzymatic mediated racemic resolution of a cyclopropanecarboxylate ester, which finds an application as a key building block of Ticagrelor, a medication used as aggregation inhibitor for the prevention of strokes and heart attacks. The resolution was catalyzed by an immobilized formulation of *Thermomyces lanuginosus* lipase. The biocatalytic reaction, run according to the two different reactor configurations, showed a significant improving of yield with flow-mode: the space time yield of batch reactor stopped to 0.4 mmol L^{-1} h^{-1}, while with a flow reactor it reached 28.2 mmol L^{-1} h^{-1} corresponding to an impressive improvement of 64 times with flow biocatalysis (Scheme 7).

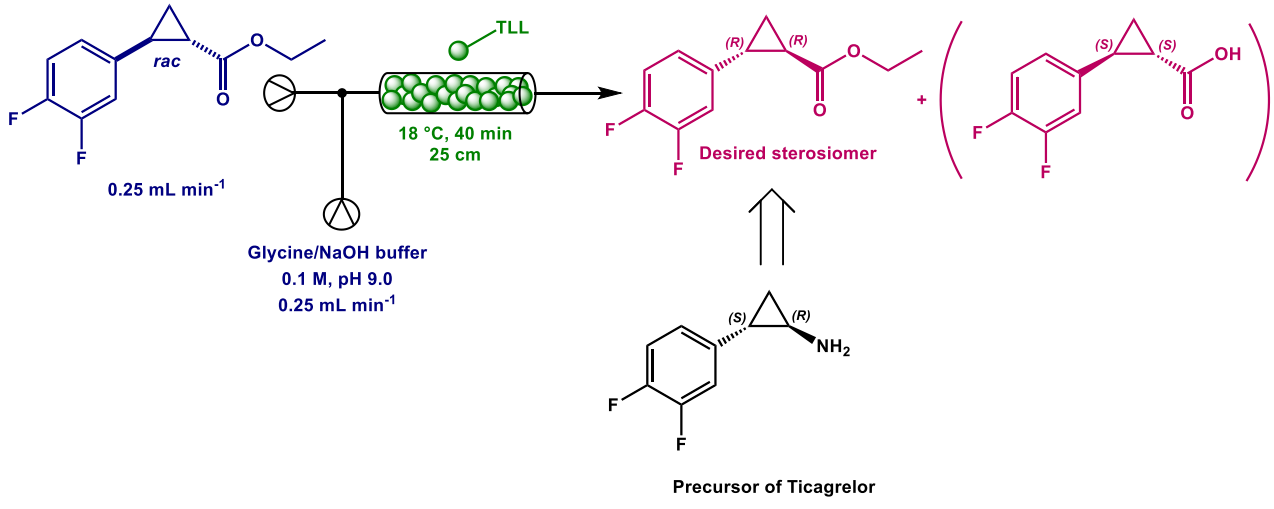

Scheme 7. Preparation of a Ticagrelor precursor by enantioselective hydrolysis mediated by *Thermomyces lanuginosus* lipase in a continuous-flow systems [106].

Process automation

One of the most important aspect that drives implementation of continuous-flow biocatalytic reaction is a desire for increasing the automation degree of the process. Specifically, it aims to set-up multiple enzymatic steps of chemo-enzymatic synthesis with an in-line work-up. and continuous product isolation and purification and without intermediate isolation. Enzymatic reactions, in enzymatic cascades or in chemo-enzymatic synthesis, implemented in continuous-flow mode with a particular attention paid to the development of purification steps, have been increasing in popularity and are well-documented [101,107-109]. One of the first successful example was reported by Baxendale *et al.* (2006) [110]. The paper deals with continuous preparation of the natural compound grossamide, a lignan amide isolated from various vegetable species. Grossamide was prepared in two steps. In the first one tyramine and ferulic acid were continuously coupled, exploiting hydroxybenzotriazole (HOBt) immobilized on a polymeric matrix as a solid activated ester. Then, the amide solution was flowed into a column packed with horseradish peroxidase (HRP) immobilized on silica in presence of hydrogen peroxide. Beyond the coupling of a synthetic and an enzymatic step and the addition of purification in-line systems, the process was equipped with inline UV detector for reaction monitoring (Scheme 8).

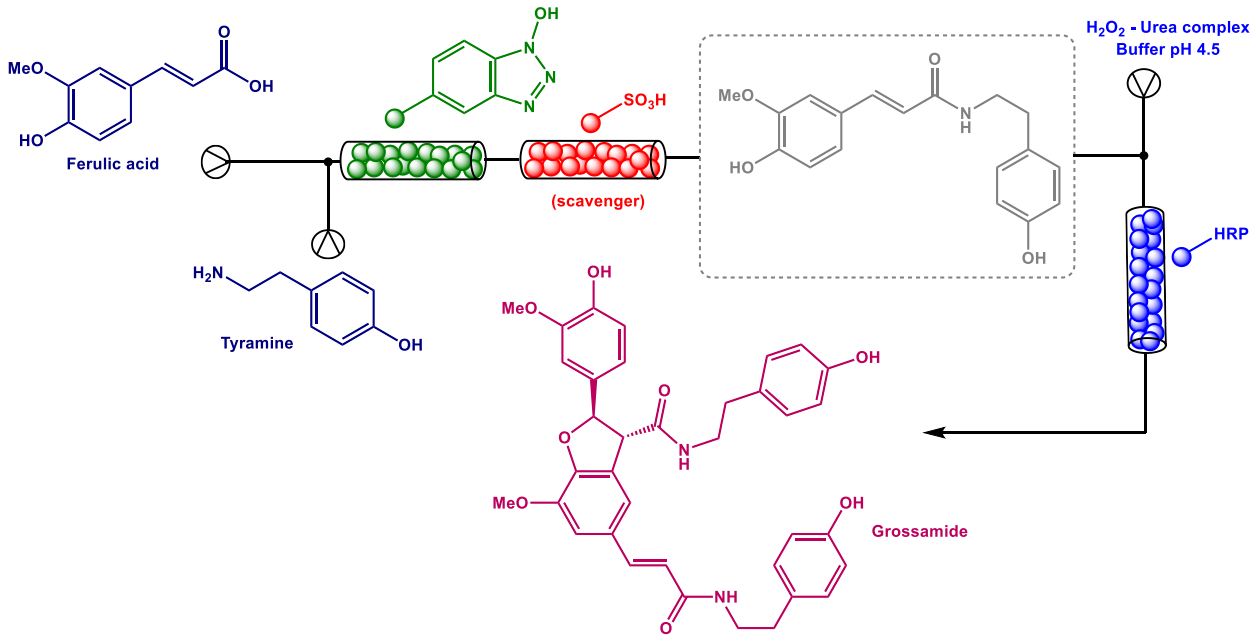

Scheme 8. Chemo-enzymatic continuous-flow synthesis of grossamide starting from ferulic acid and tyramine [110].

Farkas *et al.* (2018) [111] presented the first chemo-enzymatic kinetic dynamic resolution of an amine under totally continuous-flow conditions. The authors employed two consecutive packed-bed columns: the first was filled with a sol-gel immobilized lipase B from *Candida antarctica* (*Ca*LB-TDP10) as biocatalyst for the selective acylation of a suitable (*R*)-amine derivative using isopropyl 2-ethoxyacetate as acylating agent, followed by a column packed with both the beforementioned immobilized enzymatic formulation and a solid Pd-catalyst for racemization (palladium on aminopropyl-grafted silica Pd/AMP-KG) (Scheme 9). The system proved to successful convert six racemic benzyl amines with good isolation yields (57−96%) and excellent enantiomeric excess (>98.8%).

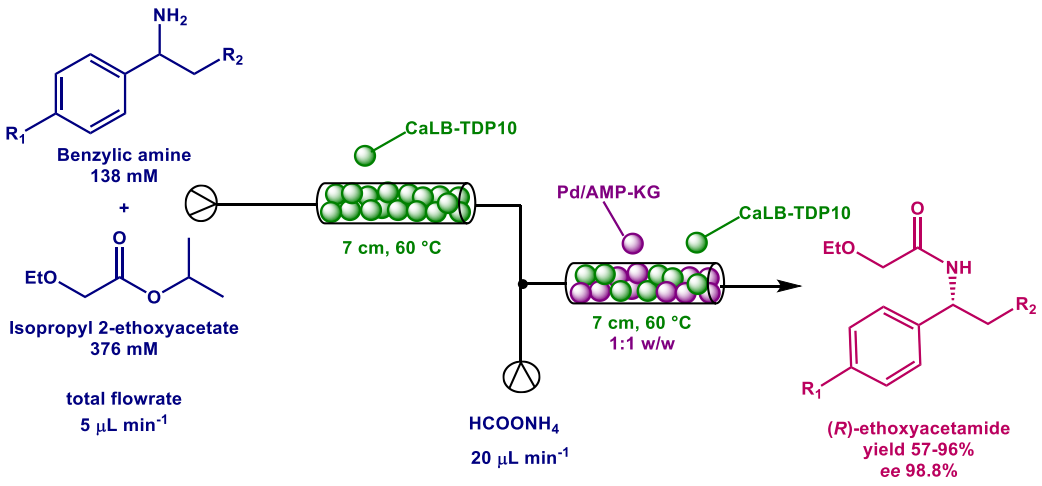

Scheme 9. Chemo-enzymatic kinetic dynamic resolution of amines under continuous-flow conditions [111].

De Vitis *et al.* (2017) [112] designed a chemo-enzymatic synthesis of captopril, a drug used for the treatment of hypertension, from the inexpensive 2-methyl-1,3-propandiol by stereoselective oxidation to the corresponding (*R*)-2-hydroxy-2-methylpropanoic acid using immobilized cells of *Acetobacter aceti*, entrapped in calcium alginate beads. The biocatalytic reaction was followed by three synthetic steps. The hydroxy acid produced by biocatalyzed oxidation was recovered as pure molecule by an in-line catch and release system, using base anion exchange resins. After acid isolation, the three synthetic steps (chlorination step, proline coupling and thiol group substitution of the chlorine) were conducted as liquid phase reactions in coil reactors without any further intermediate separation, exploiting in-line quenching and liquid-liquid separation. Such system allowed captopril recovery with an overall yield of 50% with a high enantiomeric excess (96-97%) (Scheme 10).

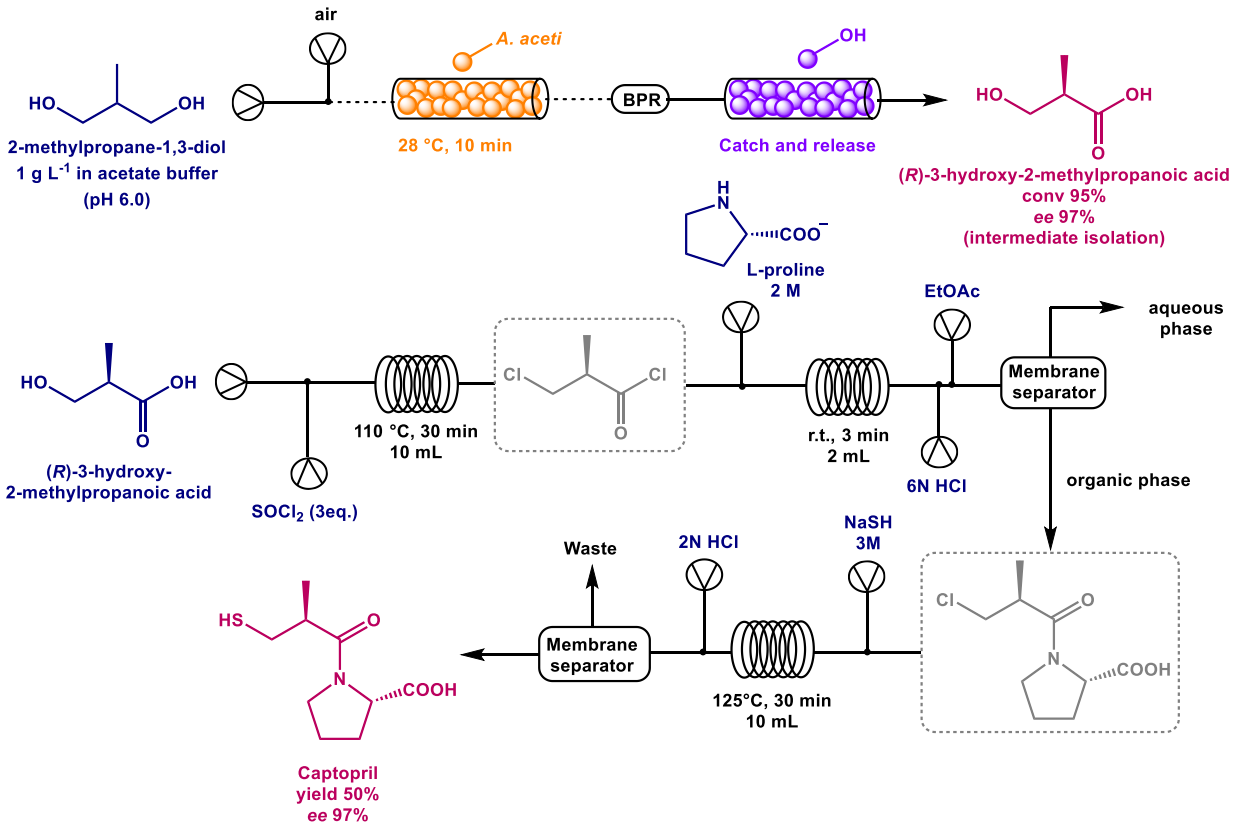

Scheme 10. Chemo-enzymatic synthesis of captopril under continuous-flow conditions [112].

Broadening the range of biocatalysis reaction when dangerous or troublesome reactants are involved

Safety issues are seldom mentioned about biocatalysis, which is often rated as completely safe. From this point of view, flow chemistry potential for handling hazardous reagents is rarely brought to the discussion for enzymatic reactions. Actually, the broad use of enzymes for organic synthesis can involve sometimes also toxic or explosive reagents and flow chemistry can address also this issue. An emblematic example of safe handling of toxic reagents for biocatalytic applications using miniaturized reactors was provided by Delville *et al.* (2015) [113]. The authors synthetized different enantiomerically pure aromatic cyanohydrins by a biocatalytic reaction. The enzyme involved belongs to hydroxynitrile lyase family, and is able to catalyze the enantioselective C–C-bond formation by adding HCN to aldehydes or ketones [114]. In the paper, the enzyme is used as crude enzyme lysates in a biphasic system: the organic solvent carries the aldehyde while the buffer carries

lysate suspension and KCN. *In situ* formation of HCN is allowed by the slightly acid pH value (5.0) of the buffer obtained by addition of citric acid (Scheme 11).

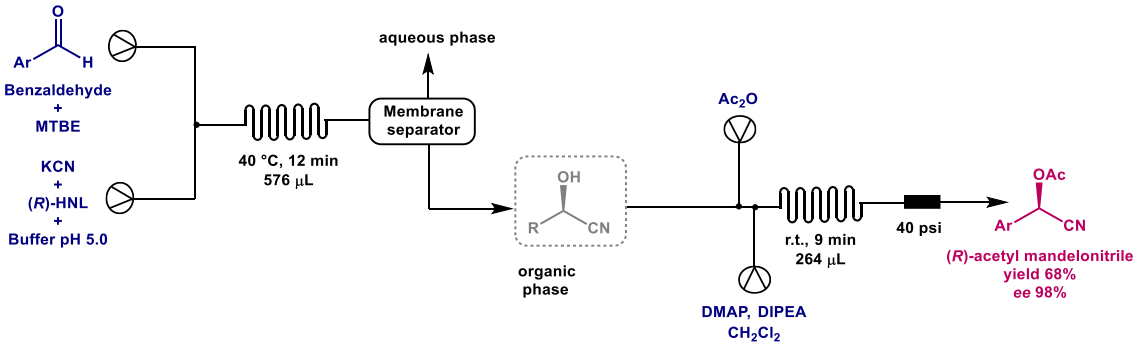

Scheme 11. Flow set-up of two-step synthesis of protected (*R*)-mandelonitrile [113].

A similar, interesting *in situ* formation and consumption of HCN was illustrated by Brahma *et al.* (2016) [115]. In this case, mandelonitrile synthesis is achieved by a two-enzymatic steps: first, HCN is generated *in situ* by enzymatic hydrolysis (promoted by immobilized *Candida antarctica* B) of ethyl cyanoformate (ECF) used as cyanide source, then after in line addition of benzaldehyde, the stereoselective nucleophilic addition is obtained by a hydroxynitrile lyase from *Arabidopsis thaliana* (*At*HNL) immobilized on celite. The system was then coupled with pyridine/acetic anhydride acetylation step (Scheme 12).

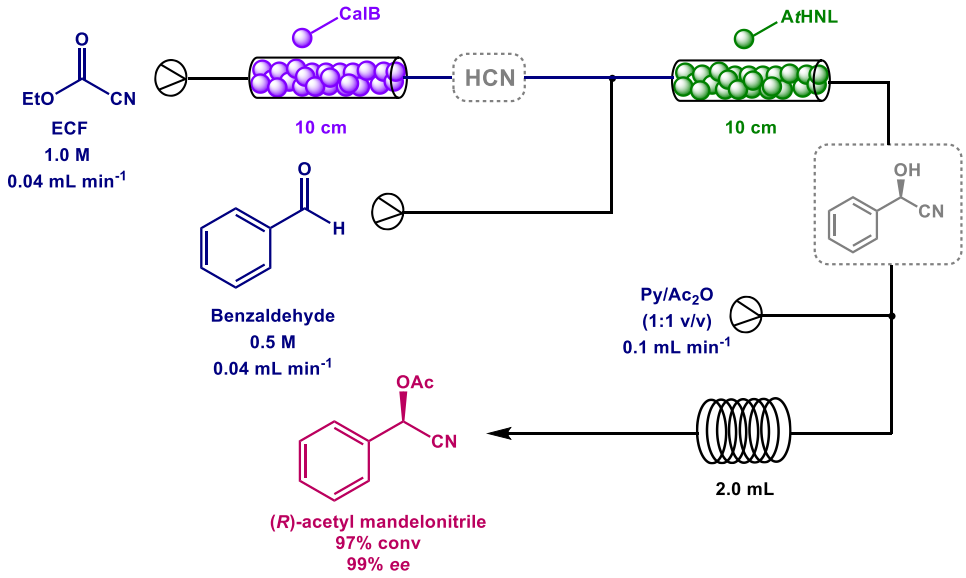

Scheme 12. Synthesis (*R*)-mandelonitrile by a two-step biotransformation (Novozym® 435 and *At*HNL), followed by chemical acetylation [115].

A second troublesome molecule which finds some popularity in biocatalysis is peroxyacetic acid (PAA), used for carbon-carbon double bonds epoxidation. The high instability of PAA makes its handling troublesome, moreover its *in situ* generation occurs only in presence of strong mineral acids as catalyst. Biocatalysis offers a safer route by providing some lipases that can catalyze peroxyacids formation from hydrogen peroxide and carboxylic acids [116]. Continuous-flow employment of biocatalytic *in situ* production and consumption of PAA has been addressed also in this thesis, and it will be discussed later.

Available tools for continuous-flow biocatalysis

As for the advantages that can push flow mode application to biocatalysis, concerning the methodologies and reactor configurations, they are not very different from the synthetic flow chemistry. Continuous enzymatic reactions can be run in a homogeneous medium (aqueous or organic, depending on the enzyme) with the catalyst in solution (free enzyme) and in the literature there are examples of homogeneous enzymatic reactions run in tubular reactors (PFR) [113,116-119] as well as in stirred reactors (CSTR) [120-122]. Usually, membranes are employed for enzyme retaining or for its recovery and recirculation [123,124]. Beyond these examples, the most part of continuous biocatalysis applications rely on enzyme immobilization as a tool to switch from a homogenous catalysis to heterogeneous catalysis and to exploit the advantages related to enzyme immobilization as illustrated before. The flourishing of enzyme immobilization literature encourages to find a suitable immobilization solution for different enzyme classes and different immobilization techniques have been used for flow applications: from covalent binding [125-127], to physical adsorption [128-130], to metal-coordination [131,132]. Immobilized enzymes are mainly used for packing reactor columns that work as packed-bed reactors (PBRs) [104-106,110-112,125-127] but examples are found also in CSTR-mode [133-137]. Other immobilization solutions find large application like biocatalyst immobilization directly on reactor inner walls [138-140] or magnetic field assisted microreactors, a recent technique that exploits functionalized magnetic nanoparticles for enzyme retention which is gaining significant popularity [141-143]. Few works report also the preparation of immobilized enzyme on monoliths, made of different materials, usually silica, that are directly inserted in the reactor [144]. Also the scales can be different: usually meso-scale reactors are the most common choice [104-106,110-112,124,125], but also microreactors are often found [113,117,145,146]. An emerging configuration for enzymatic reactions, which well fits continuous-

flow concept, is multiphase systems where the poor solubility of organic substrates in aqueous medium is overcomed by introducing a second non-aqueous phase, which can also determines an improvement in yield for near-equilibrium reactions by continuous *in situ* removal of the product. In this context, the small dimensions of the micro- and meso- reactors drastically increase the interfacial area between the phases thus causing a significant intensification in mass transfer resulting in reactor productivity [147,148].

General methods

The enzymes exploited for this work were either commercial and produced recombinantly in-house. For immobilization studies, OYE3 from *Saccharomyces cerevisiae* and GDH from *Bacillus megaterium* (employed for NAD(P)H recycling system) were prepared as His-tagged protein and purified on Ni-resins according to standard methods [149]. Conversely, the other enzymes found in the work are commercially available: the alcohol dehydrogenases were part of kit from Evoxx kit and the lipases, *Candida antarctica* lipase A and *Candida antarctica* lipase B (Novozym® 435), were purchased from Merck and Novozymes® as immobilized derivatives (adsorbed onto acrylic resins).

For OYE3 immobilization studies, two different techniques were explored: first, covalent binding of OYE3 on agarose after its derivatization using glycidol to glyoxyl agarose, then, immobilization *via* metal-coordination on a set of three commercial supports (EziG™ Opal, EziG™ Coral and EziG™ Amber) sold by EnginZyme AB®, Sweden.

All the continuous-flow reactions are referred to meso-scale reactors. Both continuously stirred systems (CSTR) and plug-flow reactors (PFR) were employed, according to the characteristics of the enzyme of interest and its most convenient flow implementation. Pumping and heating system was part of a commercial equipment sold by Vapourtec (E-Series Integrated Flow Chemistry system), provided with peristaltic pumps. For reactions performed in a PFR, a glass column (of an inner diameter of 6.6 mm and an adjustable length up to 15 cm) was used. For implementation of homogeneous enzymatic reaction under continuous conditions, a membrane reactor was chosen. This reactor consisted in an ultrafiltration chamber (63.5 mm i.d.) equipped with a magnetic stirrer that reduces the available volume from 20 mL (empty volume) to 12 mL (effective volume). The reactor was combined with regenerated cellulose membranes (63.5 mm i.d.) with a cut-off of 5 kDa. Continuous in-line extraction and phase separation was enabled by a commercial liquid-liquid separator (purchased from Zaiput Flow Technologies), employed in combination with hydrophobic OP-900 membranes from the same supplier. A last reactor configuration was used for continuously stirred flow reactions where a solid enzyme had to be dispersed in the reaction medium. A flat bottom, 3-necked, jacketed reactor (50 mL), with the mechanical stirrer inserted in the central neck was connected to the peristaltic pumps of the Vapourtec (one pump for flowing the solution from the reservoir into the reactor, the other for moving the liquid out) through the side necks. At the outlet of

the suction pump, suction solvent filter for HPLC was employed to prevent tube blocking from lipase beads.

References

[1] Vasic-Racki, D. "History of industrial biotransformations - dreams and realities". *Industrial Biotransformation*, 2nd edition, Wiley-VCH Verlag GmbH & Co., **2006**, pp. 1-36.

[2] Prescott, F. Spallanzani on spontaneous generation and digestion - life and works of Spallanzani. *Proc R. Soc. Med.* **1930**; *23*, 495-510.

[3] Armstrong, E.F. Enzymes: a discovery and its consequences. *Nature* **1933**, *131*, 535-537.

[4] Pasteur, L. Mémoir sur la fermentation de l'acide tartrique. *C.R. Acad. Sci.* **1858**, *46*, 615-618.

[5] Pasteur, L. Suite a une précédente communication sur les mycodermes; nouveau procéde industriel de fabrication du vinaigre. *Compt. Rend.* **1862**, *55*, 28-32.

[6] Kühne, W. Über das Verhalten verschiedener organisierter und sogenennter ungeformter Fermente. Über das Trypsin (enzyme das Pankreas). *Verhandlungen Des Naturhistorisch-Medicinischen Vereins Zu Heidelb* **1876**.

[7] Sumner, J.B. The isolation and crystallization of the enzyme urease. *J. Biol. Chem.* **1926**, *69*, 435-441.

[8] Fischer, E. Einfluss der Configuration auf die Wirkung der Enzyme. *Ber. Dtsch. Chem. Ges.* **1894**, *27*, 2985-2993.

[9] Michaelis, L.; Menten, M.L. The kinetics of invertin action. *Biochem. Z.* **1913**, *49*, 333-369.

[10] Weizmann, C. Improvements in the bacterial fermentation of carbohydrates and in bacterial cultures for the same. GB application 191504845, 3 June 1919.

[11] Cairns, T.C.; Nai, C.; Meyer, V. How a fungus shapes biotechnology: 100 years of *Aspergillus niger* research. *Fungal Biol. Biotechnol.* **2018**, *5*, 13.

[12] Martens, J.-H.; Barg, H.; Warren, M.J.; Jahn, D. Microbial production of vitamin B_{12}. *Appl. Microbiol. Biotechnol.* **2002**, *58*, 275-285.

[13] Neushul, P. Science, government and the mass production of penicillin. *J. Hist. Med. Allied Sci.* **1993**, *48*, 371-395.

[14] Miescher, F. Über die chemische Zusammensetzung der Eiterzellen. *Medicinisch-chemische Untersuchungen* **1871**, *4*, 441-460.

[15] Hershey, A.; Chase, M. Independent functions of viral protein and nucleic acid in growth of bacteriophage. *J. Gen. Physiol.* **1952**, *36*, 39-56.

[16] Watson, J.D.; Crick, F.H. Molecular structure of nucleic acids: a structure for deoxyribose nucleic acid. *Nature* **1953**, *171*, 737-738.

[17] Jackson, D.; Symons, R.; Berg, P. Biochemical method for inserting new genetic information into DNA of Simian Virus 40: circular SV40 DNA molecules containing lambda phage genes and the galactose operon of *Escherichia coli*. *PNAS USA* **1972**, *69*, 2904-2909.

[18] Saiki, R.K.; Scharf, S.; Faloona, F.; Mullis, K.B.; Horn, G.T.; Erlich, H.A.; Arnheim, N. Enzymatic amplification of beta-globin genomic sequences and restriction site analysis for diagnosis of sickle cell anemia. *Science* **1985**, *230*, 6-11.

[19] Chen, K.; Arnold, F. H. Tuning the activity of an enzyme for unusual environments: sequential random mutagenesis of subtilisin E for catalysis in dimethylformamide. *PNAS* **1993**, *90*, 5618-5622.

[20] Sheldon, R.A. "Biocatalysis and Green Chemistry". *Green Biocatalysis*, 1st edition, John Wiley & Sons, Inc., **2016,** pp. 1-15.

[21] Reetz, M.T. Lipases as practical biocatalysts. *Curr. Opin. Chem. Biol.* **2002**, *6*, 145-150.

[22] Sharma R., Chisti Y., Banerjee U.C. Production, purification, characterization, and applications of lipases. *Biotechnol. Adv.* **2001**, *19*, 627-662.

[23] Choudhury P., Bhunia B. Industrial application of lipase: a review. *Biopharm J.* **2015**, *1*, 41-47.

[24] Sarmah N., Revathi D., Sheelu G., Yamuna Rani K., Sridhar S., Mehtab V., Sumana C. Recent advances on sources and industrial applications of lipases. *Biotechnol. Prog.* **2018**, *34*, 1-28.

[25] Ansorge-Schumacher, M.B.; Thum, O. Immobilised lipases in the cosmetics industry. *Chem. Soc. Rev.* **2013**, *42*, 6475-6490.

[26] Verma, N.; Thakur, S. and Bhatt A.K. Microbial lipases: industrial applications and properties (a review). *Int. Res. J. Biological Sci.* **2012**, *1*, 88-92.

[27] Aravindan, R.; Anbumathi, P.; Viruthagiri, T. Lipase applications in food industry. *Indian J. Biotechnol.* **2007**, *6*, 141-158.

[28] Geoffry, K.; Achur, R.N. Screening and production of lipase from fungal organisms. *Biocatal. Agric. Biotechnol.* **2018**, *14*, 241-253.

[29] de Godoy Daiha, K.; Angeli, R.; Dias de Oliveira, S.; Volcan Almeida, R. Are lipases still important biocatalysts? A study of scientific publications and patents for technological forecasting. *PLoS ONE* **2015**, *10*, e0131624.

[30] Kroutil, W.; Mang, H.; Edegger, K.; Faber, K. Biocatalytic oxidation of primary and secondary alcohols. *Adv. Synth. Catal.* **2004**, *346*, 125-142.

[31] Holt, R.A.; Rigby, S.R. Process for microbial reduction producing 4(*S*)-hydroxy-6(*S*)methyl-thienopyran dervatives. U.S. Patent 5,580,764, 3 December 1996.

[32] Fogal, S.; Bergantino, E.; Motterle, R.; Castellin, A.; Arvotti, G. Process for the preparation of testosterone. U.S. Patent 8,592,178 B2, 26 November 2013.

[33] Toogood, H.S.; Gardiner, J.M.; Scrutton, N.S. Biocatalytic reductions and chemical versatility of the old yellow enzyme family of flavoprotein oxidoreductases. *ChemCatChem* **2010**, *2*, 892-914.

[34] von Leuenberger, H.G.W.; Boguth, W.; Widmer, E.; Zell, R. Synthese von optisch aktiven, naturlichen Carotinoiden und strukturell verwandten Naturprodukten. I. Synthese der chiralen Schlusselverbindung (4*R*, 6*R*) -4-Hydroxy -2,2,6 -trimethylcyclohexanon. *Helv. Chim. Acta* **1976**, *59*, 1832-1849.

[35] Tange, T.O.; Haerle, J.; Delegrange, F.; De Block, J.D.V.; Allan, R.C.; Berninger, P.F.; Folly, C.; Ravasio, D.A.; Labagnere, L.; Brianza, F.; Nielsen, C.A.F.; Hansen, J.; Weber, N.; Capewell, S.J. Production of citronellal and citronellol in recombinant hosts. WO 2018/069418 A2, 19 April 2018.

[36] Scrutton, N.S.; Toogood, H.S.; Gardiner, J. Biosynthetic mint. U.S. Patent 2016/02897.02 A1, 6 October 2016.

[37] Motterle, R.; Bergantino, E.; Robescu, M.S.; Niero, M.; Fogal, S. Process for the preparation of (*R*)-beta-angelica lactone from alpha-angelica lactone employing ene-reductases. E.P. Patent 3,450,567 B1, 4 September 2017.

[38] Sheldon, R.A. Enzyme immobilization: the quest for optimum performance. *Adv. Synth. Catal.* **2007**, *349*, 1289-1307.

[39] Spahn, C.; Minteer, S.D. Enzyme immobilization in biotechnology. *Recent Pat. Eng.* **2008**, *2*, 195-200.

[40] Homaei, A.A.; Sariri, R.; Vianello, F.; Stevanato, R. Enzyme immobilization: an update. *J. Chem. Biol.* **2013**, *6*, 185-205.

[41] Cantone, S.; Ferrario, V.; Corici, V.; Ebert, C.; Fattor, D.; Spizzo, P.; Gardossi, L. Efficient immobilisation of industrial biocatalysts: criteria and constraints for the selection of organic polymeric carriers and immobilisation methods. *Chem. Soc. Rev.* **2013**, *42*, 6262-6276.

[42] Nguyen, H.H.; Kim, M. An overview of techniques in enzyme immobilization. *Appl. Sci. Converg. Technol.* **2017**, *26*, 157-163.

[43] Zdarta, J.; Meyer, A.S.; Jesionowski, T.; Pinelo, M. A general overview of support materials for enzyme immobilization: characteristics, properties, practical utility. *Catalysts* **2018**, *8*, 92.

[44] Sheldon, R.A.; van Pelt, S. Enzyme immobilisation in biocatalysis: why, what and how. *Chem. Soc. Rev.* **2013**, *42*, 6223-6235.

[45] Basso, I.; Serban, S. Industrial applications of immobilized enzymes - A review. *Mol. Catal.* **2019**, *479*, 110607.

[46] DiCosimo, R.; McAuliffe, J.; Poulose, A.J.; Bohlmann, G. Industrial use of immobilized enzymes. *Chem. Soc. Rev.* **2013**, *42*, 6437.

[47] Chibata, I. Application of immobilized enzymes for asymmetric reactions V. 185 ACS Symposium Series (Ed.), Asymmetric React. Process. Chem., American Chemical Society (**1982**), 195-203.

[48] Cassimjee, K.E.; Kadow, M.; Wikmark, Y.; Svedendahl Humble, M.; Rothstein, M.L.; Rothstein, D.M.; Bäckvall, J.-E. A general protein purification and immobilization method on controlled porosity glass: biocatalytic applications. *Chem. Commun.* **2014**, *50*, 9134-9137.

[49] Böhmer, W.; Knaus, T.; Volkov, A.; Slot, T.K.; Shiju, N.R.; Cassimjee, K.E.; Mutti, F.G. Highly efficient production of chiral amines in batch and continuous flow by immobilized ω-transaminases on controlled porosity glass metal-ion affinity carrier. *J. Biotechnol.* **2019**, *291*, 52-62.

[50] Coloma, J.; Lugtenburg, T.; Afendi, M.; Lazzarotto, M.; Bracco, P.; Hagedoorn, P.-L.; Gardossi, L.; Hanefeld, U. Immobilization of *Arabidopsis thaliana* hydroxynitrile lyase (*At*HNL) on EziG Opal. *Catalysts* **2020**, *10*, 899.

[51] Zucca, P.; Fernandez-Lafuente, R.; Sanjust, E. Agarose and its derivatives as supports for enzyme immobilization. *Molecules* **2016**, *21*, 1577.

[52] Contente; M.L; Farris, S.; Tamborini, L.; Molinari, F.; Paradisi, F. Flow-based enzymatic synthesis of melatonin and other high value tryptamine derivatives: a five-minute intensified process. *Green Chem*. **2019**, *21*, 3263-3266.

[53] Guerrero, C.; Valdivia, F.; Ubilla, C.; Ramirez, N.; Gomez, M.; Aburto, C.; Vera, C.; Illanes, A. Continuous enzymatic synthesis of lactulose in packed-bed reactor with immobilized *Aspergillus oryzae* β-galactosidase. *Bioresour. Technol.* **2019**, *278*, 296-302.

[54] Fernandes, P.; de Carvalho, C.C.C.R. Multi-enzyme systems in flow chemistry. *Processes* **2021**, *9*, 225.

[55] Hills, R.L. Sir Richard Arkwright and his patent granted in 1769. *Notes Rec. R. Soc. Lond.* **1970**, *24*, 254-260.

[56] Sellers Jr., C. Oliver Evans and his inventions. *J. Franklin Inst.* **1886**, *122*, 1-16.

[57] Murty, K.G. "History of crude oil refining". *Models for Optimum Decision Making*, 1st edition, Springer, **2020**, pp 1-8.

[58] Fridenson, P. "The coming of the assembly line to Europe*". The Dynamics of Science and Technology*, 1st edition, **1978**, Springer pp 159-175.

[59] Leigh, G. J. Haber-Bosch and other industrial processes. *Catalysts for Nitrogen Fixation*, 1st edition, **2004**, Springer, pp 33-54.

[60] Fogler, H.S. *Elements of Chemical Reaction Engineering*, 6th edition, **2020**, Pearson Education (US).

[61] Homberger, E.; Reggiani, G.; Sambeth, J.; Wipf, H. K. The Seveso accident: its nature, extent and consequences. *Ann. Occup. Hyg. Pergamon Press* **1979**, *22*, 327-370.

[62] Gustin, J.-L. How the study of accident case histories can prevent runaway reaction accidents to occur again. *Process. Saf. Environ. Prot.* **2002**, *80*, 16-24.

[63] Yao, X.; Zhang, Y.; Du, L.; Liu, J.; Yao, J. Review of the applications of microreactors. *Renew. Sustain. Energy Rev.* **2015**, *47*, 519-539.

[64] Wegner, J.; Ceylan, S.; Kirschning, A. Ten key issues in modern flow chemistry. *Chem. Commun*. **2011**, *47*, 4583-4592.

[65] Malet-Sanz, L.; Susanne, F. Continuous flow synthesis. A pharma perspective. *J. Med. Chem.* **2012**, *55*, 4062-4098.

[66] Jensen, K.F. Flow chemistry - Microreaction technology comes of age. *AIChE J.* **2017**, *63*, 858-869.

[67] Wheeler, R.C.; Benali, O.; Deal, M.; Farrant, E.; MacDonald, S.J.F.; Warrington, B.H. Mesoscale flow chemistry: a plug-flow approach to reaction optimization. *Org. Process Res. Dev*. **2007**, *11*, 704-710.

[68] Styring, P.; Parracho, A.I.R. From discovery to production: scale-out of continuous flow meso reactors. *Beilstein J. Org. Chem.* **2009**, *5*, 1-10.

[69] Jovanovic, G.N.; Coblyn, M.Y.; Plazl, I. Time scale analysis & characteristic times in microscale-based chemical and biochemical processes: Part I - Concepts and origins. *Chem. Eng. Sci.* **2021**, *238*, 116502.

[70] Jovanovic, G.N.; Coblyn, M.Y.; Plazl, I. Time scale analysis & characteristic times in microscale-based bio-chemical processes: Part II - Bioreactors with immobilized cells, and process flowsheet analysis. *Chem. Eng. Sci.* **2021**, *236*, 116499.

[71] Yang, L.; Nieves-Remacha, M.J.; Jensen, K.F. Simulations and analysis of multiphase transport and reaction in segmented flow microreactors. *Chem. Eng. Sci.* **2017**, *169*, 106-116.

[72] Wolfrum, C.; Josten, A.; Götz, P. Optimization and scale-up of oligonucleotide synthesis in packed bed reactors using computational fluid dynamics modeling. *Biotechnol. Prog.* **2014**, *30*, 1048-1056.

[73] Bodla, V.K.; Seerup, R.; Krühne, U.; Woodley, J.M.; Gernaey, K.V. Microreactors and CFD as tools for biocatalysis reactor design: a case study. *Chem. Eng. Technol.* **2013**, *36*, 1017-1026.

[74] Vicente, F.A.; Plazl, I.; Ventura, S.P.M.; Žnidaršič-Plazl, P. Separation and purification of biomacromolecules based on microfluidics. *Green Chem.* **2020**, *22*, 4391-4410.

[75] Strniša, F.; Žnidaršič-Plazl, P.; Plazl, I. Lattice Boltzmann modeling-based design of a membrane-free liquid-liquid microseparator. *Chem. Biochem. Eng. Q.* **2020**, *34*, 73-78.

[76] Pamme, N. Continuous flow separations in microfluidic devices. *Lab Chip* **2007**, *7*, 1644-1659.

[77] O'Brien, M.; Koos, P.; Browne, D.L.; Ley, S.V. A prototype continuous-flow liquid-liquid extraction system using open-source technology. *Org. Biomol. Chem.* **2012**, *10*, 7031-7036.

[78] Adamo, A.; Beingessner, R.L.; Behnam, M.; Chen, J.; Jamison, T.F.; Jensen, K.F.; Monbaliu, J.C.M.; Myerson, A.S.; Revalor, E.M.; Snead, D.R.; Stelzer, T.; Weeranoppanant, N.; Wong, S.Y.; Zhang, P. On-demand continuous-flow production of pharmaceuticals in a compact, reconfigurable system. *Science* **2016**, *352*, 61-67.

[79] Johnson, M.D.; May, S.A.; Haeberle, B.; Lambertus, G.R.; Pulley, S.R.; Stout, J.R. Design and comparison of tubular and pipes-in-series continuous reactors for direct asymmetric reductive amination. *Org Process Res. Dev.* **2016**, *20*, 1305-1320.

[80] Adamo, A.; Heider, P.L.; Weeranoppanant, N.; Jensen, K.F. Membrane-based, liquid-liquid separator with integrated pressure control. *Ind. Eng. Chem. Res.* **2013**, *52*, 10802-10808.

[81] Peeva, L.; Da Silva Burgal, J.; Heckenast, Z.; Brazy, F.; Cazenave. F.; Livingston, A. Continuous consecutive reactions with inter-reaction solvent exchange by membrane separation. *Angew. Chem. Int. Ed.* **2016**, *55*, 13576-13579.

[82] Britton, J.; Raston, C.L. Multi-step continuous-flow synthesis. *Chem. Soc. Rev.* **2017**, *46*, 1250-1271.

[83] Lam, K.F.; Cao, E.; Sorensen, E., Gavriilidis, A. Development of multistage distillation in a microfluidic chip. *Lab Chip* **2011**, *11*, 1311-1317.

[84] Ziogas, A; Cominos, V.; Kolb, G.; Kost, H.J.; Werner, B.; Hessel, V. Development of a microrectification apparatus for analytical and preparative applications. *Chem. Eng. Technol.* **2012**, *35*, 58-71.

[85] Baxendale, I.R.; Storer, R.I.; Ley, S.V. "Supported reagents and scavengers in multi-step organic synthesis". *Polymeric Materials in Organic Synthesis and Catalysis*, 1st edition, Wiley-VCH Verlag GmbH & Co., **2003**, pp 53-136.

[86] Mo, Y.; Jensen, K.F. A miniature CSTR cascade for continuous flow of reactions containing solids. *React. Chem. Eng.* **2016**, *5*, 501-507.

[87] Liedtke, A.-K.; Bornette, F.; Philippe, R.; de Bellefon, C. External liquid solid mass transfer for solid particles transported in a milli-channel within a gas-liquid segmented flow. *Chem. Eng. J.* **2016**, *287*, 92-102.

[88] Ley, S.V.; Fitzpatrick, D.E.; Ingham, R.J.; Myers, R.M. Organic synthesis: march of the machines. *Angew. Chemie Int. Ed.* **2015**, *54*, 3449-3464.

[89] Moore, J.S.; Smith, C.D.; Jensen, K.F. Kinetics analysis and automated online screening of aminocarbonylation of aryl halides in flow. *React. Chem. Eng.* **2016**, *1*, 272-279.

[90] Ghislieri, D.; Gilmore, K.; Seeberger, P.H. Chemical assembly systems: layered control for divergent, continuous, multistep syntheses of active pharmaceutical ingredients. *Angew. Chemie Int. Ed.* **2015**, *54*, 678-682.

[91] Baxendale, I.R.; Deeley, J.; Griffiths-Jones, C.M.; Ley, S.V.; Saaby, S. Tranmer, G.K. A flow process for the multi-step synthesis of the alkaloid natural product oxomaritidine: a new paradigm for molecular assembly. *Chem. Commun.* **2006**, 2566-2568.

[92] Fuse, S.; Tanabe, N.; Takahashi, T. Continuous *in situ* generation and reaction of phosgene in a microflow system. *Chem. Commun.* **2011**, *47*, 12661-12663.

[93] Nagaki, A.; Kim, H.; Yoshida, J.-i. Aryllithium compounds bearing alkoxycarbonyl groups: generation and reactions using a microflow system. *Angew. Chem. Int. Ed.* **2008**, *47*, 7833-7836.

[94] Nagaki, A.; Kim, H.; Usutani, H.; Matsuo, C.; Yoshida, J.-i. Generation and reaction of cyano-substituted aryllithium compounds using microreactors. *Org. Biomol. Chem.***2010**, ***8***, 1212-1217.

[95] Schaber, S.D.; Gerogiorgis, D.I.; Ramachandran, R.; Evans, J.M.B.; Barton, P.I.; Trout, B.L. Economic Analysis of integrated continuous and batch pharmaceutical manufacturing: a case study. *Ind. Eng. Chem. Res.* **2011**, *50*, 10083-10092.

[96] Krtschil, U.; Hessel, V.; Kralisch, D.; Kreisel, G.; Küpper, M.; Schenk, R. Cost analysis of a commercial manufacturing process of a fine chemical compound using micro process engineering. *Chimia* **2006**, *60*, 611-617.

[97] Grimaldi, F.; de Leon Izeppi, G.A.; Kirschneck, D.; Lettieri, P.; Escribà-Gelonch, M. Hessel, V. Life cycle assessment and cost evaluation of emerging technologies at early stages: the case of continuous flow synthesis of Rufinamide. *J. Adv. Manuf. Process.* **2020,** *2*, e10043.

[98] Pashkova, A.; Greiner, L. Towards Small-scale continuous chemical production: technology gaps and challenges. *Chem. Ing. Tech.* **2011**, *83*, 1337-1342.

[99] Pollington, S. 10th International symposium on continuous flow reactor technology for industrial applications. *Johnson Matthey Technol. Rev*., **2019**, *63*, 157-165.

[100] Pichon, L. Flow chemistry: analysis of market trends sightseeing by skilled flow chemists. *Chem. Today* **2016**, *34*, 14.

[101] Žnidaršič-Plazl, P. Biocatalytic process intensification via efficient biocatalyst immobilization, miniaturization, and process integration. Curr. *Opin. Green Sustain. Chem.* **2021**, *32*, 100546.

[102] Bolivar, J.M.; López-Gallego, F. Characterization and evaluation of immobilized enzymes for applications in flow reactors. *Curr. Opin. Green Sustain. Chem.* **2020**, *25*, 100349.

[103] Woodley, J.M. Advances in biological conversion technologies: new opportunities for reaction engineering. *React. Chem. Eng.* **2020**, *5*, 632-640.

[104] Woodcock, L.L.; Wiles, C.; Greenway, G.M.; Watts, P.; Wells, A.; Eyley, S. Enzymatic synthesis of a series of alkyl esters using novozyme 435 in a packed-bed, miniaturized, continuous flow reactor. *Biocatal. Biotransfor*. **2008**, *26*, 501-507.

[105] Wang, J.; Gu, S.-S; Cui, H.-S.; Wu, X.-Y.; Wu, F.-A. A novel continuous flow biosynthesis of caffeic acid phenethyl ester from alkyl caffeate and phenethanol in a packed bed microreactor. *Bioresour. Technol.* **2014**, *158*, 39-47.

[106] Hugentobler, K.G.; Rasparini, M.; Thompson, L.A.; Jolley, K.E.; Blacker, A.J.; Turner, N.J. Comparison of a batch and flow approach for the lipase-catalyzed resolution of a cyclopropanecarboxylate ester, a key building block for the synthesis of Ticagrelor. *Org. Process Res. Dev.* **2017**, *21*, 195-199.

[107] Thompson, M.P.; Peñafiel, I.; Cosgrove, S.C.; Turner, N.J. Biocatalysis using immobilized enzymes in continuous flow for the synthesis of fine chemicals. *Org. Process Res. Dev.* **2019**, *23*, 9-18.

[108] Žnidaršič-Plazl, P. The promises and the challenges of biotransformations in microflow. *Biotechnol. J.* **2019**, *14*, 1800580.

[109] Tamborini, L.; Fernandes, P.; Paradisi, F.; Molinari, F. Flow bioreactors as complementary tools for biocatalytic process intensification. *Trends Biotechnol.* **2018**, *36*, 73-88.

[110] Baxendale, I.R.; Griffiths-Jones, C.M.; Ley, S.V.; Tranmer, G.K. Preparation of the neolignan natural product grossamide by a continuous-flow process. *Synlett* **2006**, *3*, 427-430.

[111] Farkas, E.; Oláh, M.; Földi, A.; Kóti, J.; Eles. J.; Nagy, J.; Gal, C.A.; Paizs, C.; Hornyánszky, G.; Poppe, L. Chemoenzymatic dynamic kinetic resolution of amines in fully continuous-flow mode. *Org. Lett.* **2018**, *20*, 8052-8056.

[112] De Vitis, V.; Dall'Oglio, F.; Pinto, A.; De Micheli, C.; Molinari, F.; Conti, P.; Romano, D.; Tamborini, L. Chemoenzymatic synthesis in flow reactors: a rapid and convenient preparation of Captopril. *ChemistryOpen* **2017**, *6*, 668-673.

[113] Delville, M.M.E., Koch, K; van Hest, J.C.M.; Rutjes, F.P.J.T. Chemoenzymatic flow cascade for the synthesis of protected mandelonitrile derivatives. *Org. Biomol. Chem.* **2015**, *13*, 1634-1638.

[114] Bracco, P.; Busch, H.; von Langermann, J.; Hanefeld, H. Enantioselective synthesis of cyanohydrins catalysed by hydroxynitrile lyases - a review. *Org. Biomol. Chem*. **2016**, *14*, 6375-6389.

[115] Brahma, A.; Musio, B.; Ismayilova, U.; Nikbin, N.; Kamptmann, S.B.; Siegert, P.; Jeromin, G.E.; Ley, S.V.; Pohl, M. An orthogonal biocatalytic approach for the safe generation and use of HCN in a multistep continuous preparation of chiral o-acetylcyanohydrins. *Synlett* **2016**, *27*, 262-266.

[116] Rüsch gen.Klaas, M.; Warwel, S. Lipase-catalyzed preparation of peroxy acids and their use for epoxidation. *J. Mol. Catal. A Chem.* **1997**, *117*, 311-319.

[117] Mashhadi, F.; Habibi, A.; Varmira, K. Enzymatic production of green epoxides from fatty acids present in soapstock in a microchannel bioreactor. *Ind. Crops Prod.* **2018**, *113*, 324-334.

[118] Gumel, A.M; Annuar, M.S.M. *Thermomyces lanuginosus* lipase-catalyzed synthesis of natural flavor esters in a continuous flow microreactor. *3 Biotech* **2016**, *6*, 24.

[119] Karande, R.; Schmid, A.; Buehler, K. Applications of multiphasic microreactors for biocatalytic reactions. *Org. Process Res. Dev.* **2016**, *20*, 361-370.

[120] Valinger, D.; Vrsalović Presečki, A.; Kurtanjek, Z.; Pohl, M.; Blažević, Z.F.; Vasić-Rački, D. Continuous enzymatic carboligation of benzaldehyde and acetaldehyde in an enzyme ultrafiltration membrane reactor and laminar flow microreactors. *J. Mol. Catal. B Enzym.* **2014**, *102*, 132-137.

[121] Wichmann, R.; Wandrey, C.; Bückmann, A.F.; Kula, M.-R. Continuous enzymatic transformation in an enzyme membrane reactor with simultaneous NAD(H) regeneration. *Biotechnol. Bioeng.* **1981**, *23*, 2789-2802.

[122] Vladisavljević, G.T. "Biocatalytic membrane reactors". *Catalytic reactors*, 1st edition, Walter de Gruyter GmbH, **2015**, pp 51-102.

[123] Ho, C.-H.; Yi, J.; Wang, X. Biocatalytic continuous manufacturing of diabetes drug: plantwide process modeling, optimization, and environmental and economic analysis. *ACS Sustain. Chem. Eng.* **2019**, *7*, 1038-1051.

[124] Chapman, M.R.; Cosgrove, S.C.; Turner, N.J.; Kapur, N.; Blacker, A.J. Highly productive oxidative biocatalysis in continuous flow by enhancing the aqueous equilibrium solubility of oxygen. *Angew. Chem. Int. Ed.* **2018**, *57*, 10535-10539.

[125] Dall'Oglio, F.; Contente, M.L.; Conti, P.; Molinari, F.; Monfredi, D.; Pinto, A.; Romano, D.; Ubiali, D.; Tamborini, L.; Serra, I. Flow-based stereoselective reduction of ketones using an immobilized ketoreductase/glucose dehydrogenase mixed bed system. *Catal. Commun.* **2017**, *93*, 29-32.

[126] Contente, M.L.; Farris, S.; Tamborini, L.; Molinari, F.; Paradisi, F. Flow-based enzymatic synthesis of melatonin and other high value tryptamine derivatives: a five-minute intensified process. *Green Chem.* **2019**, *21*, 3263-3266.

[127] Padrosa, D.R.; De Vitis, V.; Contente, M.L.; Molinari, F.; Paradisi, F. Overcoming water insolubility in flow: enantioselective hydrolysis of naproxen ester. *Catalysts* **2019**, *9*, 232.

[128] Guajardo, N.; Rodrigo, A.S.; de Maríac, P.D. From batch to fed-batch and to continuous packed-bed reactors: lipase-catalyzed esterifications in low viscous deep-eutectic-solvents with buffer as cosolvent. *Bioresour. Technol.* **2019**, *273*, 320-325.

[129] Silva, M.V.M.; Bassut, J.F.; Junior, I.I.; de Souza, S.P.; Estrada, M.L.G.; Miranda, L.S.M.; de Souza, R.O.M.A. Lipase immobilization towards improved productivity on kinetic resolutions by a continuous-flow process. *RSC Adv.* **2015**, *5*, 102409-102415.

[130] Cipolatti, E.P.; Pinto, M.C.C.; Robert, J.deM.; da Silva, T.P.; Beralto, T.daC.; Santos Jr., J.G. F.; de Castro, R.deP.V.; Fernandez-Lafuente, R.; Manoel, E.A.; Pinto, J.C.; Freire, D.M.G. Pilot-scale development of core-shell polymer supports for the immobilization of recombinant lipase B from *Candida Antarctica* and their application in the production of ethyl esters from residual fatty acids. *J. Appl. Polym. Sci.* **2018**, *135*, 46727.

[131] Thompson, M.P.; Derrington, S.R.; Heath, R.S.; Porter, J.L.; Mangas-Sanchez, J.; Devine, P.N.; Truppo, M.D.; Turner, N.J. A generic platform for the immobilisation of engineered biocatalysts. *Tetrahedron* **2019**, *75*, 327-334.

[132] Valikhani, D.; Srivastava, P.L.; Allemann, R.K.; Wirth, T. Immobilised enzymes for sesquiterpene synthesis in batch and flow systems. *ChemCatChem* **2020**, *12*, 2194-2197.

[133] Sperl, J.M.; Carsten, J.M.; Guterl, J.-K.; Lommes, P.; Sieber, V. Reaction design for the compartmented combination of heterogeneous and enzyme catalysis. *ACS Catal.* **2016**, *6*, 6329-6334.

[134] Ubilla, C.; Ramírez, N.; Valdivia, F.; Vera, C.; Illanes, A.; Guerrero, C. Synthesis of lactulose in continuous stirred tank reactor with β-galactosidase of *Apergillus oryzae* immobilized in monofunctional glyoxyl agarose support. *Front. Bioeng. Biotechnol.* **2020**, *8*, 1-14.

[135] Rakmai, J.; Cheirsilp, B. Continuous production of β-cyclodextrin by cyclodextrin glycosyltransferase immobilized in mixed gel beads: comparative study in continuous stirred tank reactor and packed bed reactor. *Biochem. Eng. J.* **2016**, *105*, 107-113.

[136] Fidalgo, W.R.R.; Ceron, A.; Freitas, L.; Santos, J.C.; de Castro, H.F. A fluidized bed reactor as an approach to enzymatic biodiesel production in a process with simultaneous glycerol removal. *J. Ind. Eng. Chem.* **2016**, *38*, 217-223.

[137] Meyer, J.; Horst, A.E.W.; Steinhagen, M.; Holtmann, D.; Ansorge-Schumacher, M.B.; Kraume, M.; Drews, A. A continuous single organic phase processfor the lipase catalyzed synthesis of peroxyacids increases productivity. *Eng. Life Sci.* **2017**, *17*, 759-767.

[138] Valikhani, D.; Bolivar, J.M.; Pfeiffer, M.; Nidetzky, B. Multivalency effects on the immobilization of sucrose phosphorylase in flow microchannels and their use in the development of a high-performance biocatalytic microreactor. *ChemCatChem* **2017**, *9*, 161-166.

[139] Miložič, N; Lubej, M; Lakner, M; Žnidaršič-Plazl, P.; Plazl, I. Theoretical and experimental study of enzyme kinetics in a microreactor system with surface-immobilized biocatalyst. *Chem. Eng. J.* **2017**, *313*, 374-381.

[140] Bolivar, J.M.; Valikhani, D.; Nidetzky, B. Demystifying the flow: biocatalytic reaction intensification in microstructured enzyme reactors. *Biotechnol. J.* **2019**, *14*, 1800244.

[141] Peschke, T.; Bitterwolf, P.; Rabe, K.S.; Niemeyer, C.M. Self-immobilizing oxidoreductases for flow biocatalysis in miniaturized packed-bed reactors. *Chem. Eng. Technol.* **2019**, *42*, 2009-2017.

[142] Zheng, D.; Wang, S.; Qiu, S.; Lin, J.; Diao, X. Synthesis of butyl oleate catalyzed by cross-linked enzyme aggregates with magnetic nanoparticles in rotating magneto-micro-reactor. *J. Biotechnol.* **2018**, *281*, 123-129.

[143] Gebreyohannes, A.Y.; Bilad, M.R.; Verbiest, T.; Courtin, C.M.; Dornez, E.; Giorno, L.; Curcio, E.; Vankelecom, I.F.J. Nanoscale tuning of enzyme localization for enhanced reactor performance in a novel magnetic-responsive biocatalytic membrane reactor. *J. Membr. Sci.* **2015**, *487*, 209-220.

[144] Rinaldi, F.; Fernández-Lucas, J.; de la Fuente, D.; Zheng, C.; Bavaro, T.; Peters, B.; Massolini, G.; Annunziata, F.; Conti, P.; de la Mata, I.; Terreni, M.; Calleri, E. Immobilized enzyme reactors based on nucleoside phosphorylases and 2′-deoxyribosyltransferase for the in-flow synthesis of pharmaceutically relevant nucleoside analogues. *Bioresour. Technol.* **2020**, *307*, 123258.

[145] Bajić, M.; Plazl, I.; Stloukal, R.; Žnidaršič-Plazl, P. Development of a miniaturized packed bed reactor with ω-transaminase immobilized in LentiKats®. *Process Biochem.* **2017**, *52*, 63-72.

[146] Miložič, N.; Stojkovič, G.; Vogel, A.; Bouwes, D.; Žnidaršič-Plazl, P. Development of microreactors with surface-immobilized biocatalysts for continuous transamination. *New Biotechnol.* **2018**, *47*, 18-24.

[147] Žnidaršič-Plazl, P. Enzymatic microreactors utilizing non-aqueous media. *Chem. Today* **2014**, *32*, 54-60.

[148] Bolivar, J.M.; Nidetzky, B. Multiphase biotransformations in microstructured reactors: opportunities for biocatalytic process intensification and smart flow processing. *Green Proc. Synth.* **2013**, *2*, 541.

[149] Brenna, E.; Gatti, F.G.; Monti, D.; Parmeggiani, F.; Sacchetti, A. cascade coupling of ene reductases with alcohol dehydrogenases: enantioselective reduction of prochiral unsaturated aldehydes. *ChemCatChem* **2012**, *4*, 653-659.

Chapter 1

Biocatalytic approach to chiral β-nitroalcohols by enantioselective alcohol dehydrogenase-mediated reduction of α-nitroketones

Francesca Tentori [1], Elisabetta Brenna [1,2], Danilo Colombo [1], Michele Crotti [1], Francesco G. Gatti [1], Maria Chiara Ghezzi [1] and Giuseppe Pedrocchi-Fantoni [2]

[1] Politecnico di Milano, Dipartimento di Chimica, Materiali e Ingegneria Chimica, via Mancinelli 7, Milano I-20131, Italy.

[2] Istituto di Chimica del Riconoscimento Molecolare - CNR, via Mancinelli 7, Milano I-20131, Italy.

Published in *Catalysts* **2018**, *8*, 308

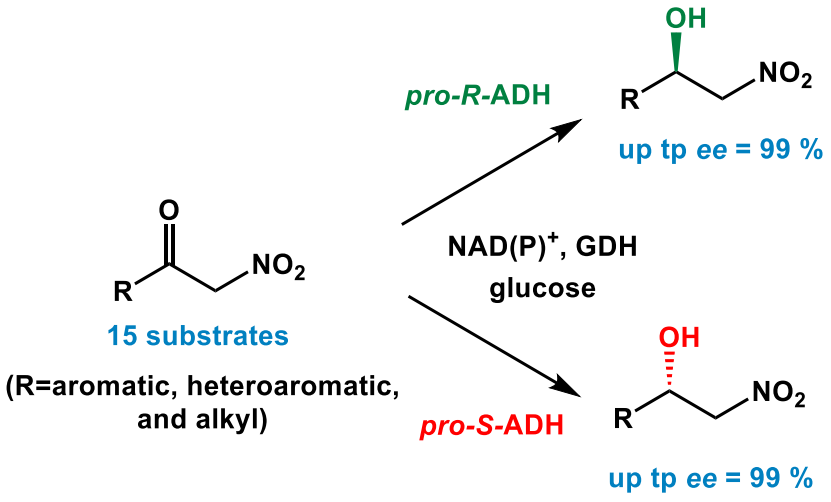

Introduction

Chiral β-nitroalcohols **1** (Scheme 1) are relevant synthetic targets in organic chemistry. They are employed as key intermediates for the preparation of a wide range of biologically active natural products and active pharmaceutical ingredients [1-5], especially because they can be readily converted into chiral β-aminoalcohols **2** by reduction of the nitro moiety.

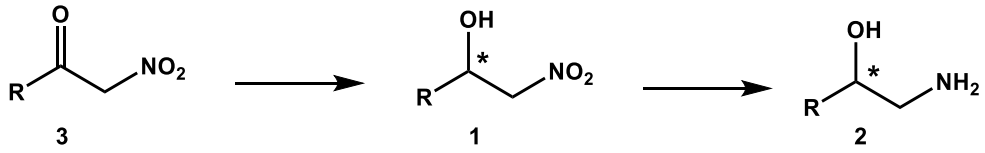

Scheme 1. Synthesis of β-amminoalcohols **2** through β-nitroalcohols **1** as intermediates.

The most common approach to compounds **1** is represented by the enantioselective Henry (nitroaldol) reaction between aldehydes and nitromethane, which is catalyzed by metal complexes or organocatalysts [1,6-16]. During the past decade, the search for greener and more sustainable synthetic procedures has promoted the investigation of biocatalyzed strategies for the synthesis of enantiopure β-nitroalcohols [17]. Several examples of kinetic resolution of racemic compounds **1** catalyzed by hydrolases have been reported in the literature [7]. It has also been discovered that some hydroxynitrile are able to promote the enantioselective addition of nitromethane to aldehydes, such as the (*S*)- selective HNLs from *Hevea brasiliensis* and from *Manihot esculenta* [18-20], and the (*R*)-selective HNLs from *Arabidopsis thaliana* [21], *Acidobacterium capsulatum*, and *Granulicella tundricula* [22]. These reactions are generally characterized by long reaction times, and strong substrate dependence. Another possible enzymatic approach, which has received scarce consideration until now, is represented by the bioreduction of α-nitroketones **3**. Only a few papers on this topic are present in the literature. In 1987 [23], the baker's yeast reduction of 3-methyl-3-nitro-2-butanone to the (*S*)- enantiomer of corresponding alcohol (enantiomeric excess = *ee* > 96%) in 57% yield was described. A few years later, Moran *et al.* [24] investigated the reduction of α-nitroacetophenone (**3a**. R = Ph) in fermenting baker's yeast. Only 6% of nitroalcohol **1a** (R = Ph) could be isolated, with benzoic acid being the main product of the biotransformation (27%). According to the authors, the formation of benzoic acid was due to the retro-Henry degradation of nitroalcohol **1a** to benzaldehyde,

followed by oxidation. In 2008, Kroutil *et al*. [25] reported on the conversion of 1-nitro-3-phenylpropan-2-one and 1-nitro-2-octanone into the enantiopure (*S*)-nitroalcohols in 47% and 75% yield, respectively, by using the lyophilized cells of *Comomonas testoteroni*. Recently [26], the whole cells of *Candida parapsilosis* ATCC 7330 were employed to catalyze the enantioselective reduction of some aliphatic derivatives **3** (only R = alkyl) in water with ethanol as a cosolvent, at room temperature, and in 4 h reaction time (conversion yields 54-76%, *e*e = 8.2-81%). The formation of the (*R*) or (*S*) enantiomer of the corresponding nitroalcohol depended upon the nature of the R group. The scarcity of experimental data on the bioreduction of α-nitroketones, especially for aromatic derivatives, and the current need for biocatalyzed synthesis of chiral building blocks for pharmaceutical applications [27-31] led us to investigate the use of commercial alcohol dehydrogenases for the enantioselective reduction of aryl and alkyl α-nitroketones **3** in controlled reaction conditions. We also studied the further manipulation of specific nitroalcohols **1** to prepare aminoalcohols **2**, which have been already employed as key intermediates for the synthesis of active pharmaceutical ingredients, such as levamisole and (*R*)-tembamide.

Results and Discussion

*Synthesis of Nitroketones 3 and Biocatalyzed Reduction to Derivatives **1***

Nitroketones **3a-o** (Scheme 2) were synthesized according to the literature by derivatization of the corresponding carboxylic acids with carbonyldiimidazole, followed by reaction with the sodium salt of nitromethane, which was obtained in turn by deprotonation of nitromethane with NaH [32].

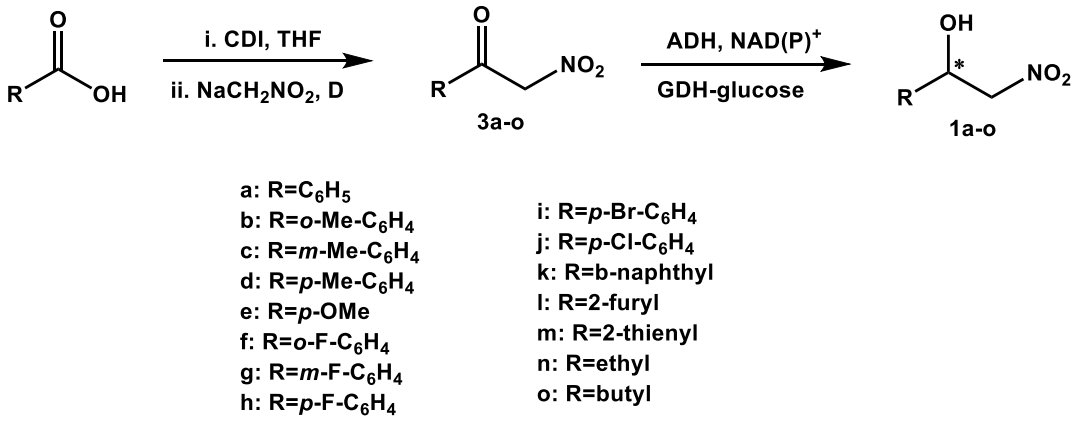

Scheme 2. Synthesis and biocatalyzed reduction of nitroketones **3a-o**.

Before starting the alcohol dehydrogenases (ADH) screening, the stability of derivatives **1** was investigated in buffer solutions at pH = 5, 7, and 9 for 4-18 h at 25 °C, using compound **1a** as a model and DMSO as a co-solvent. As expected, nitroalcohol **1a** resulted to be unstable towards retro-Henry reaction in basic and neutral medium: conversion into benzaldehyde was complete at pH = 7 and 9 after 18 h. At pH = 5 no benzaldehyde was observed. Thus, pH = 5 was selected for the investigation of the biocatalyzed reduction of compound **3a**, using a panel of 18 commercial alcohol dehydrogenases (from Evoxx). The catalytic NADPH or NADH cofactor was recycled with glucose dehydrogenase (GDH from *Bacillus megaterium*), and glucose was employed as a sacrificial co-substrate. The reactions were performed in acetate buffer solution (pH = 5) with 1% DMSO, monitored by TLC, and usually stopped after 4-5 h. The results of the screening experiments are collected in Table S1 (see Supplementary Information in Appendix *Chapter 1*). Conversion were evaluated by ^{1}H NMR spectroscopy and the enantiomeric excess values of the reduced products were determined by HPLC analysis on a chiral stationary phase. GC-analysis could not be used because

nitroalcohol **1a** undergoes partial thermal degradation to benzaldehyde. During this screening, benzaldehyde was never detected in the final reaction mixture, while the formation of benzoic acid was observed in a variable amount: from 4-6% in the most effective reductions of **3a** with ADH270 and 440, to nearly 30% in those reactions in which no nitroalcohol was formed. In order to explain the formation of benzoic acid, the stability of compound **3a** was investigated in buffer solution (pH = 5), in the presence of 1% DMSO, GDH, $NAD(P)^+$, without adding the ADH, for 4 and 18 h at 25 ◦C. Partial degradation (35%) to the carboxylic acid was observed after 4 h, while the complete conversion into benzoic acid was achieved after 18 h. A search in the literature showed that Pearson *et al.* [33] had described the hydrolytic cleavage of nitroketone **3a** to the corresponding carboxylic acid in dioxane-water solution and the possibility to suppress this side-reaction only in strong mineral acid solution. In the evaluation of the molar percentages of the reduced product **1a** reported in Table S1 (see Supplementary Information in Appendix *Chapter 1*) as calculated by ^{1}H NMR analysis of the final mixture, the formation of the carboxylic acid was taken into account. The integrals of the following well-separated signals were employed: (i) the doublet of doublets of the CH-OH of **1a** (one hydrogen atom); (ii) the singlet of the CH_2 of **3a** (two hydrogen atoms); and, (iii) the doublet of the two aromatic hydrogen atoms adjacent to the COOH group of benzoic acid. Only eight of the eighteen screened ADHs could catalyze the reduction of nitroketone **3a**. Prolonged reaction times did not improve the yield in the reduction product, instead promoted the extensive hydrolysis of unreacted starting **3a**. The ADHs giving the best results in terms of both conversion and enantioselectivity, *i.e.*, ADH270, 440 and 441, were employed to investigate the reduction of the whole set of nitroketones **3b-o**. The results are reported in Figure 1 and Table S2 (see Supplementary Information in Appendix *Chapter 1*). The absolute configuration of all the nitroalcohols **1a-o** could be established by a comparison of the corresponding HPLC analyses on chiral stationary phase with those reported in the literature in the same experimental conditions (see Supplementary Information in Appendix *Chapter 1*). (*R*)-Nitroalcohols were invariably obtained in the presence of ADH440, while opposite enantioselectivity were observed with either ADH270 or ADH441. In the reduction of 2-furyl and 2-thienyl derivatives **3l** and **3m**, obtaining the (*S*)-nitroalcohol with ADH440 and the (*R*)-enantiomer with ADH270, and 441 does not represent an inversion of enantioselectivity with respect to the reductions of the other substrates. It is a consequence of the fact that the priority order of the substituents around the stereogenic centre is different for the presence of the heteroaromatic ring. The only real inversions of configuration were observed in the reduction of **3f** (R = o-F-C_6H_4) and **3n** (R = ethyl) with ADH441 and 270, respectively, affording the corresponding (*R*)-enantiomers with *ee* =

43 and 80%. The best results were achieved while using ADH440 as a catalyst (Figure 1). This enzyme promoted the conversion of nitroketones **3** into the (*R*)-enantiomer of nitroalcohols **1** with high yields (c = 79-99%) and very good *ee* values in the range 92-99% for most of the substrates. Enantioselectivity that was slightly lower 90% was observed in the quantitative reduction of **3c** (R = m-Me-C_6H_4, *ee* = 84%) and **3l** (R = 2-furyl, *ee* = 71%). Only in the case of ethyl derivative **3n**, the corresponding reduced product was obtained in racemic form.

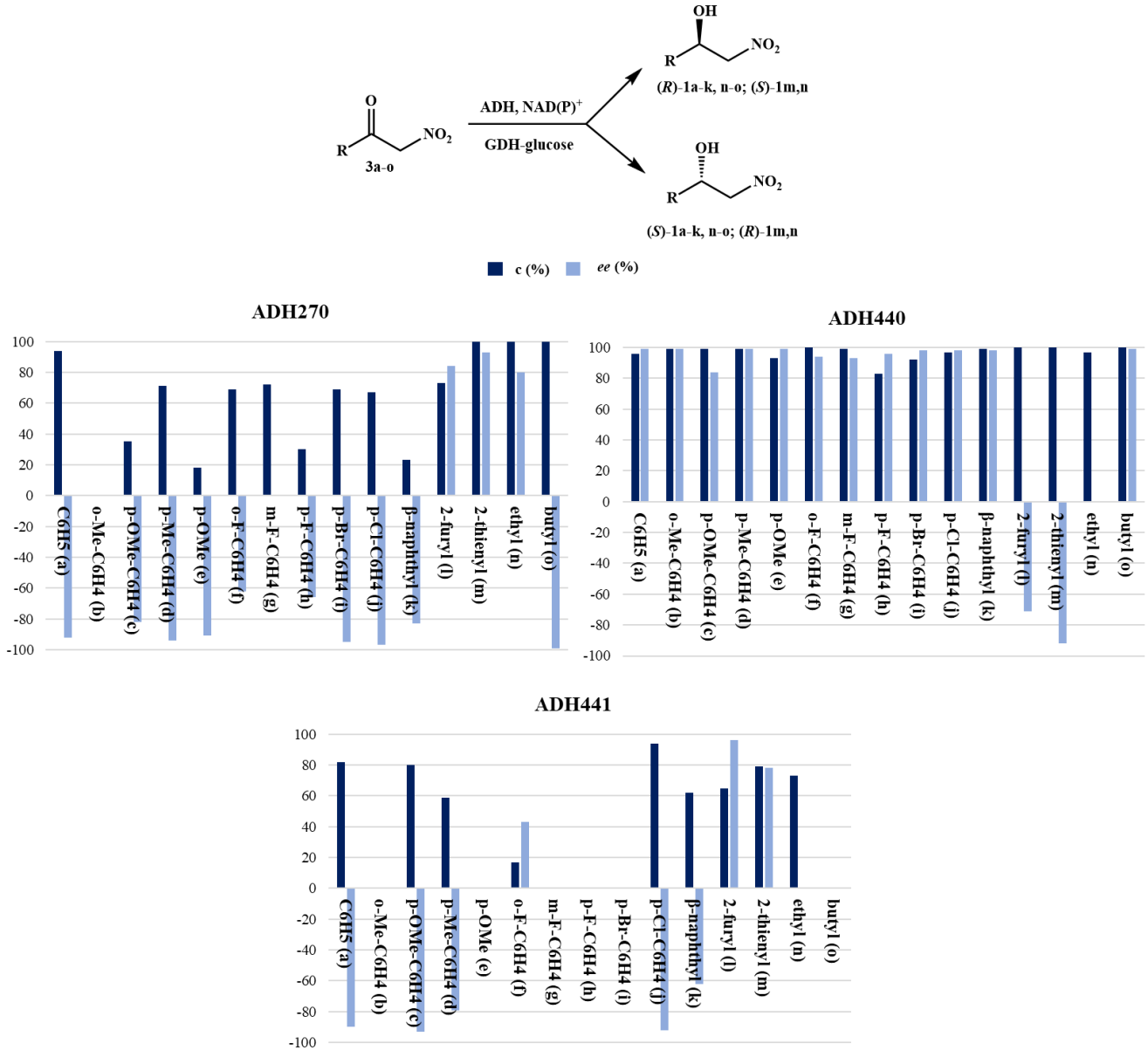

Figure 1. Alcohol dehydrogenases (ADH)-mediated reduction of nitroketones **3a-o** to nitroalcohols **1a-o** (preliminary screening). For graphic reasons the *ee* values of (*R*)-enantiomers are represented as positive values. Those of (*S*)-enantiomers are given as negative: 5 mM substrate, 16 mM glucose, ADH, glucose dehydrogenase (GDH), $NAD(P)^+$, 1% DMSO, acetate buffer pH 5.0, 25 °C, 4-5 h; conversion (c, %) calculated by ^1H NMR spectroscopy as molar percentage of the nitroalcohol **1** in the final reaction mixture after 4-5 h, taking into account the unreacted nitroketone **3**, and the

carboxylic acid obtained upon nitroketone hydrolysis; enantiomeric excess (*ee*, %) calculated on the basis of HPLC analysis on a chiral stationary phase.

ADH270 gave the (*S*)-enantiomer of the reduced product in all the bioreductions, with the exception of the reaction of compound **3n** (Figure 1, R = ethyl), affording (*R*)-**1n** (*ee* = 80%). The highest *ee* values (91-99%) were obtained in the transformation of para-substituted nitroketones **3d** (R = p-Me-C_6H_4, *ee* = 94%), **3e** (R = p-OMe-C_6H_4, *ee* = 91%), **3i** (R = p-Br-C_6H_4, *ee* = 95%), **3j** (R = p-Cl-C_6H_4, *ee* = 97%), and derivatives **3a** (R = phenyl, *ee* = 92%), **3m** (R= 2-thienyl, *ee* = 93%), and **3o** (R = butyl, *ee* = 99%). Enantioselectivity in the range 80-84% was achieved in the reduction of compounds **3c** (R = m-Me-C_6H_4, *ee* = 82%), **3k** (R = 2-naphthyl, *ee* = 83%), **3l** (R = 2-furyl, *ee* = 84%), and **3n** (R = ethyl, *ee* = 80%), while modest *ee* values could be obtained with fluoro derivatives **3f** (R = o-F-C6H4, *ee* = 62%), and **3h** (R = p-F-C_6H_4, *ee* = 66%). m-Fluoro nitroketone **3g** was converted into a racemic nitroalcohol. Only substrate **3b** (R = o-Me-C_6H_4) was recovered unreacted. When ADH441 was employed as a catalyst (Figure 1), the relevant results were achieved in the reduction of **3a** (R = Ph), **3c** (R = m-Me-C_6H_4), **3j** (R = p-Cl-C_6H_4), and **3l** (R = 2-furyl), affording the corresponding nitroalcohol with high enantiomeric purity (*ee* = 90, 93, 92 and 96%, respectively). The results of this screening clearly show that ADH270 and 440 are the most effective catalysts for the preparation of both the enantiomers of nitroalcohols **1**.

Bioreductions of Nitroketones in Biphasic Medium

In order to avoid the drawback of nitroketone hydrolysis, the use of a biphasic medium (buffer and organic solvent) was evaluated. No benzoic acid was observed when compound **3a** was stirred in toluene/buffer or EtOAc/buffer mixtures for 24 h in the presence of GDH and $NAD(P)^+$ without adding the ADH. In the presence of ADH440 and ADH270 as catalysts, the reductions proceeded affording the results that are reported in Table 1. Toluene resulted to be the solvent of choice, preserving nitroketone **3a** from hydrolysis, still maintaining the activity of the ADH.

[a] Conversion calculated on the basis of the ^{1}H NMR spectrum of the crude mixture after 24 h; [b] enantiomeric excess calculated on the basis of HPLC analysis on a chiral *stationary phase*.

ADH	Organic Solvent	Conversion[a] (%)	*ee*[b] (%)
270	AcOEt	-	-
440	AcOEt	68	98 (*R*)
270	toluene	88	95 (*S*)
440	toluene	99	97 (*R*)

Table 1. ADH-mediated reduction of nitroketone **3a** to nitroalcohol **1a** in biphasic system. Total volume 4 mL (organic solvent/water 1/1), 6 mM substrate, 20 mM glucose, ADH (2 mg), GDH (1 mg), $NAD(P)^+$ (0.25 mM), acetate buffer pH 5.0, 25 °C, 24 h.

The ADH-mediated reduction of model nitroketone **3a** was also investigated in 1:1 toluene-water (buffer pH = 5) at 25 ◦C with ADH270 and 440 in order to increase both substrate loading (mg mL^{-1}) and substrate to enzyme ratio (mg mg^{-1}). The corresponding conversions, determined after 24 h reaction time by ^{1}H NMR spectroscopy, are reported in Table 2.

[a] Conversion calculated on the basis of the ^{1}H NMR spectrum of the crude mixture after 24 h.

ADH [1]	[Substrate] (mg mL^{-1})	Substrate/Enzyme (mg mg^{-1})	Conversion [2] (%)
440	1	2.0	99
	1	8.0	94
	2	2.0	95
	2	8.0	91
	3	8.0	94
	3	24.0	80
270	1	2.0	88
	1	3.0	67
	2	2.0	84
	2	3.0	74
	3	3.0	73
	3	4.0	58

Table 2. Effect of substrate concentration and substrate/enzyme ratio on conversion for the ADH-mediated reduction of **3a**. Total volume 4 mL (organic solvent/water 1/1), substrate, glucose (3.2 eq), ADH, GDH, NAD(P)$^+$ (0.04 eq), acetate buffer pH 5.0, 25 °C, 24 h.

ADH440 was found to be very effective in promoting the reduction of substrate **3a**: in batch conditions, with a substrate concentration of 3 mg mL^{-1}, conversion remained still satisfactory (80%) when the enzyme concentration was decreased from 0.38 mg mL $^{-1}$ (substrate/enzyme = 8) to 0.12 mg mL^{-1} (substrate/enzyme = 24). ADH 270 showed less efficiency than ADH440 in these bioreductions. When substrate loading was increased to 3 mg mL $^{-1}$ the use of 1 mg mL^{-1} enzyme (substrate/enzyme = 3) afforded 73% conversion, while a further decrease of enzyme concentration to 0.75 mg mL^{-1} (substrate/enzyme = 4) led only to 58% of reduced product.

*Synthesis of Boc-protected β-Aminoalcohols **2***

The conversion of β-nitroalcohols **1** into β-aminoalcohols **2** was investigated, in order to establish the synthetic potential of the ADH-mediated reduction of nitroketones **3** and highlight its value within organic chemistry procedures. Compounds **1a** and **1e** were employed as model substrates, since the corresponding amino derivatives (*S*)-**2a** and (*R*)-**2e** are the key intermediates in the synthesis of active pharmaceutical ingredients, such as levamisole and (*R*)-tembamide (Scheme 3).

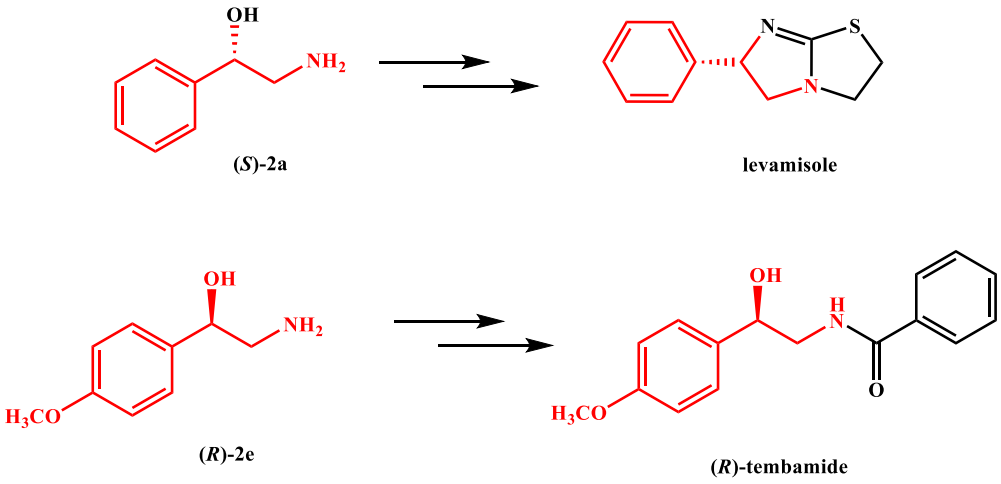

Scheme 3. Active pharmaceutical ingredients prepared starting from amino alcohols (*S*)-**2a** and (*R*)-**2e**.

Levamisole, which is the (*S*)-enantiomer of tetramisole, is a broad spectrum anthelmintic [34], which has found wide application in the treatment of worm infestations and in the elimination of intestinal parasites in both humans and animals. It is also one of the nonspecific immunomodulating agents that are used in clinical practice [35-37]. The known synthetic asymmetric approaches are based on the use of optically active phenylethylenediamine [38-41] or amino alcohol (*S*)-**2a** as intermediates [42]. (*R*)-(−)-Tembamide is a naturally occurring β-hydroxyamide isolated from various members of the Rutaceae family. This compound has been reported to have insecticide and adrenaline-like activity. Extracts of Aegle marmelos, containing tembamide, have been used in the Indian traditional medicine as a control for hypoglycemia [43]. Most of the enantioselective procedures to (*R*)-tembamide involve the use of the corresponding amino alcohol (*R*)-**2e** as a key building block [44]. The nitro moiety of model compounds (*S*)-**1a** and (*R*)-**1e** was converted into the corresponding amino functionality by reaction with $NiCl_2 \cdot 6H_2O$ and $NaBH_4$ (Scheme 4), followed by treatment with $(Boc)_2O$, in order to facilitate the isolation of the aminoalcohol from the reaction mixture. The reaction was fast and is

characterized by complete conversion. The Boc derivatives could be recovered as solid compounds, and easily purified by crystallization. The procedure was carried out directly in the reaction medium of the biocatalyzed reaction, after removal of the aqueous phase, avoiding the isolation of the intermediate nitroalcohols, in order to achieve a one-pot chemo-catalyzed conversion of nitroketones **3a** and **3e** into Boc-protected derivatives (*S*)-**2a** and (*R*)-**2e**, in 57 and 63% isolation yields.

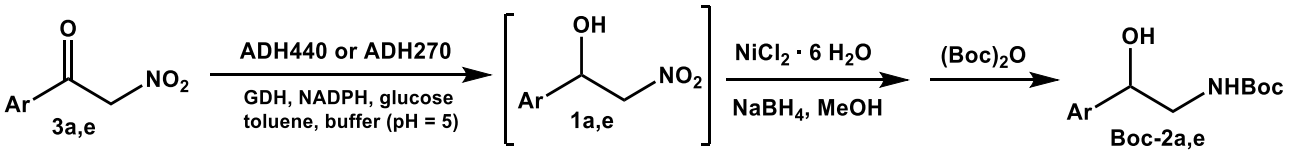

Scheme 4. Synthesis of Boc-protected derivatives **2**.

Conclusions

The results that are reported in this work show that the biocatalytic reduction of α-nitroketones **3** mediated by ADHs is a convenient and useful procedure for the synthesis of both the enantiomers of the corresponding β-nitroalcohols **1** with high enantiomeric purity. In particular, for the first time the reduction of aryl and heteroaryl α-nitroketones (R = aryl or heteroaryl) has been successfully achieved by enzymatic catalysis, enlarging the known methods for the reduction of these compounds limited up to now to the asymmetric transfer hydrogenation in the presence of ruthenium [45], and iridium [46] chiral complexes, with formic acid as a reductant. The bioreduction is performed under mild conditions (ambient temperature and pressure), with low energy consumption, at the expense of glucose, which is employed as a sacrificial substrate for the enzymatic regeneration of the cofactor. The enzymes catalyzing this transformation with either (*R*)- and (*S*)-selectivity are commercially available, and they can be manipulated easily and safely. The use of a biphasic reaction medium with toluene as an organic solvent does not inhibit the activity of the selected ADHs, helps in preserving the starting substrate from hydrolytic degradation, and it improves work-up procedures. The further manipulation of nitroketones into aminoalcohols was carried out without isolation of the nitroalcohol intermediate, thus telescoping the synthetic sequence. Future work will be devoted to increase the productivity of the reaction, for example, by immobilizing the most suitable ADHs on solid supports and performing the reaction in flow conditions.

References

[1] Luzzio, F.A. The Henry reaction: recent examples. *Tetrahedron* **2001**, *57*, 915-945.

[2] Klingler, F.D. Asymmetric hydrogenation of prochiral amino ketones to amino alcohols for pharmaceutical use. *Acc. Chem. Res.* **2007**, *40*, 1367-1376.

[3] Takasu, T.; Ukai, M.; Sato, S.; Matsui, T.; Nagase, I.; Maruyama, T.; Sasamata, M.; Miyata, K.; Uchida, H.; Yamaguchi, O. Effect of (*R*)-2-(2-aminothiazol-4-yl)-4-{2-[(2-hydroxy-2-phenylethyl)amino]ethyl} acetanilide (YM178), a novel selective beta(3)-adrenoceptor agonist, on bladder function. *J. Pharmacol. Exp. Ther.* **2007**, *321*, 642-647.

[4] Hicks, A.; McCafferty, G.P.; Riedel, E.; Aiyar, N.; Pullen, M.; Evans, C.; Luce, T.D.; Coatney, R.W.; Rivera, G.C.; Westfall, T.D. GW427353 (solabegron), a novel, selective beta(3)-adrenergic receptor agonist, evokes bladder relaxation and increases micturition reflex threshold in the dog. *J. Pharmacol. Exp. Ther.* **2007**, *323*, 202-209.

[5] Blay, G.; Hernández-Olmos, V.; Pedro, J.P. Synthesis of (*S*)-(+)-sotalol and (*R*)-(–)-isoproterenol via a catalytic enantioselective Henry reaction. *Tetrahedron* **2010**, *21*, 578-581.

[6] Alvarez-Casao, Y.; Marques-Lopez, E.; Herrera, R.P. Organocatalytic enantioselective Henry reactions. *Symmetry* **2011**, *3*, 220-245.

[7] Palomo, C.; Oiarbide, M.; Laso, A. Recent advances in the catalytic asymmetric nitroaldol Henry reaction. *Eur. J. Org. Chem.* **2007**, 2561-2574.

[8] Marcelli, T.; van der Haas, R.N.S.; van Maarseveen, J.H.; Hiemstra, H. Asymmetric organocatalytic Henry reaction. *Angew. Chem. Int. Ed.* **2006**, *45*, 929-931.

[9] Shibazaki, M.; Kumagaya, N.; Nitabara, T. Preparation of Optically Active Anti-1,2-Nitroalcohols by Stereoselective Nitroaldol Reaction. Jpn. Kokai Tokkyo Koho JP 2009114071 A, 28 May 2009.

[10] Shibazaki, M.; Matsunaga, S.; Handa, S. Preparation of Optically Active Anti-1,2-Nitroalcohols by Stereoselective Nitroaldol Reaction with Palladium Lanthanum-Schiff Base Complex Catalysts. Jpn. Kokai Tokkyo Koho JP 2009108012 A, 21 May 2009.

[11] Ooi, T.; Uraguchi, D. Chiral Tetraaminophosphonium salts, catalyst for asymmetric synthesis and method for producing chiral beta Nitroalcohol. US 20090131716 A1, 21 May 2009.

[12] Baxter, C.E.J. Preparation of (1*R**,2*S**)-1-Phenyl-2-Nitroalcohols from Benzaldehyde and the Corresponding Nitroalkane in the Presence of Amine Catalysts. US 5750802 A, 12 May 1998.

[13] Kodama, K.; Sugawara, K.; Hirose, T. Synthesis of chiral 1,3-diamines derived fromcis-2-benzamidocyclohexane carboxylic acid and their application in the Cu-catalyzed enantioselective Henry reaction. *Chem. Eur. J.* **2011**, *17*, 13584-13592.

[14] Chinnaraja, E.; Arunachalam, R.; Subramanian, P.S. Enantio- and diastereoselective synthesis of beta-nitroalcohol via Henry reaction catalyzed by Cu(II), Ni(II), Zn(II) complexes of chiral BINIM ligands. *ChemistrySelect* **2016**, *1*, 5331-5338.

[15] Cwiek, R.; Niedziejko, P.; Kaluzia, Z. Synthesis of tunable diamine ligands with spiro indane-2,2-pyrrolidine backbone and their applications in enantioselective Henry reaction. *J. Org. Chem.* **2014**, *79*, 1222-1234.

[16] Angelin, M.; Vongvilai, P.; Fischer, A.; Ramström, O. Crystallization-driven asymmetric synthesis of pyridine-beta-nitroalcohols via discovery-oriented self-resolution of a dynamic system. *Eur. J. Org. Chem.* **2010**, 6315-6318.

[17] Milner, S.E.; Moody, T.S.; Maguire, A.R. Biocatalytic approaches to the Henry (nitroaldol) reaction. *Eur. J. Org. Chem.* **2012**, 3059-3067.

[18] Purkarthofer, T.; Gruber, K.; Gruber-Khadjawi, M.; Waich, K.; Skranc,W.; Mink, D.; Griengl, H. A biocatalytic Henry reaction-the hydroxynitrile lyase from Hevea brasiliensis also catalyzes nitroaldol. *Angew. Chem.Int. Ed.* **2006**, *45*, 3454-3456.

[19] Gruber-Khadjawi, M.; Purkarthofer, T.; Skranc, W.; Griengl, H. A biocatalytic Henry reaction-The hydroxynitrile lyase from Hevea brasiliensis also catalyzes nitroaldol reactions. *Adv. Synth. Catal.* **2007**, *349*, 1445-1450.

[20] Yuryev, R.; Purkarthofer, T.; Gruber, M.; Griengl, H.; Liese, A. Kinetic studies of the asymmetric Henry reaction catalyzed by hydroxynitrile lyase from *Hevea brasiliensis*. *Biocatal. Biotransform.* **2010**, *28*, 348-356.

[21] Fuhshuku, K.; Asano, Y. Synthesis of (*R*)-beta-nitro alcohols catalyzed by *R*-selective hydroxynitrile lyase from Arabidopsis thaliana in the aqueous-organic biphasic system. *J. Biotechnol.* **2011**, *153*, 153-159.

[22] Bekerle-Bogner, M.; Gruber-Khadjawi, M.; Wiltsche, H.; Wiedner, R.; Schwab, H.; Steiner, K. (*R*)-Selective nitroaldol reaction catalyzed by metal-dependent bacterial hydroxynitrile lyase. *ChemCatChem* **2016**, *8*, 214-2216.

[23] Fujisawa, T.; Hayashi, H.; Kishioka, Y. Enantioselective Synthesis of Optically Pure Amino Alcohol Derivatives by Yeast Reduction. *Chem. Lett.* **1987**, *16*, 129-132.

[24] Brenelli, E.; de Carvalho, M.; Marques, M.; Moran, P.J.S.; Rodrigues, J.A.R.; Sorrilha, A.E.P.M. Enantioselective synthesis of (*R*)-(-)-phenylethanolamines using Baker's yeast reduction of some substituted methyl phenyl ketones. *Indian J. Chem.* **1992**, *31B*, 821-823.

[25] Wallner, S.R.; Lavandera, I.; Mayer, S.F.; Öhrlein, R.; Hafner, A.; Edegger, K.; Faber, K.; Kroutil, W. Stereoselective anti-Prelog reduction of ketones by whole cells of *Comamonas testosteroni* in a substrate-coupled approach. *J. Mol. Catal. B.* **2008**, *55*, 126-129.

[26] Venkataraman, S.; Chadha, A. Enantio- & chemo-selective preparation of enantiomerically enriched aliphatic nitro alcohols using *Candida parapsilosis* ATCC 7330. *RSC Adv.* **2015**, *5*, 73807-73813.

[27] Albarrán-Velo, J.; González-Martínez, D.; Gotor-Fernández, V. Stereoselective biocatalysis: A mature technology for the asymmetric synthesis of pharmaceutical building blocks. *Biocatal. Biotransform.* **2017**, *36*, 102-130.

[28] Brenna, E.; Crotti, M.; Gatti, F.G.; Monti, D.; Parmeggiani, F.; Pugliese, A.; Tentori, F. Biocatalytic synthesis of chiral cyclic gamma-oxoesters by sequential C–H hydroxylation, alcohol oxidation and alkene reduction. *Green Chem.* **2017**, *19*, 5122-5130.

[29] Brenna, E.; Crotti, M.; Gatti, F.G.; Monti, D.; Parmeggiani, F.; Santangelo, S. Asymmetric bioreduction of beta-acylaminonitroalkenes: Easy access to chiral building blocks with two vicinal nitrogen-containing functional groups. *ChemCatChem* **2017**, *9*, 2480-2487.

[30] Brenna, E.; Cannavale, F.; Crotti, M.; De Vitis, V.; Gatti, F.G.; Migliazza, G.; Molinari, F.; Parmeggiani, F.; Romano, D.; Santangelo, S. Synthesis of enantiomerically enriched 2-hydroxymethylalkanoic acids by oxidative desymmetrisation of achiral 1,3-diols mediated by *Acetobacter aceti. ChemCatChem* **2016**, *8*, 3796-3803.

[31] Brenna, E.; Crotti, M.; Gatti, F.G.; Monti, D.; Parmeggiani, F.; Powell, R.W.; Santangelo, S.; Stewart, J.D. Opposite enantioselectivity in the bioreduction of (*Z*)-beta-aryl-beta-cyanoacrylates mediated by the tryptophan 116 mutants of Old Yellow Enzyme 1: synthetic approach to (*R*)- and (*S*)-beta-aryl-gamma-lactams. *Adv. Synth. Catal.* **2015**, *357*, 1849-1860.

[32] Lindsay, V.N.G.; Lin, W.; Charette, A.B. Experimental evidence for the all-up reactive conformation of chiral rhodium(II) carboxylate catalysts: enantioselective synthesis of cis-cyclopropane alpha-amino acids. *J. Am. Chem. Soc.* **2009**, *131*, 16383-16385.

[33] Pearson, R.G.; Anderson, D.H.; Alt, L.L. Mechanism of the hydrolytic cleavage of carbon-carbon bonds. III. Hydrolysis of alpha-nitro and alpha-sulfonyl ketones. *J. Am. Chem. Soc.* **1955**, *77*, 527-529.

[34] Thienpont, D.C.I.; Vanparijs, O.; Raeymaekers, A.; Vandenberk, J.; Demoen, P.; Allewijn, F.; Marsboom, R.; Niemegeers, C.; Schellekens, K.; Janssen, P. Tetramisole (R 8299), a new, potent broad spectrum anthelmintic. *Nature* **1966**, *209*, 1084-1086.

[35] Moertel, C.G.; Fleming, T.T.; Macdonald, J.S.; Haller, D.G.; Laurie, J.A.; Tangen, C.M.; Ungerleider, J.S.; Emerson,W.A.; Tormey, D.C.; Glick, J.H. Fluorouracil plus levamisole as effective adjuvant therapy after resection of stage III colon carcinoma: a final report. *Anal. Int. Med.* **1995**, *122*, 321-326.

[36] Moertal, G.G.; Fleming, T.R.; Macdonald, J.S. Levamisole and fluorouracil for adjuvant therapy of resected colon-carcinoma. *New Engl. J. Med.* **1990**, *322*, 352-358.

[37] Gwilt, P.; Tempero, M.; Kremer, A.; Connolly, M.; Ding, C. Pharmacokinetics of levamisole in cancer patients treated with 5-fluorouracil. Cancer Chemother. *Pharmacol.* **2000**, *45*, 247-251.

[38] Raeymaekers, A.H.M.; Roevens, L.F.C.; Janssen, P.A.J. The absolute configurations of the optical isomers of the broad spectrum anthelmintic tetramisole. *Tetrahedron Lett.* **1967**, *8*, 1467-1470.

[39] Choudhary, M.K.; Rajkumar Tak, R.; Kureshy, R.I.; Ansari, A.; Khan, N.H.; Abdi, S.H.R.; Bajaj, H.C. Enantioselective aza-Henry reaction for the synthesis of (*S*)-levamisole using efficient recyclable chiral Cu(II)-amino alcohol derived complexes. *J. Mol. Catal. A.* **2015**, *409*, 85-93.

[40] Roeben, C.; Souto, J.A.; Gonzalez, Y.; Lishchynskyi, A.; Muniz, K. Enantioselective metal-free diamination of styrenes. *Angew. Chem., Int. Ed*. **2011**, *50*, 9478-9482.

[41] Sadhukhan, A.; Sahu, D.; Ganguly, B.; Khan, N.H.; Kureshy, R.I.; Abdi, S.H.R.S.; Bajaj, H.C. Oxazoline-based organocatalyst for enantioselective Strecker reactions: A protocol for the synthesis of levamisole. *Chem. Eur. J.* **2013**, *19*, 14224-14232.

[42] Kamal, A.; Ramesh Khanna, G.B.; Krishnaji, T.; Ramu, R. A new facile chemoenzymatic synthesis of levamisole. *Biorg. Med. Chem. Lett.* **2005**, *15*, 613-615.

[43] Shoeb, A.; Kapil, R.S.; Popli, S.P. Coumarins and alkaloids of Aegle-marmelos. *Phytochemistry* **1973**, *12*, 2071-2072.

[44] Das, A.; Choudhary, M.K.; Kureshy, R.I.; Roy, T.; Khan, N.H.; Abdi, S.H.R.; Bajaj, H.C. Enantioselective Henry and aza-Henry reaction in the synthesis of (*R*)-tembamide using efficient, recyclable polymeric CuII complexes as catalyst. *ChemPlusChem* **2014**, *79*, 1138-1146.

[45] Watanabe, M.; Murata, K.; Ikariya, T. Practical synthesis of optically active amino alcohols *via* asymmetric transfer hydrogenation of functionalized aromatic ketones. *J. Org. Chem.* **2002**, *67*, 1712-1715.

[46] Soltani, O.; Ariger, M.A.; Vázquez-Villa, H.E.; Carreira, M. Transfer hydrogenation in water: enantioselective, catalytic reduction of alpha-cyano and alpha-nitro substituted acetophenones. *Org. Lett.* **2010**, *12*, 2893-2895

Chapter 2

Immobilization of Old Yellow Enzymes via covalent or coordination bonds

Francesca Tentori [1], Teodora Bavaro [2], Elisabetta Brenna [1,3], Danilo Colombo [1], Daniela Monti [3], Riccardo Semproli [2] and Daniela Ubiali [2]

[1] Politecnico di Milano, Dipartimento di Chimica, Materiali e Ingegneria Chimica, via Mancinelli 7, Milano I-20131, Italy.

[2] Università degli Studi di Pavia, Dipartimento di Scienze del Farmaco, viale Taramelli 12, Pavia I-27100, Italy.

[3] Istituto di Chimica del Riconoscimento Molecolare - CNR, via Mancinelli 7, Milano I-20131, Italy.

Published in *Catalysts* **2020**, *10*, 260

Introduction

Ene-reductases (ERs) belonging to the old yellow enzyme (OYE) family (EC 1.6.99.1) are flavin mononucleotide (FMN)-containing oxidoreductases, which are able to catalyze the stereoselective reduction of C=C double bonds activated by the presence of a suitable electron-withdrawing group (EWG) as a substituent of the alkene moiety [1,2]. The reaction occurs through a stereospecific anti hydrogen addition to the C=C double bond, according to the following steps [3]. The enzyme-bound flavin (reduced by NAD(P)H cofactor to $FMNH_2$) transfers a hydride to the olefin carbon atom in β position with respect to the EWG. A proton is delivered by a tyrosine side-chain (Tyr196 for OYE1-3) of the enzyme active site to the α-carbon atom (with respect to EWG) on the opposite face of the alkene. For the application of OYE-mediated reductions in synthetic sequences of practical interest, it is advantageous to promote the *in situ* regeneration of the reduced nicotinamide cofactor by using a NAD(P)H-dependent glucose dehydrogenase (GDH) with glucose as a sacrificial co-substrate. The OYE-mediated bioreduction has been widely investigated in the last decade to establish substrate scope and stereoselectivity of these enzymes [4-6], and to study the combination of this reaction with other chemo- and/or biocatalyzed transformations, both in concomitant and subsequent cascade procedures [7,8]. Several works showed the advantages of using OYE-catalyzed hydrogenation to prepare chiral building blocks for the synthesis of APIs (Active Pharmaceutical Ingredients) [9-12], flavors and fragrances [13-15]. The synthetic potential of the OYE-mediated bioreduction can be further expanded by OYE immobilization on solid carriers. If OYEs are converted into stable, readily-recoverable and recyclable heterogeneous catalysts, then their suitability for large-scale applications can be enhanced, in agreement with one of the key green chemistry research areas established by the ACS Green Chemistry Institute® Pharmaceutical Roundtable (catalyst immobilization without significant loss in kinetics) [16]. Studies on the immobilization of oxidoreductases are gradually increasing, but still only a few examples of ER immobilization have been described to date. Recently, a recombinant ER from the OYE family and its cofactor-recycling partner enzyme GDH (commercially available from Amano Enzyme Inc.) were co-immobilized by using two immobilization methods (*i.e.*, cross-linked enzyme aggregates (CLEAs) and a so-called "biomimetic" immobilization (BI)) by entrapment within a network of fused silica particles. Activity recovery of both enzyme preparations were about 45%. Immobilization enhanced the thermal stability (50 °C) of both enzymes and markedly increased their resistance to acidic pH (5-6) in comparison with the non-immobilized enzyme. Moreover, both immobilized enzymes were successfully recycled and re-used

for up to 14 reaction cycles. The catalytic "performance" of the CLEA preparation in the reduction of 4-(4-methoxyphenyl)-3-buten-2-one resulted to be superior, both to the non-immobilized enzymes and the entrapped enzymes by BI [17]. In a very recent study, an ER from *Thermus scotoductus* SA-01 (*Ts*OYE) was encapsulated with a light-harvesting dye in an alginate hydrogel for NADH-free, photobiocatalytic asymmetric hydrogenation of 2-methylcyclohexenone. The *Ts*OYE encapsulated in alginate hydrogel exhibited enhanced stability against external stresses (e.g., heat, organic solvents), also on a repeated use. However, the long-term reusability of *Ts*OYE alginate hydrogel was hampered by photobleaching and leakage of the dye used [18]. OYE immobilization is still under-investigated and, to the best of our knowledge, no attempt of immobilization has ever been reported for OYE3, one of the most performing members of this enzyme class. The impressive results obtained in OYE3-catalyzed biotransformations in the past years and the benefits envisaged for ER immobilization urged us to undergo a "seed-study" in this frame. In this work, OYE3 was immobilized both by covalent binding on glyoxyl-agarose (OYE3-GA), and by metal affinity interaction on EziG™ particles (OYE3-EziG). The GA carrier [19,20], widely explored for the irreversible immobilization of enzymes by multipoint attachment, has proven its efficiency and versatility as immobilization support by affording robust biocatalysts, both for batch and flow applications [21,22]. On the other hand, EziG™ is a novel carrier made of controlled porosity glass (CPG) particles containing chelated Fe(III) for His-tag binding. This carrier can specifically immobilize tagged enzymes from a crude mixture by affinity interaction and is, thus, frequently used to combine immobilization and purification steps [23,24]. In this context, EziG™ was studied to explore a milder immobilization technique based on non-covalent interaction.

Results and Discussion

Enzyme Activity Assays

In order to characterize OYE3, the enzyme activity was assessed spectrophotometrically, as described for other ERs [25-27], by measuring the consumption of NADH at 340 nm in the reduction of cyclohex-2-enone (**1**) (see Experimental Part in Appendix *Chapter 2*). This assay was found to be suitable for the soluble enzyme, but not for assessing the activity of the immobilized enzyme (and, indeed, to calculate the activity recovery after immobilization) because of the interference of the solid carrier with the spectrophotometric readouts. Therefore, a GC/MS assay (see Experimental Part in Appendix *Chapter 2*) based on the reduction of (*R*)-carvone (**2**) in the presence of stoichiometric NADH was used. Unless otherwise stated, this latter assay was used to determine the activity of both soluble and immobilized OYE3.

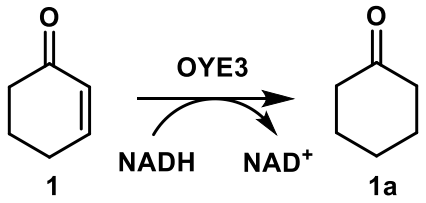

Scheme 1. Reduction of cyclohex-2-enone (**1**) to cyclohexanone (**1a**) catalyzed by OYE3 (spectrophotometric activity assay). Experimental conditions: 50 mM phosphate buffer pH 7 (0.5% DMSO), [substrate] = 0.05 mM, [NADH] = 0.2 mM, 28 °C, reaction time: 80 sec, volume = 1 mL.

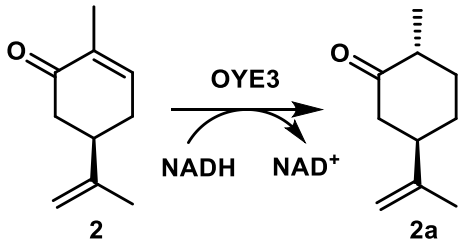

Scheme 2. Reduction of (*R*)-carvone (**2**) to (2*S*,3*R*)-dihydrocarvone (**2a**) catalyzed by OYE3 (GC/MS activity assay). Experimental conditions: 50 mM phosphate buffer pH 7 (1% DMSO), [substrate] = 1 mM, [NADH] = 1 mM, 28 °C, reaction time = 30 min., volume = 1 mL.

A spectrophotometric assay was also used to assess the activity of soluble GDH by measuring the formation of NADH over time at 340 nm as a result of glucose oxidation (experimental conditions: 50 mM phosphate buffer pH 7, [substrate] = 20 mM, [NAD^+] = 0.2 mM, 28 °C, reaction time = 2

min, volume = 1 mL). Glucose dehydrogenasewas coupled to OYE3 for cofactor regeneration in the reduction of α-methyl-*trans*-cinnamaldehyde (**3**) (see Experimental Part in Appendix *Chapter 2*).

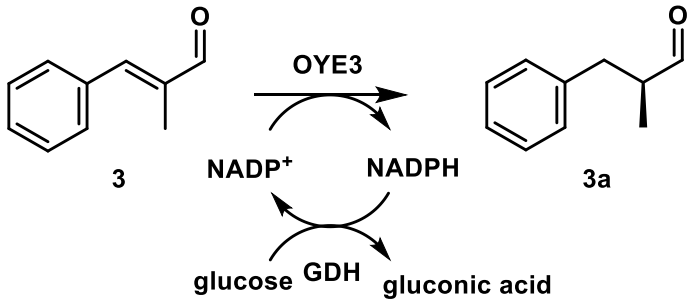

Scheme 3. Reduction of α-methyl-*trans*-cinnamaldehyde (**3**) to (*S*)-α-methyl-β-phenylpropanal (**3a**) catalyzed by OYE3. The regeneration of $NADP^+$ was ensured by the GDH/glucose system. Experimental conditions: 50 mM phosphate buffer pH 7 (1% DMSO), [substrate] = 5 mM, [$NADP^+$] = 0.1 mM, [glucose] = 20 mM, GDH = 10 µL; 5 mg mL^{-1}, 28 °C, reaction time = 1 h, volume = 1 mL.

Preliminary Study of OYE3 Stability at Alkaline pH

Covalent immobilization of enzymes on glyoxyl-agarose (GA) relies on the formation of imino bonds between the non-protonated "ε-amino groups of enzyme Lys residues and the aldehyde groups of the carrier [19,20]. This immobilization is required to be carried out at alkaline pH (*i.e.*, pH ≥10) and a final chemical reduction step is necessary for the generation of irreversible C-N bonds. Whenever compatible with the enzyme stability, sodium borohydride is used to this aim, since it transforms Schiff's bases into secondary amino bonds and the unreacted aldehyde groups of the carrier into inert hydroxyl moieties. Alternatively, the milder sodium cyanoborohydride or 2-picoline borane can be used for those enzymes which are sensitive to sodium borohydride reduction (but unreacted aldehyde groups of the carrier remain unchanged in this case) [28]. Thus, the first step before immobilization on GA was to assay the stability of OYE3 at alkaline pH. A pH "window" of 8-10 was considered and 3 h was selected as the endpoint (according to the general protocol for this type of immobilization) [19]. Enzyme activity before and after incubation at pH 8-10 (see Experimental part in Appendix *Chapter 2*) was assessed spectrophotometrically using the cyclohex-2-enone assay (Scheme 1). Data of the stability assay at pH 8-10 are reported in Figure 1. The residual activity of OYE3 after 3 h at pH 10 was about 70%. This result was considered acceptable for the immobilization on GA.

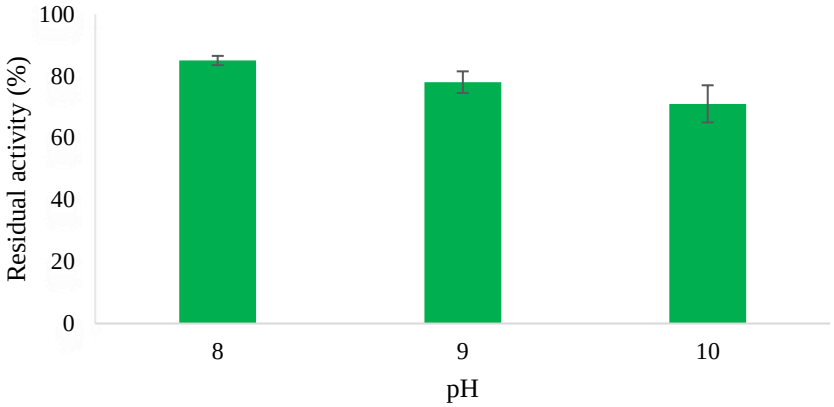

Figure 1. Residual activity (%) of soluble OYE3 upon incubation at pH 8-10 (endpoint: 3 h). Experimental conditions: 50 mM phosphate buffer, pH 8; 50 mM Tris-HCl buffer, pH 9; 50 mM NaOH/glycine buffer, pH 10; 20 °C. Enzyme activity was determined as r Enzyme activity was determined as reported in Scheme 1.

Immobilization of OYE3

Immobilization of OYE3 on GA (OYE3-GA) was performed according to a standard protocol by using a 2 mg g^{-1} protein loading [19]. In order to extend the enzyme stability during the immobilization, the reaction was performed at 4 °C. After 3 h, almost all the protein was immobilized (immobilization yield = 95%), as revealed by protein measurements of the supernatant from the immobilization reaction. The activity recovery, after reduction of the immobilized enzyme with $NaBH_4$, was 52% (Table 1).

[a] Calculated as described in Experimental Part, Appendix *Chapter 2*. [b] Determined by the (*R*)-carvone (**2**) assay (see Scheme 2). [c] Calculated as described in Experimental Part, Appendix *Chapter 2*. Activity measurements were performed at least in duplicate. Deviation from mean values was below 5%.

Carrier	**Enzyme loading (mg g^{-1})**	**Immobilization yield [a] (%)**	**Activity [b] (U g^{-1})**	**Activity recovery [c] (%)**
Glyoxyl-agarose	2.0	95	0.023	52
EziG™ Opal	4.2	100	0.037	54
EziG™ Coral	4.2	100	0.015	23
EziG™ Amber	4.2	100	0.014	19

Table 1. Results of OYE3 immobilization.

For the immobilization by metal-coordination, three EziG™ resins were tested (namely Opal or EziG 1, Coral or EziG 2, and Amber or EziG 3). According to the indications of the supplier, Opal is a hydrophilic carrier (glass), whereas Coral and Amber are hydrophobic and semi-hydrophilic, respectively. The lower hydrophilicity of Coral and Amber in comparison with Opal is due to the presence of different polymeric coatings on the particle silica surface [30]. Specifically, EziG™ Coral is made from hybrid CPG with polyvinyl benzyl chloride, whereas EziG™ Amber is produced from hybrid CPG with a blended co-polymer. Pore size distribution of the carriers ranges from ~500 Å as standard (Opal) to ~300 Å (Coral and Amber, due to the polymer coating). According to the indications of the supplier, a higher protein loading (4.2 mg g^{-1}) was applied to EziG™ carriers. In all cases, the immobilization was complete. The activity recovery for EziG™ Opal was 54%, thus resulting comparable to that previously obtained with GA. In the case of the hybrid CPG Coral and Amber, the activity recovery was less than half with respect to EziG™ Opal. Under the same binding chemistry, it is plausible that this result may be ascribed to the effect of the polymer coating in tuning the hydrophilicity-hydrophobicity balance of the carrier. However, a systematic study on these carriers was not performed at this stage. Due to the positive result achieved with EziG™ Opal, this

carrier was selected for the full characterization of this type of enzyme preparation (stability, recycling, re-use, enzyme leakage).

Stability of Immobilized OYE3

Increased stability is recognized as one of the most important advantages of immobilized enzymes [31,32]. To verify whether this "general rule" might be applied also to immobilized OYE3 preparations, the stability of both OYE3-GA and OYE3-EziG (Opal) was tested under the experimental conditions used for the reduction of (*R*)-carvone (**2**) (Scheme 2). The stability assay was carried on for six days (Figure 2). From the stability time course, it clearly emerged that immobilization exerted a stabilizing effect on the soluble enzyme. The OYE3-GA retained almost 100% of its activity, whereas the activity of the non-immobilized enzyme dropped to 50% after two days. On the other hand, OYE3-EziG was slightly less stable than OYE3-GA, but it still retained about 90% of its starting activity after 144 h.

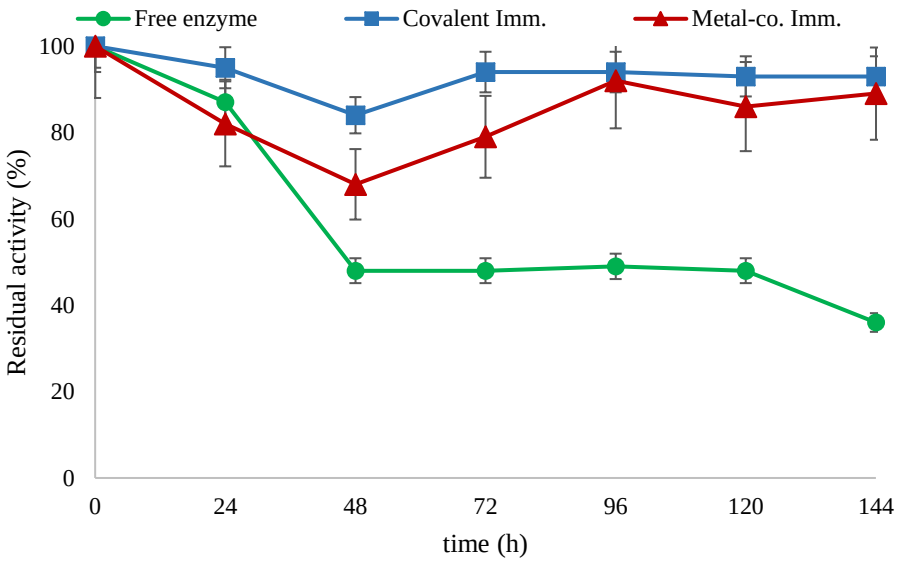

Figure 2. Stability of soluble OYE3 (green circles), OYE3-GA (blue squares) and OYE3-EziG (red triangles). Experimental conditions: 50 mM phosphate nuffer pH 7 (1% DMSO), (*R*)-carvone and NADH=1 mM, 28 °C, volume=1 mL.

Recycling of Immobilized OYE3

Biocatalyst recycling and re-use is a further strength point of immobilized enzymes [31-33]. Thus, both OYE3-GA and OYE3-EziG were used in the bioreduction of α-methyl-*trans*-cinnamaldehyde (**3**, Scheme 3), then recovered and added to a newly-prepared reaction mixture. A catalytic amount of the cofactor ($NADP^+$) was used since a GDH glucose regeneration system was coupled to the main biotransformation. In the case of OYE3-GA, GDH was added as a soluble enzyme to each reaction cycle. In the case of OYE3-EziG, a co-immobilized preparation OYE3/GDH was used, taking advantage of the His-tag displayed by both enzymes. The enzymes (OYE3 and GDH) were incubated with EziGTM. Activity recovery for OYE3 was 55%. OYE3-GA could be recycled and re-used for up to 12 reaction cycles. The highest conversion achieved after 12 runs was 40% (Figure 3). Moreover, it is worth noting that OYE3-GA retained completely its activity up to the fifth reaction cycle. In the case of OYE3/GDH-EziG, the initial conversion dropped to 56% after two reaction cycles. Interestingly, when the conversion % was almost negligible (reaction 11) and the biotransformation was supplemented with a fresh aliquot of soluble GDH, the reaction afforded a 30% conversion, thus suggesting that the gradual drop of the conversions registered for OYE3/GDH-EziG might depend either on the loss of activity of immobilized GDH or on its leakage from the carrier and/or deactivation, thereof.

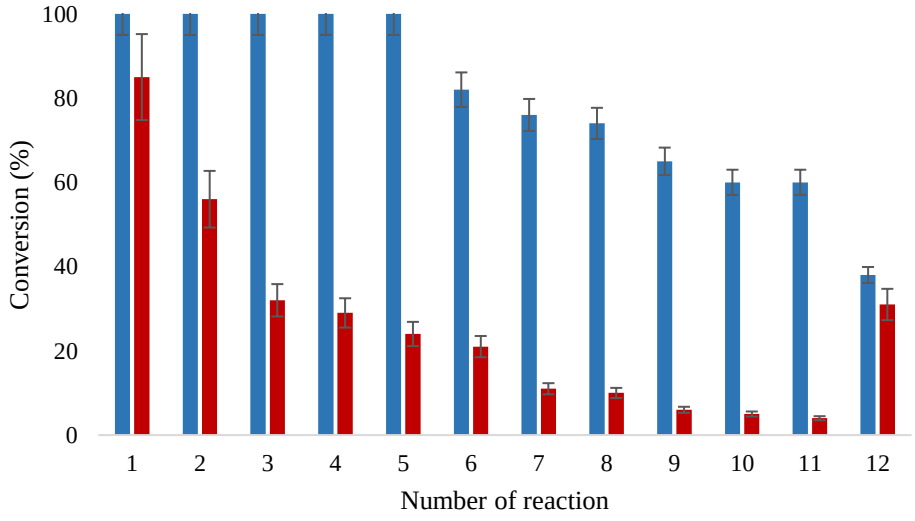

Figure 3. Recycling of immobilized OYE3-GA (blue) and OYE3/GDH-EziG (red). Experimental conditions as reported in Scheme 2.

Protein Leakage Assay of Immobilized OYE3

Protein leakage from the immobilization carrier is undesirable for several reasons: Loss of activity of the biocatalyst, lack of data reproducibility in the investigated biotransformation, costs and product contamination, to name a few [29]. Covalent immobilization of the enzyme to the carrier generally prevents the protein from leaching from the support surface. In this context, glyoxylagarose and other surface-functionalized carriers (*i.e.*, epoxy carriers) are frequently preferred because of the "irreversible" nature of the bonds generated between the enzyme and the carrier. On the other hand, the high affinity and the specificity of the binding interaction based on the His-tag as in EziGTM-type carriers is plausible to generate a strong enzyme ‒ support interaction which might prevent enzyme leakage. However, predictions about how an enzyme will respond to an immobilization process are often hard to make. Enzyme leakage is routinely verified by protein measurements [34] of the supernatant in which the immobilized preparation is incubated under specific conditions dictated by the type of information needed (e.g., reaction or storage conditions). Both OYE3-GA and OYE3/GDH-EziG were, thus, incubated in the reaction buffer (50 mM phosphate buffer pH 7) at 28 ◦C under stirring for 48 h. At scheduled times, samples of the incubation buffer were collected and submitted to SDS-PAGE analysis; silver staining, due to its high sensitivity in the low nanogram range, was used to detect protein traces after electrophoretic separation [35]. From the inspection of the SDS-PAGE gel (data not reported), no enzyme traces were detected for either OYE3-GA or OYE3/GDH-EziG. This suggests that the loss of activity of both immobilized enzymes registered during the recycling and re-use study, although to a different extent, cannot be ascribed to protein leakage phenomena.

Conclusions

Ene-reductases are a powerful tool for the stereoselective reduction of activated C=C double bonds under mild and environmentally friendly conditions. Due to the great interest in these enzymes for preparative applications, the access to stable and reusable heterogeneous biocatalysts is being sought. Immobilization of OYE3 both on the well-known glyoxyl-agarose (GA) by covalent binding and on controlled pore glass EziG^{TM} by affinity-based adsorption was shown to produce active, stable and reusable biocatalysts. Although activity recovery for both enzyme preparations was similar (≈50%), OYE3-GA appeared to be superior about stability and recycling properties. In this latter regard, OYE3-GA could be re-used up to five reaction cycles without any loss of activity. Still, upon a prolonged re-use (up to 12 runs), this immobilized biocatalyst allowed to obtain a 40% conversion in the reduction of α-methyl-*trans*-cinnamaldehyde (**3**). On the other hand, in the case of the co-immobilized OYE3/GDH-EziG, a drop of conversion was observed after two reaction cycles, presumably due to deactivation of GDH. Interestingly, no evidence of enzyme leaching from both the supports was registered.

References

[1] Winkler, C.K.; Tasnádi, G.; Clay, D.; Hall, M.; Faber, K. Asymmetric bioreduction of activated alkenes to industrially relevant optically active compounds. *J. Biotechnol.* **2012**, *162*, 381-389.

[2] Toogood, H.S.; Scrutton, N.S. New developments in 'ene'-reductase catalysed biological hydrogenations. *Curr. Opin. Chem. Biol.* **2014**, *19*, 107-115.

[3] Vaz, A.D.N.; Chakraborty, S.; Massey, V. Old yellow enzyme: aromatization of cyclic enones and the mechanism of a novel dismutation reaction. *Biochemistry* **1995**, *34*, 4246-4256.

[4] Gatti, F.G.; Parmeggiani, F.; Sacchetti, A. Synthetic strategies based on C=C bioreductions for the preparation of biologically active molecules. In Synthetic Methods for Biologically Active Molecules; Brenna, E., Ed.;WILEY-VCH Verlag GmbH & Co. KGaA:Weinheim, Germany, 2013; pp. 49-84.

[5] Toogood, H.S.; Scrutton, N.S. Discovery, characterization, engineering, and applications of ene-reductases for industrial biocatalysis. *ACS Catal.* **2018**, *8*, 3532-3549.

[6] Winkler, C.K.; Faber, K.; Hall, M. Biocatalytic reduction of activated C=C-bonds and beyond: Emerging trends. *Curr. Opin. Chem. Biol.* **2018**, *43*, 97-105.

[7] Classen, T.; Korpak, M.; Schölzel, M.; Pietruszka, J. Stereoselective enzyme cascades: An efficient synthesis of chiral -butyrolactones. *ACS Catal.* **2014**, *4*, 1321-1331.

[8] Brenna, E.; Crotti, M.; Gatti, F.G.; Monti, D.; Parmeggiani, F.; Pugliese, A.; Tentori, F. Biocatalytic synthesis of chiral cyclic -oxoesters by sequential C–H hydroxylation, alcohol oxidation and alkene reduction. *Green Chem.* **2017**, *19*, 5122-5130.

[9] Winkler, C.K.; Clay, D.; Davies, S.; O'Neill, P.; McDaid, P.; Debarge, S.; Steflik, J.; Karmilowicz, M.;Wong, J.W.; Faber, K. Chemoenzymatic asymmetric synthesis of pregabalin precursors via asymmetric bioreduction of β-cyanoacrylate esters using ene-reductases. *J. Org. Chem.* **2013**, *78*, 1525-1533.

[10] Brenna, E.; Gatti, F.G.; Manfredi, A.; Monti, D.; Parmeggiani, F. Biocatalyzed enantioselective reduction of activated C=C bonds: Synthesis of enantiomerically enriched α-halo-β-arylpropionic acids. *Eur. J. Org. Chem.* **2011**, 4015-4022.

[11] Brenna, E.; Crotti, M.; Gatti, F.G.; Monti, D.; Parmeggiani, F.; Powell, R.W.; Santangelo, S.; Stewart, J.D. Opposite enantioselectivity in the bioreduction of (*Z*)-β -aryl-β-cyanoacrylates mediated by the tryptophan 116 mutants of old yellow enzyme 1: Synthetic approach to (*R*)- and (*S*)-β-aryl-γ-lactams. *Adv. Synth. Catal.* **2015**, *357*, 1849-1860.

[12] Waller, J.; Toogood,H.S.; Karuppiah, V.; Rattray,N.J.W.;Mansell,D.J.; Leys,D.; Gardiner, J.M.; Fryszkowska,A.; Ahmed, S.T.; Bandichhor, R. Structural insights into the ene-reductase synthesis of profens. *Org. Biomol. Chem.* **2017**, *15*, 4440-4448.

[13] Kumru, C.; Classen, T.; Pietruszka, J. Enantioselective, catalytic one-pot synthesis of -butyrolactone-based fragrances. *ChemCatChem* **2018**, *10*, 4931-4940.

[14] Guo, J.; Zhang, R.; Ouyang, J.; Zhang, F.; Qin, F.; Liu, G.; Zhang, W.; Li, H.; Ji, X.; Jia, X. Stereodivergent synthesis of carveol and dihydrocarveol through ketoreductasesene-reductases catalyzed asymmetric reduction. *ChemCatChem* **2018**, *10*, 5496-5504.

[15] Stueckler, C.; Mueller, N.J.; Winkler, C.K.; Glueck, S.M.; Gruber, K.; Steinkellner, G.; Faber, K. Bioreduction of α-methylcinnamaldehyde derivatives: Chemo-enzymatic asymmetric synthesis of Lilial. and Helional. *Dalton Trans.* **2010**, *39*, 8472-8476.

[16] Bryan, M.C.; Dunn, P.J.; Entwistle, D.; Gallou, F.; Koenig, S.G.; Hayler, J.D.; Hickey, M.R.; Hughes, S.; Kopach, M.E.; Moine, G. Key Green Chemistry research areas from a pharmaceutical manufacturers' perspective revisited. *Green Chem.* **2018**, *20*, 5082-5103.

[17] Li, H.; Xiao, W.; Xie, P.; Zheng, L. Co-immobilization of enoate reductase with a cofactor-recycling partner enzyme. *Enzym. Microb. Technol.* **2018**, *109*, 66-73.

[18] Yoon, J.; Lee, S.H.; Tieves, F.; Rauch, M.; Hollmann, F.; Park, C.B. Light-harvesting dye-alginate hydrogel for solar-driven, sustainable biocatalysis of asymmetric hydrogenation. *ACS Sustain. Chem. Eng.* **2019**, *7*, 5632-5637.

[19] Guisán, J.M. Aldehyde-agarose gels as activated supports for immobilization-stabilization of enzymes. *Enzyme Microb. Technol.* **1988**, *10*, 375-382.

[20] Zucca, P.; Fernandez-Lafuente, R.; Sanjust, E. Agarose and its derivatives as supports for enzyme immobilization. *Molecules* **2016**, *21*, 1577.

[21] Fernández-Lorente, G.; Lopez-Gallego, F.; Bolivar, J.M.; Rocha-Martin, J.; Moreno-Perez, S.; Guisán, J.M. Immobilization of proteins on highly activated glyoxyl supports: Dramatic increase of the enzyme stability via multipoint immobilization on pre-existing carriers. *Curr. Org. Chem.* **2015**, *19*, 1-13.

[22] Dall'Oglio, F.; Contente,M.L.; Conti, P.;Molinari, F.;Monfredi,D.; Pinto,A.; Romano,D.; Ubiali,D.; Tamborini, L.; Serra, I. Flow-based stereoselective reduction of ketones using an immobilized ketoreductaseglucose dehydrogenase mixed bed system. *Catal. Commun.* **2017**, *93*, 29-32.

[23] Cassimjee, K.E.; Kadow, M.; Wikmark, Y.; Svedendahl Humble, M.; Rothstein, M.L.; Rothstein, D.M.; Bäckvall, J.-E. A general protein purification and immobilization method on controlled porosity glass: Biocatalytic applications. *Chem. Commun.* **2014**, *50*, 9134-9137.

[24] Thompson, M.P.; Derrington, S.R.; Heath, R.S.; Porter, J.L.; Mangas-Sanchez, J.; Devine, P.N.; Truppo, M.D.; Turner, N.J. A generic platform for the immobilisation of engineered biocatalysts. *Tetrahedron* **2019**, *75*, 327-334.

[25] Chaparro-Riggers, J.F.; Rogers, T.A.; Vazquez-Figueroa, E.; Polizzi, K.M.; Bommarius, A.S. Comparison of three enoate reductases and their potential use for biotransformations. *Adv. Synth. Catal.* **2007**, *309*, 1521-1531.

[26] Kohli, R.M.;Massey, V. The oxidative half-reaction of Old YellowEnzyme. *J. Biol. Chem.* **1998**, *273*, 32763-32770.

[27] Hulley, M.E.; Toogood, H.S.; Fryszkowska, A.; Mansell, D.; Stephens, G.M.; Gardiner, J.M.; Scrutton, N.S. Focused directed evolution of pentaerythritol tetranitrate reductase by using automated anaerobic kinetic screening of site-saturated libraries. *ChemBioChem* **2010**, *11*, 2433-2447.

[28] Orrego, A.H.; Romero-Fernández, M.; Millán-Linares, M.C.; Yust, M.M.; Guisán, J.M.; Rocha-Martin, J. Stabilization of enzymes by multipoint covalent attachment on aldehyde-supports: 2-picoline borane as an alternative reducing agent. *Catalysts* **2018**, *8*, 333.

[29] Sheldon, R.A.; van Pelt, S. Enzyme immobilisation in biocatalysis: Why, what and how. *Chem. Soc. Rev.* **2013**, *42*, 6223-6235.

[30] EnginZyme: Enzyme Carrier, Biocatalysis Research. Available online: http://enginzyme.com/ (accessed on 30 January 2020).

[31] Mateo, C.; Palomo, J.M.; Fernandez-Lorente, G.; Guisán, J.M.; Fernandez-Lafuente, R. Improvement of enzyme activity, stability and selectivity via immobilization techniques. *Enzym. Microb. Technol.* **2007**, *40*, 1451-1463.

[32] Foley, A.M.; Maguire, A.R. The impact of recent developments in technologies which enable the increased use of biocatalysts. *Eur. J. Org. Chem.* **2019**, 3713-3734.

[33] Sheldon, R.A.; Brady, D. The limits to biocatalysis: Pushing the envelope. *Chem. Commun.* **2018**, *54*, 6088-6104.

[34] Bradford, M.M. A rapid and sensitive method for the quantitation of microgram quantities of protein utilizing the principle of protein-dye binding. *Anal. Biochem.* **1976**, *27*, 248-254.

[35] Chevallet, M.; Luche, S.; Rabilloud, T. Silver staining of proteins in polyacrylamide gels. *Nat. Protoc.* **2006**, *1*, 1852-1858.

Chapter 3

Continuous-flow biocatalytic process for the synthesis of the best stereoisomers of the commercial fragrances leather cyclohexanol (4-isopropylcyclohexanol) and woody acetate (4-(*tert*-butyl)cyclohexyl acetate)

Francesca Tentori [1], Elisabetta Brenna [1,2], Michele Crotti [1], Giuseppe Pedrocchi-Fantoni [2], Maria Chiara Ghezzi [1] and Davide Tessaro [1]

[1] Politecnico di Milano, Dipartimento di Chimica, Materiali e Ingegneria Chimica, via Mancinelli 7, Milano I-20131, Italy.

[2] Istituto di Chimica del Riconoscimento Molecolare - CNR, via Mancinelli 7, Milano I-20131, Italy.

Published in *Catalysts* **2020**, *10*, 102

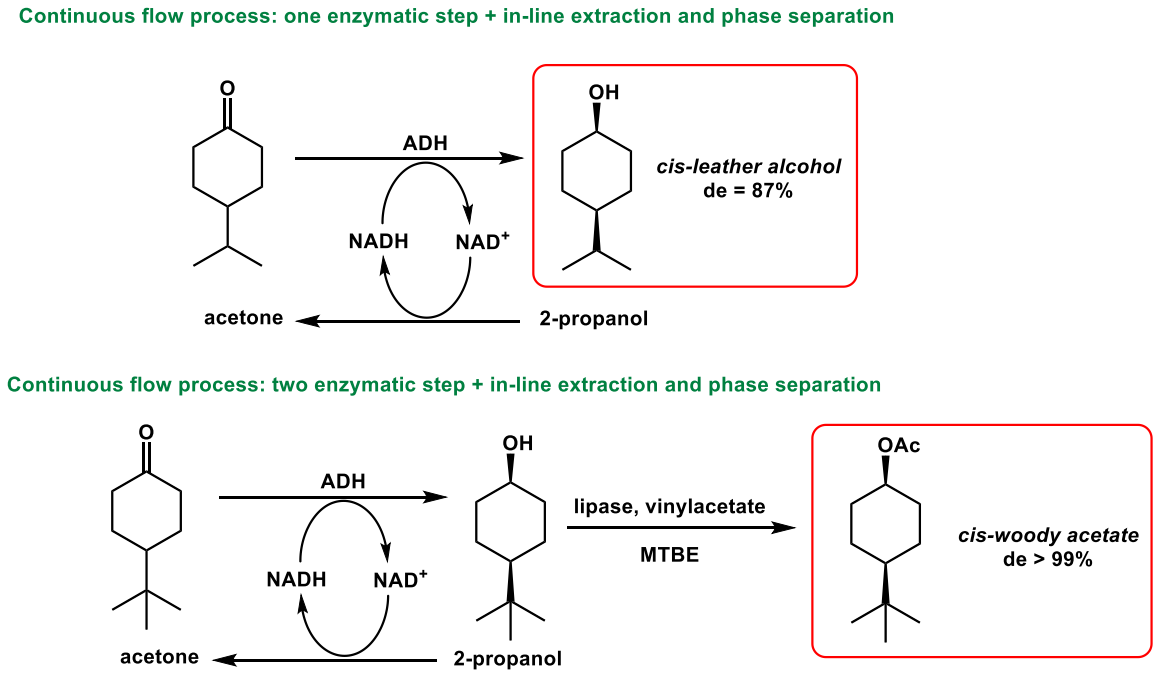

Introduction

Known respectively as leather cyclohexanol and woody acetate, 4-isopropylcyclohexanol (**1**) and 4-*tert*-butylcyclohexylacetate (**2**) (Figure 1) are commercialized as fragrance ingredients for applications in the field of functional perfumery, such as beauty care, soap, laundry care, and household products. The first (Apo Patchone Coeur - IFF; Folrosia - Givaudan) has a diffusive leathery and floral effect, reminiscent of lilac, rose and geranium [1], and it is generally available as a mixture of *cis* (25%-35%) and *trans*-diastereoisomers (65%-75%). The latter (Vertenex- IFF; Lorysia - Firmenich) is sweet, rich, floral, with woody-orris character [2], and it is usually sold as a sum of *cis*- (> 27%) and *trans*-isomers (69%-73%). Vertenex High Cis is also available with a minimum 68% of the *cis*-isomer, because *cis*-**2** has been found to show more valuable odor characteristics than the *trans*-isomer. It is very likely that the same difference does exist for compounds *cis*- and *trans*-**1**.

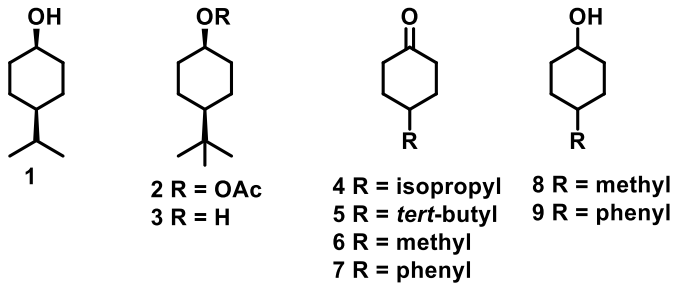

Figure 1. Chemical structures of leather cyclohexanol (**1**), woody acetate (**2**), and related compounds.

Mixtures of *cis*- and *trans*-4-alkylcyclohexanols **1** and **3** are usually obtained by liquid-phase hydrogenation of 4-alkylphenols over supported metal catalysts in organic solvent [3-5]. In these conditions, however, the thermodynamically more stable *trans*- isomer is also formed simultaneously, most frequently as the main product. Good stereoselectivity (*de* = 58%) towards *cis*-*tert*-butylcyclohexanol (**3**) was also obtained by the hydrogenation (H_2(g) p = 2 MPa) of 4-*tert*-butylphenol over a charcoal-supported rhodium catalyst at 313 K in supercritical carbon dioxide ($scCO_2$) as a solvent [6]. In a further development of this procedure, the addition of hydrochloric acid to the catalytic system was reported to be effective in controlling the stereoselectivity of 4-*tert*-isopropylphenol hydrogenation [7], and to afford *cis*-**1** with *de* = 76%. As for the reduction of the corresponding 4-alkylcyclohexanones **4** and **5**, the use of sterically hindered L-selectride in THF at

−78 ◦C was described by Brown [8] to afford *cis*-**3** with *de* = 93%. The effect of solvent on the stereoselectivity of cyclic ketone reduction by Al-isopropoxydiisobutylalane (DIBAiOPr) has been also investigated. In dichloromethane, DIBAiOPr behaves as a bulky reducing agent, and approaches the carbonyl group along an equatorial trajectory, affording *cis*-**3** with >10:1 stereoselectivity [9]. In 1999, Takasago patented a process for the production of *cis*-**3** with *de* = 90% by reduction of ketone **5** with rhodium based-catalysts under high temperature and pressure conditions in the presence of an alkali metal and an alkylenediamine [10]. To our knowledge, the only biocatalytic approach to alcohols **1** and **3** described in the literature is the reduction of ketones **4** and **5** mediated by horse liver dehydrogenase (HLDH) in the presence of stoichiometric NADH. Derivative *trans*-**1** (*de* = 48%) and *cis*-**3** (*de* = 94%) were obtained [11]. Since the availability of commercial ADHs has greatly increased during the last years, we undertook the investigation of these enzymes for the stereoselective reduction of ketones **4** and **5**, in order to achieve high selectivity values towards the corresponding *cis*-alcohols. The aim of the work was the development of a low energy procedure, operating at room temperature and pressure with renewable catalysts, as a sustainable alternative to known synthetic methods, based on either the use of metal catalysts under H_2 pressure or the employment of reducing agents in anhydrous inert solvents at low temperature, requiring troublesome work-up procedures. For woody acetate, the reduction step was combined with the lipase-mediated acetylation of *cis*-**3** to provide an all-enzymatic route to the fragrance. Furthermore, in order to meet the expectations of a new industrial culture demanding manufacturing processes characterized by flexibility, automation and interconnected production units [12,13], we took up the challenge to apply continuous-flow conditions to this biocatalytic procedure. While synthetic chemistry has been widely involved in flow-mode applications [14-16] in the past decade, biocatalysis has raised its attention to continuous-flow techniques only recently. Biocatalysis could greatly take advantage of this operational mode, especially when a multistep synthesis is involved. As a matter of fact, very different, even incompatible, reaction conditions may be controlled and optimized separately, thus making the coupling of chemical and biocatalytic steps easier. Then, the possibility to couple reaction steps with in-line work-up reduces waste and operational complexity in recovering the intermediate to be submitted to the subsequent reaction step [17-20]. Thus intrigued by the great opportunities that flow chemistry delivers to the future of industrial biocatalysis, in this work, we describe the optimization of a highly selective preparation of *cis*-4-alkylcyclohexanols, employing *cis*-**1** and *cis*-**3** as model target compounds showing commercial interest in the field of synthetic fragrances. We present the development of a continuous-flow process also for *cis*-**2**, based on a two-step all-enzymatic

procedure, as a case study involving some experimental hurdles, such as the handling of the strongly insoluble ketone **5** and the necessity to combine two reactions (ADH-reduction and lipase-mediated acetylation) characterized by rather incompatible experimental conditions.

Results and Discussion

Screening of ADH-mediated Reduction of 4-alkycyclohexanones 4-7

The biocatalytic reduction of differently substituted 4-alkylcyclohexanones by ADHs has been rarely documented [11]. With the aim of finding an enzyme providing complete reduction to the corresponding *cis*-diastereoisomer and, at the same time, of better understanding the influence of the substituent in position 4, the four commercially available compounds **4**-**7** were submitted to ADH-mediated reduction, using a commercial kit of 18 enzymes. NAD(P)H cofactor was employed in catalytic amount and regenerated using glucose dehydrogenase (GDH from Bacillus megaterium), in the presence of glucose as a sacrificial cosubstrate. DMSO was employed as a cosolvent. For each ADH, the optimal pH value suggested by the producer was employed. The product distribution after 18 h reaction time was determined by GC/MS analysis. Considering that, in general, at least half of the ADHs of the kit were almost ineffective, we gathered the best results in Figure 2, providing conversions and diastereoisomeric excess (*de*) values for the reactions mediated by the six most active ADHs (EVO30, 200, 441, 270, 420, 440) in 18 h reaction time. The complete results of this screening are reported in Table S1 and Table S2 in Supplementary Information (Appendix *Chapter 3*). These results show a broad variety of behavior in terms of conversion and diastereoisomeric excess. As a general view, ketone **6**, bearing the smallest substituent (methyl) in position 4, was modestly accepted by most of the ADHs of the kit, hardly reaching a conversion of 80% in most cases. With the other substituents, although much bulkier than methyl, conversions were surprisingly almost complete when submitted to the most active ADHs. More interestingly, with five of the six most active ADHs (EVO30, 200, 441, 270, 420), the thermodynamically less stable *cis* isomers of the four alcohols were obtained, providing in general good de values. In particular, in the reduction of substrates **4** and **5**, ADHs EVO30, 200, 441, 270 and 420 afforded complete reduction with the formation of *cis*-**1** and *cis*-**3** showing *de* = 72%-88% and 66%-99%, respectively. ADH 440 completely reduced both **4** and **5** to the *trans* isomer with *de* = 87% and >99%, respectively. The other twelve ADHs reduced the two substrates with modest conversions, to afford mixtures of the two isomers (data reported in the Supplementary Information, Appendix *Chapter 3*).

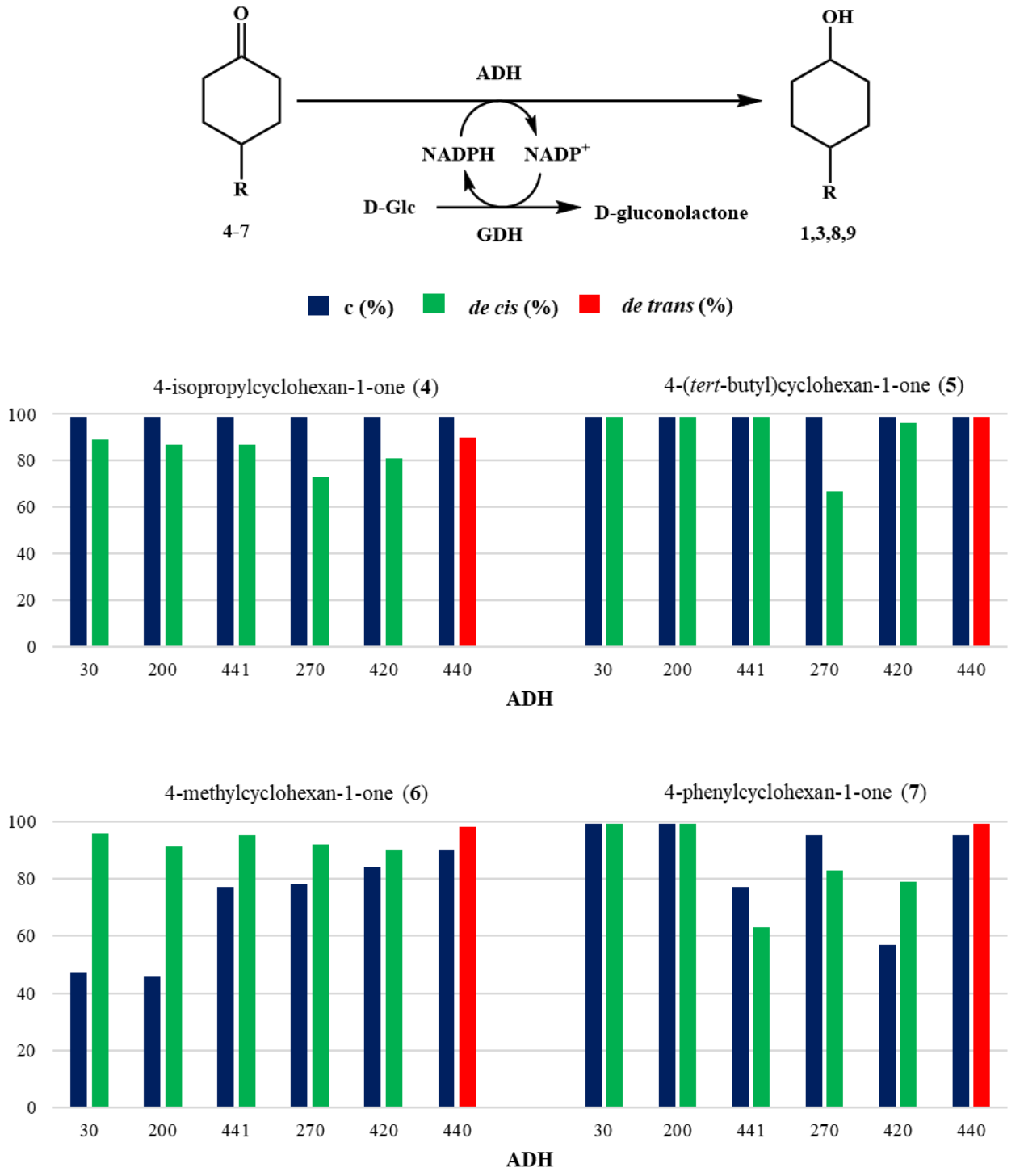

Figure 2. Screening of ADH-mediated reduction of 4-alkylcyclohexanones **4-7** to 4-alkylcyclohexanols **1,3,8,9**. Results are reported only for the six most performant ADHs (for the complete results see Supplementary Information in Appendix *Chapter 3*). 5 mM substrate, 20 mM glucose, ADH (200 μg mL $^{-1}$), GDH (5 UmL $^{-1}$), NADH and NADP^{+} (0.1 mmol each), 1% DMSO, phosphate buffer pH 7.0, 30°C, 18 h; conversion (c%) and diastereoisomeric excess (*de*%) calculated by GC/MS.

Screening of lipase-mediated Acetylation of cis-***3*** *to Afford Derivative* cis-***2***

After having obtained *cis*-**3** with high *de* value by ADH-mediated reduction, we thought to employ a second biocatalytic step to complete the synthetic approach to the corresponding high *cis*-acetyl ester derivative **2**, and obtain a product showing better olfactory properties than the commercial formulation, through an all-enzymatic procedure. The classical acetylation process employing acetic anhydride or acetyl chloride in organic solvent in the presence of an equimolar amount of pyridine or triethylamine is without any doubt economic and easy to perform but shows several negative effects on the sustainability of the reaction. Chlorinated solvents are usually employed with excess of acylating agents, and heating or long reaction time are required. The loss of one mol of either acetic acid or chloride per mol of ester, together with the loss of the tertiary base employed for its neutralization, negatively influences the atom economy of the transformation. Furthermore, the aqueous effluents coming from work-up have to be properly treated before final disposal. Thus, we investigated the lipase - mediated acetylation of derivative *cis*-**3** in methyl *tert*-butyl ether (MTBE) as a solvent, in the presence of vinyl acetate as an acyl donor [21,22] in 18 h reaction time. Five different lipases were tested, and *Candida antarctica* lipase A (CALA) was selected as the best performer (Table 1). CALA was found to be effective also in the acylation of *trans*-**3**, affording 85% conversion in 18 h reaction time.

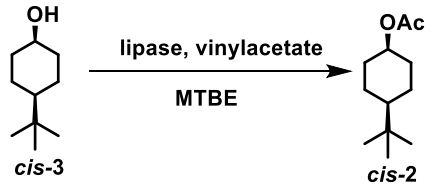

Lipase	Conversion (%)
Lipase PS	<1
Candida rugosa lipase	<1
CALA	79
CALB	35

Table 2. Screening of lipase-mediated acetylation of *cis*-**3**. 50 mg mL^{-1} substrate concentration, MTBE, vinyl acetate (10% v/v), lipase (10 mg mL^{-1}), 30 °C, 12 h. Conversion (c, %) calculated by GC/MS.

Semi-Preparative Scale Preparation of cis-***1*** *and* cis-***2*** *and Olfactory Evaluation*

In order to obtain an acceptable quantity of *cis*-**1** and *cis*-**2**, two semi-preparative reductions were carried out on 500 mg of ketones **4** and **5**. 2-Propanol was used not only as a co-solvent, but also to regenerate the cofactor in the reduced form, thus avoiding the recycling system based on GDH and glucose employed in preliminary investigations. Substrates **4** and **5** were dissolved in 2-propanol (2.2 mL on a total volume of 40 mL), using ADH 200 as a catalyst (10 mg), in the presence of a catalytic quantity of NADH (10 mg). After complete conversion in 24 h reaction time, derivatives *cis*-**1** (*de* = 87%) and *cis*-**3** (*de* > 99%) were isolated in 91 and 95% yield, respectively, by filtration of the enzyme and solvent removal by in vacuo distillation. Alcohol *cis*-**3** (450 mg) was submitted to CALA-mediated acetylation (150 mg), in MTBE as a solvent (9 mL), in the presence of vinyl acetate (1 mL). Acetylation was complete after 24 h and acetate derivative *cis*-**2** was obtained in 95% isolated yields and high diastereoisomeric purity (*de* > 99%). The same procedure was used for a semi-preparative production of the *trans* isomers of compounds **1** and **3**. In this case, ADH 440 was employed, being the only active ADH providing quantitative conversion into the *trans* isomers. *Trans*-**3** was then converted into *trans*-**2** by CALA-mediated acetylation. The samples of *cis*- and *trans*-**1** and *cis*- and *trans*-**2** were submitted to bulb-to-bulb distillation, then their odor properties were evaluated by professional perfumers at Givaudan. The results are reported in Table 3.

Compound (*de* %)	Odor threshold (ng L^{-1} air)	
cis-**1** (86)	13	floral animalic, phenolic - leathery earthy, tea tree, p-cresol, green, folrosia, slightly medicinal
trans-**1** (86)	63	floral animalic, leathery, green, folrosia, less green and leathery than the *cis*-isomer, softer, more oily, and more pronounced floral.
cis-**2** (99)	14.8	floral fruity, reminiscent of red fruits, red berries, dry, woody with aspects of Koavone and Isoraldein, and slight pear facets.
trans-**2** (99)	110	Floral, oily, muguet, slightly agrestic, clearly weaker than the *cis*-isomer

Table 3. Odor description of samples *cis*- and *trans*-**1,** *cis*- and *trans*-**2**.

The odor description highlights the difference between *cis* and *trans* isomers. *Cis*-**1** is almost five times more potent than *trans*-**1**, and for the two isomers of derivative **2** the difference in odor threshold is even much more pronounced.

Continuous-Flow Processes

The successive step was the optimization of these synthetic sequences in continuous-flow mode. Although the preferential way for implementing biocatalytic continuous-flow processes goes through biocatalyst immobilization with several positive effects on enzyme stability and reusability [23,24], we thought more convenient to avoid the immobilization of a commercial enzyme with unknown characteristics and limited availability. As an alternative to obtain enzyme confinement inside the process, an ultrafiltration system was adopted: a membrane entraps the enzyme inside the reactor (kept under stirring), while reagents and products are continuously moved in and out, according to the CSTR model. For the continuous-flow production of leather alcohol *cis*-**1** (Figure 3), a phosphate buffer solution (100 mM, pH 7) of ketone **4** (10 mM) and NADH (0.2 mM) was fed to a jacketed membrane reactor (12 mL) kept at 30 ◦C, at a flow rate of 200 μL min^{-1}. In order to achieve complete substrate dissolution, a high amount of 2-propanol (20%) was required. Among ADHs showing high selectivity for the *cis*-isomer, ADH200 was chosen for being active in presence of up to 30% 2-

propanol. Subsequently, 3 mg of ADH were loaded in the chamber and confined by a regenerated cellulose membrane (cut-off 5kDa). Complete conversion was reached at the reactor outlet after 60 min residence time. Then, the reaction solution was connected to an organic solvent flow at a flowrate of 200 μL min^{-1} by means of a tee piece assembly, to carry out in-line extraction. Hexane was chosen for this extraction process. As a matter of fact, high 2-propanol content represents an issue for phase separation through Zaiput® membrane devices: the highest the interfacial tension between the two phases, the more performant is the separation. Since a 20% of 2-propanol causes a drop in water surface tension [25], n-hexane (the most hydrophobic among common organic solvents, *i.e.*, the one with the highest interfacial tension with water) was found to be the best candidate for a satisfactory separation. The segmented water-hexane flow was then directed to Zaiput® system. The ^{1}H-NMR analysis of the hexane solution recovered from the in-line extraction showed the presence of 2% of the starting 2-propanol, besides the desired alcohol *cis*-**1**. Evaporation under reduced pressure gave compound *cis*-**1** with an isolation yield of 90%. In order to evaluate process stability, the enzymatic reduction was run for 24 h, showing after this period a slight decrease of conversion to a final value of 80% (GC/MS).

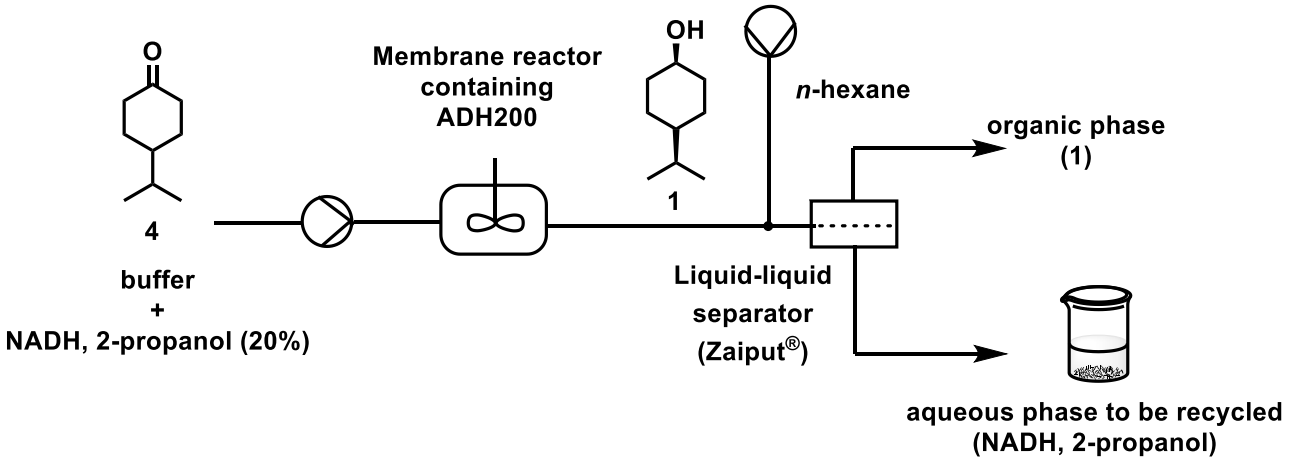

Figure 3. Continuous-flow process for the synthesis of leather alcohol *cis*-**1**.

In order to minimize NADH process consumption, we collected the corresponding aqueous phase (containing NADH and most of 2-propanol) with the aim to verify whether it could be recycled inside the system. Thus, after collection, the starting ketone **4** and the amount of 2-propanol lost with hexane extraction were added to the aqueous phase and the solution was re-fed to the membrane reactor. The aqueous phase recovered from extraction (100 mL) was submitted to enzymatic reduction and n-

hexane extraction twice for 8 h and no significant loss of conversion was observed, neither the first nor the second time. For the synthesis of acetate *cis*-**2** the first step of ketone reduction was performed according to the same conditions described for the conversion of derivative **4** into *cis*-**1** (Figure 4). The combination of this ADH-reduction with lipase-acetylation raised some concerns about the in-line work-up procedure, because the two enzymatic steps occur in different reaction media (respectively buffer and organic solvent), and, moreover, 2-propanol (used in high amount in the first step) is detrimental to CALA [26] and competes with *cis*-**3** in the acetylation reaction. However, the in-line hexane extraction described for compound *cis*-**1** was found to be effective also in this case to solve these issues. In-line separation made the organic phase easily available for the subsequent enzymatic acetylation, with most of 2-propanol remaining in the water phase. Aqueous and organic phases were mixed by using a segmented biphasic flow, and phase separation was achieved using a commercial in-line membrane separator Zaiput®. Vinyl acetate was added after phase separation (100 µL min^{-1}).

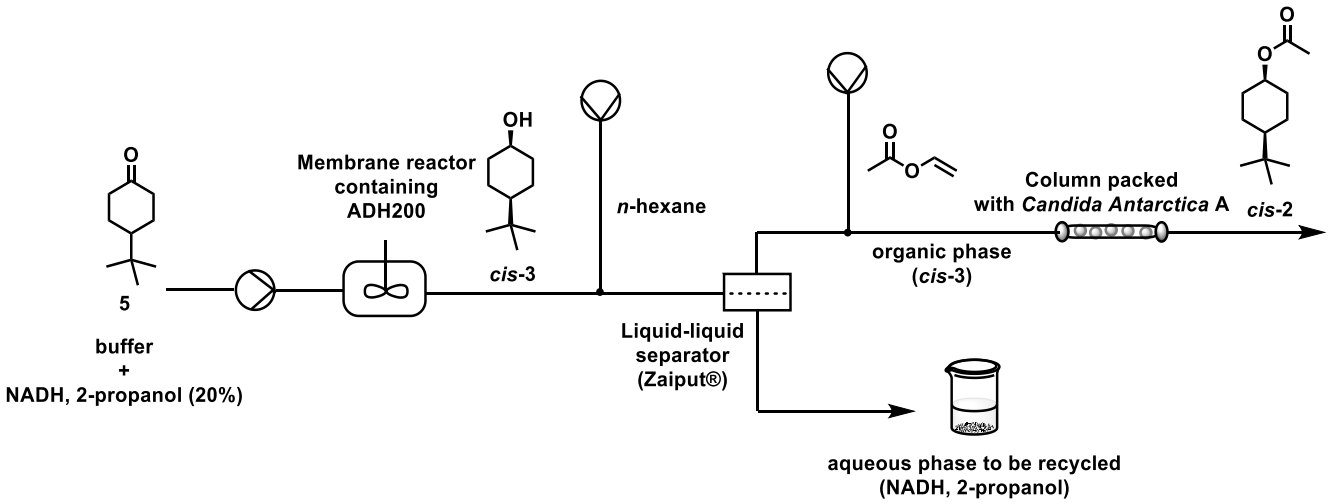

Figure 4. Continuous-flow process for the synthesis of woody acetate *cis*-**2**.

For the enzymatic acetylation of compound *cis*-**3**, the commercial form of CALA, which is sold as an immobilized enzyme, allowed us to easily set up a packed bed reactor (PFR-like reactor). The column reactor was filled with 500 mg of CALA, which had been previously swelled overnight in hexane. The acetylation step provided 85% conversion (GC/MS) of *cis*-**3** into *cis*-**2** at the outlet with a residence time of 11 min: acetate derivative *cis*-**2** was recovered by solvent evaporation with an isolated yield of 81%. Also, in this case, as already described for the production of alcohol **1**, the aqueous phase containing NADH and most of 2-propanol was collected and, after substrate **5**

addition, reused in the membrane reactor. When the whole process was run for 24 h, the conversion of ketone **5** into alcohol *cis*-**3** slightly decreased to a final value of 80% (GC/MS), while lipase acetylation maintained a constant value of 85% (GC/MS) for all the reaction time.

Conclusions

Advantages connected to enzymatic transformations for the stereoselective production of fine chemicals are well established. In the field of functional perfumery, the availability of inexpensive and sustainable synthetic methods to the most odorous isomers of commercial fragrances is appreciated, not only to help reduce the environmental burden of manufacturing routes, but also to make available more performant products that can be employed in lower amounts in final products. We report herein the case of leather alcohol and woody acetate: the odor thresholds of *cis*-isomers are respectively 5 and 10 times lower than those of the *trans*-isomer but, unfortunately, being less thermodynamically stable, they are hardly formed by reduction of the corresponding ketones with traditional reagents. The most selective chemical synthetic routes to *cis*-enriched samples reported in the literature are characterized by high environmental impact or delicate reaction conditions. For this reason, we wanted to explore alcohol dehydrogenases as a possible tool for a greener and more selective production of these two commercial fragrances. By submitting ketones **4** and **5** to ADHs from a commercial kit, we found that some of these enzymes were exceptionally active in providing the corresponding *cis* alcohols with high conversions (up to 99%) and high *de* values (up to 99%). In particular, ADH200 was selected for the preparation of *cis*-**1** and **3** with *de* = 87% and > 99%, respectively. We successfully tested also 4-methyl- and 4-phenyl-cyclohexanone (6, 7) to verify whether the same ADHs could be used on a wider range of differently substituted cyclohexanones (conversions: 85%-99%; *cis*-isomer *de*: 90%-99%). Focusing on compound *cis*-**2**, we were able to select a second enzymatic step for acetylation of *cis*-**3** (through lipase CALA in the presence of vinyl acetate), finally achieving a complete enzymatic synthesis of *cis*-**2** (*de*>99%) from ketone **5**. To meet the demand of more efficient and automatic processes, we designed a completely continuous-flow process both for *cis*-**1** and *cis*-**2**. We could couple in line enzymatic reduction and in line work-up for *cis*-**1**, with completely automatic synthesis and easy recovery of the product. Concerning production of *cis*-**2**, two biocatalytic reactions, requiring almost incompatible conditions, were successfully coupled. The continuous flow process allowed us, by means of in-line extraction and phase separation, to obtain the final product without intermediate isolation. Furthermore, processes were shown to be conveniently stable for 24 h in terms of conversion, confirming the potential of flow chemistry for biocatalytic applications.

References

[1] Available online: http://www.thegoodscentscompany.com/data/rw1001961.html (accessed on 1 December 2019).

[2] Available online: http://www.thegoodscentscompany.com/data/rw1001372.html (accessed on 1 December 2019).

[3] Murugesan, K.; Senthamarai, T.; Alshammari, A.S.; Altamimi, R.M.; Kreyenschulte, C.; Pohl, M.-M.; Lund, H.; Jagadeesh, R.V.; Beller, M. Cobalt-nanoparticles catalyzed efficient and selective hydrogenation of aromatic hydrocarbons. *ACS Catal.* **2019**, *9*, 8581-8591.

[4] Nie, Y.; Jaenicke, S.; van Bekkum, H.; Chuah, G.-K. Stereoselective cascade hydrogenation of 4-*tert*-butylphenol and *p*-cresol over Zr-zeolite beta-supported rhodium. *J. Catal.* **2009**, *246*, 223-231.

[5] Tan, S.-L.; Liu, G.-B.; Gao, X.; Thiemann, T. Raney Ni-Al alloy-mediated reduction of alkylated phenols in water. *J. Chem. Res.* **2009**, *2009*, 5-7.

[6] Hiyoshi, N.; Rode, C.V.; Sato, O.; Tetsuka, H.; Shirai, M. Stereoselective hydrogenation of *tert*-butylphenols over charcoal-supported rhodium catalyst in supercritical carbon dioxide solvent. *J. Catal.* **2007**, *252*, 57-68.

[7] Hiyoshi, N.; Sato, O.; Yamaguchi, A.; Rode, C.V.; Shirai, M. Kinetic analysis of 4-isopropylphenol hydrogenation over activated carbon-supported rhodium catalysts in supercritical carbon dioxide solvent. *Green Chem.* **2012**, *14*, 633-638.

[8] Brown, H.C.; Krishnamurthy, S.J. Lithium tri-*sec*-butylborohydride. A new reagent for the reduction of cyclic and bicyclic ketones with super stereoselectivity. A remarkably simple and practical procedure for the conversion of ketones to alcohols in exceptionally high stereochemical purity. *J. Am. Chem. Soc.* **1972**, *94*, 7159-7161.

[9] Bahia, P.S.; Jones, M.A.; Snaith, J.S. Al-isopropoxydiisobutylalane: a study of the effect of solvent on the rate and stereoselectivity of cyclic ketone reduction. *J. Org. Chem.* **2004**, *69*, 9289-9291.

[10] Emura, M.; Toyoda, T.; Seldo, N.; Ikariya, T.; Ohkuma, T. Process for producing *cis*-4-t-butylcyclohexanol. U.S. Patent No. 5,856,590, 5 January 1999.

[11] van Osselaer, T.A.; Lemière, G.L.; Lepoivre, J.A.; Alderweireld, F.C. Enzymatic in vitro reduction of ketones VI (1) reduction rates and stereochemistry of the HLAD-catalyzed reduction of 3-alkyl- and 4-alkylcyclohexanones. *Bull. Soc. Chim. Belg.* **1980**, *89*, 133-149.

[12] Fitzpatrick, D.E.; Ley, S.V. Engineering chemistry for the future of chemical synthesis. *Tetrahedron* **2018**, *74*, 3087-3100.

[13] Poechlauer, P.; Colberg, J.; Fisher, E.; Jansen, M.; Johnson, M.D.; Koenig, S.G.; Lawler, M.; Laporte, T.; Manley, J.; Martin, B. Pharmaceutical roundtable study demonstrates the value of continuous manufacturing in the design of greener processes. *Org. Process Res. Dev*. **2013**, *17*, 1472-1478.

[14] Bennett, J.A.; Campbell, Z.S.; Abolhasani, M. Role of continuous flow processes in green manufacturing of pharmaceuticals and specialty chemicals. *Curr. Opin. Chem. Eng*. **2019**, *26*, 9-19.

[15] Rossetti, I.; Compagnoni, M. Chemical reaction engineering, process design and scale-up issues at the frontier of synthesis: flow chemistry. *Chem. Eng. J*. **2016**, *296*, 56-70.

[16] Baumann, M.; Baxendale, I.R. The synthesis of active pharmaceutical ingredients (APIs) using continuous flow chemistry. *Beilstein J. Org. Chem*. **2015**, *11*, 1194-1219.

[17] Farkas, E.; Oláh, M.; Földi, A.; Kóti, J.; Éles, J.; Nagy, J.; Gal, C.A.; Paizs, C.; Hornyánszky, G.; Poppe, L. chemoenzymatic dynamic kinetic resolution of amines in fully continuous-flow mode. *Org. Lett*. **2018**, *20*, 8052-8056.

[18] De Vitis, V.; Dall'Oglio, F.; Pinto, A.; De Micheli, C.; Molinari, F.; Conti, P.; Romano, D.; Tamborini, L. Chemoenzymatic synthesis in flow reactors: a rapid and convenient preparation of Captopril. *ChemistryOpen* **2017**, *6*, 668-673.

[19] Brahma, A.; Musio, B.; Ismayilova, U.; Nikbin, N.; Siegert, P.; Jeromin, G.E.; Ley, S.V.; Pohl, M. An orthogonal biocatalytic approach for the safe generation and use of HCN in a multistep continuous preparation of chiral *O*-acetylcyanohydrins. *Synlett* **2016**, *27*, 262-266.

[20] Delville, M.M.E.; Koch, K.; van Hest, J.C.M.; Rutjes, F.P.J.T. Chemoenzymatic flow cascade for the synthesis of protected mendelonitrile derivatives. *Org. Biomol. Chem*. **2015**, *13*, 1634-1638.

[21] Acetti, D.; Brenna, E.; Fuganti, C.; Gatti, F.G.; Serra, S. Enzyme-catalysed approach to the preparation of triazole antifungals: Synthesis of (−)-genaconazole. *Tetrahedron Asymmetry* **2009**, *20*, 2413-2420.

[22] Brenna, E.; Fuganti, C.; Gatti, F.G.; Parmeggiani, F. Enzyme-mediated synthesis of EEHP and EMHP, useful pharmaceutical intermediates of PPAR agonists. *Tetrahedron Asymmetry* **2009**, *20*, 2594-2599.

[23] Contente, M.L.; Farris, S.; Tamborini, L.; Molinari, F.; Paradisi, F. Flow-based enzymatic synthesis of melatonin and other high value tryptamine derivatives: A five-minute intensified process. *Green Chem*. **2019**, *21*, 3263-3266.

[24] Dall'Oglio, F.; Contente, M.L.; Conti, P.; Molinari, F.; Monfredi, D.; Pinto, A.; Romano, D.; Ubiali, D.; Tamborini, L.; Serra, I. Flow-based stereoselective reduction of ketones using an immobilized ketoreductase/glucose dehydrogenase mixed bed system. *Catal. Commun*. **2017**, *93*, 29-32.

[25] Vázquez, G.; Alvarez, E.; Navaza, J.M. Surface tension of alcohol + water from 20 to 50 ◦C. *J. Chem. Eng. Data* **1995**, *40*, 611-614.

[26] Yang, C.; Wang, F.; Lan, D.; Whiteley, C.; Yang, B.; Wang, Y. Effects of organic solvents on activity and conformation of recombinant *Candida antarctica* A produced by Pichia pastoris. *Process Biochem.* **2012**, *47*, 533-537.

Chapter 4

Chemo-enzymatic oxidative cleavage of isosafrole for the synthesis of piperonal

Francesca Tentori [1], Elisabetta Brenna [1,2], Chiara Ferrari [1], Francesco G. Gatti [1], Maria Chiara Ghezzi [1] and Fabio Parmeggiani [1]

[1] Politecnico di Milano, Dipartimento di Chimica, Materiali e Ingegneria Chimica, via Mancinelli 7, Milano I-20131, Italy.

[2] Istituto di Chimica del Riconoscimento Molecolare - CNR, via Mancinelli 7, Milano I-20131, Italy.

Published in *React. Chem. Eng.* **2021**

DOI: 10.1039/D1RE00173F

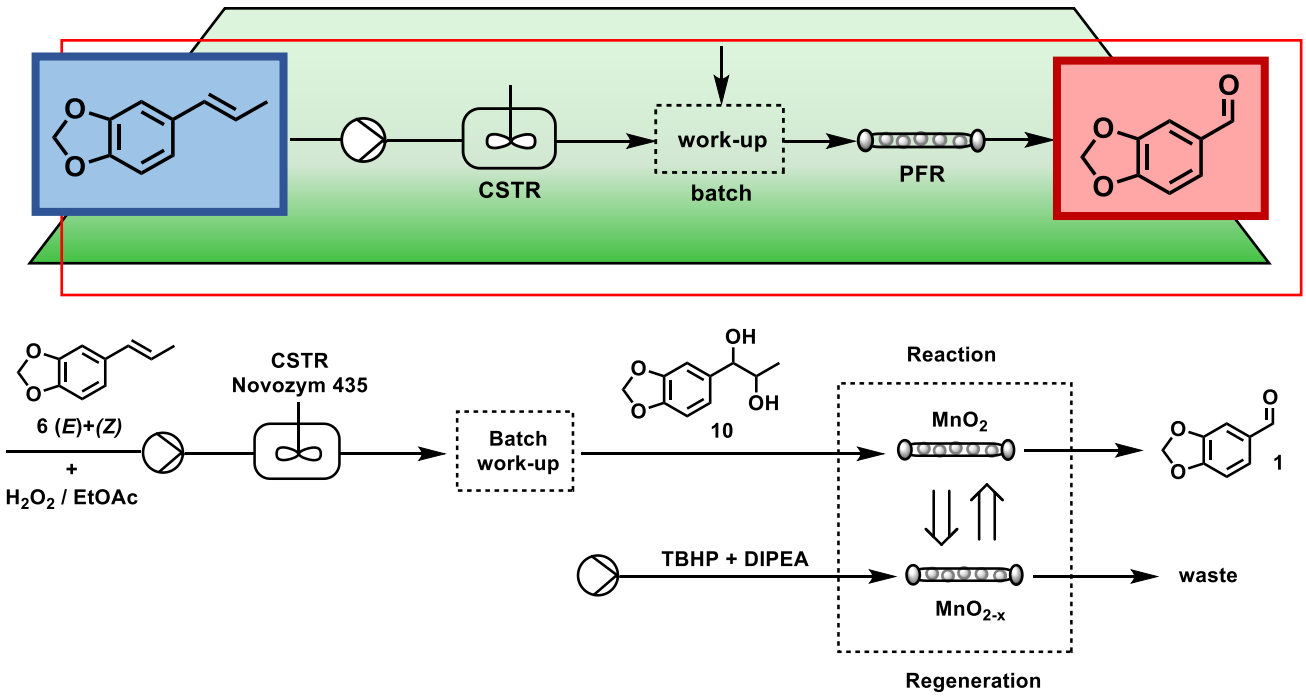

Introduction

Phenylpropenoids such as safrole, eugenol, and estragole are widespread in essential oils, representing a relevant and abundant class of renewable feedstock. Many commercial processes have been developed to isomerise them into their conjugated isomers, *i.e.* isosafrole, isoeugenol, and anethole, respectively, which are further transformed by oxidative cleavage into flavoring aromatic aldehydes, namely piperonal, vanillin and anisaldehyde [1,2]. In recent years the increasing attention gained by the concepts of green chemistry has promoted the investigation of more sustainable and energy-effective approaches for the synthetic exploitation of these plant-based starting materials [3,4].

One of these procedures is represented by the commercial process for the production of piperonal, also known as heliotropine (**1**, Figure 1), obtained by base-catalyzed isomerization of safrole (**2**) into isosafrole (**3**) and subsequent oxidation by treatment with either chromic acid [5] or ozone combined with sulfur or zinc reduction [6]. Isosafrole is not particularly abundant in nature, while safrole is extracted in high yield from the root-bark or the fruit of *Sassafras albidum* [7] or from *Ocotea odorifera* [8]. A more sustainable source is pimenta-longa (*Piper hispidinervium*), a pioneer shrub of Amazonian forest: the essential oil extracted from the leaves and thin branches contains 90−94% safrole [9].

Piperonal has a relevant role in the flavor industry, in spite of its rare occurrence in Nature. It resembles heliotrope flowers, being however absent in their natural scent. It is also reminiscent of hay and vanilla, with a marked floral, powdery edge [10]. Even though the odor of piperonal does not closely resemble that of coumarin, they both have in common the powdery note. This aspect makes piperonal a suitable candidate for the replacement of coumarin in flavor applications. Piperonal is widely employed in French-style vanilla flavors, in other closely related ‘brown’ flavors (toffee, caramel, butterscotch, chocolate, coffee), and in fruit and dairy flavors. It is also used as a scent in perfumes, candles, air fresheners, laundry products, deodorants, sunscreens, and mosquito repellents [11].

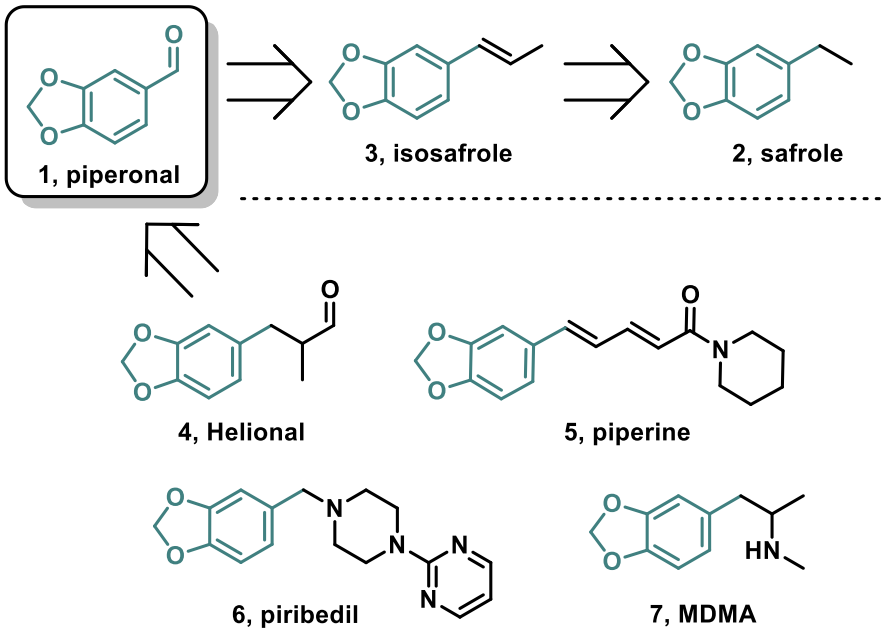

Figure 1. Piperonal (**1**) and related products.

Besides these applications due to its odor properties, piperonal is an essential starting material for the synthesis of a range of fine chemicals, such as the widely commercialized fragrance 3-(1,3-benzodioxol-5-yl)-2-methylpropanal (**4**, known as Helional or Tropional), the pungent, burning, and spicy flavoring ingredient piperine (**5**) [12], and the antiparkinsonian agent piribedil (**6**) [13]. Furthermore, a sadly notorious illegal use of piperonal is its conversion into the psychoactive drug 3,4-methylenedioxy-*N*-methylamphetamine (**7**, MDMA), which is under strict legal control in most of the world within the UN Convention on Psychotropic Substances and other international agreements [14]. Thus, the production, trading and storage of piperonal and of its precursors is obviously subject to stringent regulatory control in many countries.

Besides the commercial route from safrole, other synthetic methods have been studied, all starting from petroleum-based chemicals: (i) from 3,4-dihydroxybenzaldehyde, prepared from catechol [15] by alkylation with dichloro- or dibromomethane [16] in DMF solution in the presence of a suitable base; (ii) by oxidation of benzo[*d*][1,3]dioxol-5-ylmethanol (piperonol) [17], generally prepared by chloromethylation of 1,2-methylenedioxybenzene (another derivative of catechol), followed by hydrolysis [18]. Some enzymatic approaches have been investigated for the direct conversion of

isosafrole into piperonal [19]. Unfortunately, the development of a practical synthetic process based on such microbiological transformations is hampered by exceedingly low productivity values. The only promising procedure [20] is represented by a novel whole-cell process based on the use of engineered *Escherichia coli* co-expressing a suitably selected *trans*-anethole oxygenase mutant for the conversion of (*E*)-isosafrole into piperonal, and formate dehydrogenase for cofactor regeneration. After optimization, 96% yield (calculated only considering the (*E*)-isomer of starting isosafrole) was obtained with a space-time yield (STY) of 3.89 $g \cdot L^{-1} \cdot h^{-1}$. No isolation yield was reported in the paper.

We envisaged the possibility to optimize a new route for the conversion of both (*E*)- and (*Z*)-isosafrole into piperonal (Scheme 1). Isosafrole (**3**) was submitted to chemo-enzymatic epoxidation, using H_2O_2 as an oxidant, with concomitant partial *in situ* epoxide cleavage, to afford a mixture of epoxide **8**, monoacetate derivatives **9a,b**, and vicinal diol **10**, in varying relative concentrations depending on the peroxide addition method. Complete epoxide opening and ester saponification to diol **10**, followed by MnO_2 oxidation, afforded piperonal.

The enzyme-mediated epoxidation of isosafrole and the MnO_2 oxidation of the corresponding vicinal diol **10** were implemented in continuous-flow conditions to increase the productivity and stability of the overall process. A continuously-stirred tank reactor (CSTR) was employed for the first step, and a column reactor packed with activated MnO_2, regenerated by means of *tert*-butylhydroperoxide (TBHP) and *N*,*N*-diisopropylethylamine (DIPEA) in a plug-flow reactor mode, was developed for the final oxidative cleavage. The two steps were connected by the isolation of diol **10** after hydrolysis of the reaction mixture recovered from the epoxidation reaction.

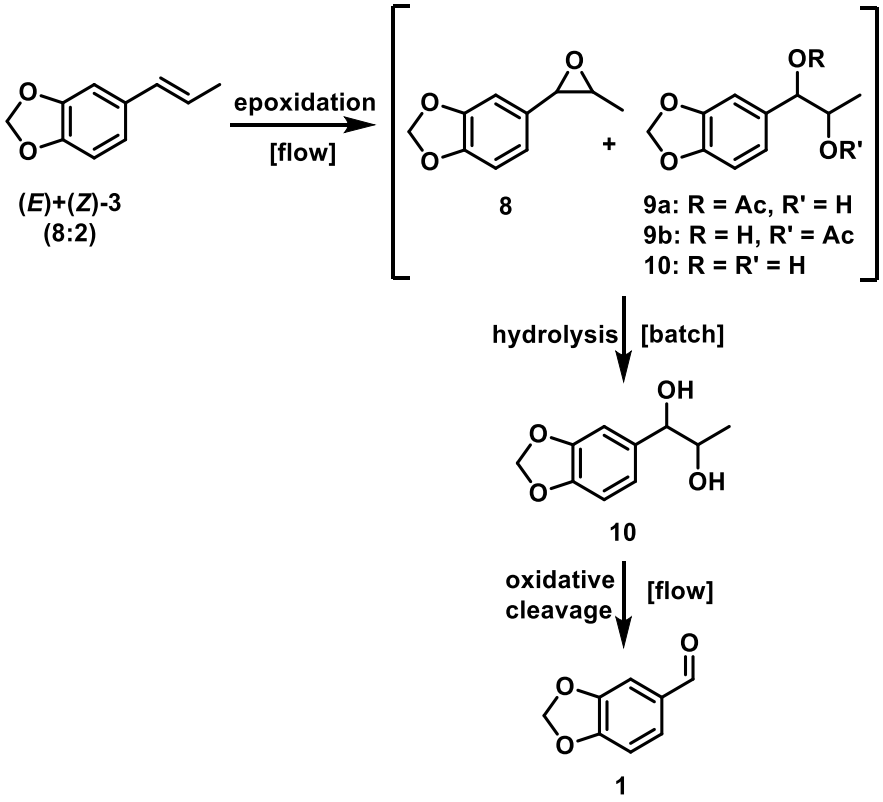

Scheme 1. Chemo-enzymatic conversion of isosafrole (**3**) into piperonal (**1**) described in this work.

Results and Discussion

Enzymatic epoxidation of isosafrole: preliminary batch experiments

The first step of our synthetic route is the epoxidation of isosafrole. According to the literature, the classical Prilezhaev epoxidation of isosafrole with *m*-chloroperbenzoic acid occurs reportedly with low yield (10%) [21] whereas the electrooxidation in MeCN-H_2O (7:2) containing 1.5-2.0 equiv. of sodium bromide at room temperature on platinum electrodes afforded a mixture of epoxide **8** (71%) and diol **10** (23%) [22]. In 2010, the reaction of isosafrole with hydrogen peroxide, catalyzed by methyltrioxorhenium, was described to give the corresponding epoxide (99 %, GC/MS analysis), using 3-methylpyrazole and 1-methylimidazole as additives to prevent ring opening and rearrangement [23].

We investigated an alternative approach, consisting in the Prilezhaev reaction of isosafrole performed under extremely mild conditions by employing a peroxycarboxylic acid obtained *in situ* by lipase-catalyzed perhydrolysis of the corresponding carboxylic acid in the presence of hydrogen peroxide. The application of this method of peroxyacid production in the epoxidation of alkenes was first described in 1990 by Björkling [24]. In this pioneering work, octanoic acid was employed to generate the peroxyacid, working in a water/toluene biphasic mixture as a solvent. Commercial immobilized lipase B from *Candida antarctica* (Novozym® 435) was found to have the highest perhydrolase activity among other conventional lipases. A further improvement of the procedure was reported in 2006 [25]: urea-H_2O_2 adduct (UHP) was employed in place of aqueous H_2O_2, and ethyl acetate was used as a solvent. The use of ethyl acetate, that can undergo lipase-mediated perhydrolysis releasing ethanol and peroxyacetic acid, avoided the need for octanoic acid or other carboxylic acids to promote the reaction.

Accordingly, it was decided to run preliminary experiments of isosafrole epoxidation (Scheme 2) in ethyl acetate, in the presence of either aqueous hydrogen peroxide or UHP to compare the two methods of H_2O_2 delivery, employing Novozym® 435 as a catalyst in batch conditions.

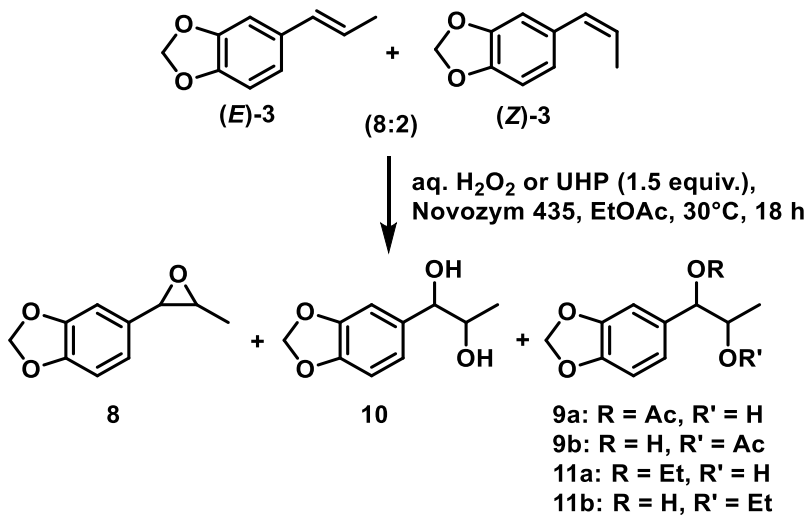

Scheme 2. Epoxidation of isosafrole in batch conditions (with either aq. H_2O_2 or UHP).

The two hydrogen peroxide sources were tested in parallel under the following general conditions: to a dispersion of 10 mg of Novozym® 435 in 15 mL of a 0.2 M solution of isosafrole in EtOAc, 1.5 equiv. of H_2O_2 were added, either as a 35% w/w aqueous solution or as UHP adduct. After 18 h at 30°C, the two reactions were submitted to work-up (addition of Na_2SO_3, then of $NaHCO_3$ sat. solution, followed by extraction with EtOAc) and were analyzed by GC/MS. Starting from commercial isosafrole, which is sold as a 8:2 mixture of (*E*)/(*Z*) diastereoisomers, all the reaction products 8-11 (Scheme 2) were mixtures of two diastereoisomers. The results are reported in Table 1.

[a] Reaction conditions: 10 mg of Novozym® 435, 15 mL of a solution of isosafrole (0.2 M) in EtOAc, 1.5 equivalents of H_2O_2, 18 h, 30 °C. [b] As sum of two diastereoisomers. [c] As sum of regio- and diastereoisomers.

H_2O_2 source	Isosafrole (**6**)[b]	Epoxide (**8**)[b]	Diol (**10**)[b]	Mono acetates (**9a**+**9b**)[c]	Monoethyl ethers (**11a**+**11b**)[c]
35% *w/w* aq. H_2O_2	7	18	7	62	6
UHP	6	88	0	6	0

Table 1. Product distributions obtained by batch epoxidation of isosafrole with either aq. H_2O_2 or UHP (percentage values from GC/MS analysis as mean value of two replicates)[a].

Notably, although isosafrole conversion seemed comparable in both cases, the distribution of products was found to be quite different. A clear prevalence of epoxide **8** was observed when UHP was supplied, while the use of 35% w/w H_2O_2 solution afforded monoacetate derivatives **9a,b** as the main products. The formation of the latter compounds was ascribed to acid hydrolysis of the intermediate epoxide, followed by lipase- mediated esterification. On the other hand, when UHP was employed, no water was present in the reaction medium and **8** resulted therefore more stable.

Conveniently, both the epoxide and the monoacetate derivatives can be easily converted into the corresponding vicinal diol **10**, the key intermediate for completing the oxidative cleavage to piperonal. Thus, in spite of its wider distribution of reaction products, aqueous H_2O_2 solution was chosen for further development, being more easily handled in continuous flow conditions. The treatment of the corresponding epoxidation mixture with methanolic KOH completed oxirane ring cleavage and promoted monoacetate hydrolysis. Under these conditions, the only real by-products were ethyl ethers **11a,b** (formed upon oxirane ring opening by ethanol released from perhydrolysis of EtOAc) and unreacted isosafrole diastereoisomers, all present in minor amounts. After trituration with hexane/EtOAc 8:2 of the residue recovered from alkaline hydrolysis, a 3:1 mixture of (*R*,S**)- and (*R*,R**)-**10** (Scheme 3) could be recovered in 69% overall isolation yield (corresponding to 0.400 g of product). The relative configuration of the two diastereoisomers of diol **10** was established on the basis of the fact that the starting isosafrole was enriched in the (*E*)-stereoisomer and that the hydrolytic epoxide cleavage occurs with *anti* mechanism.

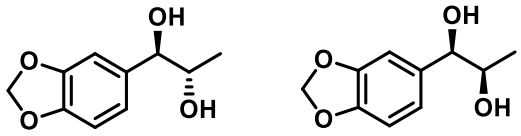

Scheme 3. Diols (*R**,*S**)- and (*R**,*R**)-**10** isolated after H_2O_2 epoxidation of isosafrole and hydrolysis of the reaction mixture with KOH in methanol.

Attempts to recover and recycle the immobilised lipase failed: nearly complete enzyme deactivation was observed within 18 h reaction time.

Enzymatic epoxidation of isosafrole: from batch to continuous-flow conditions

Continuous-flow approach has been increasing in popularity also among biocatalysis specialists [26]. In particular, lipase-mediated epoxidation under flow conditions has been already extensively studied and described by Meyer-Waßewitz [27] for α-pinene, and the beneficial effects of this technique evaluated in depth. At the end of their analysis, the authors concluded that the best technological solution for this kind of reaction was a continuously-stirred tank reactor (CSTR), employing a saturated solution of H_2O_2 in EtOAc, instead of aqueous H_2O_2. On the basis of these reports, we chose to adopt the same strategy and investigate CSTR epoxidation of isosafrole as well. The flow modality was expected to increase process productivity [28-31], having usually a beneficial effect on mass transfer enhancement. Moreover, the possibility of prolonged operation in continuous mode enables the effective and simple re-use of the catalyst, generally with concomitant reduction of reaction time.

Before implementing the flow process, we decided to investigate the effect of the amount of enzyme and the concentration of isosafrole and H_2O_2 on the reaction course, with the aim of finding the most suitable operative batch conditions in a reaction time shorter than 18 h.

For the purpose, we adopted a factorial design (elaborated through Minitab) according to the design of experiments (DOE) approach: the total conversion of isosafrole into the corresponding transformation products (epoxide **8**, diol **10**, monoacetates **9a,b** and ethyl ethers **11a,b**) was considered as the system response (**9a,b** and **8** can be easily converted into diol **10** under alkaline conditions) and its variation was analysed within the domain of the three variables (for details see Experimental Part in Appendix *Chapter 4*).

In order to shorten reaction times, since Novozym® 435 is reported to work well at significantly high temperature, reactions were performed at 50°C and conversions were evaluated after 4 h. H_2O_2 in EtOAc at the suitable concentration was employed and prepared by dilution of a 3 M solution obtained by extraction of the commercial aq. H_2O_2 35% solution with EtOAc (see Experimental Part in Appendix *Chapter 4*).

The results obtained by factorial design analysis showed that (i) the concentration of the undesired monoethyl ethers **11a,b** was always low (approximately 10%) and only slightly affected by different reaction conditions: (ii) the conversion into diol **10**, epoxide **8** and monoacetates **9a,b** was strongly

disfavored by high concentration of isosafrole and was slightly to moderately increased by higher enzyme and H_2O_2 content. The optimal reaction conditions and the corresponding product distribution obtained by batch epoxidation of isosafrole after DOE optimization are reported in Table 2.

[a] As sum of two diastereoisomers. [b] As sum of regio- and diastereoisomers.

[Isosafrole]	32.4 g L^{-1}
Equiv. H_2O_2	3.0
[Enzyme]	1.33 g L^{-1}
T	55 °C
Reaction time	4 h
Product distribution	Isosafrole (**6**)[a]: 15%
	Epoxide (**8**)[a]: 15%
	Diol (**10**)[a]: 16%
	Monoacetates (**9a** + **9b**)[b]: 44%
	Monoethyl ethers (**11a** + **11b**)[b]: 10%

Table 2. Reaction conditions and product distribution obtained by batch epoxidation of isosafrole after DOE optimization (percentage values from GC/MS analysis as mean value of two replicates).

These conditions were successfully implemented in continuous-flow mode in a CSTR, charged with 45 mL reaction mixture and 60 mg of immobilized enzyme (1.33 g·L^{-1}), working under a flowrate value of 188 µL min^{-1} with a residence time of 4 h (the same value of the reaction time of batch experiments for DOE investigation). We tested also a lower flowrate (150 µL min^{-1}) increasing residence time to 5 h, but we did not observe any significant improvement of the conversion values (less than 5 %) and, moreover, the time necessary to reach the stationary state increased to more than 5 hours. Then, we considered convenient to keep the first tested residence time.

The reactor was kept at a constant temperature of 50°C. Being Novozym® 435 an immobilized enzyme, there was no need of ultrafiltration for enzyme confinement in the reactor. In order to prevent blockages by enzyme beads, a HPLC solvent filter was fitted at the end of the suction tube. The stationary state was reached after 5 h, with a conversion value of 80%. Sampling and analysis were

performed till 12 h: the conversion of the stationary state was maintained for 3 h, then a gradual deflection was observed until reaching the value 62 % in the last analysed sample (Figure 2). The reaction operation time was prolonged overnight without sampling and analysis: conversion was found to be 26 % in the solution collected from 12 to 24 h.

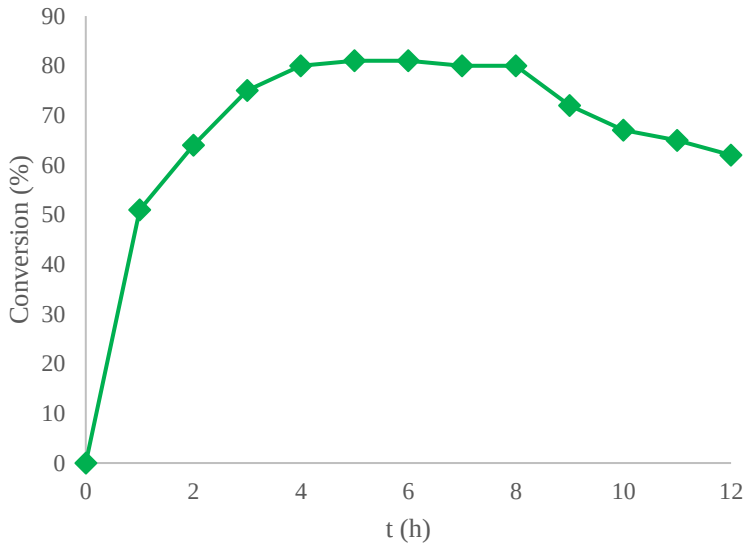

Figure 2. Conversion of isosafrole (by GC/MS) during 12 h continuous operating time of CSTR.

The reaction mixture collected at the outlet of the epoxidation reactor required further manipulation for the hydrolysis of monoacetate derivatives **9a,b** and the opening of the unreacted epoxide **8**. The fractions, characterized by a conversion value included in the range 62-81 % (from 2 to 12 h, 112.5 mL total volume), were collected, quenched first with Na_2SO_3, then with $NaHCO_3$ sat. solution, extracted with EtOAc, dried and submitted to solvent removal under reduced pressure. The crude reaction mixture was treated with methanolic KOH in batch conditions, to afford, after work-up, a residue containing 73% of diols (*R**,*S**)- and (*R**,*R**)-**10**, 20 % of starting isosafrole and 7 % of ethyl ethers **11a,b** (GC/MS). Trituration of the residue with hexane/EtOAc 8:2 afforded the 3:1 mixture of (*R**,*S**)- and (*R**,*R**)-10 in 68% overall isolation yield (corresponding to 3.0 g of product).

*Oxidative conversion of diol **10** into piperonal*

The synthesis of an aldehyde from a vicinal diol by oxidative cleavage is a highly sought-after reaction. Still nowadays, it is often performed using traditional oxidants, such as periodic acid or lead

tetraacetate, notwithstanding the high toxicity and critical waste disposal issues. However, efforts to optimize new procedures for vicinal diol oxidation have been carried out in parallel. Recently, a new protocol using graphitic carbon nitride with nitrogen vacancies as a metal-free recyclable photocatalyst in water solution in the presence of cetyltrimethylammonium bromide as surfactant, has been described [32], and an exhaustive overview of alternative metal-catalyzed procedures developed in the last decade is reported in the Introduction.

As for the oxidation of diol **10** to piperonal, an electrolytic process in benzene / 0.5% aq. NaOH (6:4) at 65°C was published in 1984 [33]. The electrochemical method was shown to be more advantageous than the classical chemical oxidation strategies (sodium periodate, cerium ammonium nitrate, or calcium hypochlorite). In 2004, Sumitomo patented a procedure for the oxidative cleavage of diols, including diol **10**, based on the use of bromine, or an inorganic bromine compound, in the presence of a Bi(III) compound, such as triphenylbismuthane, and of a base, such as potassium carbonate, in aqueous acetonitrile at 55°C [34].

An interesting, mild reaction for oxidative cleavage of vicinal diols was described in 1973 by Ohloff [35] using activated manganese dioxide in heterogeneous phase: the reactions proceeded to quantitative yield and good selectivity for many different cyclic compounds in dichloromethane at room temperature, showing as the main drawback the massive amount of MnO_2 needed to reach complete conversion (up to 20 equivalents). MnO_2 was studied under similar conditions by Outram in 2002 [36] by coupling MnO_2 oxidative cleavage of vicinal diols with a Wittig reaction, to the aim of preparing olefins directly from diols avoiding aldehyde isolation. The comparison between sodium periodate and manganese dioxide as reagents to achieve this cleavage proved MnO_2 a valid choice, especially for the oxidation of diols characterized by a benzylic OH group, providing in this case higher yields than $NaIO_4$. To the best of our knowledge, no other examples of MnO_2 oxidation of diols have been reported so far, probably because of the high excess of the oxidant required. As an alternative, Escande *et al.* in 2017 [37] developed a manganese layered mixed oxide, mainly containing MnO_2 (average oxidation state +3.7), that was used in catalytic amount to afford quantitative conversions of a range of different diols with benzylic OH groups into the corresponding aldehyde under aerobic conditions, using oxygen or air as stoichiometric oxidant.

MnO_2 is particularly attractive for its availability [38] and low toxicity [39]; moreover, the possibility to produce manganese oxides for organic synthesis applications by using Mn oxidizing bacteria has been recently reported in the literature [40]. This kind of research is very attractive and still in its

infancy. Thus, we considered worth doing a preliminary investigation of the efficiency of MnO_2 for the conversion of diol **10** into piperonal by using the commercial product, planning a future development of the procedure with such bacteria. The reaction of 200 mg of diol **10** with 10 equiv. of MnO_2 (890 mg) in 17 mL of dichloromethane afforded complete conversion to piperonal after 2 h at room temperature.

This reaction perfectly suited the conditions for the implementation of a continuous-flow process. Indeed, the literature provides several examples of the effective use of MnO_2 in continuous-flow conditions [41]. In most cases celite is used at the ends of the column as a filtering medium, enabling the construction of a simultaneous reaction/filtering unit and avoiding laborious batch filtering of heterogeneous systems at the end of the reaction.

We tested the same approach, packing a glass Omnifit column (6.6 mm i.d.) with 890 mg (10 equiv.) of MnO_2 (corresponding to a packed-bed length of approximately 1 cm) and a 1 cm plug of celite at each end. The solution of diol **10** in dichloromethane was flowed into the column at a flowrate of 200 µL min^{-1} (corresponding to a residence time of 1.7 min). Fractions of about 5 mL were collected to monitor the conversion. The first fraction showed complete conversion to piperonal, demonstrating the effectiveness of continuous system. MnO_2 was rapidly consumed and soon after the first fraction, conversion started to decline, reaching 27% at the third one.

The problem of regenerating MnO_2 when it is used as a stoichiometric reagent was faced also by Battilocchio *et al.* [42] and brilliantly solved by oxidizing spent MnO_2 using a solution of TBHP (4 M in decane, diluted to 0.24 M with DCM) and DIPEA, which allowed the reusability of the same column for three times. Thus, TBHP in decane represents, overall, the terminal oxidant of the reaction. We tested a similar system: after flowing a 0.06 M solution of diols **10** in DCM (200 mg in 17 mL DCM) for 85 min, the column was treated with a solution of TBHP and DIPEA as illustrated in reference 42 with a flowrate of 200 µL min^{-1}. The alternation between the reaction step (85 min) and the regeneration step (85 min) was carried out for 5 times. At any regeneration cycle, the first sample showed high conversion to piperonal (>90%) while at the third one conversion dropped to about 20%. All the fractions collected during the five-cycle experiment (corresponding to a final volume of 85 mL and 850 min reaction time) were collected and underwent solvent distillation under vacuum. The crude reaction mixture showed 60% of piperonal **1** and 40% of unreacted diols **10** (GC/MS). Piperonal was then recovered by column chromatography with an isolation yield of 52% (corresponding to 0.398 g).

We also tested ethyl acetate as an alternative solvent for the reaction. Batch and continuous-flow conditions showed similar performances to those obtained in DCM. Unfortunately, reactivation with TBHP/DIPEA in EtOAc as solvent failed, as shown in Figure 3.

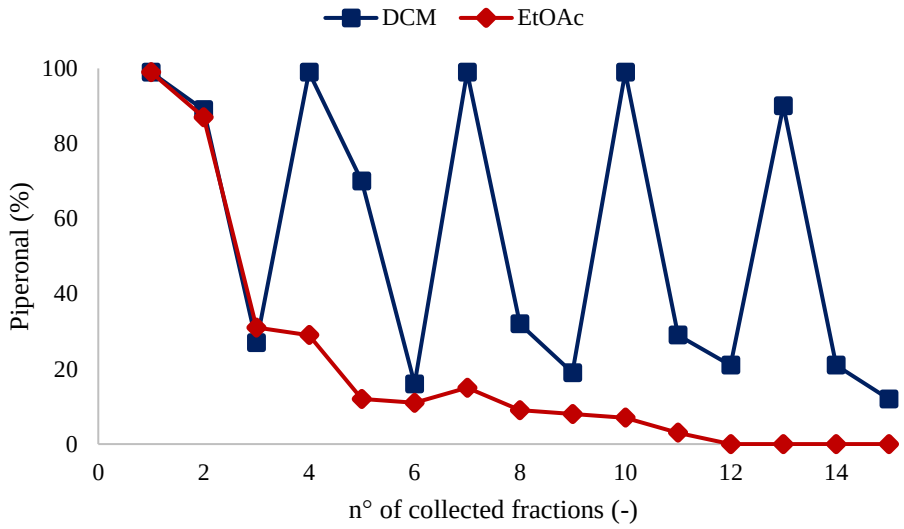

Figure 3. Percentage of piperonal (GC/MS) produced during continuous-flow MnO_2 oxidation of diol **10** with regeneration of the catalyst with TBHP and DIPEA after fractions **6, 9** and **12**.

Three-step synthesis of piperonal from isosafrole: batch versus *flow*

A flow diagram of the complete chemo-enzymatic process for the oxidative cleavage of **6** to piperonal is shown in Figure 4.

The epoxidation of isosafrole was implemented under continuous-flow conditions in a thermostated CSTR. To avoid the formation of aqueous/organic biphasic systems and limit miscibility problems in the reactor inlet lines a homogeneous solution of H_2O_2 in EtOAc was employed. The system was operated for 8 h with constant 80% conversion of isosafrole.

The amount of by-products **11a,b** remained nearly constant (10% by GC/MS analysis) during the whole process. After work-up and methanolic KOH treatment to complete epoxide **8** opening and hydrolyse monoacetate **9a,b**, total 4.02 g of starting isosafrole were transformed in 11 h using 60 mg of enzyme to produce 3.31 g of intermediate diol (*R**,*R**)-**10** (68% isolation yield, *de* = 50%). In order to compare the efficiency of flow and batch configurations in terms of yield, the STYs of the

two approaches [43] were calculated as amount of generated product per catalyst amount per time, and expressed in mmol g^{-1} h^{-1}:

$$\mathbf{STY_{batch}} = \frac{n_{\text{isosafrole}} \cdot C}{m_{\text{N435}} \cdot \Delta t} = 28 \text{ mmol } g^{-1}h^{-1}$$

$$\mathbf{STY_{flow}} = \frac{n_{\text{isosafrole}} \cdot C}{m_{\text{N435}} \cdot \Delta t} = 75 \text{ mmol } g^{-1}h^{-1}$$

$n_{\text{isosafrole}}$ = starting isosafrole amount (mmol); C = global conversion of isosafrole by GC/MS, excluding ethyl ethers (%); m_{N435} = enzyme load (g); Δt = reaction time (for batch) (h); τ = residence time (for flow) (h).

The following data were employed for the calculation of STY values:

(i) batch mode: 0.020 g Novozym® 435, 3 mmol isosafrole, reaction time 4 h, *C* = 75% (*i.e.* the results of DOE optimization);

(ii) continuous flow mode: 0.060 g Novozym® 435, 24.8 mmol isosafrole, residence time 4 h, *C* = 73% (considering a total reaction volume of 124 mL collected from 2 to 12 h continuous operation).

The last step of the procedure is the oxidation of intermediate diol **10** catalyzed by MnO_2, regenerated at the expense of TBHP in the presence of DIPEA. The following data were employed for the calculation of STY values:

(i) batch mode: 0.890 g MnO_2, 1.0 mmol diol, reaction time 2 h, *C* = 99%;

(ii) continuous flow mode: 0.890 g MnO_2, 5.0 mmol diol, residence time 0.028 h, C = 60% (after 5 reaction steps and 4 regeneration treatments).

$$\mathbf{STY_{batch}} = \frac{n_{\text{diol}} \cdot C}{m_{\text{MnO}_2} \cdot \Delta t} = 0.58 \text{ mmol } g^{-1}h^{-1}$$

$$\mathbf{STY_{flow}} = \frac{n_{\text{diol}} \cdot C}{m_{\text{MnO}_2} \cdot \tau} = 120 \text{ mmol } g^{-1}h^{-1}$$

n_{diol} = diol amount (mmol); C = conversion of diol **10** by GC/ MS (%); m_{MnO_2} = manganese dioxide load (g); Δt = reaction time (for batch) (h); τ = residence time (for flow) (h).

In both cases, the increase in STY is mainly due to the possibility to improve the amount of starting material converted per gram of catalyst. In the MnO_2 oxidation step, the positive effect on STY

observed in flow conditions could be ascribed not only to the regeneration of the catalyst, but also to the short residence time achieved with this configuration. Some considerations can be made by comparing this chemo-enzymatic procedure to the one using recombinant *trans*-anethole oxidase mutant (described in ref. 20), to convert the (*E*)-isomer of isosafrole in a single batch reaction to piperonal with a productivity of 3.89 g L^{-1} h^{-1} , *i.e.* 26 mmol L^{-1} h^{-1} . In our procedure both the isomers of isosafrole are transformed through three subsequent steps, characterized by the following STY values, calculated as mmoles of product per liter per hour for an easier comparison (see Experimental Part in Appendix *Chapter 4*): (i) batch epoxidation 38 mmol L^{-1} h^{-1}; (ii) hydrolysis of intermediate diol **10** 150 mmol L^{-1} h^{-1} ; (iii) batch MnO_2 oxidation 30 mmol L^{-1} h^{-1} . The least productive step, limiting the overall productivity of the process, was the oxidation of diol **10** to piperonal. This was the one gaining the highest advantage from the use of the continuous flow mode with concomitant cyclic regeneration of MnO_2.

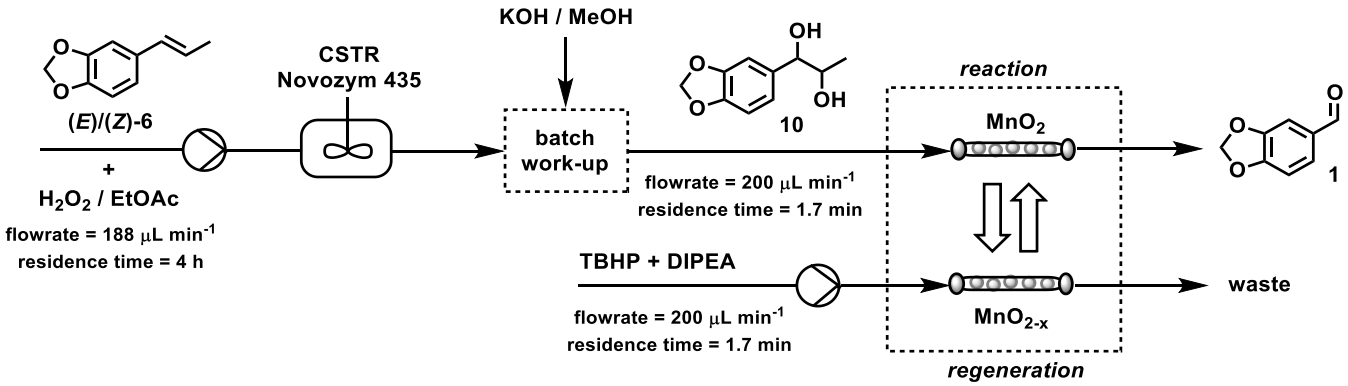

Figure 4. Flow diagram of the three-step chemo-enzymatic synthesis of piperonal (**1**) from isosafrole (**6**) developed in this work.

.

Conclusions

An innovative chemo-enzymatic synthesis of piperonal was developed starting from readily available isosafrole. The lipase-mediated perhydrolysis of EtOAc in the presence of H_2O_2 is an effective method to safely produce peracetic acid in the reaction medium, and promote isosafrole epoxidation, in both batch and flow conditions. Either aq. H_2O_2 35% w/w or sat. H_2O_2 solution in EtOAc can be employed to supply H_2O_2. In both cases, the presence of water, albeit in trace amounts in EtOAc, favours oxirane ring opening, which is soon followed by lipase-mediated esterification. The use of UHP is a suitable alternative to exclude water and preserve the epoxide derivative for other synthetic applications.

The stability of the chemo-enzymatic system decreased overnight, reaching conversions as low as 26% after 24 h, the main problem being enzyme deactivation due to the oxidative medium. The phenomenon is still present in the continuous-flow mode, though to a lesser extent with respect to batch reactions. The use of a homogeneous solution of reactants, with limited water content, possesses the advantage of avoiding high local concentration of H_2O_2 and of reducing interfacial deactivation of the enzyme.

The final oxidative cleavage of diol **10** to piperonal could be achieved in a packed bed reactor using MnO_2 as a catalyst which was periodically regenerated by treatment with TBHP and DIPEA in DCM. The flow configuration makes the work-up process rapid and clean, and reduces down-stream waste. The anhydrous TBHP in alkane solution employed in this application is commercially available only for small-scale laboratory use. However, being a powerful and versatile oxidizing agent in many chemical transformations, much effort is currently devoted to developing safe procedures for its production and storage. For example, recently, a membrane pervaporation method has been optimized [44] for the safer production of anhydrous TBHP in nonane solution in continuous manner, starting from 70% w/w TBHP in water, already manufactured in bulk quantities.

The use of biogenic manganese oxides, already successfully employed as bioremediation methods for the removal of toxic contaminants from the environment [45], is under investigation to improve the sustainability of the process even further. Unfortunately, the alkaline hydrolysis step was too laborious to be implemented in flow as a complete automatic three-steps system and we had to manually attend to the process for this step, that was performed in batch conditions. Nevertheless, the excellent results in terms of productivity and stability over time of enzymatic epoxidation and MnO_2

oxidation were very satisfactory and clearly demonstrated flow chemistry as a powerful tool also for the synthesis of piperonal from isosafrole, avoiding ozonolysis or the handling of peracids.

References

[1] Luu, T.X.T.; Lam, T.T.; Le, T.N.; Duus, F. Fast and green microwave-assisted conversion of essential oil allylbenzenes into the corresponding aldehydes via alkene isomerization and subsequent potassium permanganate promoted oxidative alkene group cleavage. *Molecules* **2009**, *14*, 3411-3424.

[2] Lummiss, J.A.M.; Oliveira, K.C.; Pranckevicius, A.M.T.; Santos, A.G.; dos Santos, E.N.; Fogg, D.E. Chemical plants: high-value molecules from essential oils. *J. Am. Chem. Soc.* **2012**, *134*, 18889-18891.

[3] Hassam, M.; Taher, A.; Arnott, G.E.; Green, I.R.; van Otterlo, W. A.L. Isomerization of allylbenzenes. *Chem. Rev.* **2015**, *115*, 5462-5569.

[4] Rajagopalan, A.; Lara, M.; Kroutil, W. Oxidative alkene cleavage by chemical and enzymatic methods. *Adv. Synth. Catal.* **2013**, *355*, 3321-3335.

[5] N. T. Farinacci, US Pat., US2794813, 1957.

[6] (a) H. E. Mains, US Pat., US3799940, Emery Industries Inc., 1974; (b) P. R. Story, E. A. Whited, J. A. Alford, W. C. Ray, W. C. Ray and J. R. Burgess, US Pat., US3862142, Research Corporation, 1975; (c) R. B. Long, C. E. Heath and V. Kevorkian, US Pat., US3160639, Esso Research and Engineering Company, 1964.

[7] Kamdem, D.P.; Gage, D.A. Chemical composition of essential oil from the root bark of *Sassafras albidum*. *Planta Med.* **1995**, *61*, 574-575.

[8] Almeida, R.S.; Freitas, P.R.; Araújo, A.C.J.; Alencar Menezes, I.R.; Santos, E.L.; Tintino, S.R.; Moura, T.F.; Filho, J.R.; Ferreira, V.A.; Silva, A.C.A.; Silva, L.E.; do Amaral, W.; Deschamps, C.; Iriti, M.; Melo Coutinho, H.D. GC-MS profile and enhancement of antibiotic activity by the essential oil of ocotea odorífera and safrole: inhibition of *Staphylococcus aureus* efflux pumps. *Antibiotics* **2020**, *9*, 247.

[9] Maia, J.G.S.; Andrade, E.H.A. Database of the Amazon aromatic plants and their essential oils. *Quim. Nova* **2009**, *32*, 595-622.

[10] Wright, J. Perfum. Flavor., 2015, 40.

[11] National Library of Medicine, Piperonal, https://pubchem.ncbi.nlm.nih.gov/compound/piperonal#section=Use-andManufacturing, (accessed 12 April 2021).

[12] Zviely, M. Perfum. Flavor., 2012, 37.

[13] Millan, M.M.; Cussac, D.; Milligan, G.; Carr, C.; Audinot, V.; Gobert, A.; Lejeune, F.; Rivet, J.-M.; Brocco, M.; Duqueyriox, D.; Nicolas, J.-P.; Boutin, J. A.; Newman-Tancredi, A. Antiparkinsonian agent

Piribedil displays antagonist properties at native, rat, and cloned, human α_2 -adrenoceptors: cellular and functional characterization. *J. Pharmacol. Exp. Ther.* **2001**, *297*, 876-887.

[14] National Institute on Drug Abuse, MDMA, https://www.drugabuse.gov/drugs-abuse/mdma-ecstasymolly, (accessed 12 April 2021).

[15] Umemura, S.; Takamitsu, N.; Enomiya, T.; Shiraishi, H.; Nakamura, T. US Pat., US4165341, Ube Industries Ltd., 1979.

[16] (a) Joshi, K.S.; Sivakumar, M.; Aware, V.S.; Wagh, V.S.; Deshpande, A.; Gangaram, A.G.; Sharma, S. WO2008/ 026125A2, Piramal Life Sciences Limited, 2008; (b) Oslob, J.; Anderson, R.; Aubele, D.; Evanchik, M.; Fox, J.C.; Kane, B.; Lu, P.; Mcdowell, R.; Rodriguez, H.; Song, Y.; Sran, A. WO2014/ 205223A1, Myokardia Inc., 2014.

[17] Lucarelli, C.; Lolli, A.; Giugni, A.; Grazia, L.; Albonetti, S.; Monticelli, D.; Vaccari, A. Efficient and ecofriendly route for the solvent-free synthesis of piperonal and aromatic aldehydes using Au/CeO_2 catalyst. *Appl. Catal. B* **2017**, *203*, 314-323.

[18] Borzatta, V.; Capparelli, E.; Gobbi, C.; Poluzzi, E. WO2005/ 042512, Endura S.p.A, 2005.

[19] (a) Santos, A.S.; Pereira Jr., N.; Da Silva, I.I.; Sarquis, M.I.; Antunes, O.A.C. microbiologic oxidation of isosafrole into piperonal. *Appl. Biochem. Biotechnol.* **2003**, *649*, 105-108; (b) Santos, A.S.; Pereira Jr., N.; Da Silva, I.I.; Sarquis, M.I.M.; Antunes, O.A.C. Peroxidase catalyzed microbiological oxidation of isosafrol into piperonal. *Process Biochem.* **2004**, *39*, 2269-2275; (c) Han, D.; Sandowsky, M.J.; Chong, Y.; Hur, H.-G. Characterization of a self-sufficient *trans*-anethole oxygenase from *Pseudomonas putida* JYR-1. *PLoS One* **2013**, *8*, e73350; (d) Lara, M.; Mutti, F.G.; Glueck, S.M.; Kroutil, W. Oxidative enzymatic alkene cleavage: indications for a nonclassical enzyme mechanism. *Eur. J. Org. Chem.* **2008**, *131*, 3668-3672; (e) Schwendenwein, D.; Fiume, G.; Weber, H.; Rudroff, F.; Winkler, M. Selective enzymatic transformation to aldehydes *in vivo* by fungal carboxylate reductase from *Neurospora crassa*. *Adv. Synth. Catal.* **2016**, *358*, 3414-3421; (f) Zhao, M.; Zheng, P.; Chen, P.; Liu, S. Biosynthesis of heliotropin by a novel strain of *Serratia liquefaciens*. *Appl. Biochem. Biotechnol*. **2017**, *183*, 1282-1294.

[20] (a) Han, D.; Kurusarttra, S.; Ryu, J.-Y.; Kanaly, R. A.; Hur, H.-G. Production of natural fragrance aromatic acids by coexpression of *trans*-anethole oxygenase and *p*-anisaldehyde dehydrogenase genes of *Pseudomonas putida* JYR-1 in *Escherichia coli*. *J. Agric. Food Chem.* **2012**, *60*, 11972-11979; (b) Wen, P.; Wu, D.; Zheng, P.; Chen, P.; Liu, S.; Fu, Y. highly efficient biosynthesis of heliotropin by engineered *Escherichia coli* coexpressing *trans*-anethole oxygenase and formate dehydrogenase. *J. Agric. Food Chem.* **2019**, *67*, 14121-14128.

[21] Nagashima, H; Sato, K.; Tsuii, J. Palladium-catalysed oxidation of alcohols with carbon tetrachloride, formation of 4,4,4-trichloro ketones from allylic alcohols and carbon tetrachlorid. *Tetrahedron* **1985**, *41*, 5645-5651.

[22] Torii, S.; Uneyama, K.; Ueda, K. Electrochemical procedure for a practical preparation of piperonal from isosafrole. *J. Org. Chem.* **1984**, *49*, 1830-1832.

[23] Yamazaki, S. An effective procedure for the synthesis of acid-sensitive epoxides: Use of 1-methylimidazole as the additive on methyltrioxorhenium-catalyzed epoxidation of alkenes with hydrogen peroxide. *Org. Biomol. Chem.* **2010**, *8*, 2377-2385.

[24] Björkling, F.; Godtfredsen, S.E.; Kirk, O. Lipase-mediated Formation of Peroxycarboxylic Acids used in Catalytic Epoxidation of Alkenes. *J. Chem. Soc. Chem. Commun.* **1990**, 1301-1303.

[25] Ankudey, E.G.; Olivo, H.F.; Peeples, T.L. Lipase-mediated epoxidation utilizing urea-hydrogen peroxide in ethyl acetate. *Green Chem.* **2006**, *8*, 923-926.

[26] (a) Britton, J.; Majumdar, J.; Weiss, G.A. Continuous flow biocatalysis. *Chem. Soc. Rev.* **2018**, *47*, 5891-5918; (b) Tamborini, L.; Fernandes, P.; Paradisi, F.; Molinari, F. Flow bioreactors as complementary tools for biocatalytic process intensification. *Trends Biotechnol.* **2018**, *36*, 73-88.

[27] (a) Meyer-Waßewitz, J.; Holtmann, D.; Ansorge-Schumacher, M.B.; Kraume, M.; Drews, A. An organic-single-phase CSTR process for the chemo-enzymatic epoxidation of α-pinene enables high selectivity and productivity. *Biochem. Eng. J.* **2017**, *126*, 68-77; (b) Meyer, J.; Horst, A.E.W.; Steinhagen, M; Holtmann, D.; Ansorge-Schumacher, M.B.; Kraume, M.; Drews, A. A continuous single organic phase process for the lipase catalyzed synthesis of peroxy acids increases productivity. *Eng. Life Sci.* **2017**, *17*, 759-767; (c) Meyer-Waßewitz, J.; Elyorgun, D.; Conradi, C.; Drews, A. Dynamic modeling of the chemo-enzymatic epoxidation of α-pinene and prediction of continuous process performance. *Chem. Eng. Res. Des.* **2018**, *134*, 463-475.

[28] Hugentobler, K.G.; Rasparini, M.; Thompson, L.A.; Jolley, K.E.; Blacker, A.J.; Turner, N.J. Comparison of a batch and flow approach for the lipase-catalyzed resolution of a cyclopropanecarboxylate ester, a key building block for the synthesis of Ticagrelor. *Org. Process Res. Dev.* **2017**, *21*, 195-199.

[29] Silva, M.V.M.; Bassut, J.F.; Junior, I.I.; de Souza, S.P.; Estrada, M.L.G.; Miranda, L.S.M.; de Souza, R.O.M.A. Lipase immobilization towards improved productivity on kinetic resolutions by a continuous-flow process. *RSC Adv.* **2015**, *5*, 102409-102415.

[30] Rao, N.N.; Lütz, S.; Würges, K.; Minör, D. Continuous biocatalytic processes. *Org. Process Res. Dev.* **2009**, *13*, 607-616.

[31] Wang, J.; Gu, S.-S; Cui, H.-S.; Wu, X.-Y.; Wu, F.-A. A novel continuous flow biosynthesis of caffeic acid phenethyl ester from alkyl caffeate and phenethanol in a packed bed microreactor. *Bioresour. Technol.* **2014**, *158*, 39-47.

[32] Niu, T.; Chen, S.; Hong, M.; Zhang, T.; Chen, J.; Donga, X.; Ni, B. Heterogeneous carbon nitride photocatalyst for C–C bond oxidative cleavage of vicinal diols in aerobic micellar medium. *Green Chem*. **2020**, *22*, 5042-5049.

[33] Torii, S.; Uneyama, K.; Ueda, K. Electrochemical procedure for a practical preparation of piperonal from isosafrole. *J. Org. Chem.* **1984**, *49*, 1830-1832.

[34] N. Takano and K. Hagiya, EP1609776B1, Sumitomo Chemical Company Limited, 2005.

[35] Ohloff, G.; Giersch, W. Conversion of vicinal diols into dicarbonyl compounds by manganese dioxide. *Angew. Chem. Int. Ed* **1973**, *12*, 401-402.

[36] Outram, H.S.; Raw, S.A.; Taylor, R.J. K. *In situ* oxidative diol cleavage-Wittig processes. *Tetrahedron Lett.* **2002**, *43*, 6185-6187.

[37] Escande, V.; Lam, C.H.; Coish, P.; Anastas, P.T. Heterogeneous sodium-manganese oxide catalyzed aerobic oxidative cleavage of 1,2-diols. *Angew. Chem. Int. Ed.* **2017**, *56*, 9561-9565.

[38] Dixon, J.B.; White, G.N. in "Soil mineralogy with environmental applications", ed. J. B. Dixon and D. G. Schulze, Soil Science Society of America, Inc., Madison, Wisconsin, USA, 2002, ch. 11, vol. 7, pp. 367-388.

[39] Gerber, G.B.; Léonard, A.; Hantson, P. Carcinogenicity, mutagenicity and teratogenicity of manganese compounds. *Crit. Rev. Oncol. Hematol.* **2002**, *42*, 25-34.

[40] Guo, J.; Guo, H.; Liu, J.; Zhong, F.; Wu, Y. Manganese(II) oxidizing bacteria as whole-cell catalyst for β-keto ester oxidation. *Int. J. Mol. Sci.* **2020**, *21*, 1709.

[41] (a) Scott, C.D.; Labes, R.; Depardieu, M.; Battilocchio, C.; Davidson, M.G.; Ley, S.V.; Wilson, C.C.; Robertson, K. Integrated plug flow synthesis and crystallisation of pyrazinamide. *React. Chem. Eng.* **2018**, *3*, 631-634; (b) Battilocchio, C.; Hawkins, J.M.; Ley, S.V. Mild and selective heterogeneous catalytic hydration of nitriles to amides by flowing through manganese dioxide. *Org. Lett.* **2014**, *16*, 1060-1063; (c) Lawrence, J.F.; Wong, B. Development of a manganese dioxide solid-phase reactor for oxidation of toxins associated with paralytic shellfish poisoning. *J. Chromatogr. A* **1996**, *755*, 227-233; (d) Glöckner, S.; Tran, D.N.; Inngham, R.J.; Fenner, S.; Wilson, Z.E.; Battilocchio, C.; Ley, S.V. The rapid synthesis of oxazolines and their heterogeneous oxidation to oxazoles under flow conditions. *Org. Biomol. Chem.* **2015**, *13*, 207-214.

[42] Tran, D.N.; Battilocchio, C.; Lou, S.-B.; Hawkins, J.M.; Ley, S.V. Flow chemistry as a discovery tool to access sp2-sp3 cross-coupling reactions via diazo compounds. *Chem. Sci.* **2015**, *6*, 1120-1125.

[43] Plutschack, M.B.; Pieber, B.; Gilmore, K.; Seeberger, P.H. The hitchhiker's guide to flow chemistry. *Chem. Rev.* **2017**, *117*, 11796-11893.

[44] Li, B.; Guinness, S.M.; Hoagland, S.; Fchtner, M.; Kim, H.; Li, S.; Maguire, R.J.; McWilliams, J.C.; Mustakis, J.; Raggon, J.; Campos, D.; Voss, C.R.; Sohodski, E.; Feyock, B.; Murnen, H.; Gonzalez, M.; Johnson, M.; Lu, J.; Feng, X.; Sun, X.; Zheng, S.; Wu, B. Continuous production of anhydrous *tert*-butyl hydroperoxide in nonane using membrane pervaporation and its application in flow oxidation of a γ-butyrolactam. *Org. Process Res. Dev.* **2018**, *22*, 707-720.

[45] Cai, Y.; He, J.; Li, J.; Zhang, J.; Luo, Y. Release of manganese and *in situ* regeneration of manganese dioxide during the degradation of ciprofloxacin. *Biochem. Eng. J.* **2020**, 107600.

Chapter 5

Multi-step chemo-enzymatic synthesis of azelaic and pelargonic acids from the soapstock of high-oleic sunflower oil refinement

Francesca Tentori [1], Elisabetta Brenna [1,2], Beatrice Casali [1], Fabio Parmeggiani [1]and Davide Tessaro [1]

[1] Politecnico di Milano, Dipartimento di Chimica, Materiali e Ingegneria Chimica, via Mancinelli 7, Milano I-20131, Italy.

[2] Istituto di Chimica del Riconoscimento Molecolare - CNR, via Mancinelli 7, Milano I-20131, Italy.

Manuscript in preparation

Introduction

Global production of vegetable oilseeds is forecast at nearly 600 million metric tons (Mt) for the year 2020-21, with a corresponding production of vegetable seed oil of 209 Mt [1]. The refinement of such a high amount of oil is characterized by huge environmental footprint. Indeed, after extraction from seeds (mainly soybean and sunflower seeds), raw vegetable oil would not be suitable for human consumption because of the presence of different compounds hampering oil quality in terms of both organoleptic and nutritional qualities, and lowering its shelf life. Their removal is achieved through a process, producing a significant amount of waste. One of the most abundant by-products of vegetable oil refinement is the so-called *soapstock*, obtained by neutralization of raw oil with an alkaline solution (typically aqueous NaOH) to remove free fatty acids (FFAs). It consists of a heavy, alkaline emulsion containing approximately 50% water, FFA sodium salts (10%), triglycerides (10%) and small percentages of partially hydrolyzed lipids (diacylglycerols and monoacylglycerols) [2,3]. Since about 6% of total refined oil volume is discharged as soapstock [4], its fate is a critical issue in vegetable oil refining, especially for its alkaline pH. In the refinement plant, soapstock, recovered by decantation, is generally treated with a concentrated acid solution (usually sulfuric or hydrochloric acid), and the resulting organic fraction is removed from water by settling and/or centrifugation [5]. This effluent is a dark-coloured mixture of triglycerides, partially hydrolyzed derivatives and FFAs, containing also small amounts of mineral acids, phospholipids, and sterols [6]. It is called *high-acid oil* or *acidulated soapstock* or *oleins*.[7] Acid splitting of soapstock has several limitations: concentrated acid is required, the resulting acidic aqueous phase must be neutralized before disposal and the treatment of such wastewater is critical because of the high concentration of sulphate or chloride ions [6].

Being soapstock characterized by a wide variability in composition, it is considered a low-value source of FFAs, and it is currently employed in the production of soaps [8] or for methane production in anaerobic biodigesters [9]. It can also be added as an additive to animal feeding in limited and controlled amount [10]. Increasing the sustainability of the vegetable seed oil refining process is an urging industrial call to be achieved by both reducing the environmental burden of the process and increasing the recycle of the related by-products [11].

In this context, biocatalysis can offer interesting strategies. The enzymatic class of lipases is a valuable and broad source of effective catalysts for esterification or hydrolysis reactions, showing

high efficiency, selectivity, stability and flexibility in a wide range of operative conditions. Lipases, many of which are produced industrially and marketed at a reasonable cost, can be employed in soapstock splitting as a convenient alternative to acid treatment, affording complete hydrolysis to the corresponding mixture of fatty acids.

Soapstock recovered from the refinement of high-oleic sunflower oil is characterized by 60-80% oleic acid (**1**, Figure 1), which is of interest to the fine chemical industry, in particular as starting material for the production of pelargonic (**2**) and azelaic acids (**3**) by oxidative cleavage of the C=C double bond, currently carried out by ozonolysis [12]. Pelargonic acid is used as a natural herbicide, a weed killer, a blossom thinner and for the synthesis of plasticizers, and flavours [13]; azelaic acid is employed as an additive in anti-acne preparations and hair growth stimulators, as well as for the production of bio-based polyesters [14].

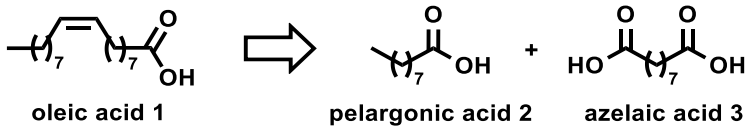

Figure 1. Oleic acid and the products of its oxidative cleavage.

A few years ago, our research group started a collaboration with Oleificio Zucchi, an Italian enterprise for vegetable seed oil refining settled in Cremona, aiming at the valorization of soapstock by biocatalytic methods. We started our investigation on high-oleic acid soapstock, and the first studies were performed on commercial oleic acid. In a recent paper,[15] we discussed the use of a lipase-mediated Prilezhaev epoxidation of oleic acid with an immobilized form of *Candida antarctica* lipase B (Novozym® 435) to obtain, after subsequent oxirane hydrolysis, *threo*-9,10-dihydroxystearic acid (**4**, Scheme 2), which represents the key intermediate towards the synthesis of azelaic and pelargonic acids.

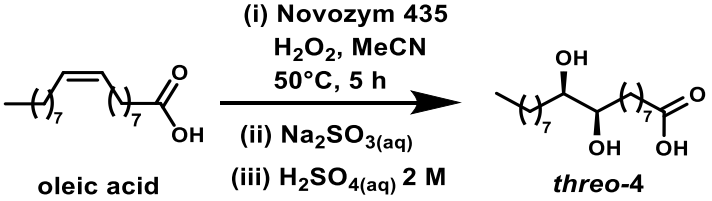

Scheme 1. Synthesis of diol **4** from oleic acid.

Oxidation to 9,10-dioxostearic acid (**5**) by means of catalytic quantities of $Fe(NO_3)_3 \cdot 9H_2O$, (2,2,6,6-tetramethylpiperidin-1-yl)oxyl (TEMPO), and NaCl in presence of atmospheric oxygen as stoichiometric oxidant (Scheme 2a) followed by cleavage with 35% aq. H_2O_2 completed the procedure to final products **2** and **3**. In a further development of this work, [16] we investigated the enzymatic oxidation of diol **4** by the recombinant alcohol dehydrogenase (ADH) from *Micrococcus luteus* NCTC2665, affording quantitative conversion into a mixture of the two regioisomeric hydroxyketones **6a**,**b**, as an alternative to chemical oxidation (Scheme 2b). The final oxidation to azelaic and pelargonic acids could be achieved by treatment with NaClO 10% aq. solution.

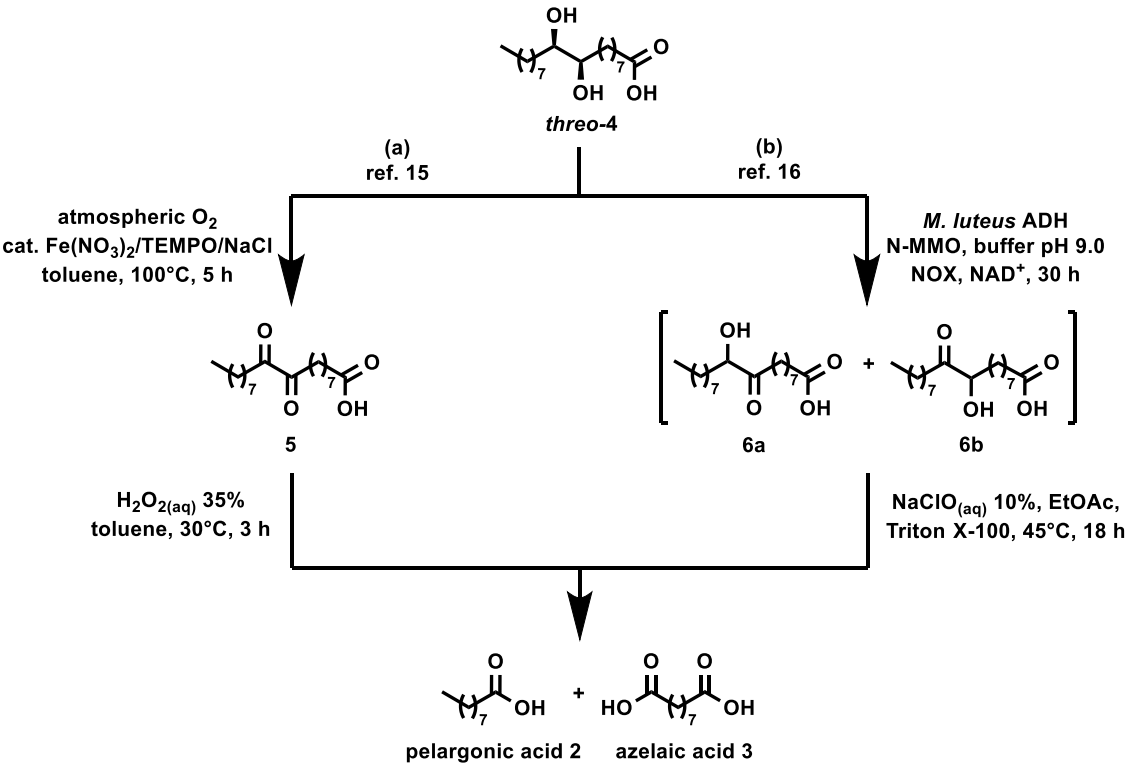

Scheme 2. Conversion of diol **4** into pelargonic and azelaic acids, already described in previous works.

We herein report on the results we attained when this chemo-enzymatic procedure, so far studied on commercial oleic acid, was applied to the actual mixture of FFAs recovered after the enzymatic hydrolysis of high-oleic sunflower oil soapstock provided by Oleificio Zucchi. The intermediate diol **4** was obtained as a crystalline product after Novozym® 435 mediated epoxidation to derivative **7**, followed by oxirane hydrolysis (Scheme 3). To shorten the reaction path, we found that sodium hypochlorite could promote the direct oxidative cleavage of diol **4** to compounds **2** and **3**. In order to

increase the efficiency of the proposed synthesis, a statistical approach was applied to optimize both epoxidation and diol cleavage steps, and perform them in continuous-flow reactors.

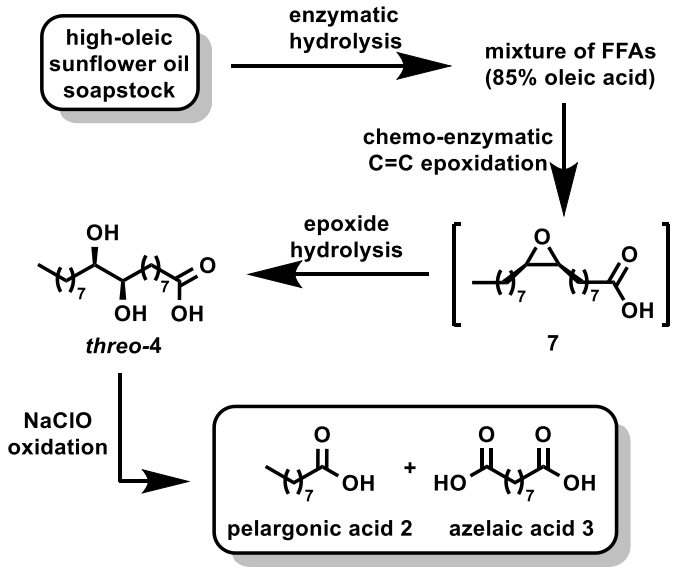

Scheme 3. Multistep process for the conversion of soapstock into pelargonic and azelaic acids described in this work.

Results and Discussion

Enzymatic splitting of high oleic sunflower oil soapstock

Enzymatic hydrolysis can constitute a more effective and sustainable alternative to acid splitting already employed at the industrial level. In order to increase the efficiency of this step and reduce the associated waste, biocatalysis represents an advantageous approach, and several examples of soapstock treatment with lipases are described in the literature [17-19], although no reference could be found to any industrial large-scale application. Most of the published papers refer to lab-scale results: the lack of scale-up projects was mainly ascribed to high enzyme load and cost, long reaction times and low efficiency.[17,20] Moreover, the high pH value of soapstock (9-10) usually has to be lowered in order to ensure the stability of most lipases, which adds a further step to the process. Recently, Novozymes® has developed commercial enzymes working in a wide range of pH values [21], that are particularly suited to implement industrial-scale enzymatic splitting of soapstock. To achieve both the conversion of fatty acid sodium salts into the corresponding free acids, and the complete hydrolysis of residual triglycerides and phospholipids, a combination of the following preparations at pH 5 is suggested: lipase from *Thermomyces lanuginosus* (Eversa® Transform 2.0, aqueous solution) together with the two phospholipases, Novozym 40121 and Lecitase Ultra (aqueous solution).

We received from Oleificio Zucchi samples of high- oleic sunflower oil soapstock showing pH ~ 10. The molar ratio between triglycerides and free fatty acids was approximately 1:1 (^{1}H NMR analysis, see Supplementary Information in Appendix *Chapter 5*). No phospholipids were found in the samples (^{31}P NMR analysis), thus only lipase Eversa® Transform 2.0 was employed. Soapstock was submitted to enzymatic hydrolysis without any acidification or pretreatment, by simply dispersing the material in water, and adding lipase Eversa® Transform 2.0 directly to the suspension. The reaction mixture was mechanically stirred at 25°C. Conversion was monitored by ^{1}H NMR (see Supplementary Information in Appendix *Chapter 5*) and complete hydrolysis was obtained after 12 h. After centrifugation of the final mixture, the organic phase (showing the following molar distribution of fatty acids by ^{1}H NMR analysis: 80-87% oleic acid, 9% linoleic acid, 4-11% saturated acids, see Supplementary Information in Appendix *Chapter 5*) was recovered and submitted to the epoxidation step. Enzymatic soapstock hydrolysis proved to be a very advantageous and convenient alternative to

acid splitting, occurring in mild reaction conditions, with high efficiency, producing smaller amounts of wastewater, that could be neutralized with phosphoric acid and disposed of with less drawbacks than that from acid splitting. Furthermore, since the lipase employed promotes complete triglyceride conversion, the corresponding product is richer in FFAs than commonly produced oleins.

Chemo-enzymatic soapstock epoxidation (batch)

The most discussed example of soapstock valorization is the conversion into biodiesel [11], but no systematic evaluation of the economical applicability of the process has been reported in literature so far [2]. Other added-value products, such as lipases [22-24] and surfactants [25-27], have been obtained by using soapstock as medium for fermentation processes. The functionalization of the C=C double bond of unsaturated FFAs as a strategy for soapstock valorization is scarcely documented. To the best of our knowledge only in Mashhadi *et al*. [28] soapstock samples containing 16.7% by weight of total fatty acids were used for producing natural epoxides to be studied as biodegradable plasticizers for PVC. The epoxidation reaction was promoted by producing peroxycarboxylic acids *in situ* by lipase-mediated perhydrolysis of the free fatty acids contained in the soapstock sample in the presence of H_2O_2 [29]. *Candida rugosa* lipase was dispersed directly in soapstock and combined in a microchannel reactor with the aqueous phase containing H_2O_2. When the reaction was performed at 36°C and pH 6.5, with a H_2O_2/C=C molar ratio of 1.61 and a feed flow rate of 42 mL h^{-1}, 85% epoxidation yield (with respect to the starting FFA content) was achieved.

In a previous paper [15], we used the same strategy for the self-epoxidation of commercial oleic acid, using an immobilized form of lipase B from *Candida antarctica* (Novozym® 435) as a catalyst. The epoxidation was carried out in acetonitrile as a solvent, because of its ability to solubilize both oleic acid and aqueous H_2O_2 35%. Final quantitative conversion was achieved in 5 h, at 50°C with 0.15 M oleic acid and 0.27 M H_2O_2 with an enzyme loading of 5 g L^{-1}. The reaction mixture was treated first with Na_2SO_3 sat. solution, then with H_2SO_4 2 M to promote oxirane hydrolysis. Compound 9,10-dihydroxystearic acid (**4**) was recovered directly by filtration (72%), after spontaneous crystallization from the reaction mixture. On the basis of these results, we planned the application of the same procedure to the mixture of FFAs produced by enzymatic hydrolysis of a sample of soapstock (from the refinement of high-oleic sunflower oil at Oleificio Zucchi) as described in the previous paragraph.

First, optimization of the epoxidation conditions in batch mode was carried out on the fatty acid mixture recovered from the enzymatic splitting of high-oleic sunflower soapstock (83% oleic acid),

using a factorial design (elaborated through Minitab) according to the design of experiments (DOE) approach. This method allowed us to gain a better understanding of the system response to the reaction variables, with the final aim of finding the optimal conditions for continuous-flow implementation. A four-variables (oleic acid and H_2O_2 concentrations, temperature, and enzyme amount) factorial design, with a replicate for each point, was designed and analyzed through the software Minitab. We considered a range of 10-50 g L^{-1} of oleic acid concentration, that corresponded to 12-60 g L^{-1} of hydrolyzed mixture. As for the other conditions, we chose to evaluate system response to temperature in the range 30-50°C, hydrogen peroxide concentration in the range 1-4% *v/v* (referred to 35% w/w aq. solution), Novozym® 435 in the range 1-2 g L^{-1}. We observed that oleic acid concentration was by far the most influential parameter, and that the best conversions were reached with the highest oleic acid concentration. The increase of enzyme load and temperature showed as well a beneficial effect on conversion, while H_2O_2 variation appeared almost irrelevant. The final optimized conditions were the following: 50 g L^{-1} oleic acid, 2 g L^{-1} Novozym® 435, 50°C and 1% *v/v* H_2O_2 35% aq. solution (for detailes see Supplementary Information in Appendix *Chapter 5*).

When the reaction was performed under these conditions starting from 60 g L^{-1} of hydrolyzed soapstock (83% oleic acid by ^{1}H NMR analysis), diol **4** was obtained in 40% yield in batch mode after 5 h. The presence of 9% linoleic acid (^{1}H NMR analysis) in the starting mixture of fatty acids, had no influence on the quality of diol **4**, that crystallized selectively from the reaction medium in pure form (35% isolated yield). In a separate experiment, we observed that when commercial linoleic acid **8** was submitted to epoxidation and hydrolysis in the same reaction conditions, no tetrahydroxy derivatives of stearic acid were formed, rather a complex mixture of stereoisomers of the two dihydroxy tetrahydrofuran derivatives **9** and **10** was obtained (Scheme 4). These compounds were identified by Li *et al.* (2018) [30] as sea lamprey migratory pheromones, and fully characterized. Their formation was attributed to an intramolecular dehydration of dihydroxy derivatives formed by partial hydrolysis of the diepoxy stearic acid stereoisomers **11a** and **11b**. These compounds were also detected in the GC/MS analysis of the mother liquors after the filtration of diol **4**.

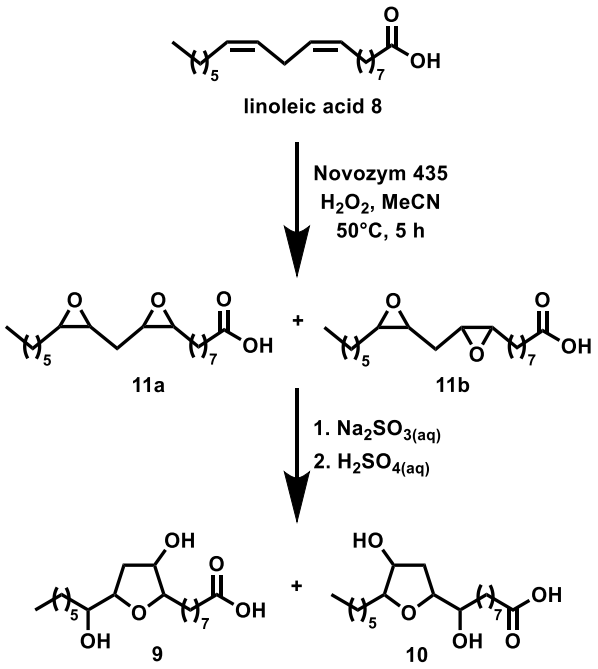

Scheme 4. Products of epoxidation and epoxide hydrolysis of linoleic acid **8**.

Chemo-enzymatic soapstock epoxidation (continuous-flow)

Over the past decades, flow chemistry has gained exceptional interest in the field of organic synthesis for its advantages over conventional batch chemistry: due to the small size of flow reactors, the high surface to volume ratio affords a fast and efficient heat and mass transfer [31]. The advantages are mainly related to an improvement of productivity, yield and safety, as well as a considerably easier scalability.

In the paper by Mashadi *et al.*,[28] a biphasic aqueous-organic continuous system could be used for the lipase-mediated epoxidation of soapstock in a micro-channel reactor, since an aqueous solution of *C. rugosa* lipase was employed. In our work, Novozym® 435 was the catalyst of choice and, being an immobilized enzyme, a different configuration had to be devised.

As an alternative to the PFR mode, Meyer *et al.* [32,33] employed a stirred-tank reactor, working according to a CSTR mode, to promote the perhydrolysis of ethyl acetate by using a commercial formulation of immobilized *C. antarctica* lipase B dispersed in the liquid phase. We adopted a similar configuration, transferring into continuous-flow mode the best batch conditions found in our factorial design analysis. Although statistical analysis suggested to adopt the highest amount of oleic acid (50

g L^{-1}, corresponding to 60 g L^{-1} of hydrolyzed soapstock), the maximum concentration of hydrolyzed soapstock we could obtain in MeCN was 52 g L^{-1} (corresponding to 43 g L^{-1} of oleic acid). This limitation was due to the fact that the solubility of oleic acid was lowered by the presence of other fatty acids and components in the starting mixture, and it was not observed working on lower amounts for DOE experiments in batch conditions.

To the final MeCN solution (160 mL), H_2O_2 35% (1.6 mL, 1% *v/v*) was added. The reactor volume was set to 45 mL and the flowrate at 150 µL min^{-1} to ensure a residence time of 5 h (equal to the reaction time in batch conditions). The reactor was kept at 50°C and loaded with 90 mg of Novozym® 435 (corresponding to 2 g L^{-1}) (Figure 2). The outlet conversion was monitored every hour, for 12 h (Figure 2): stationary state conversion was reached after 4 h and maintained for 4 h. From 8 h to 12 h a gradual decrease of conversion was observed, up to a final conversion of 45% in the last sample. The remaining solution inside the reactor was also analyzed, showing a similar conversion value (44%).

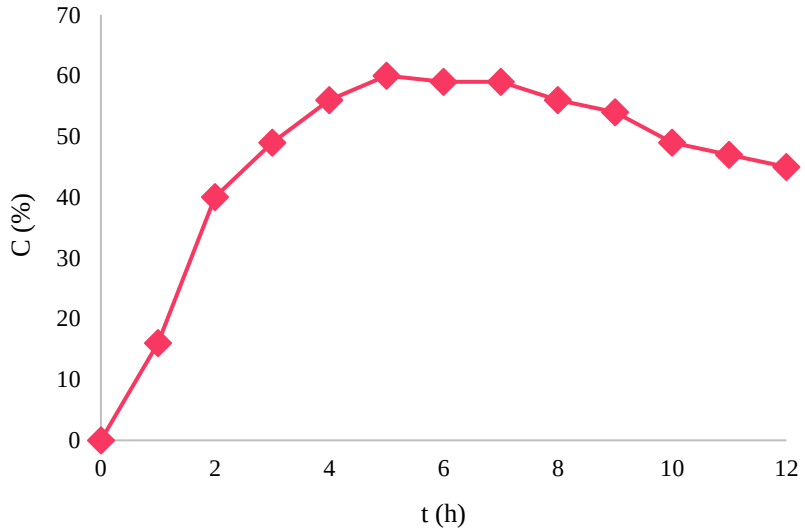

Figure 2. Enzymatic conversion of oleic acid from hydrolyzed soapstock (by GC/MS) in the CSTR during 12 h of continuous operating time.

The fractions from 2 to 12 h, corresponding to a conversion value in the range of 40-60% (100 mL) and the solution inside the reactor (45 mL) were collected (total volume of 145 mL) and quenched by

adding a saturated solution of Na_2SO_3 (6 mL). In the end, the solution was treated with 0.25 equiv. of H_2SO_4 2 M, to recover diol **4** as a pure and white solid after filtration. Starting from 7.3 g of hydrolyzed soapstock (corresponding to 6.2 g of oleic acid) we could recover 3.3 g of diol **4** (47 % yield).

In order to compare the efficiency of batch and continuous-flow approaches, the space-time yield values (STY, amount of generated product per unit catalyst weight per unit time) [34] were calculated in mmol g_{cat}^{-1} h^{-1} according to the following formula.

$$\mathbf{STY_{batch}} = \frac{n_{reagent} \cdot C}{m_{N435} \cdot \Delta t} = 7.1 \text{ mmol } g_{cat}^{-1} \text{ h}^{-1}$$

$$\mathbf{STY_{flow}} = \frac{n_{reagent} \cdot C}{m_{N435} \cdot \tau} = 25.4 \text{ mmol } g_{cat}^{-1} \text{ h}^{-1}$$

$n_{reagent}$ (mmol) = amount of reagent; C (%) = conversion of the reagent into the desired product determined by GC/MS analysis; m_{N435} (g) = Novozym® 435 load; Δt (h) = reaction time (for batch); τ (h) = residence time (for continuous-flow).

(i) batch mode: 0.030 g Novozym® 435, 2.7 mmol oleic acid from hydrolyzed soapstock, 5 h reaction time, 40% conversion.

(ii) continuous-flow mode: 0.090 g Novozym® 435, 22.0 mmol oleic acid from hydrolyzed soapstock, 5 h residence time, 52% conversion.

For the batch conditions and conversion, we considered the best result obtained using the factorial design. For the flow reaction, we took into account all the fractions collected from 2 to 12 h and the volume inside the reactor (145 mL) with a total epoxidation yield of nearly 52%.

As it can be observed, the reaction performed in a continuous-flow reactor led to an approximately three-fold higher STY with respect to the batch process, which accounts for the better exploitation of the same catalyst for a longer operation time.

*Oxidative cleavage of diol **4** (batch)*

Vicinal diol oxidative cleavage is a widely explored reaction, especially in carbohydrate chemistry [35]. Typically, this transformation is carried out using either hypervalent iodine reagents, *i.e.*, $NaIO_4$, HIO_4, $Pb(OAc)_4$ [35], or H_2CrO_4 and $KMnO_4$ when a highly oxidant environment is required for the

preparation of the corresponding (di)carboxylic acid. When milder reaction conditions are preferable, transition metal-based catalysts have to be employed, as ions (especially W [36] and Mo [37] derivatives) or nanoparticles [38]. Unfortunately, these methods are often plagued by several disadvantages like the toxicity of the reagents, the harsh conditions required or the troublesome workups. Some alternative reagents for diol cleavage to (di)carboxylic acids have been recently proposed, such as tetrapropylammonium perruthenate [39] or nitroxyl radicals like TEMPO [40].

A much more available and inexpensive oxidant, sodium hypochlorite, was tested also for glycol cleavage with appreciable results, favoring carboxylic acids instead of aldehydes as final products. In 2007, Khurana *et al.* [41] successfully tested NaClO on various 1,2-diaryl- and dialkyl-1,2-diols, and in 2019 Kirihara *et al*. [42] employed $NaOCl \cdot 5H_2O$ on sterically hindered *trans*-cyclic vicinal diols. The wide availability of NaClO attracted us as an interesting and economically viable replacement of traditional catalysts for the preparation of azelaic and pelargonic acids from diol **4**. NaClO has already been reported to oxidize **4** into acids **2** and **3** in a patent by Lemaire *et al.* 2013 [43]: starting from 120 g L^{-1} of **4** in 1.1 M NaClO complete conversion into azelaic and pelargonic acids was achieved after 5 h. Unfortunately, in our hands this methodology did not provide the desired products with significant conversion. By diluting the system and increasing the reaction time, we obtained a 55% conversion of diol **4** after 3 days, with a concentration of 25 g L^{-1} in a 10% NaClO solution. Beyond **2** and **3**, a small amount of the two isomers of hydroxyoxostearic acid (**6a,b**, Scheme 1) were formed, suggesting these are the intermediates in the cleavage of the glycol C–C bond. The addition of acetonitrile as a cosolvent to enhance the solubility of diol **4** in aqueous NaClO solution, as described in Khurana *et al.* (2007) [41], had no significant effect to reduce reaction time and increase concentration.

The use of biphasic aqueous-organic systems to improve NaClO oxidation of poorly soluble molecules has been already studied [44], using tetrabutylammonium bromide to favor phase transfer. We tested a biphasic system EtOAc/aq. NaClO for the oxidative cleavage of diol **4** using either a quaternary ammonium salt (tetraethylammonium bromide), or a non-ionic surfactant (Triton-X 100) as a phase transfer catalyst. While the former prevented the reaction from happening and did not provide any conversion, the latter showed an impressive increase of conversion with respect to the previous monophasic experiments, affording complete conversion in 48 h. Besides the substantial increase in yield, the biphasic approach showed a significant advantage in the isolation of products **2** and **3**. We observed that pelargonic acid **2** was extracted completely in the organic phase, while

azelaic acid **3** was retained in the alkaline aqueous phase and could be isolated after treatment with a saturated solution of Na_2SO_3, acidification to pH 6 and extraction with EtOAc.

After these promising results, we attempted to optimize reaction efficiency by implementing a statistical analysis through a factorial DOE approach, already employed for the first step of this procedure. After some preliminary experiments that showed that surfactant concentration was not a strongly determining variable, we chose to keep substrate and surfactant concentrations constant for all the experiments. For the application of the factorial design, the global conversion of diol **4** into products **2** and **3** (determined by GC/MS analysis) was taken as the system response, choosing as variable parameters the volumes of EtOAc (in the range 5-13 mL) and aq. NaClO 10% solution (in the range 4-10 mL). EtOAc proved to be more determinant than NaClO and the highest conversion (62%) was obtained with the highest volumes of the two phases (for detailes see Supplementary Information in Appendix *Chapter 5*).

*Oxidative cleavage of diol **4** (continuous-flow conditions)*

Multiphase reactions constitute one of the main research areas in flow chemistry. When two immiscible solvents with high interfacial tension are introduced in the small-diameter channels of a flow system through two different inlets connected by a T-junction, a segmented flow is formed [45], in which the two liquids form short alternating segments with a regular periodic pattern depending on the flow rates. The application of phase-transfer catalysis is known to increase the interfacial area for the exchange of chemical species, thanks to the transfer of reactants from one phase to the other, where the main reaction occurs. Comparing phase-transfer catalyzed reactions in flow and batch reactors, the flow reactions result more efficient and sustainable [46,47]. Nevertheless, the presence of the liquid-liquid interface limits overall kinetics, and flow chemistry has been more and more explored to push the yields. A biphasic segmented liquid-liquid flow system was thus considered the most suitable solution for the oxidative cleavage of diol **4**. The best conditions obtained by DOE analysis were applied to a 10 mL tubular coil. The optimal ratio between NaClO solution and EtOAc was obtained by setting the flowrates as follows: 100 µL min^{-1} for aq. NaClO 10% solution and 120 µL min^{-1} for the organic solution. The two flows joined in a T-junction and entered the 10 mL tubular coil, thermostated at 45°C, with a 45 min residence time. The solution collected at the outlet was quenched with a saturated aq. Na_2SO_3, the organic layer was separated and dried over Na_2SO_4. Its composition (by GC/MS) was 80% **6a**,**b** isomers, 10% dioxo derivative **5**, and 10% diol **4**. To

complete the reaction, the organic phase was flowed in a second 10 mL tubular coil with fresh aq. NaClO solution. At the outlet of the second coil, the conversion of hydroxyketones **6a**,**b** into final products was nearly complete (90%). Since the reaction does not depend on the presence of a catalyst, the STY is evaluated per unit of reaction volume: 23 mL for the batch reaction (13 mL EtOAc + 10 mL NaClO) and 20 mL for the two runs of the flow oxidation.

$$\mathbf{STY_{batch}} = \frac{n_{reagent} \cdot C}{V_{reactor} \cdot \Delta t} = 0.2 \text{ mmol L}^{-1} \text{ h}^{-1}$$

$$\mathbf{STY_{flow}} = \frac{n_{reagent} \cdot C}{V_{reactor} \cdot \tau} = 5.2 \text{ mmol L}^{-1} \text{ h}^{-1}$$

(i) batch mode: 23 mL biphasic system, 0.158 mmol diol **4**, 24 h reaction time, 62% conversion (i.e., the results of DOE optimization).

(ii) continuous flow mode: 20 mL volume (considering the two subsequent flow reactions), 0.158 mmol diol **4**, 1.5 h residence time, 99% conversion.

These results show that the reaction performed in a continuous flow reactor led to a 25 times higher STY when than in a batch process. The properties and reaction conditions in such microreactors are different to large-scale systems. The application of a biphasic reaction in microreactors, especially when phase-transfer catalysis is combined with segmentation, led to a dramatic increase the reaction rate, due to a high surface-to-volume ratio, short diffusion distances, fast and efficient heat dissipation and mass transfer.

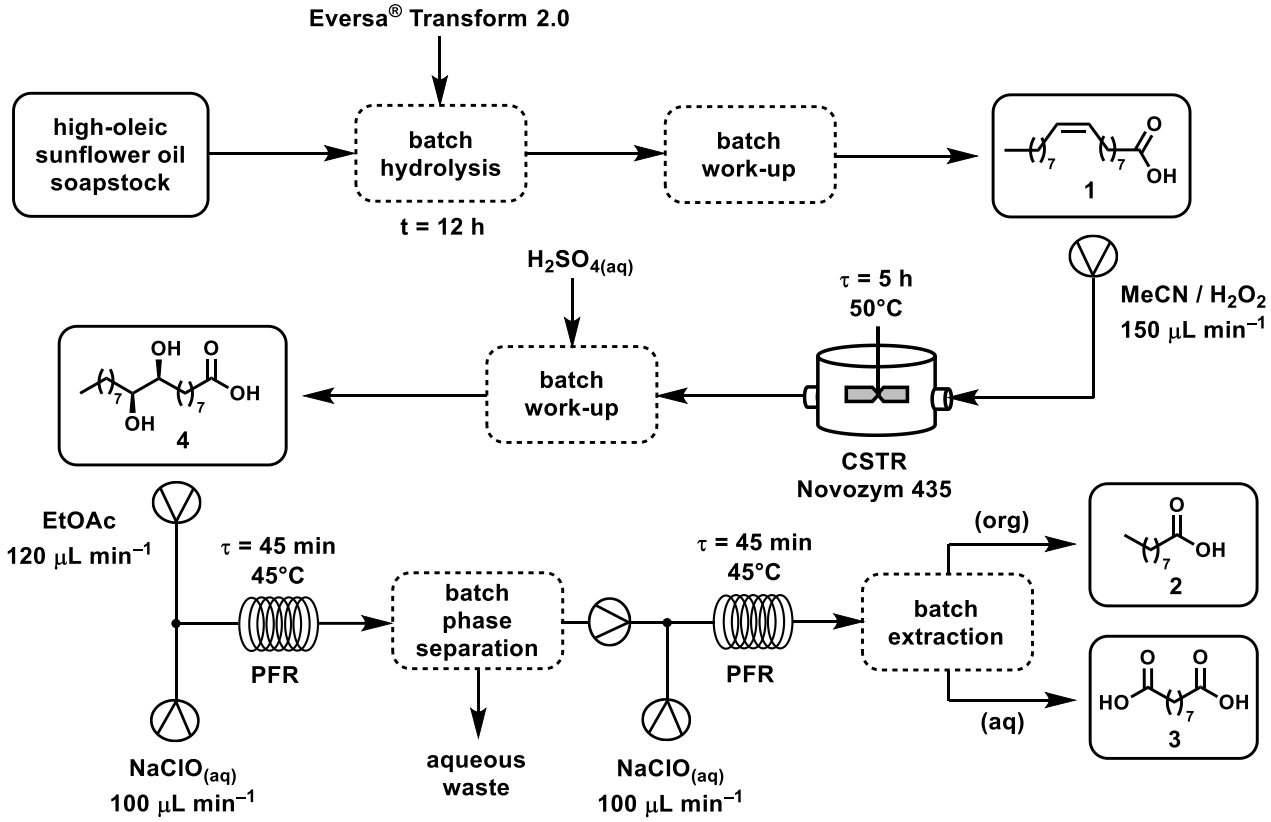

Figure 3. Overall scheme of the optimized process for the conversion of high-oleic sunflower oil soapstock into azelaic and pelargonic acids.

Conclusions

Soapstock splitting and disposal are critical issues in the vegetable oil refining industry. The potential of lipases in the manipulation of FFAs is well known but, at industrial scale, the complex composition and the highly alkaline pH of soapstock hinder lipase application for large scale enzymatic splitting. The three-step process described in this paper and summarized in Figure 3 offers a possible solution apt to process-scale development.

The collaboration with Oleificio Zucchi allowed us to test a new lipase (Eversa Transform 2.0) from Novozymes directly on a sunflower soapstock with a high content of oleic acid (~83%) as it was provided from the refining plant. Soapstock was completely hydrolyzed in 12 h without preliminary acidification and the mixture of FFAs was simply recovered by centrifugation. In order to valorize the hydrolyzed product, we aimed to prepare pelargonic and azelaic acids by oxidative C=C bond cleavage of oleic acid. The FFAs (mainly composed of oleic acid with ~9% of linoleic) was submitted to epoxidation promoted by the immobilized *Candida antarctica* lipase B (Novozym® 435) in the presence of hydrogen peroxide according to the Prilezhaev reaction mechanism. Using acetonitrile as solvent, the addition of sulfuric acid caused precipitation of diol **4** as a pure solid, leaving in the solution all impurities, including side-products from linoleic acid epoxidation. Then, diol **4** was easily submitted to oxidative cleavage to the final products in a biphasic EtOAc/aq. NaClO system using Triton-X 100 as phase-transfer catalyst. For both reaction steps, a statistical approach was applied to optimize the conversions, through a factorial DOE analysis. The optimal conditions obtained through the analysis were implemented on different reaction configurations, demonstrating and exploiting the advantages of continuous-flow chemistry. The epoxidation was run in a stirred-tank reactor in a CSTR mode, while for the oxidative cleavage a tubular coil in PFR mode was chosen. Both configurations proved to be stable and efficient, determining a substantial increase of the reaction yields, clearly demonstrating potential for further development and scale-up to industrial application in seed and vegetable oil refining plants.

References

[1] United States Department of Agriculture Foreign Agricultural Service Oilseeds: World Markets and Trade, April 2021, https://apps.fas.usda.gov/psdonline/circulars/oilseeds.pdf (accessed on 9 July 2021).

[2] Dumont, M.-J.; Narine, S.S. Soapstock and deodorizer distillates from North American vegetable oils: review on their characterization, extraction and utilization. *Food Res. Int.* **2007**, *40*, 957-974.

[3] Haas, M.J.; Cichowicz, D.J.; Jun, W.; Scott, K. The enzymatic hydrolysis of triglyceride-phospholipid mixtures in an organic solvent. *J. Am. Oil Chem. Soc.* **1995**, *72*, 519-525.

[4] Haas, M.J.; Bloomer, S.; Scott, K. Simple, high-efficiency synthesis of fatty acid methyl esters from soapstock. *JAOCS* **2000**, *77*, 373-379.

[5] Haas, M.J.; Michalski, P.J.; Runyon, S.; Nunez, A.; Scott, K.M. Production of FAME from acid oil, a by-product of vegetable oil refining. *JAOCS* **2003**, *80*, 97-102.

[6] Wang, Z.-M.; Lee, J.-S.; Park, J.-Y.; Wu, C.-Z.; Yuan, Z.-H. Novel biodiesel production technology from soybean soapstock. *Korean J. Chem. Eng.* **2007**, *24*, 1027-1030.

[7] Lin, C.-Y.; Lin, Y.-W. Fuel characteristics of biodiesel produced from a high-acid oil from soybean soapstock by supercritical-methanol transesterification. *Energies* **2012**, *5*, 2370-2380.

[8] Pandey, R.A.; Sanyal, P.B.; Chattopadhyay, N.; Kaul, S.N. Treatment and reuse of wastes of a vegetable oil refining. *Resour. Conserv. Recy.* **2003**, *37*, 101-117.

[9] Cherif, S.; Aloui, F.; Carrière, F.; Sayadi, S. Lipase pre-hydrolysis enhance anaerobic biodigestion of soap stock from an oil refining industry. *J. Oleo Sci.* **2014**, *2*, 109-114.

[10] Beal, R.E.; Lauderback, L.L.; Ford, J.R. Soybean soapstock utilization: fatty acid adducts with ethylene and 1-butene. *JAOCS* **1975**, *52*, 400-403.

[11] Casali, B.; Brenna, E.; Parmeggiani, F.; Tessaro, D.; Tentori, F. Enzymatic methods for the manipulation and valorization of soapstock from vegetable oil refining processes. *Sustain. Chem.* **2021**, *2*, 74-91.

[12] Ackman, R.G.; Retson, M.E.; Gallay, L.R.; Vandenheuvel, F.A. Ozonolysis of unsaturated fatty acids: i. ozonolysis of oleic acid. *Can. J. Chem.* **1961**, *39*, 1956-1963.

[13] Pohanish, R.P. Sittig's Handbook of Pesticides and Agricultural Chemicals, 2nd edition, William Andrew: Norwich, New York, 2015.

[14] a) Azelaic acid topical, https://www.drugs.com/mtm/azelaic-acid-topical.html (accessed on 9 July 2021); b) Sasmaz, S.; Arican, O. Comparison of azelaic acid and anthralin for the therapy of patchy alopecia areata. *Am. J. Clin. Dermatol.* **2005**, *6*, 403-406; c) Brydson, J.A. Plastics Materials, 7th ed, Chapter 18, Butterworth Heinemann, Oxford, 1999, pp. 478-530.

[15] Brenna, E.; Colombo, D.; Di Lecce, G.; Gatti, F.G.; Ghezzi, M.C.; Tentori, F.; Tessaro, D.; Viola, M. Conversion of oleic acid into azelaic and pelargonic acid by chemo-enzymatic route. *Molecules* **2020**, *25*, 1882.

[16] Colombo, D.; Brenna, E.; Casali, B.; Ghezzi, M.C.; Parmeggiani, F.; Tentori, F.; Tessaro, D.; Boratyński, F. Oxidation of threo-9,10-dihydroxystearic acid mediated by *Micrococcus luteus* as a key step in the conversion of oleic acid into pelargonic and azelaic acids. *ChemCatChem* **2021**, *13*, 1-9.

[17] Brunner, K.; Frische, R.; Kilian, D. Method for enzymatic splitting of oils and fats. U.S. Patent 2002/0197687A1, 26 December 2002.

[18] Haas, M.J.; Cichowicz, D.J.; Jun, W.; Scott, K. The enzymatic hydrolysis of triglyceride-phospholipid mixtures in an organic solvent. *JAOCS* **1995**, *72*, 519-525.

[19] Kempers, P.; Schőrken, U.; Wolf, T.; Sato, S.; Bueno de Almdeida, W.; Bizzarri, P.S.; Araujo, A.S. Process for production of fatty acids, fatty acid esters and sterolesters from soapstock. U.S. Patent 8426622B2, 23 April 2013.

[20] Haas, M.J.; Scott, K.M. Combined nonenzymatic-enzymatic method for the synthesis of simple alkyl fatty acid esters from soapstock. *JAOCS* **1996**, *73*, 1393-1401.

[21] Feedstock flexibility for your biodiesel plant - with Eversa® Transform, https://www.novozymes.com/en/advance-your-business/food-and-beverage/vegetable-oils-rocessing/biodiesel (accessed on 9 July 2021).

[22] Davranov, K.D.; Gulyamova, K.A.; Alimova, B.K.; Turapova, N.M. Enzymatic utilization of cotton oil soap stock. *Appl. Biochem. Microbiol.* **2000**, *36*, 19-22.

[23] Damaso, M.C.T.; Passianoto, M.A.; de Freitas, S.C.; Freire, D.M.G.; Lago, R.C.A.; Couri, S. Utilization of agroindustrial residues for lipase production by solid-state fermentation. *Braz. J. Microbiol.* **2008**, *39*, 676-681.

[24] Silveira, E.A.; Tardioli, P.W.; Farinas, C.S. Valorization of palm oil industrial waste as feedstock for lipase production. *Appl. Biochem. Biotechnol.* **2016**, *179*, 558-571.

[25] Benincasa, M.; Contiero, J.; Manresa, M.A.; Moraes, I.O. Rhamnolipid production by *Pseudomonas aeruginosa* LBI growing on soapstock as the sole carbon source. *J. Food Eng.* **2002**, *54*, 283-288.

[26] Benincasa, M.; Accorsini, F.R. *Pseudomonas aeruginosa* LBI production as an integrated process using the wastes from sunflower-oil refining as a substrate. *Bioresour. Technol.* **2008**, *99*, 3843-3849.

[27] Shabtai, Y. Production of exopolysaccharides by *Acinetobacter* strains in a controlled fed-batch fermentation process using soapstock oil (SSO) as carbon source. *Int. J. Biol. Macromol.* **1990**, *12*, 145-152.

[28] Mashhadi, F.; Habibi, A.; Varmira, K. Enzymatic production of green epoxides from fatty acids present in soapstock in a microchannel bioreactor. *Ind. Crop. Prod.* **2018**, *113*, 324-334.

[29] Björkling, F.; Frykman, H.; Godtfredsen, S.E.; Kirk, O. Lipase catalyzed synthesis of peroxycarboxylic acids and lipase mediated oxidations. *Tetrahedron* **1992**, *48*, 4587-4592.

[30] Li, K.; Brant, O.; Huertas, M.; Hessler, E.J.; Mezei, G.; Scott, A.M.; Hoye, T.R.; Li, W. Fatty-acid derivative acts as a sea lamprey migratory pheromone. *PNAS* **2018**, *155*, 8603-8608.

[31] De Zani, D.; Colombo, M. Phase-transfer catalysis under continuous flow conditions: an alternative approach to the biphasic liquid/liquid o-alkylation of phenols. *J. Flow Chem.* **2012**, *1*, 5-7.

[32] Meyer, J.; Horst, A.E.W.; Steinhagen, M.; Holtmann, D.; Ansorge-Schumacher, M.B.; Kraume, M.; Drews, A. A continuous single organic phase process for the lipase catalyzed synthesis of peroxy acids increases productivity. *Eng. Life Sci.* **2017**, *17*, 759-767.

[33] Meyer-Waßewitz, J.; Holtmann, D.; Ansorge-Schumacher, M.B.; Kraume, M.; Drews, A. An organic-single-phase CSTR process for the chemo-enzymatic epoxidation of α-pinene enables high selectivity and productivity. *Biochem. Eng J.* **2017**, *126*, 68-77.

[34] Plutschack, M.B.; Pieber, B.; Gilmore, K.; Seeberger, P.H. The hitchhiker's guide to flow chemistry, *Chem. Rev.* **2017**, *117*, 11796-11893.

[35] Perlin, A.S. Glycol-Cleavage Oxidation. *Adv. Carbohydr. Chem. Biochem.* **2006**, *60*, 183-250.

[36] Venturello, C.; Ricci, M. Oxidative cleavage of 1,2-diols to carboxylic acids by hydrogen peroxide. *J. Org. Chem.* **1986**, *51*, 1599-1602.

[37] Pultinas Jr., E.P. Preparation of carboxylic acids by the oxidation of vicinal glycols. U.S. Patent 3855257, 17 December 1974.

[38] Solmi, S.; Rozhko, E.; Malmusi, A.; Tabanelli, T.; Albonetti, S.; Basile, F.; Agnoli, S.; Cavani, F. The oxidative cleavage of trans-1, 2-cyclohexanediol with O_2: catalysis by supported Au nanoparticles. *Appl. Catal. A Gen.* **2018**, *557*, 89-98.

[39] Schmidt, A.-K.C.; Stark, C.B.W. Tetrapropylammonium perruthenate catalyzed glycol cleavage to carboxylic (di)acids. *Org. Lett.* **2011**, *13*, 5788-5791.

[40] Shibuya, M.; Shibuta, T.; Fukuda, H.; Iwabuchi, Y. Nitroxyl radical/PhI(OAc)2: one-pot oxidative cleavage of vicinal diols to (di)carboxylic acids. *Org. Lett.* **2012**, *14*, 5010-5013.

[41] Khurana, J.M.; Sharma, P.; Gogia, A.; Kandpal, B.M. Oxidative cleavage of 1, 2-diols, α-ketols and 1, 2-diketones with aqueous sodium hypochlorite. *Org. Prep. Proced. Int.* **2007**, *39*, 185-202.

[42] Kirihara, M.; Osugi, R.; Saito, K.; Adachi, K.; Yamazaki, K.; Matsushima, R.; Kimura, Y. Sodium hypochlorite pentahydrate as a reagent for the cleavage of trans-cyclic glycols. *J. Org. Chem.* **2019**, *84*, 8330-8336.

[43] Lemaire, M.; Favre-Reguillon, A.; Paquit, B.; Claude, S.; Raoul, Y. Method for preparing carboxylic acids by oxidative cleavage of a vicinal diol. U.S. Patent 2013/0131379 A1, 23 May 2013.

[44] Mirafzal, G. A.; Lozeva, A.M. Phase transfer catalyzed oxidation of alcohols with sodium hypochlorite. *Tetrahedron Letters* **1998**, *39*, 7263-7266.

[45] Ahmed-Omer, B.; Barrow, D.; Wirth, T. Effect of segmented fluid flow, sonication and phase transfer catalysis on biphasic reactions in capillary microreactors. *Chem. Eng. J.* **2008**, *135*, 280-283.

[46] Reichart, B.; Kappe, C.O.; Glasnov, T.N. Phase-transfer catalysis: mixing effects in continuous-flow liquid/liquid O-and S-alkylation processes. *Synlett* **2013**, *24*, 2393-2396.

[47] Teoh, S.K.; Sa-ei, K.; Noorulameen, M.S.; Toh, Q.Y.; Ng, Y.L.; Sharratt, P.N. Sustainability benefits of a continuous phase transfer catalyzed process for a model pharmaceutical intermediate. *Chem. Eng. Res. Des.* **2015**, *100*, 467-480.

Appendix

Chapter 1

Supplementary Information

Preliminary screening: ADH-mediated reduction of nitroketone 3a to nitroalcohol 1a.

[a] Conversion calculated by ^{1}H NMR spectroscopy as molar percentage of the nitroalcohol **1a** in the final reaction mixture after 4-5 h, taking into account the molar amount of the unreacted nitroketone **3a**, and of the carboxylic acid obtained upon nitroketone hydrolysis; [b] enantiomeric excess calculated on the basis of HPLC analysis on a chiral stationary phase.

ADH	Conversion (%) [a]	*ee* of **1a** (%) [b]
10	27	75 (*R*)
20	-	
30	15	96 (*R*)
40	-	
130	<10	n.d.
140	44	92 (*R*)
190	<10	n.d.
200	15	12 (*R*)
210	-	
250	-	
260	-	
270	94	92 (*R*)

380	-	
420	-	
430	-	
440	96	99 (*R*)
441	82	90 (*S*)
442	52	40 (*R*)

Table S1. ADH-mediated reduction of nitroketone **3a** to nitroalcohol **1a** (preliminary screening).15 mM substrate, 16 mM glucose, ADH (3 mg), GDH (1.5 mg), $NAD(P)^+$ (1 μmol), 1% DMSO, acetate buffer pH 5.0, 25°C, 4-5 h.

Complete screening results of ADH-Mediated Reduction of α-Nitroketones 1a-o

[a] Conversion calculated by ^{1}H NMR spectroscopy as molar percentage of nitroalcohol **1** in the final reaction mixture after 4-5 h, taking into account the molar amount of the unreacted nitroketone **3**, and of the carboxylic acid obtained upon nitroketone hydrolysis; [b] enantiomeric excess calculated on the basis of HPLC analysis on a chiral stationary phase.

Substrate	**ADH**	**Conversion(%) [a]**	***ee* of nitroalcohol 1 (%) [b]**
C_6H_5 (3a)	270	94	92 (*S*)
	440	96	99 (*R*)
	441	82	90 (*S*)
***o*-Me-C_6H_4 (3b)**	270	<5	
	440	99	99 (*R*)
	441	n.r.	
***m*-Me-C_6H_4 (3c)**	270	35	82 (*S*)
	440	99	84 (*R*)
	441	80	93 (*S*)
***p*-Me-C_6H_4 (3d)**	270	71	94 (*S*)

	440	99	99 (*R*)
	441	59	79 (*S*)
***p*-OMe-C$_6$H$_4$ (3e)**	270	18	91 (*S*)
	440	93	99 (*R*)
	441	n.r.	
***o*-F-C$_6$H$_4$ (3f)**	270	69	62 (*S*)
	440	100	94 (*R*)
	441	17	43 (*R*)
***m*-F-C$_6$H$_4$ (3g)**	270	72	rac
	440	99	93 (*R*)
	441	n.r.	
***p*-F-C$_6$H$_4$ (3h)**	270	30	66 (*S*)
	440	83	96 (*R*)
	441	n.r.	
***p*-Br-C$_6$H$_4$ (3i)**	270	69	95 (*S*)
	440	92	98 (*R*)
	441	n.r.	
***p*-Cl-C$_6$H$_4$ (3j)**	270	67	97 (*S*)
	440	97	98 (*R*)
	441	94	92 (*S*)
β-Naphthyl (3k)	270	23	83 (*S*)
	440	99	98 (*R*)

	441	62	62 (*S*)
2-Furyl (3l)	270	73	84 (*R*)
	440	100	71 (*S*)
	441	65	96 (*R*)
2-Thienyl (3m)	270	100	93 (*R*)
	440	100	92 (*S*)
	441	79	78 (*R*)
Ethyl (3n)	270	100	80 (*R*)
	440	97	rac
	441	73	rac
Butyl (3o)	270	100	99 (*S*)
	440	100	99 (*R*)
	441	n.r.	

Table S2. ADH-mediated reduction of nitroketones **3a-o** to nitroalcohols **1a-o** (preliminary screening). 15 mM substrate, 16 mM glucose, ADH (3 mg), GDH (1.5 mg), $NAD(P)^+$ (1 μmol), 1% DMSO, acetate buffer pH 5.0, 25°C, 4-5 h.

Experimental Part

General analytical methods

^{1}H and ^{13}C NMR spectra were recorded on a 400 or 500 MHz spectrometer in $CDCl_3$ solution at r.t.. The chemical shift scale was based on internal tetramethylsilane. GC/MS analyses were performed using a HP-5MS column (30 m × 0.25 mm × 0.25 μm, Agilent). The following temperature program was employed: 60°C (1 min) / 6°C min^{-1} / 150°C (1 min) /12°C min^{-1} / 280°C (5 min). Chiral HPLC analyses were performed on a Chiralcel OD column (4.6 mm × 250 mm, Daicel) or on Chiralart Amylose SA (4.6 mm × 250 mm, YMC) installed on instruments with UV detector. TLC analyses were performed on Merck Kieselgel 60 F254 plates. All the chromatographic separations were carried out on silica gel columns.

General Procedure for the ADH-Mediated Reduction of α-Nitroketones 1a-o (Screening)

A solution of the substrate in DMSO (50 μL, 500 mM) was added to an acetate buffer solution (5 mL, 50 mM, pH 5.0) containing glucose (80 μmol), $NADP^+$ (1 μmol, Sigma-Aldrich, Milan, Italy) or NAD^+ (1 μmol, Sigma-Aldrich, Milan, Italy) (according to the ADH preference), GDH (1.5 mg), and the required ADH (3 mg, Evoxx, Monheim am Rhein, Germany). The mixture was incubated for 4-5 h in an orbital shaker (150 rpm, 30 °C). The solution was extracted with EtOAc (2 × 1 mL, Sigma-Aldrich, Milan, Italy), centrifuging after each extraction (15,000 g, 1.5 min). The combined organic solutions were dried over anhydrous Na_2SO_4, and concentrated under reduced pressure. The residue was submitted to ^{1}H NMR analysis (Bruker, Milan, Italy) to determine conversion. Two replicates were performed for each biotransformation: no significant differences (less than 5%) were observed for conversion and enantiomeric excess values. The enantiomeric excess values of each nitroalcohol was determined by HPLC analysis (Agilent, Cernusco sul Naviglio, Italy) on a chiral stationary phase. The comparison of these HPLC analyses with those that were reported in the literature in the same experimental conditions allowed for the absolute configuration of nitroalcohols **1a-o** to be established.

General Procedure for the Reduction of Nitroketone 3a in a Biphasic System Mediated by ADH440 and ADH270.

A solution of nitroketone **3a** (4 mg, 25 μmol) in toluene (2 mL) was mixed with an acetate buffer solution (2 mL, 50 mM, pH = 5), containing glucose (80 μmol), $NADP^+$ (1 μmol), GDH (1 mg), and the required ADH (2 mg). The mixture was incubated for 24 h in an orbital shaker (150 rpm, 30 °C). The mixture was extracted with EtOAc (2 x 1 mL), centrifuging after each extraction (15,000 g, 1.5 min). The combined organic solutions were dried over anhydrous Na_2SO_4, and concentrated under reduced pressure. The residue was submitted to ^1H NMR analysis to determine conversion. Two replicates were performed for each biotransformation: no significant differences (less than 5%) were observed for the conversion and enantiomeric excess values. The same procedure was employed to investigate the effect on conversion due to substrate loading and substrate to enzyme ratio, by changing the amount of nitroketone and ADH.

General Procedure for the Conversion α-Nitroketones 3a and 3e into Boc Protected Amino Alcohols 2a and 2e

The enantioselective reduction of the nitroketone was performed with the required ADH on 100 mg of nitroketone (20 mL of toluene, 20 mL of buffer pH = 5, 15 mg of ADH440 or 35 mg of ADH270, 10 mg $NADP^+$, 7.5 or 18 mg GDH, 150 mg glucose), following the procedure already described in the previous paragraph for biotransformations in biphasic medium. After 24 h, the aqueous phase was removed, methanol was added (0.5 mL), followed by the cautious addition of $NiCl_2 \cdot 6H_2O$ (1 eq) and $NaBH_4$ (3 eq) under vigorous stirring. After 30 min, $(Boc)_2O$ (1.2 eq) was added. The mixture was stirred for 30 min, filtered through a celite pad, and extracted with EtOAc. The organic layers were dried over anhydrous Na_2SO_4, and the residue was purified by crystallization from hexane-EtOAc.

*(*S*)-*Tert*-butyl (2-hydroxy-2-phenylethyl) carbamate ((*S*)-**2a**)*

From compound **3a** (100 mg, 0.61 mmol), using ADH270, derivative (*S*)-**2a** was obtained (83 mg, 57%): *ee* (HPLC) = 92%, $[\alpha]_D$ = +46.8 (c 0.85, $CHCl_3$) [lit. ref. [1] $[\alpha]_D$ = +45.1. (*c* 0.6, $CHCl_3$) for (*S*)-**1a** with *ee* = 93%]; ^1H NMR ($CDCl_3$, 400 MHz) [2]: δ = 7.40-7.27 (m, 5H, Ar*H*), 4.92 (br s, 1H, *NH*), 4.83 (m, 1H, *CH*OH), 3.48 (m, 1H, *CH*N), 3.26 (m, 1H, *CH*N), 3.01 (br s, 1H, *OH*), 1.45 (s, 9H, $(CH_3)_3C$); ^{13}C NMR ($CDCl_3$, 100.6 MHz) [1]: δ = 157.1, 142.0, 128.6, 127.9, 126.0, 80.0, 74.0,

48.5, 28.5; GC/MS (EI) tr= 21.5 min *m/z* (%) = 181 (M^+ – 56, 14), 107 (100), 79 (47), 57 (100). HPLC analysis [1]: Chiralcel OD, 95/5 hexane/*i*-PrOH, 0.6 mL min^{-1}, 215 nm, (*R*)-**2a** t_r = 19.1 min, (*S*)-**2a** t_r = 23.4 min.

*(*R*)*-Tert-*butyl (2-hydroxy-2-(4-methoxyphenyl)ethyl) carbamate ((*R*)-**2e**)*

From compound **3e** (100 mg, 0.51mmol), using ADH440, derivative (*R*)-**2e** was obtained (86.3 g, 63%): *ee* (HPLC) = 96%, $[\alpha]_D$ = -37.7 (*c* 0.7, $CHCl_3$); ^{1}H NMR ($CDCl_3$, 400 MHz) [3]: δ = 7.28 (d, *J* = 8.7 Hz, 2H, Ar*H*), 6.88 (d, *J* = 8.7 Hz, 2H, Ar*H*), 4.95 (br s, 1H, N*H*), 4.76 (m, 1H, C*H*OH), 3.80 (s, 3H, OCH_3), 3.43 (m, 1H, C*H*N), 3.23 (m, 1H, C*H*N), 3.00 (br s, 1H, OH), 1.44 (s, 9H, (CH_3)$_3$C); ^{13}C NMR ($CDCl_3$, 100.6 MHz): δ = 159.4, 157.0, 134.1, 127.2, 114.1, 79.9, 73.2, 55.4, 48.5, 28.5; GC/MS (EI) t_r= 23.8 min *m/z* (%) = 267 (M^+, 0.5), 211 (5), 137 (100), 109 (15), 57 (18). HPLC analysis: Chiralcel OD, 95/5 hexane/*i*-PrOH, 0.6 mL min^{-1}, 215 nm, (*R*)-**2a** t_r = 26.9 min, (*S*)-**2a** t_r = 34.9 min.

General procedure for the synthesis of nitroketones 3a-o [4]

A solution of the suitable carboxylic acid (0.083 mol) and CDI (*N*,*N'*-carbonyldiimidazole, 0.10 mol) in dry THF (150 mL) was refluxed for 1 h (solution A). During that time, CH_3NO_2 (2.32 mol) was slowly added at room temperature to a suspension of NaH (0.10 mmol) in dry THF (100 mL). The resulting solution was stirred for further 30 minutes at room temperature (solution B). Solution A was cooled to room temperature, then transferred to the flask containing solution B. The resulting mixture was refluxed for a few hours with vigorous stirring, affording a light-yellow heterogeneous solution, which was cooled to room temperature. Approximately 2/3 of the solvent was removed *in vacuo*, then the mixture was poured into water and extracted with EtOAc. The aqueous phase was acidified with conc. HCl, to promote the formation of a solid, which was extracted with EtOAc. The combined organic phases of this second extraction were washed with brine, dried on Na_2SO_4 and concentrated *in vacuo* to afford the corresponding crude α-nitroketone, which was purified by crystallization and used for the biocatalyzed reductions. The two aliphatic derivatives **3n** and **3o** were purified by column chromatography. The characterization data of nitroketones **3a**-**k** have been already reported by the authors in a previous paper [5]. The synthetic details and characterization data of nitroketones **3l**-**o** are herein reported.

1-(Furan-2-yl)-2-nitroethan-1-one (3l)

From 2-furoic acid (9.3 g, 0.083 mol) derivative **3l** was obtained (8.7 g, 68 %): ^{1}H NMR ($CDCl_3$, 400 MHz) [6]: δ =7.68 (dd, 1H, *J* = 1.7 and 0.75 Hz, ArH), 7.42 (dd, 1H, *J* =3.7 and 0.75 Hz, ArH), 6.67 (dd,1H, *J* = 3.7 and 1.7 Hz, ArH), 5.70 (s, 2H, CH_2); 13C NMR ($CDCl_3$, 100.6 MHz) [6]: δ = 174.5, 150.0, 148.2, 120.0, 113.7, 80.3; GC/MS (EI) t_r= 14.4 min: *m/z* (%)= 155 (M^+, 5), 83 (100).

2-Nitro-1-(thiophen-2-yl)-ethan-1-one (3m)

From 2-thiophenecarboxylic acid (10.2 g, 0.080 mol) derivative **3m** was obtained (10.0 g, 73 %): ^{1}H NMR ($CDCl_3$, 400 MHz) [7]: δ = 7.84 (dd, 1H , *J* = 5.0 and 1.1 Hz, ArH), 7.73 (dd, 1H, *J* = 3.9 and 1.1 Hz, ArH), 7.22 (dd, 1H, *J* = 5.0 and 3.9 Hz, ArH), 5.76 (s, 2H, CH_2); ^{13}C NMR ($CDCl_3$, 100.6 MHz) [7]: δ = 178.4, 139.9, 136.8, 133.8, 129.3, 80.9; GC/MS (EI) t_r= 18.2 min: *m/z* (%) = 171 (M^+, 14), 111 (100), 99 (53).

1-Nitrobutan-2-one (3n)

From propionic acid (6.7 g, 0.090 mmol) derivative **3n** was obtained (7.0 g, 66 %): ^{1}H NMR ($CDCl_3$, 400 MHz) [8]: δ =5.27 (s, 2H, CH_2-NO_2), 2.59 (q, 2H, *J* = 7.1 Hz, CH_2-CH_3), 1.17 (t, 3H, *J* =7.2 Hz, CH_3); ^{13}C NMR ($CDCl_3$, 100.6 MHz) [8]: δ = 196.6, 83.1, 34.0, 7.3; GC/MS (EI) t_r= 5.9 min: *m/z* (%)= 117 (M^+, 3), 88 (10), 57 (100).

1-Nitrohexane-2-one (3o)

From valeric acid (9.7 g, 0.095 mmol) derivative **3o** was obtained (8.9 g, 65 %): ^{1}H NMR ($CDCl_3$, 400 MHz): δ = 5.26 (s, 2H, CH_2-NO_2), 2.55 (t, 2H, *J* = 7.2 Hz, CH_2-CO), 1.64 (quintuplet, *J* = 7.2 Hz, 2H, CH_2-CH_2 -CO), 1.36 (sextet, *J* = 7.6 Hz, 2H, CH_2-CH_2CH_2 -CO), 0.92 (t, 3H, *J* = 7.6 Hz, CH_3); ^{13}C NMR ($CDCl_3$, 100.6 MHz): δ = 196.3, 83.3, 40.3, 25.3, 22.2, 13.8; GC/MS (EI) t_r= 10.2 min: *m/z* (%)= 98 (M^+ – 47, 10), 85 (65), 57 (100).

General procedure for the synthesis of racemic β-nitroalcohols 1a-o

To a stirred solution of aldehyde (1.50 mmol) in nitromethane (10 mL) triethylamine (1 mL) was added and the resulting solution was stirred at room temperature and monitored by TLC analysis. The solution was diluted with ethyl acetate (200 mL) and washed with water. The organic layers were dried over anhydrous Na_2SO_4 and concentrated *in vacuo*. The crude products were purified by silica gel column chromatography eluting with hexane and increasing amount of ethyl acetate.

2-Nitro-1-phenylethan-1-ol (1a)

From benzaldehyde (0.16 g, 1.5 mmol) derivative **1a** was obtained (0.15 g, 60%). ^{1}H NMR ($CDCl_3$, 400 MHz) [9]: δ = 7.43-7.34 (m, 5H, ArH), 5.46 (dt, 1H, *J* = 9.5 and 3.4 Hz, *CH*-OH), 4.62 (dd, 1H, *J*= 13.4 and 9.5 Hz, C*H*H-NO_2), 4.52 (dd,1H, *J* = 13.4 and 3.3 Hz, C*H*H-NO_2), 2.81 (d, 1H, *J* = 3.4 Hz, *OH*);^{13}C NMR ($CDCl_3$, 100.6 MHz) [9]: δ = 138.3, 129.1, 129.0, 126.0, 81.3, 71.1. HPLC [9]: Chiralcel OD, 95/5 hexane/*i*-PrOH, 0.6 mL min^{-1}, 215 nm, (*R*)-**1a** t_r = 43.2 min, (*S*)-**1a** t_r = 52.4 min.

2-Nitro-1-(*o*-tolyl)ethan-1-ol (1b)

From 2-tolualdehyde (0.18 g, 1.50 mmol) derivative **1b** was obtained (0.14 g, 52 %). ^{1}H NMR ($CDCl_3$, 400 MHz) [10]: δ = 7.52-7.44 (m, 1H, ArH), 7.30-7.15 (m, 3H, ArH), 5.64 (dd, 1H, *J* = 9.6 and 2.7 Hz, *CH*-OH), 4.51 (dd,1H, *J*= 13.3 and 9.6 Hz, C*H*H-NO_2), 4.40 (dd, 1H, *J* = 13.3 and 2.7 Hz, C*H*H-NO_2), 2.36 (s, 3H, CH_3); δ = ^{13}C NMR ($CDCl_3$, 100.6 MHz) [10]: δ = 136.4, 134.6, 131.0, 128.8, 126.9, 125.7, 80.4, 68.1, 19.0. HPLC [10]: Chiralcel OD, 90/10 hexane/*i*-PrOH, 0.6 mL min^{-1}, 215 nm, (*R*)-**1b** t_r = 17.8 min, (*S*)-**1b** t_r = 20.0 min.

2-Nitro-1-(*m*-tolyl)ethan-1-ol (1c):

From 3-tolualdehyde (0.18 g, 1.5 mmol) derivative **1b** was obtained (0.15 g, 56 %). ^{1}H NMR (400 MHz, $CDCl_3$) [11]: δ = 7.26 (m, 1H, Ar–H), 7.16 (m, 3H, Ar–H), 5.43 (dd, *J* = 9.6 and 3.1 Hz, 1H, *CH*OH), 4.61 (dd, *J* = 13.2 and 9.5, 1H, C*H*H-NO_2), 4.49 (dd, *J* =13.2 and 3.1 Hz, C*H*H-NO_2); 2.37 (s, 3H, CH_3); ^{13}C NMR (400 MHz, $CDCl_3$) [11]: δ = 138.9, 138.6, 129.6, 129.0, 126.7, 123.1, 81.7, 71.1, 21.5. HPLC [12]: Chiralcel OD, 90/10 hexane/*i*-PrOH, 0.6 mL min^{-1}, 215 nm, (*R*)-**1c** t_r = 19.3 min, (*S*)-**1c** t_r = 22.2 min.

2-Nitro-1-(p-tolyl)ethan-1-ol (1d)

From 4-tolualdehyde (0.18 g, 1.5 mmol) derivative **1d** was obtained (0.18 g, 66 %). ^{1}H NMR ($CDCl_3$, 400 MHz) [11]: δ = 7.31-7.27 (d, 2H, *J* = 8.0 Hz, ArH), 7.23-7.19 (d, 2H, *J* = 8.0 Hz, ArH), 5.43 (dd, 1H, *J* = 9.5 and 3.0 Hz, *CH*-OH), 4.61 (dd,1H, *J*= 13.3 and 9.5 Hz, C*H*H-NO_2), 4.49 (dd, 1H, *J* = 13.3 and 3.0 Hz, C*H*H-NO_2), 2.36 (s, 3H, CH_3); ^{13}C NMR ($CDCl_3$, 100.6 MHz) [11]: δ = 139.3, 135.4, 129.8, 126.0, 81.4, 71.1, 21.3. HPLC [12]: Chiralcel OD, 90/10 hexane/*i*-PrOH, 0.6 mL min^{-1}, 215 nm, (*R*)-**1d** t_r = 22.3 min, (*S*)-**1d** t_r = 28.8 min.

1-(4-Methoxyphenyl)-2-nitroethan-1-ol (1e)

From 4-anisaldehyde (0.20 g, 1.5 mmol) derivative **1e** was obtained (0.19 g, 64%). ^{1}H NMR ($CDCl_3$, 400 MHz) [10]: δ = 7.33 - 7.31 (m, 2H, ArH), 6.93 - 6.90 (m, 2H, ArH), 5.42 (dd, 1H, *J* = 9.6 and

3.1 Hz, *CH*-OH), 4.61 (dd,1H, *J* = 13.3 and 9.5 Hz, C*H*H-NO_2), 4.61 (dd, 1H, *J* = 13.3 and 9.5 Hz, C*H*H-NO_2), 4.48 (dd, 1H, *J* = 13.3 and 3.1 Hz, C*H*H-NO_2), 3.81 (s, 3H, OCH_3);^{13}C NMR ($CDCl_3$, 100.6 MHz) [10]: δ = 160.2, 130.4, 127.4, 114.6, 81.4, 70.8, 55.5. HPLC [10]: Chiralcel OD, 90/10 hexane/*i*-PrOH, 0.6 mL min^{-1}, 215 nm, (*R*)-**1e** t_r = 31.8 min, (*S*)-**1e** t_r = 40.7 min.

1-(2-Fluorophenyl)-2-nitroethan-1-ol (1f)

From 2-fluorobenzaldehyde (0.19 g, 1.5 mmol) derivative **1f** was obtained (0.17 g, 61 %). ^{1}H NMR ($CDCl_3$, 400 MHz) [13]: δ =7.57 (m, 1H, Ar–H), 7.34 (m, 1H, Ar–H), 7.22 (m, 1H, Ar–H), 7.08 (m, 1H, Ar–H), 5.75 (dd, *J* = 8.5 and 3.8 Hz, 1H, C*H*OH), 4.61 (m, 2H, CH_2NO_2); ^{13}C NMR (400 MHz, $CDCl_3$): δ = 159.5 (d, *J* = 246 Hz), 136.5 (d, *J* = 9.2 Hz), 130.4 (d, *J* = 8.3 Hz), 127.8 (d, *J* = 3.8 Hz), 124.9 (d, *J* = 3.6 Hz), 116.6 (d, *J* = 20.4 Hz), 115.7 (d, *J* = 21.2 Hz), 80.2, 65.4. HPLC [13]: Chiralart Amylose SA, 97/3 hexane/*i*-PrOH, 0.6 mL min^{-1}, 215 nm, (*S*)-**1f** t_r = 32.7 min, (*R*)-**1f** t_r = 36.2 min.

1-(3-Fluorophenyl)-2-nitroethan-1-ol (1g)

From 3-fluorobenzaldehyde (0.19 g, 1.5 mmol) derivative **1g** was obtained (0.16 g, 57 %). ^{1}H NMR ($CDCl_3$, 400 MHz) [14]: δ = 7.40 - 7.33 (m, 1H, ArH), 7.20 -7.12 (m, 2H, ArH), 7.08 - 7.01 (m, 1H, ArH), 5.47 (dd, 1H, *J* = 9.2 and 3.3 Hz, *CH*-OH), 4.59 (dd, 1H, *J* = 13.4 and 9.4 Hz, C*H*H-NO_2), 4.52 (dd, 1H, *J* = 13.4 and 3.3 Hz, C*H*H-NO_2); ^{13}C NMR ($CDCl_3$, 100.6 MHz) [14]: δ = 163.2 (d, *J* = 247 Hz), 141.5 (*J* = 7.2 Hz), 130.7 (d, *J* = 8.1 Hz), 121.6 (d, *J* = 3.4 Hz), 115.9 (d, *J* = 21.2 Hz), 113.4 (d, *J* = 22.4 Hz), 81.5, 70.4. HPLC [14]: Chiralcel OD, 90/10 hexane/*i*-PrOH, 0.6 mL min^{-1}, 215 nm, (*R*)-**1g** t_r = 21.0 min, (*S*)-**1g** t_r = 24.3 min.

1-(4-Fluorophenyl)-2-nitroethan-1-ol (1h)

From 4-fluorobenzaldehyde (0.19 g, 1.5 mmol) derivative **1h** was obtained (0.18 g, 65 %). ^{1}H NMR ($CDCl_3$, 400 MHz) [9]: δ = 7.42-7.37 (m, 2H, ArH), 7.12-7.07 (m, 2H,ArH), 5.46 (dd, 1H, *J* =9.4 and 3.2 Hz, *CH*-OH), 4.59 (dd, 1H, *J* = 13.4 and 9.4 Hz, C*H*H-NO_2), 4.50 (dd, 1H, *J* = 13.4 and 3.1 Hz, C*H*H-NO_2);^{13}C NMR ($CDCl_3$, 100.6 MHz) [9]: δ = 163.1 (d, *J* = 248 Hz), 134.0 (d, *J* = 3.2 Hz), 127.9 (d, *J* = 8.2 Hz), 116.2 (d, *J* = 22 Hz), 81.3, 70.5. HPLC [9]: Chiralcel OD, 90/10 hexane/*i*-PrOH, 0.6 mL min^{-1}, 215 nm, (*R*)-**1h** t_r = 18.9 min, (*S*)-**1h** t_r = 22.5 min.

1-(4-Bromophenyl)-2-nitroethan-1-ol (1i)

From 4-bromobenzaldehyde (0.28 g, 1.5 mmol) derivative **1i** was obtained (0.19 g, 52%). ^{1}H NMR ($CDCl_3$, 400 MHz) [11]: δ =7.56-7.52 (m, 2H, ArH), 7.31-7.28 (m, 2H, ArH), 5.44 (dd, 1H, *J* = 9.3

and 3.2 Hz, *CH*-OH), 4.57 (dd, 1H, *J* = 13.5 ad 9.2 Hz, C*H*H-NO_2),4.49 (dd, 1H, *J* = 13.5 and 3.2 Hz, C*H*H-NO_2); ^{13}C NMR ($CDCl_3$, 100.6 MHz) [11]: δ = 137.2, 132.3, 127.8, 123.1, 81.1, 70.5. HPLC [11]: Chiralcel OD, 95/5 hexane/*i*-PrOH, 0.6 mL min^{-1}, 215 nm, (*R*)-**1i** t_r = 49.5 min, (*S*)-**1i** t_r = 65.9 min.

1-(4-Chlorophenyl)-2-nitroethan-1-ol (1j)

From 4-chlorobenzaldehyde (0.21 g, 1.5 mmol) derivative **1j** was obtained (0.19 g, 63%). ^{1}H NMR ($CDCl_3$, 400 MHz) [9]: δ = 7.41-7.33 (m, 4H, ArH), 5.45 (dd, 1H, *J* = 9.4 and 3.1 Hz, *CH*-OH), 4.58 (dd, 1H, *J* = 13.4 and 9.3 Hz, C*H*H-NO_2), 4.50 (dd, 1H, *J* = 13.4 and 3.2 Hz, C*H*H-NO_2); ^{13}C NMR ($CDCl_3$, 100.6 MHz) [9]: δ = 136.8, 134.8, 129.2, 127.4, 81.1, 70.4. HPLC [9]: Chiralcel OD, 90/10 hexane/*i*-PrOH, 0.6 mL min^{-1}, 215 nm, (*R*)-**1j** t_r = 20.6 min, (*S*)-**1j** t_r = 25.6 min.

1-(Naphthalen-2-yl)-2-nitroethan-1-ol (1k)

From 2- naphtaldehyde (0.23 g, 1.5 mmol) derivative **1k** was obtained (0.20 g, 62 %). ^{1}H NMR ($CDCl_3$, 400 MHz) [15]: δ = 7.90 - 7.75 (m, 4H, ArH), 7.53 - 7.47 (m, 2H, ArH), 7.44 (dd, 1H, *J* = 8.4 and 1.8 Hz, ArH), 5.59 (dd, 1H, *J* = 9.5 and 3.2 Hz, *CH*-OH), 4.67 (dd, 1H, *J* = 13.2 and 9.5 Hz , C*H*H-NO_2), 4.56 (dd, 1H, *J* = 13.2 and 3.2 Hz, C*H*H-NO_2); ^{13}C NMR ($CDCl_3$, 100.6 MHz) [15]: δ = 136.0, 133.4, 133.2, 128.8, 128.1, 127.8, 126.61, 126.57, 125.3, 123.4, 81.3, 71.1. HPLC [16]: Chiralcel OD, 80/20 hexane/*i*-PrOH, 0.8 mL min^{-1}, 215 nm, (*R*)-**1k** t_r = 25.2 min, (*S*)-**1k** t_r = 36.8 min.

1-(Furan-2-yl)-2-nitroethan-1-ol (1l)

From 2- furanaldehyde (0.14 g, 1.5 mmol) derivative **1l** was obtained (0.14 g, 59 %). ^{1}H NMR ($CDCl_3$, 400 MHz) [11]: δ = 7.43-7.41(m, 1H, furan H), 6.42-6.37 (m,2H, furan H), 4.79 (dd, 1H, *J* = 13.5 and 8.8 Hz , C*H*H-NO_2), 4.68 (dd, 1H, *J* = 13.5 and 3.5 Hz, C*H*H-NO_2);^{13}C NMR ($CDCl_3$, 100.6 MHz) [11]: δ = 150.9, 143.3, 110.8, 108.3, 78.6, 65.0. HPLC [17]: Chiralart Amylose SA, 90/10 hexane/*i*-PrOH, 0.5 mL min^{-1}, 215 nm, (*S*)-**1l** t_r = 20.5 min, (*R*)-**1l** t_r = 22.1 min.

2-Nitro-1-(thiophen-2-yl)ethan-1-ol (1m)

From thiophen-2-aldehyde (0.17 g, 1.50 mmol) derivative **1m** was obtained (0.15 g, 58%).^{1}H NMR ($CDCl_3$, 400 MHz) [12]: δ = 7.34 (dd, 1H, *J* = 5.1 and 1.3 Hz, thiophen H), 7.08-7.06 (m, 1H, thiophen H), 7.02 (dd, 1H, *J* = 5.1 and 3.5 Hz, thiophen H), 5.73 (dd, 1H, *J* = 9.3 and 3.3 Hz, *CH*OH), 4.72 (dd, 1H, *J* = 13.5 and 9.2 Hz, C*H*H-NO_2), 4.62 (dd, 1H, *J*= 13.5 and 3.3 Hz, C*H*H-NO_2); ^{13} C NMR

($CDCl_3$, 100.6 MHz) [12]: δ = 141.3, 127.0, 126.4, 124.9, 80.6, 67.1. HPLC [18]: Chiralcel OD, 90/10 hexane/*i*-PrOH, 0.6 mL min^{-1}, 215 nm, (*S*)-**1m** t_r = 22.8 min, (*R*)- **1m** t_r = 24.7 min.

1-Nitrobutan-2-ol (1n)

Frompropanaldehyde (0.087 g, 1.5 mmol) derivative **1n** was obtained (0.19 g, 62 %). ^{1}H NMR ($CDCl_3$, 400 MHz) [14]: δ = 4.48 - 4.34 (m, 2H, CH_2-NO_2), 4.30 - 4.20 (m, 1H, *CH*-OH), 1.65 - 1.45 (m, 2H, CH_2-CH_3), 1.03 (t, 3H, *J* = 7.4 Hz, CH_3); ^{13}C NMR ($CDCl_3$, 100.6 MHz) [14]: δ = 80.6, 69.9, 27.0, 9.4. HPLC [14]: Chiralcel OD, 97/3 hexane/*i*-PrOH, 0.6 mL min^{-1}, 215 nm, (*R*)-**1n** t_r = 30.2 min, (*S*)-**1n** t_r = 32.8 min.

1-Nitrohexan-2-ol (1o)

From valeraldehyde (0.13 g, 1.5 mmol) derivative **1o** was obtained (0.16 g, 73%). ^{1}H NMR ($CDCl_3$, 400 MHz) [9]: δ = 4.46 - 4.28 (m, 3H, *CH*-OH + CH_2NO_2), 1.60 -1.30 (m, 6H, 3 CH_2), 0.93 (t, 3H, *J*= 7.0 Hz, CH_3); ^{13}C NMR ($CDCl_3$, 100.6 MHz) [9]: δ = 80.8, 68.8, 33.6, 27.5, 22.6, 14.0. HPLC [16]: Chiralcel OD, 97/3 hexane/*i*-PrOH, 0.6 mL min^{-1}, 215 nm, (*R*)-**1o** t_r = 23.8 min, (*S*)-**1o** t_r = 24.9 min.

References

[1] Russo, A.; Lattanzi, A. Catalytic asymmetric beta-peroxidation of nitroalkenes. *Adv. Synth. Catal.* **2008**, *350*, 1991-1995.

[2] Choudhary, M.K.; Rajkumar Tak, R.; Kureshy, R.I.; Ansari, A.; Khan, N.H.; Abdi, S.H.R.; Bajaj, H.C. Enantioselective aza-Henry reaction for the synthesis of (*S*)-levamisole using efficient recyclable chiral Cu(II)-amino alcohol derived complexes. *J. Mol. Catal. A.* **2015**, *409*, 85-93.

[3] O'Brien, P.; Osborne, S.A.; Parker, D.D. Asymmetric aminohydroxylation of substituted styrenes: applications in the synthesis of enantiomerically enriched arylglycinols and a diamine. *J. Chem. Soc. Perkin Trans.* **1998**, *1*, 2519-2526.

[4] Lindsay, V.N.G.; Cyril, N.; Charette, A.B. Asymmetric Rh(II)-catalyzed cyclopropanation of alkenes with diacceptor diazo compounds: *p*-methoxyphenyl ketone as a general stereoselectivity controlling group. *J. Am. Chem. Soc.* **2011**, *133*, 8972-8981.

[5] Brenna, E.; Crotti, M.; Gatti, F.G.; Monti, D.; Parmeggiani, F.; Santangelo, S. Asymmetric bioreduction of β-acylaminonitroalkenes: easy access to chiral building blocks with two vicinal nitrogen-containing functional groups. *ChemCatChem*, **2017**, *9*, 2480-2487.

[6] Katritzky, A.R.; Abdel-Fattah, A.A.A.; Gromova, A.V.; Witek, R.; Steel, P.J. α-Nitro ketone synthesis using *N*-acylbenzotriazoles. *J. Org. Chem* **2005**, *70*, 9211-9214.

[7] Lian, Z.; Friis, S.D.; Skrydstrup, T. Palladium-catalysed carbonylative α-arylation of nitromethane. *Chem. Commun.* **2015**, *51*, 3600-3603.

[8] Takamoto, M.; Kurouchi, H.; Otani, Y.; Ohwada, T. Phenylation reaction of α-acylnitromethanes to give 1,2-diketone monooximes: involvement of carbon electrophile at the position α to the nitro group. *Synthesis* **2009**, 4129-4136.

[9] Evans, D.A., Seidel, D.; Rueping, M.; Wai Lam, H.; Shaw, J.T.; Downey, C.W. A new copper acetate-bis(oxazoline)-catalyzed, enantioselective Henry reaction. *J. Am. Chem. Soc*. **2003**, *125*, 12692-12693.

[10] Kottala Vijaya, P.; Murugesan, S.; Siva, A. Highly enantioselective asymmetric Henry reaction catalyzed by novel chiral phase transfer catalysts derived from cinchona alkaloids. *Org. Biomol. Chem*. **2016**, *14*, 10101-10109.

[11] Xu, D.; Sun, Q.; Quan, Z.; Sun, W.; Wang, X. The synthesis of chiral tridentate ligands from l-proline and their application in the copper(II)-catalyzed enantioselective Henry reaction. *Tetrahedron:Asymmetry* **2017**, *28*, 954-963.

[12] Boobalan, R.; Lee, G.H.; Chen, C. Copper complex of aminoisoborneol Schiff base Cu_2(SBAIB-d)$_2$: an efficient catalyst for direct catalytic asymmetric nitroaldol (Henry) reaction. *Adv. Synth. Catal.,* **2012**, *354*, 2511-2520.

[13] Khong, D.T.; Judeh, Z.M.A. Synthesis of chiral tetrahydroisoquinoline and C_2-symmetric bistetrahydroisoquinoline ligands and their application in the enantioselective Henry reaction. *Synthesis* **2016**; *48*, 2271-2279.

[14] Lu, G.; Zheng, F.; Wang, L.; Guo, Y.; Li, X.; Cao, X.; Wang, C.; Chi, H.; Dong, Y.; Zhang, Z. Asymmetric Henry reaction catalyzed by Cu(II)-based chiral amino alcohol complexes with C_2-symmetry *Tetrahedron: Asymmetry* **2016**, *27*, 732-739.

[15] Park, J.; Lang, K.; Abboud, K.A.; Hong, S. Asymmetric Henry reaction catalyzed by Cu(II)-based chiral amino alcohol complexes with C_2-symmetry. *J. Am. Chem. Soc.,* **2008**, *130*, 16484-16485.

[16] Chunhong, Z.; Liu, F.; Gou, S. Application of chiral *N,N′*-dialkyl-1,2-cyclohexanediamine derivatives in asymmetric copper(II)-catalyzed Henry reactions. *Tetrahedron: Asymmetry* **2014**, *25*, 278-283.

[17] Scharnagel, D.; Prause, F.; Kaldun, J.; Haase, R.G.; Breuning, M. (2*S*,5*R*)-2-Methylaminomethyl-1-methyl-5-phenylpyrrolidine, a chiral diamine ligand for copper(II)-catalysed Henry reactions with superb enantiocontrol. *Chem. Commun*. **2014**, *50*, 6623-6625.

[18] Ao, C.; Men, J.; Wang, Y.; Shao, T.; Huang, Y.; Huo, J.; Gao, G. The development of new amine-amide ligands for application in Cu(II)-catalyzed enantioselective Henry reactions. *Tetrahedron: Asymmetry* **2016**, *27*, 589-595.

Chapter 2

Experimental Part

General analytical methods

GC/MS analyses were performed using a HP-5MS column (30 m × 0.25 mm × 0.25 μm, Agilent). The following temperature program was employed: 60 °C (1 min), 6 °C min^{-1}/150 °C (1 min), 12 °C min^{-1}/280 °C (5 min). Bradford assay [1] was performed by using a Shimadzu UV-1601 spectrophotometer and bovine serum albumin (BSA) was used as reference standard protein.

Activity Assays

Spectrophotometric Enzymatic Assay

a) For the OYE activity assay, in a 2 mL cuvette, a solution of cyclohex-2-enone (5 μL; stock solution = 10 mM in DMSO) and a solution of NADH (20 μL; stock solution = 10 mM in water) were added to 50 mM phosphate buffer pH 7 (916 μL). The reaction was carried out at 28 °C and started by adding to the blank solution 59 μL of OYE3 (177 μg, conc. = 3 mg-mL^{-1}).

b) For the GDH activity assay, in a 2 mL cuvette, a solution of glucose (205 μL; stock solution = 1 M in water) and a solution of NAD^+ (20 μL; stock solution = 10 mM in water) were added to 50 mM phosphate buffer pH 7 (960 μL). The reaction was carried out at 28 °C and started by adding to the blank solution 2 μL of GDH (6 μg, conc. = 3 mg mL^{-1}).

The enzymatic activity (U mL^{-1}) was calculated from the consumption/formation of NADH, for a) and b), respectively, at 340 nm ($\varepsilon_{NAD(P)H}$=6200 M^{-1} cm^{-1}) according to the following equation:

$$\frac{U}{mL} = \frac{\Delta Abs/min \cdot V_{tot}}{V_E \cdot \varepsilon}$$

ΔAbs/min: slope of Abs *vs* time curve (mAU min^{-1}), V_{tot}: total assay volume (mL), V_E: volume of soluble enzyme used in the assay (mL), ε: NAD(P)H molar absorbivity (6200 M^{-1} cm^{-1}).

One Unit (U) is defined as the amount of enzyme that converts 1 μmol of substrate in the product in 1 min under specific temperature and pH conditions.

GC/MS enzymatic assay

In a 2 mL test-tube, a solution of (*R*)-carvone (10 µL; stock solution= 100 mM in DMSO) and 15 µL of soluble OYE3 (conc.: 3 mg mL^{-1}) or immobilized OYE3 (ca. 20 mg for OYE3-GA or 45 mg for OYE3-EziG) were added to 50 mM phosphate buffer, pH 7 (final volume = 1 mL). The reaction was started by adding NADH (100 µL; stock solution = 10 mM in water) and the mixture was kept at 28 °C under stirring (thermoshaker) for 30 min, then vortexed for 30 sec in the presence of CH_2Cl_2 (200 µL). The organic phase was separated by centrifugation (2 min, 13500 rpm), dried over Na_2SO_4 for 5 min, and analyzed by GC/MS. (*R*)-carvone: GC/MS (EI) t_r = 12.99 min: *m/z* (%) = 150 (M^+, 15), 135 (10), 108 (40), 93 (40), 82 (100). Product: GC/MS (EI) t_r = 11.83 min: *m/z* (%) = 152 (M^+, 30), 137 (25), 123 (10), 109 (55), 95 (100). The enzymatic activity (U mL^{-1} for the non-immobilized enzyme, or U g^{-1} for the immobilized enzyme) was calculated from the percentage of substrate conversion after 30 min according to the following equation:

$$\frac{U}{mL\ or\ g} = \frac{[S] \cdot c}{t_R \cdot E}$$

[S]: substrate concentration (mM), c: conversion (%), t: reaction time (30 min), E: amount of soluble enzyme (mL) or immobilized enzyme (g).

One unit (U) is defined as the amount of enzyme that converts 1 µmol of substrate in the product in 1 min under specific temperature and pH conditions.

*OYE3-Mediated reduction of α-methyl-*trans*-cinnamaldehyde (3)*

In a 2 mL test tube, a solution of α-methyl-*trans*-cinnamaldehyde (10 µL; stock solution= 500 mM in DMSO) was added to 50 mM phosphate buffer pH 7 (838 µL) followed by a solution of $NADP^+$ (10 µL; stock solution = 10 mM in water), glucose (20 µL; stock solution = 1 M in water), and GDH (10 µL; 5 mg mL^{-1}). The reaction (final volume=1 mL) was started by adding 160 µg of OYE3 (non-immobilized enzyme: 53 µL; OYE3-GA=80 mg; OYE3-EziG=170 mg) and kept under stirring (thermoshaker) at 28 °C for 1 h. At the endpoint, in the case of the immobilized enzyme, the reaction was stopped by removing the biocatalyst by centrifugation (4 min, 13200 rpm). The reaction mixture was vortexed for 30 sec in the presence of CH_2Cl_2 (400 µL). The organic phase was separated by centrifugation (2 min, 13200 rpm), dried over Na_2SO_4 for 5 min, and analyzed by GC/MS. α-Methyl-*trans*-cinnamaldehyde: GC/MS (EI) t_r = 14.60 min: *m/z* (%) = 146 (M^+, 70), 145 (100), 117 (80), 115

(70), 91 (50). Product: GC/MS (EI) t_r = 11.68 min: *m/z* (%) = 148 (M^+, 45), 133 (25), 105 (25), 91 (100). The conversion was evaluated from the ratio of the peak areas of product and substrate.

Stability of OYE3 in the pH range 8-10

The stability of non-immobilized OYE3 was assayed in the pH range 8-10 by incubating 100 µL of the enzyme solution (stored in 20 mM phosphate buffer pH 8.5 containing 200 mM imidazole and 500 mM NaCl) in 100 µL of 50 mM phosphate buffer pH 7.5 (final pH=8), 50 mM Tris-HCl buffer pH 9.5 (final pH=9), or 50 mM NaOH/glycine buffer pH 11.5 (final pH=10) at 20 °C. After 3 h, 100 µL were withdrawn from each sample and the enzymatic activity was measured spectrophotometrically in the reduction of cyclohex-2-enone. The residual activity was calculated according to the following equation:

$$Residual\ activity\ (\%) = \frac{observed\ activity\ at\ the\ endpoint}{starting\ activity} \times 100$$

Covalent immobilization of OYE3 on glyoxyl-agarose (OYE3-GA)

Immobilization of OYE3 on glyoxyl-agarose was performed following the protocol previously reported [19]. Briefly, glyoxyl-agarose (1.8 g = 2.52 mL) was suspended in 50 mM Na_2CO_3 buffer (14.3 mL) at pH 10. After the addition of the desired amount of protein (1.2 mL, loading: 2 mg g^{-1}), the suspension was kept under mechanical stirring for 3 h at 4 °C. Chemical reduction of Schiff bases and unreacted aldehyde groups was carried out over 30 min by adding $NaBH_4$ to the mixture (18 mg; 1 mg mL^{-1} of suspension). The immobilized enzyme was then filtered and washed with 10 mM phosphate buffer pH 7 and deionized water.

The immobilization reaction was monitored by measuring the amount of protein in the supernatant before the addition of the carrier and after 1.5 h and 3 h [1]. The immobilization yield (%, endpoint: 3 h) was calculated according to the following equation [2]:

$$Yield\ (\%) = \frac{immobilized\ protein}{starting\ protein} \times 100$$

The activity of the immobilized OYE3 was measured by the GC/MS enzymatic assay (reduction of (*R*)-carvone, **2**). The activity recovery (%) was calculated according to the following equation [2]:

$$Activity\ recovery\ (\%) = \frac{observed\ activity}{starting\ activity} \times 100$$

Immobilization of OYE3 by affinity-based adsorption (OYE3-EziG)

Immobilization of OYE3 by affinity-based adsorption on EziG™ (Opal, Coral, and Amber) was performed following the protocol of the supplier with minor modifications. EziG™ (100 mg) was added to a 2 mL test tube containing the enzyme (140 µL, loading: 4.2 mg g^{-1} of dry carrier) diluted in 50 mM phosphate buffer pH 7 (1.5 mL) at r.t. After 30 min, the test tube was centrifugated (5 min, 13200 rpm) and the supernatant was removed by pipetting. Following supplier's instructions, the wet enzyme preparation was stored as such (when the immobilized enzyme was filtered under vacuum, it showed an almost complete loss of activity. The weight of the wet carrier was estimated to be 4.5-fold higher than the dry carrier. The activity recovery (%) was referred to the wet carrier weight).
The immobilization yield (%, endpoint: 30 min) was calculated as reported above. The activity of the immobilized OYE3 was measured by the (*R*)-carvone assay and the activity recovery (%) was calculated as described above.
Co-immobilization of OYE3 and GDH on EziG™ Opal was carried out by following the procedure applied to OYE3 immobilization. Briefly, EziG™ Opal (100 mg) was added to 50 mM phosphate buffer pH 7 (1.5 mL) containing OYE3 (140 µL, U = 0.06) and GDH (45 µL, U = 0.87). Monitoring and work-up of the immobilization mixture was performed as above reported.

Stability of non-immobilized OYE3, OYE3-GA, and OYE3-EziG

For each endpoint, non-immobilized or immobilized OYE3 (42 µg of protein) was incubated in a solution containing 50 mM phosphate buffer pH 7 (890 µL) and (*R*)-carvone (10 µL; stock solution: 100 mM in DMSO) at 28 °C. Each reaction was started by adding NADH (100 µL; stock solution: 10 mM in water). The final volume was 1 mL. The enzyme activity was assessed by the standard activity assay (reduction of (*R*)-carvone). The enzyme activity was compared with the starting activity which was considered as 100%.

Protein leakage assay

For each endpoint (1-3-6-24-48 h), 42 µg of protein (corresponding to 21 mg of OYE3-GA and 45 mg of OYE3/GDH-EziG) were incubated in 50 mM phosphate buffer pH 7 (200 µL). The suspensions were kept at 28 °C under stirring (thermoshaker). At each endpoint, a sample (15 µL) was withdrawn from the supernatant and analyzed by SDS-PAGE. GDH and OYE3 (450 ng, corresponding to 0.15 µL of each stock solution) were loaded in the gel as reference standards. Precision Plus Protein™

Unstained Protein Standards (10-250 kD) was used as molecular weight proteins size marker. PAGE analysis was performed in a Mini-Protean 3 system (Bio-Rad). SDS-PAGE was carried out on 12% polyacrylamide (running buffer: 50 mM MES, 50 mM Tris base, 0.1 % w/v SDS and 1 mM EDTA). Proteins were stained by means of a silver staining kit (SilverQuest™ kit, Thermofisher) according to supplier's protocol.

Recycling of immobilized enzymes

Recycling of immobilized OYE3-GA and OYE3/GDH-EziG was performed by evaluating the conversion (%) of α-methyl-*trans*-cinnamaldehyde (**3**) into **3a**. At the end of the reaction, the immobilized biocatalyst was washed twice with 1 mL of 50 mM phosphate buffer pH 7, separated through centrifugation, and then re-suspended under the conditions above described for the next reaction cycle.

References

[1] Bradford, M.M. A rapid and sensitive method for the quantitation of microgram quantities of protein utilizing the principle of protein-dye binding. *Anal. Biochem.* **1976**, *27*, 248-254.

[2] Sheldon, R.A.; van Pelt, S. Enzyme immobilisation in biocatalysis: Why, what and how. *Chem. Soc. Rev.* **2013**, *42*, 6223-6235.

Chapter 3

Supplementary Information

Preliminary screening of ADH-mediated reduction of 4-alkylcyclohexanones 4 and 5 to 4-alkylcyclohexanols 1 and 3

[a] 5 mM substrate, 20 mM glucose, ADH (200 µg mL^{-1}), GDH (5 U mL^{-1}), NADH and $NADP^+$ (0.1 mmol each), 1% DMSO, phosphate buffer pH 7.0, 30°C, 18 h; conversion (c %) and diastereoisomeric excess (*de* %) calculated by GC/MS.

	4-isopropylcyclohexan-1-one		**4-(*tert*-butyl)cyclohexan-1-one**	
ADH	**c (%)**	***de* (%)**	**c (%)**	***de* (%)**
10	60	77 (*trans*)	7	71 (*trans*)
20	45	91 (*trans*)	4	>99 (*trans*)
30	>99	89 (*cis*)	>99	>99 (*cis*)
40	20	90 (*trans*)	5	>99 (*trans*)
130	16	80 (*trans*)	5	>99 (*trans*)
140	32	50 (*trans*)	<1	-
190	16	75 (*trans*)	<1	-
200	>99	87 (*cis*)	>99	>99 (*cis*)
210	27	48 (*trans*)	8	50 (*trans*)
250	31	23 (*trans*)	34	94 (*cis*)
260	<1	-	<1	-
270	>99	73 (*cis*)	>99	67 (*cis*)
380	63	17 (*trans*)	42	>99 (*trans*)
420	>99	81 (*cis*)	>99	97 (*cis*)

430	5	60 (*trans*)	16	>99 (*trans*)
440	>99	87 (*trans*)	>99	>99 (*trans*)
441	>99	87 (*cis*)	>99	>99 (*cis*)
442	31	61 (*trans*)	65	78 (*trans*)

Table S1. ADH-mediated reduction of 4-alkylcyclohexanones **4** and **5** to 4-alkylcyclohexanols **1** and **3** (preliminary screening) [a].

Preliminary screening of ADH-mediated reduction of 4-alkylcyclohexanones 6 and 7 to 4-alkylcyclohexanols 8 and 9

[a] 5 mM substrate, 20 mM glucose, ADH (200 µg mL^{-1}), GDH (5 U mL^{-1}), NADH and $NADP^+$ (0.1 mmol each), 1% DMSO, phosphate buffer pH 7.0, 30°C, 18 h; conversion (c %) and diastereoisomeric excess (*de* %) calculated by GC/MS.

	4-methylcyclohexan-1-one		**4-phenylcyclohexan-1-one**	
ADH	**c (%)**	***de* (%)**	**c (%)**	***de* (%)**
10	11	64 (*trans*)	32	>99 (*trans*)
20	12	>99 (*trans*)	53	>99 (*trans*)
30	47	96 (*cis*)	>99	>99 (*cis*)
40	<1	-	7	>99 (*trans*)
130	<1	-	6	>99 (*trans*)
140	<1	-	<1	-
190	<1	-	9	33 (*cis*)
200	46	91 (*cis*)	>99	>99 (*cis*)
210	23	39 (*trans*)	<1	-
250	18	78 (*cis*)	34	94 (*cis*)
260	<1	-	<1	-
270	78	92 (*cis*)	95	83 (*cis*)

380	86	7 (*trans*)	76	61 (*trans*)
420	85	90 (*cis*)	57	79 (*cis*)
430	11	45 (*cis*)	17	88 (*trans*)
440	90	98 (*trans*)	95	>99 (*trans*)
441	77	95 (*cis*)	77	64 (*cis*)
442	<1	-	97	94 (*trans*)

Table S2. ADH-mediated reduction of 4-alkylcyclohexanones **6** and **7** to 4-alkylcyclohexanols **8** and **9** (preliminary screening) [a].

Experimental Part

General analytical methods

^{1}H and ^{13}C NMR spectra were recorded on a 400 or 500 MHz spectrometer in $CDCl_3$ solution at r.t. The chemical shift scale was based on internal tetramethylsilane. GC/MS analyses were performed using a HP-5MS column (30 m × 0.25 mm × 0.25 μm, Agilent Technologies Italia Spa (Cernusco sul Naviglio, Italy)). The following temperature program was employed: 60 °C (1 min) / 6 °C min^{-1} / 150 °C (1 min) / 12°C min^{-1} / 280 °C (5 min).

General Procedure for the ADH-mediated reduction of cyclohexanones 4-7 (Screening Scale)

The suitable substrate (5 μmol), dissolved in DMSO (10 μL), was added to a phosphate buffer solution (1 mL, 50 mM, pH 7) containing glucose (20 mM, 4 eq. with respect to the substrate), NADH and $NADP^+$ (0.1 mM each), GDH (5 U mL^{-1}), and an ADH (200 μg mL^{-1}). The mixture was kept for 18 h in an orbital shaker (160 rpm, 30 °C). The solution was extracted with EtOAc (3 × 500 μL) and centrifuged (15000 g, 1.5 min). The combined organic phases were dried over Na_2SO_4 and analyzed.

General Procedure for Lipase-Mediated Acetylation of cis-4-(tert-butyl)cyclohexan-1-ol (cis-3) (Screening Scale)

Alcohol *cis*-**3** (50 mg mL^{-1} final concentration) was dissolved in a solution of MTBE and vinyl acetate (10% v/v). A suitable lipase was added (10 mg mL^{-1}). The reaction mixture was shaken (160 rpm, 30 °C) for 18 h in an orbital shaker.

General Procedure for **cis***-selective ADH-Mediated Reduction of Cyclohexanones 4-7 (Semi-preparative Scale)*

The suitable substrate (500 mg), dissolved in 2-propanol (2.2 mL), was added to a phosphate buffer solution (50 mM, pH 7) for a total volume of 40 mL together with ADH200 (10 mg) and NADH (10 mg). The mixture was kept for 24 h in an orbital shaker (160 rpm, 30 °C), then extracted with EtOAc (3 × 40 mL). The combined organic phases were dried over Na_2SO_4 and concentrated *in vacuo* to

afford the corresponding alcohol derivative without the need for further purification except for compound *cis*-**8.**

***Cis*-4-isopropylcyclohexan-1-ol (*cis*-1)**

From compound **4** (500 mg, 3.57 mmol), derivative *cis*-**1** was obtained (461 mg, 91%, *de* = 87%):

^{1}H NMR ($CDCl_3$, 400 MHz) [1]: δ = 3.99 (m, 1H, C*H*OH), 1.79-1.72 (m, 2H, hydrogens of cyclohexane ring), 1.53-1.41 (m, 7H, hydrogens of cyclohexane ring), 1.09-1.02 (m, 1H, $CH(CH_3)_2$), 0.88 (d, 6H, *J* = 6.8 Hz, $C(CH_3)_2$). ^{13}C NMR ($CDCl_3$, 100.6 MHz): δ = 66.6, 43.4, 32.7, 32.0, 23.7, 19.9. GC/MS (EI) t_r = 10.23 min: *m/z* (%) = 141 (M^+ – 1, 1), 124 (25), 109 (25), 95 (10), 81 (100). Compound *cis*-**1** was submitted to bulb-to-bulb distillation (85-88 °C, 10 mmHg) to obtain a sample for olfactory evaluation.

***Cis*-4-(*tert*-butyl)cyclohexan-1-ol (*cis*-3)**

From compound **5** (500 mg, 3.25 mmol), derivative *cis*-**3** was obtained (481 mg, 95%, *de* > 99%): ^{1}H NMR ($CDCl_3$, 400 MHz) [2]: δ = 4.03 (m, 1H, C*H*OH), 1.85-1.81 (m, 2H, hydrogens of cyclohexane ring), 1.56-1.31 (m, 6H, hydrogens of cyclohexane ring), 1.02-0.96 (m, 1H, *CH*-C(CH_3)3), 0.86 (s, 9H, $C(CH_3)_3$); ^{13}C NMR ($CDCl_3$, 100.6 MHz) [2]: δ = 66.0, 48.2, 33.6, 32.6, 27.6, 21.1; GC/MS (EI) t_r = 11.52 min: *m/z* (%) = 156 (M^+, 1), 123 (25), 99 (25), 81 (60), 67 (67), 57 (100).

***Cis*-4-methylcyclohexan-1-ol (*cis*-8)**

From compound **6** (500 mg, 4.46 mmol), derivative *cis*-**8** was obtained after silica gel column chromatography using hexane and ethyl acetate as eluents (462 mg, 40%, *de* = 91%): ^{1}H NMR ($CDCl_3$, 400 MHz) [3]: δ = 3.93 (m, 1H, *CH*OH), 1.75-1.31 (m, 9H, hydrogens of cyclohexane ring), 0.91 (d, 3H, *J* = 6.2 Hz, CH_3); ^{13}C NMR ($CDCl_3$, 100.6 MHz) [3]: δ = 67.1, 32.4, 31.3, 29.2, 21.8; GC/MS (EI) t_r = 5.54 min: *m/z* (%) = 114 (M^+, 5), 96 (20), 81 (39), 70 (34), 57 (100).

***Cis*-4-phenylcyclohexan-1-ol (*cis*-9)**

From compound **7** (500 mg, 2.87 mmol), derivative *cis*-**9** was obtained (450 mg, 89%, *de* > 99%): ^{1}H NMR ($CDCl_3$, 400 MHz) [4]: δ = 7.32-7.17 (m, 5H, ArH), 4.14 (m, 1H, *CH*OH), 2.54 (m, 1H, CH-Ph), 1.96-1.85 (m, 4H, $2CH_2$), 1.73-1.64 (m, 4H, $2CH_2$); ^{13}C NMR ($CDCl_3$, 100.6 MHz) [4]: δ = 147.4, 128.4, 126.9, 126.0, 65.7, 43.9, 33.1, 27.8; GC/MS (EI) t_r = 19.63 min: *m/z* (%) = 176 (M^+, 58), 158 (25), 143 (35),129 (30), 117 (60), 104 (100), 91 (63).

General Procedure for Trans-Selective ADH-Mediated Reduction of Cyclohexanones 4-7 (Semi-preparative Scale)

The suitable substrate (500 mg) dissolved in 2-propanol (2.2 mL) was added to a phosphate buffer solution (50 mM, pH 7) for a total volume of 40 mL together with ADH440 (10 mg) and NADH (10 mg). The mixture was kept for 24 h in an orbital shaker (160 rpm, 30 °C). The solution was extracted with EtOAc (3 × 40 mL). The solution was extracted with EtOAc (3 × 40 mL). The combined organic phases were dried over Na_2SO_4 and concentrated in vacuo to afford the corresponding alcohol derivative without the need for further purification, except for compounds *trans*-**8** and *trans*-**9.**

***Trans*-4-isopropylcyclohexan-1-ol (*trans*-1)**

From compound **4** (500 mg, 3.57 mmol), derivative *trans*-**1** was obtained (450 mg, 89%, *de* = 87%): ^{1}H NMR ($CDCl_3$, 400 MHz) [1]: δ = 3.53 (m, 1H, *CH*OH), 2.02-1.96 (m, 2H, hydrogens of cyclohexane ring, 1.78-1.68 (m, 2H, hydrogens of cyclohexane ring), 1.48-1.35 (m, 1H, hydrogen of cyclohexane ring), 1.27-1.18 (m, 2H, hydrogens of cyclohexane ring), 1.08-0.98 (m, 3H, hydrogens of cyclohexane ring + $CH(CH_3)_2$), 0.86 (d, 6H, J = 6.8 Hz, $C(CH_3)_2$). ^{13}C NMR ($CDCl_3$, 100.6 MHz): δ = 70.4, 42.9, 35.3, 32.2, 27.7, 19.7; GC/MS (EI) t_r = 10.59 min: *m/z* (%) = 141 (M^+ – 1, 1), 124 (25), 109 (30), 95 (10), 81 (100). Compound *trans*-**1** was submitted to bulb-to-bulb distillation (90-95 °C, 10 mmHg) to obtain a sample for olfactory evaluation.

***Trans*-4-(*tert*-butyl)cyclohexan-1-ol (*trans*-3)**

From compound **5** (500 mg, 3.25 mmol), derivative *trans*-**3** was obtained (460 mg, 91%, *de*>99%): ^{1}H NMR ($CDCl_3$, 400 MHz) [2]: δ = 3.51 (m, 1H, *CH*OH), 2.04-1.98 (m, 2H, hydrogens of cyclohexane ring), 1.81-1.76 (m, 2H, hydrogens of cyclohexane ring), 1.30-0.97 (m, 5H, hydrogens of cyclohexane ring), 0.85 (s, 9H, $C(CH_3)_3$); ^{13}C NMR ($CDCl_3$, 100.6 MHz) [2]: δ = 71.4, 47.4, 36.3, 32.4, 27.8, 25.8; GC/MS (EI) t_r = 11.82 min: *m/z* (%) = 138 (M^+ – 18, 13), 123 (27), 81 (47), 67 (40), 57 (100).

***Trans*-4-methylcyclohexan-1-ol (*trans*-8)**

From compound **6** (500 mg, 4.46 mmol), derivative *trans*-**8** was obtained after silica gel column chromatography using hexane and ethyl acetate as eluents (457 mg, 90%, *de* = 98%): ^{1}H NMR ($CDCl_3$, 400 MHz) [3]: δ = 3.53 (tt, 1H, J_1 = 10.8 Hz, J_2 = 4.3 Hz, *CH*OH), 1.99-1.88 (m, 2H, hydrogens of cyclohexane ring), 1.74-1.65 (m, 2H, hydrogens of cyclohexane ring), 1.39-0.89 (m,

5H, hydrogens of cyclohexane ring), 0.87 (d, 3H, J = 6.5 Hz, CH_3); ^{13}C NMR ($CDCl_3$, 100.6 MHz) [3]: δ = 70.9, 35.6, 33.4, 31.9, 22.0; GC/MS (EI) t_r = 5.56 min: m/z (%) = 113 (M^+ – 1, 1), 96 (15), 81 (54), 70 (46), 67 (27), 57 (100).

***Trans*-4-phenylcyclohexan-1-ol (*trans*-9)**

From compound **7** (500 mg, 2.87 mmol), derivative *trans*-**9** was obtained after silica gel column chromatography using hexane and ethyl acetate as eluents (440 mg, 87%, *de*>99%): ^1H NMR ($CDCl_3$, 400 MHz) [4]: δ = 7.31-7.16 (m, 5H, ArH), 3.68 (m, 1H, *CH*OH), 2.50 (tt, 1H, J_1 = 12.9 Hz, J_2 = 3.5 Hz, *CH*-Ph), 2.14-2.06 (m, 2H, hydrogens of cyclohexane ring), 1.98-1.90 (m, 2H, hydrogens of cyclohexane ring), 1.61-1.37 (m, 4H, hydrogens of cyclohexane ring); ^{13}C NMR ($CDCl_3$, 100.6 MHz) [4]: δ = 146.7, 128.5, 126.9, 126.2, 70.8, 43.6, 36.1, 32.6; GC/MS (EI) t_r = 19.69 min: *m/z* (%) = 176 (M^+, 10), 158 (100), 143 (90), 130 (60), 117 (50), 104 (75), 91 (60).

General Procedure for Lipase-Mediated Acetylation of cis- *and* trans-*4-(*tert-*butyl)cyclohexan-1-ol (*cis- *and* trans-*3) (Semi-preparative Scale)*

Compounds *cis*- and *trans*-**3** (isolated from the semi-preparative ADH-mediated reductions) were added to a solution of MTBE (9 mL) and vinyl acetate (1 mL) together with CALA (150 mg). The mixture was kept for 24 h in an orbital shaker (160 rpm, 30 °C) and then concentrated *in vacuo*.

Cis-*4-(*tert-*butyl)cyclohexyl Acetate (*cis-*2)*

From compound *cis*-**3** (460 mg, 2.95 mmol), derivative *cis*-**2** was obtained (560 mg, 96%): ^1H NMR ($CDCl_3$, 400 MHz): δ = 4.99 (m, 1H, *CH*OAc), 2.05 (s, 3H, CH_3CO), 1.96-1.90 (m, 2H, hydrogens of cyclohexane ring), 1.61-1.55 (m, 2H, hydrogens of cyclohexane ring), 1.45 (tt, 2H, J_1 = 13.9 Hz, J_2 = 3.2 Hz, hydrogens of cyclohexane ring), 1.33-1.23 (m, 2H, hydrogens of cyclohexane ring), 1.02 (tt, 1H, J_1 = 12.0 Hz, J_2 = 3.0 Hz, *CH*-$C(CH_3)_3$), 0.86 (s, 9H, $C(CH_3)_3$); ^{13}C NMR ($CDCl_3$, 100.6 MHz): δ = 170.8, 69.6, 47.8, 32.7, 30.8, 27.6, 21.8, 21.6; GC/MS (EI) t_r = 14.89 min: *m/z* (%) = 138 (M^+ – 60, 29), 123 (46), 82 (86), 67 (71), 57 (100). Compound *cis*-**2** was submitted to bulb-to-bulb distillation (110-115 °C, 10 mmHg) to obtain a sample for olfactory evaluation.

Trans-*4-(*tert-*butyl)cyclohexyl Acetate (*trans-*2)*

From compound *trans*-**3** (450 mg, 2.89 mmol), derivative *trans*-**2** was obtained (540 mg, 94%) (460 mg, 2.95 mmol), derivative *trans*-**2** was obtained (540 mg, 93%): ^{1}HNMR ($CDCl_3$, 400 MHz): δ = 4.61 (tt, 1H, J_1 = 11.3 Hz, J_2 = 4.4 Hz, *CH*OAc), 2.01 (s, 3H, CH_3CO), 2.05- 1.95 (m, 2H, hydrogens of cyclohexane ring), 1.82-1.77 (m, 2H, hydrogens of cyclohexane ring), 1.34-1.24 (m, 2H, hydrogens of cyclohexane ring), 1.15-0.96 (m, 3H, hydrogens of cyclohexane ring + *CH*-$C(CH_3)_3$), 0.84 (s, 9H, $C(CH_3)_3$); ^{13}C NMR ($CDCl_3$, 100.6 MHz): _ = 170.4, 73.5, 47.0, 32.2, 27.5, 25.4, 21.9, 21.2; GC/MS (EI) t_r = 15.73 min: *m/z* (%) = 138 (M^+ – 60, 15), 123 (30), 82 (70), 67 (55), 57 (100). Compound *trans*-**2** was submitted to bulb-to-bulb distillation (115-120 °C, 10 mmHg) to obtain a sample for olfactory evaluation.

Continuous-Flow Production of cis-*4-isopropylcyclohexan-1-ol (*cis-*1)*

280 mL of a buffer solution (phosphate buffer, 100 mM, pH 7) containing 2-propanol (20% v/v), 4-isopropyl cyclohexanone (**4**) (10 mM) and NADH (0.2 mM) were continuously fed to a stirred membrane reactor (12 mL reaction volume, 5 kDa membrane cut-off, 30 °C) containing ADH200 (3 mg) at 200 μL min^{-1} (60 min residence time) for 24 h. At the membrane reactor outlet, buffer solution was mixed to *n*-hexane (fed at μL min^{-1}) in a tee piece. The biphasic segmented flow thus formed entered a commercial in-line liquid-liquid separator (Zaiput®, hydrophobic membrane OP-900). The two phases were then collected at the respective outlets. The total hexane solution collected in 24 h reaction time was submitted to solvent removal by in vacuo distillation to give *cis*-**1** (3.66 g, 92%) containing 5% (GC/MS) of starting ketone **4**.

Continuous-Flow Production of cis-*4-(*tert-*butyl)cyclohexyl Acetate (*cis-*2)*

Briefly, 280 mL of a buffer solution (phosphate buffer, 100 mM, pH 7) containing 2-propanol (20% v/v), 4-(*tert*-butyl) cyclohexanone (**5**) (10 mM) and NADH (0.2 mM) were continuously fed to a stirred membrane reactor (12 mL reaction volume, 5 kDa membrane cut-off, 30 °C) containing ADH200 (3 mg) at 200 μL min^{-1} (60 min residence time) for 24 h. At the membrane reactor outlet, buffer solution was mixed to *n*-hexane (fed at 200 μL min^{-1}) in a tee piece. The biphasic segmented flow thus formed entered a commercial in-line liquid-liquid separator (Zaiput®, hydrophobic membrane OP-900). Aqueous phase was collected. Organic phase was continuously mixed with vinyl acetate (fed at 100 μL min^{-1}) in a tee piece. The resulting solution entered a column reactor packed

with *Candida antarctica* lipase A (500 mg of dry weight, pre-swelled, column i.d. 6.6 mm, 30 °C) with a residence time of 11 min. The total hexane solution collected in 24 h reaction time was submitted to solvent removal by in vacuo distillation to give *cis*-**2** (4.93 g, 89%) containing 4% (GC/MS) of starting ketone **5** and 10% (GC/MS) of intermediate alcohol *cis*-**3**.

References

[1] Tan, S.-L.; Liu, G.-B.; Gao, X.; Thiemann, T. Raney Ni-Al alloy-mediated reduction of alkylated phenols in water. *J. Chem. Res.* **2009**, *2009*, 5-7.

[2] Spiniello, M.; White, J.M. Low-temperature X-ray structural studies of the ester and ether derivatives of *cis* and *trans*-4-*tert*-butyl cyclohexanol and 2-adamantanol: application of the variable oxygen probe to determine the relative σ-donor ability of C–H and C–C bonds. *Org. Biomol. Chem.* **2003**, *1*, 3094-3101.

[3] Wiitala, K.W.; Al-Rashid, Z.F.; Dvornikovs, V.; Hoye, T.R.; Cramer, C.J. Evaluation of various DFT protocols for computing ^{1}H and ^{13}C chemical shifts to distinguish stereoisomers: diastereomeric 2-, 3-, and 4-methylcyclohexanols as a test set. *J. Phys. Org. Chem.* **2007**, *20*, 345-354.

[4] Hodgson, D.M.; Chung, Y.K.; Paris, J.-M. Intramolecular cyclopropanation of unsaturated terminal epoxides. *J. Am. Chem. Soc.* **2004**, *126*, 8664-8665.

Chapter 4

Supplementary Information

Epoxidation of isosafrole: experimental design

A 2^3 full factorial experimental design was applied. The conversion of isosafrole isomers into all the oxidation products (*Y*), calculated by GC/MS analysis as a conversion percentage, was taken as response. The three factors (X_1 - X_3) and their values were: enzyme load X_1 (10 - 20 mg), isosafrole concentration X_2 (0.2 - 0.5 M), H_2O_2 concentration X_3 (0.3 - 0.6 M). The ranges of X_1 - X_3 were selected from preliminary experiments. The final reaction volume was 15 mL. Hydrogen peroxide was extracted in EtOAc as explained above and then diluted with fresh EtOAc to the desired final concentration. All the reactions were incubated in a thermoshaker at the controlled temperature of 50 °C for 4 h. The sum of the percentages of epoxides **8**, monoacetate derivatives **9a, b**, diols **10** and monoethyl ethers **11a, b**, obtained by GC/MS analysis, was taken as system response. All the experiments were conducted in duplicates, for a total of 16 reactions. The response was elaborated using Minitab. The following multivariate regression model was obtained: $Y = 56.25 + 6.125X_1 - 15.375X_2 + 9.125X_3 - 2.00X_1X_2 - 1.250X_1X_3 + 0.500X_2X_3 + 2.125X_1X_2X_3$.

Experimental design for epoxidation of isosafrole: results

[a] Conversion calculated on the basis of GC/MS analysis.

n° run	Enzyme [mg]	Isosafrole [M]	H_2O_2 [M]	Isosafrole conversion [%][a]
1	10	0.5	0.3	27
2	20	0.2	0.6	87
3	20	0.5	0.6	56
4	20	0.2	0.3	72
5	10	0.2	0.6	77

6	10	0.5	0.6	47
7	20	0.5	0.3	35
8	10	0.2	0.6	74
9	20	0.5	0.6	55
10	20	0.2	0.6	83
11	10	0.5	0.3	29
12	10	0.2	0.3	48
13	20	0.5	0.3	34
14	10	0.5	0.6	44
15	20	0.2	0.3	77
16	10	0.2	0.3	55

Table S1. Factorial design for the enzymatic epoxidation of isosafrole.

[a] Conversion calculated on the basis of GC/MS analysis.

n° run	**Epoxide (8) [%][a]**	**Monoethyl ethers (11a,b) [%][a]**	**Diol (10) [%][a]**	**Monoacetates (9a,b) [%][a]**	**Isosafrole ((*E*)- and (*Z*)-3) [%][a]**
1	3	4	16	4	73
2	16	10	16	45	13
3	7	5	11	33	44
4	6	7	38	21	28
5	18	5	33	21	23
6	7	4	18	18	53
7	3	7	22	3	65
8	16	5	25	28	26

9	7	5	14	29	45
10	14	10	16	43	17
11	3	3	18	5	71
12	4	5	31	8	52
13	3	5	19	7	66
14	7	3	15	19	56
15	8	5	38	26	23
16	5	7	31	12	45

Table S2. Results of factorial design experiments.

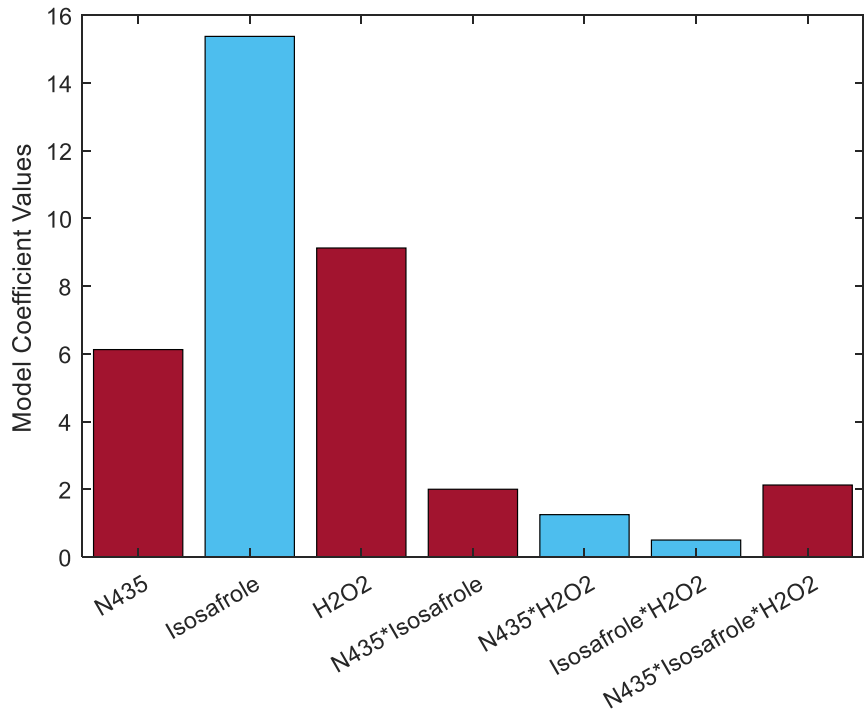

Figure S1. Coefficient plot showing the effects of the three variables (enzyme load, isosafrole concentration and H_2O_2 concentration) and of their interactions on conversion: red=positive value = positive effect; light blue= negative value = negative effect.

(multivariate regression model obtained by DOE analysis: $Y = 56.25 + 6.125X_1 - 15.375X_2 + 9.125X_3 - 2.00X_1X_2 - 1.250X_1X_3 + 0.500X_2X_3 + 2.125X_1X_2X_3$ - enzyme load X_1, isosafrole concentration X_2, H_2O_2 concentration X_3).

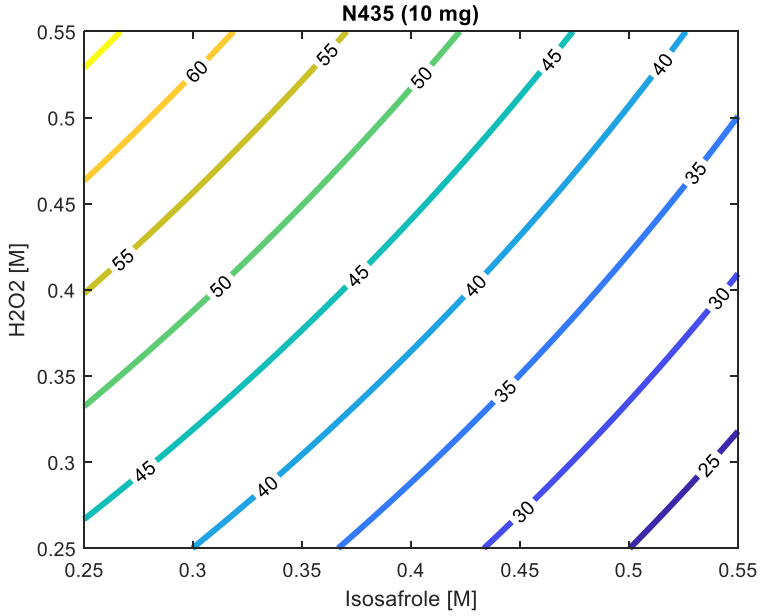

Figure S2. Contour plot of conversion [%] as a function of isosafrole concentration [M] and hydrogen peroxide concentration [M] evaluated at an enzyme load of 10 mg. Lines refer to constant conversion corresponding to the value reported on the labels.

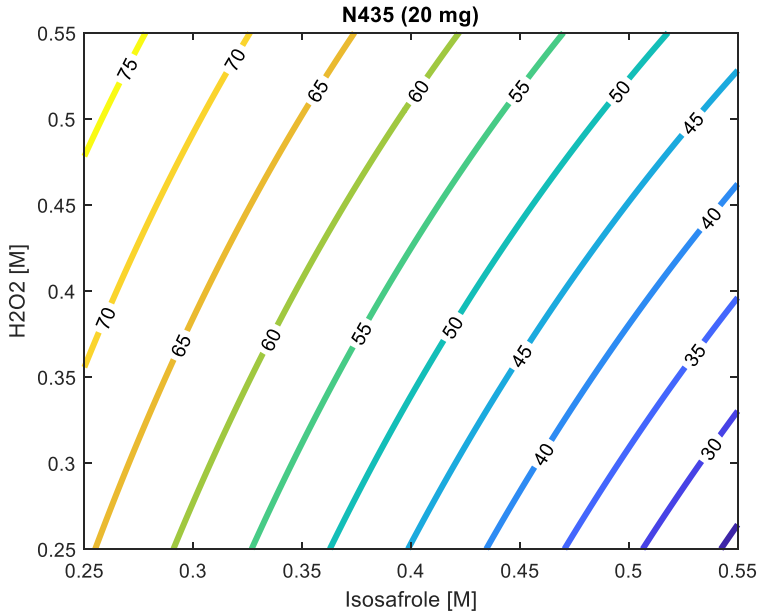

Figure S3. Contour plot of conversion [%] as a function of isosafrole concentration [M] and hydrogen peroxide concentration [M] evaluated at an enzyme load of 20 mg. Lines refer to constant conversion corresponding to the value reported on the labels.

Experimental Part

General analytical methods

^{1}H and ^{13}C NMR spectra were recorded on a 400 or 500 MHz spectrometer in $CDCl_3$ solution at r.t. The chemical shift scale was based on internal tetramethylsilane. GC/MS analyses were performed using a HP-5MS column (30 m × 0.25 mm × 0.25 μm, Agilent Technologies Italia Spa (Cernusco sul Naviglio, Italy)). The following temperature program was employed: 60 °C (1 min) / 6 °C min^{-1} / 150 °C (1 min) / 12°C min^{-1} / 280 °C (5 min).

Hydrogen peroxide extraction with EtOAc **[1]**

A 35% (w/w) H_2O_2 solution (15 mL) was added to EtOAc (10 mL) and left under stirring at r.t. for 1 h. The two phases were separated. Hydrogen peroxide concentration was evaluated by HPLC analysis according to a published procedure [2] and resulted to be about 3 M. The solution was diluted with fresh EtOAc according to the need. The authors have also developed a method for determining H_2O_2 concentration in EtOAc, using NMR spectroscopy which will be published elsewhere.

Epoxidation of isosafrole (batch conditions)

Isosafrole **3** (480 mg, 2.96 mmol) was dissolved in EtOAc (15 mL). UHP (417 mg, 4.44 mmol) and Novozym® 435 (10 mg) were then added to the solution, which was incubated in a thermoshaker for 18 h at 30 °C. Insoluble UHP and enzyme were removed by filtration and the reaction mixture was quenched first with Na_2SO_3, then with $NaHCO_3$ sat. solution. Extraction with EtOAc afforded an organic phase that was dried (Na_2SO_4) and concentrated under reduced pressure. The residue was chromatographed on a silica gel column, eluting with hexane and increasing amount of EtOAc, in order to recover the 4:1 mixture of the two diastereoisomers of epoxide **8** (379 mg, 72%) for analytical characterization. The NMR signal descriptions herein reported were obtained by examining the NMR spectra of the mixture and are in agreement with those reported in the literature [3]

5-((2*R,3*R**)-3-Methyloxiran-2-yl)benzo[*d*][1,3]dioxole ((2*R**,3*R**)-8)**

^{1}H NMR ($CDCl_3$, 400 MHz): δ = 6.78-6.74 (m, 2H, Ar–*H*), 6.70-6.67 (m, 1H, Ar–*H*), 5.93 (s, 2H, CH_2), 3.49 (d, 1H, J = 2.0 Hz, C*H*OCH), 2.97 (qd, 1H, J_1 = 5.1 Hz, J_2 = 2.1 Hz, C*H*OCH), 1.42 (d, 3H, J = 5.1 Hz, CH_3); ^{13}C NMR ($CDCl_3$, 100.6 MHz): δ = 148.1, 147.6, 131.8, 119.6, 108.3, 105.7,

101.2, 59.6, 58.8, 17.9. GC/MS (EI) t_r = 18.38 min: *m/z* (%) = 178 (M^+, 55), 163 (20), 149 (25), 135 (100).

5-((2*R,3*S**)-3-Methyloxiran-2-yl)benzo[*d*][1,3]dioxole ((2*R**,3*S**)-8)**

^{1}H NMR ($CDCl_3$, 400 MHz): δ = 6.78-6.74 (m, 3H, Ar–*H*), 5.95 (s, 2H, C*H*$_2$), 3.97 (d, *J* = 4.1 Hz, 1H, C*H*OCH), 3.27 (m, 1H, C*H*OCH), 1.09 (d, 3H, *J* = 5.4, C*H*$_3$); ^{13}C NMR ($CDCl_3$, 100.6 MHz): δ = 147.6, 147.1, 129.6, 120.0, 108.1, 107.2, 101.1, 57.5, 55.3, 12.6. GC/MS (EI) t_r = 17.92 min: *m/z* (%) = 178 (M^+, 50), 163 (20), 149 (30), 135 (100).

Epoxidation of isosafrole followed by diol 10 isolation (batch conditions)

Isosafrole **3** (480 mg, 2.96 mmol) was dissolved in EtOAc (15 mL). A 35% w/w aqueous solution of hydrogen peroxide (382 μL, 4.44 mmol) and Novozym® 435 (10 mg) were added to the solution, which was incubated in a thermoshaker for 18 h at 30 °C. At the end, the enzyme was filtered and the reaction mixture was quenched first with Na_2SO_3, then with $NaHCO_3$ sat. solution. Extraction with EtOAc afforded an organic phase that was dried (Na_2SO_4) and concentrated under reduced pressure. The resulting residue was dissolved in MeOH (15 mL) and an excess of KOH (250 mg, 1.5 equiv.) was added to the solution. The reaction was left under magnetic stirring at room temperature for 24 h. The solution volume was reduced to one third under vacuum, poured into diluted H_2SO_4 solution, and extracted with EtOAc. The organic phase was dried (Na_2SO_4) and concentrated under vacuum. Trituration of the solid residue with hexane/EtOAc (8:2) afforded a 3:1 mixture of (*R**,*S**)- and (*R**,*R**)-**10** as a pure compound (0.401 g, 69%).

(1*R,2*S**)-1-(Benzo[*d*][1,3]dioxol-5-yl)propane-1,2-diol ((1*R**,2*S**)-10)**

^{1}H NMR ($CDCl_3$, 400 MHz): δ = 6.86-6.84 (m, 1H, Ar–*H*), 6.81-6.76 (m, 2H, Ar–*H*), 5.96 (s, 2H, C*H*$_2$), 4.29 (d, 1H, *J* = 7.4 Hz, C*H*OH), 3.81 (m,1H, C*H*OH), 2.56 (s, 1H, O*H*), 2.42 (s, 1H; O*H*), 1.06 (d, 3H, *J* = 6.3 Hz, C*H*$_3$); ^{13}C NMR ($CDCl_3$, 100.6 MHz): δ = 147.95, 147.5, 135.2, 120.6, 108.3, 107.2, 101.21, 79.5, 72.4, 18.9; GC/MS (EI) t_r = 21.85 min: *m/z* (%) = 196 (M^+, 16), 178 (8), 162 (8), 151 (100), 135 (25), 123 (25).

(1*R,2*R**)-1-(Benzo[*d*][1,3]dioxol-5-yl)propane-1,2-diol ((1*R**,2*R**)-10)**

^{1}H NMR ($CDCl_3$, 400 MHz): δ = 6.90-6.89 (m, 1H, Ar–*H*), 6.80-6.78 (m, 2H, Ar–*H*), 5.95 (s, 2H, C*H*$_2$), 4.57 (d, 1H, *J* = 4.6 Hz, C*H*OH), 3.96 (m,1H, C*H*OH), 2.28 (s, 1H, O*H*), 1.83 (s, 1H; O*H*),

1.11 (d, 3H, J = 6.4 Hz, CH_3); ^{13}C NMR ($CDCl_3$, 100.6 MHz): δ = 147.9, 147.3, 134.5, 120.3, 108.2, 107.3, 101.17, 77.6, 71.4, 17.6; GC/MS (EI) t_r = 21.95 min: *m/z* (%) = 196 (M^+, 16), 178 (8), 162 (8), 151 (100), 135 (25), 123 (25).

Epoxidation of isosafrole followed by diol 10 isolation (DOE optimal conditions, batch mode)

Isosafrole **3** (486 mg, 3.00 mmol) was dissolved in EtOAc (12 mL). A 3 M solution of H_2O_2 in EtOAc (3.00 mL, 9.00 mmol) and Novozym® 435 (20 mg) were added to the solution, which was incubated in a thermoshaker for 4 h at 50 °C. At the end, the enzyme was filtered and the reaction mixture was quenched first with Na_2SO_3, then with $NaHCO_3$ sat. solution. Extraction with EtOAc afforded an organic phase that was dried (Na_2SO_4) and concentrated under reduced pressure, to give a residue showing the following product distribution by GC/MS analysis: 15% epoxide **8**, 10% monoethyl ethers **11a, b**, 16% diols 10, 44% monoacetates **9a, b** with 15% unreacted isosafrole isomers (*E*)- and (*Z*)-**6**. STY epoxidation step = 38 mmol L^{-1} h^{-1}.

The crude product was dissolved in MeOH (15 mL) and an excess of KOH (252 mg, 1.5 equiv.) was added to the solution. The reaction was refluxed for 1 h. The solution volume was reduced to one third under vacuum, poured into diluted H_2SO_4 solution, and extracted with EtOAc. The organic phase was dried (Na_2SO_4) and concentrated under vacuum, to give a residue showing the following product distribution by GC/MS analysis: 10% monoethyl ethers **11a, b**, 75% diols **10**, 15% unreacted isosafrole isomers (*E*)- and (*Z*)-6. STY hydrolysis = 150 mmol L^{-1} h^{-1}.

Trituration of the solid residue with hexane/EtOAc (8:2) afforded a 3:1 mixture of (*R**,*S**)- and (*R**,*R**)-**10** as a pure compound (0.417 g, 71%).

Epoxidation of isosafrole followed by diol 10 isolation (continuous-flow conditions)

An EtOAc solution (final volume 45 mL) of isosafrole (0.2 M) and of H_2O_2 (0.6 M) was continuously added and pumped out at a constant flowrate of 188 μL min^{-1} in a 50 mL jacketed stirred tank reactor containing 45 mL of the same solution and of Novozym® 435 (60 mg) dispersed in the liquid phase. The residence time inside the reactor was 4 h. The reactor was kept at 50 °C. The system continuously operated for 24 h. The outlet composition was periodically sampled and analysed by GC/MS during the first 12 h. The fractions collected from 2 to 12 h (124 mL) were combined, submitted first to work

up, then to reaction with KOH/MeOH as described in the previous paragraph, in order to recover diol **10** (3.31 g, 68%).

Synthesis of piperonal (batch conditions)

Diol (*R**,*S**)-**10** (200 mg) was dissolved in EtOAc or DCM (17 mL). MnO_2 (890 mg) was dispersed in the solution and reaction was kept under stirring at r.t. for 2 h till diol complete consumption (TLC and GC/MS). STY = 30 mmol L^{-1} h^{-1}.

Synthesis of piperonal (continuous flow conditions)

A glass column (6.6 mm i.d., adjustable length) was filled with MnO_2 (890 mg, 1 cm of bed length). At each end of MnO_2, a layer of celite was added (1 cm). A solution of diol **10** (200 mg) in DCM (17 mL) was flowed into the column at a flowrate of 200 μL min^{-1} (residence time of 1.7 min). After 85 min reaction time, the column was regenerated by flowing a solution of TBHP 0.24 M in *n*-decane (1 mL) and DIPEA (1 mL) in DCM (15 mL) at a flowrate of 200 μL min^{-1} (85 min). The overall process consisted in 5 reactions steps and 4 regeneration treatments. The procedure of reaction and regeneration was repeated four times. The outlet solution (85 mL) was quenched with a saturated solution of Na_2SO_3. Between oxidation and regeneration, the column was washed by flowing DCM at 1 mL min^{-1} for 5 min. The collected solution contained 60% piperonal and 40% of unreacted diol **10** (GC/MS). Piperonal was recovered by column chromatography with a final yield of 52% (0.398 g).

^{1}H NMR ($CDCl_3$, 400 MHz) [4]: δ = 9.82 (s, 1H, CO*H*), 7.41 (dd, 1H, J_1 = 7.9 Hz, J_2 = 1.6 Hz, Ar–*H*), 7.34 (d, 1H, *J* = 1.6 Hz, Ar–*H*), 6.93 (d, 1H, *J* = 7.9 Hz, Ar–H), 6.08 (s, 2H, CH_2); ^{13}C NMR ($CDCl_3$, 100.6 MHz): δ = 190.2, 154.1, 148.7, 131.9, 128.6, 108.3 m 106.8, 102.1; GC/MS (EI) t_r = 15.30 min: *m/z* (%) = 149 (M^+ −1, 100), 135 (1), 131 (1), 124 (1), 121 (40).

References

[1] Walton, J.H.; Lewis, H.A. The partition coefficients of hydrogen peroxide between water and certain organic solvents. *J. Am. Chem. Soc.* **1916**, *38*, 633-638.

[2] Pinkernell, U.; Effkemann, S.; Karst, U. Simultaneous HPLC determination of peroxyacetic acid and hydrogen peroxide. *Anal. Chem.* **1997**, *69*, 3623-3627.

[3] Yamazaki, S. An effective procedure for the synthesis of acid-sensitive epoxides: use of 1-methylimidazole as the additive on methyltrioxorhenium-catalyzed epoxidation of alkenes with hydrogen peroxide. *Org. Biomol. Chem.* **2010**, *8*, 2377-2385.

[4] Iinuma, M.; Moriyama, K.; Togo, H. Oxidation of alcohols to aldehydes or ketones with 1-acetoxy-1,2-benziodoxole-3(1*H*)-one derivatives. *Eur. J. Org. Chem.* **2014**, 772-780.

Chapter 5

Supplementary Information

Evaluation of the molar ratio between triglycerides and free fatty acids in samples of high oleic sunflower soapstock

A suitable sample of soapstock (1 g) was dispersed in distilled water (15 mL). The value of pH was lowered from 10 to 6 by adding a diluted solution of H_3PO_4, then the mixture was extracted with EtOAc, dried over Na_2SO_4 and evaporated under vacuum. The molar ratio between triglycerides and free fatty acids was estimated by ^1H NMR by considering the integrals of the following signals: 4.40-4.00 ppm, multiplet of the 2 CH_2 units of triglycerides, 2.38-2.24 ppm, multiplet of the CH_2 units of triglycerides (3 units) and free fatty acids (1 CH_2 unit) in α position with respect to the carboxylic moiety. The analyzed samples always showed an equimolar quantity of triglycerides and free fatty acids.

The ^{31}P NMR spectrum recorded in $CDCl_3$ showed the lack of any phospholipid. A representative ^1H NMR spectrum of a sample of high oleic sunflower oil soapstock is shown below.

^1H NMR of high oleic sunflower soapstock:

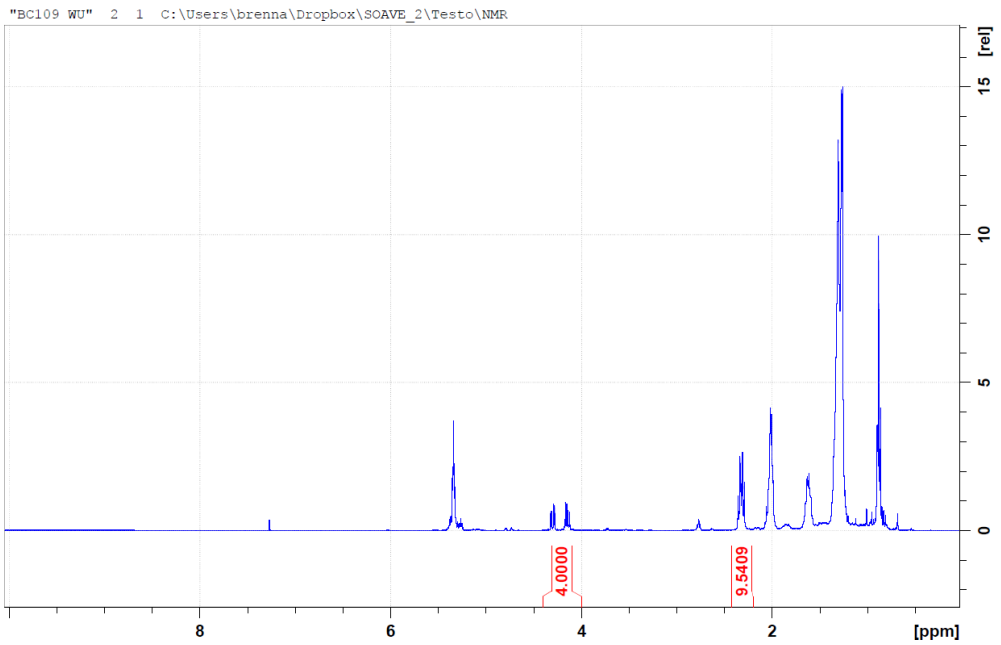

Evaluation of the molar distribution of the main fatty acids in the mixtures obtained by enzymatic splitting of samples of high oleic sunflower soapstock

A suitable sample of soapstock was submitted to enzymatic hydrolysis according to the procedure reported in the main text. The molar distribution of the main fatty acids contained in each sample was estimated by ^{1}H NMR by considering the integrals of the following signals: 2.83-2.71 ppm, 1 CH_2 unit between the two C=C double bonds of polyunsaturated acids (mainly linoleic acid); 2.41-2.23 ppm, 1 CH_2 unit in α position with respect to the carboxylic moiety of all free fatty acids; 2.09-2.14 ppm, 2 CH_2 units in allylic position with respect to the C=C double bond of monounsaturated fatty acids (mainly oleic acid) and polyunsaturated acids (mainly linoleic acid). The following distributions were obtained: 80-87% monounsaturated fatty acids (mainly oleic acid), 9% polyunsaturated fatty acids (mainly linoleic acid), 4-11% saturated acids (mainly palmitic and stearic acids). These results were confirmed by GC/MS analysis of the corresponding mixture of methyl esters.

A representative example of ^{1}H NMR spectrum of the mixture of free fatty acids recovered from high oleic sunflower oil soapstock is shown below.

<u>^{1}H NMR, mixture of free fatty acids obtained by enzymatic hydrolysis of a sample of high oleic sunflower oil soapstock:</u>

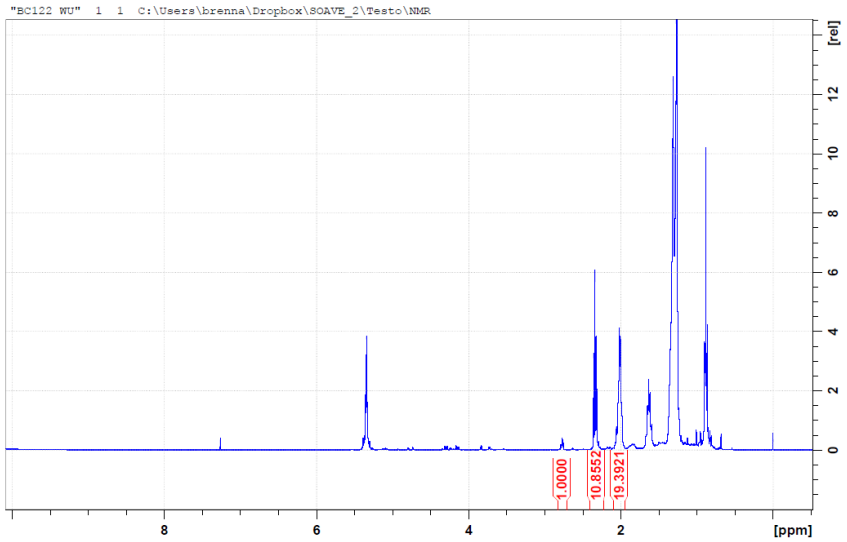

Factorial design - Enzymatic epoxidation of hydrolyzed soapstock

[a] Conversion calculated on the basis of GC/MS analysis

n° run	Oleic acid [g L^{-1}] X_1	N435 [g L^{-1}] X_2	H_2O_2 [% v/v] X_3	T [°C] X_4	Conversion to oleic acid epoxide [%][a] Y
1	10	2	10	30	12
2	10	1	40	30	3
3	50	1	40	30	17
4	50	1	40	30	21
5	10	1	10	30	5
6	10	1	40	50	21
7	10	1	10	50	15
8	10	1	40	30	5
9	10	2	40	50	25
10	50	2	10	50	36
11	50	1	10	50	24
12	10	1	40	50	20
13	50	1	40	50	18
14	10	2	40	50	16
15	50	2	10	50	41
16	10	1	10	50	10
17	10	2	10	30	10
18	50	1	10	50	30

19	10	2	40	30	7
20	50	2	40	30	39
21	50	1	10	30	14
22	50	1	40	50	30
23	10	2	40	30	3
24	50	2	40	50	34
25	10	2	10	50	30
26	50	2	10	30	32
27	50	2	40	30	42
28	10	1	10	30	5
29	50	1	10	30	23
30	50	2	10	30	39
31	10	2	10	50	30
32	50	2	40	50	38

Table S1. Factorial design for the enzymatic epoxidation of oleic acid from hydrolyzed soapstock.

A four-variables (oleic acid and H_2O_2 concentrations, temperature, and enzyme amount) factorial design, with a replicate for each point, was designed and analyzed through Minitab. We considered a range of 10-50 g L^{-1} of oleic acid concentration that corresponded to 12-60 g L^{-1} of hydrolyzed mixture. As for the other conditions, we chose to evaluate system response to temperature (30-50 °C), hydrogen peroxide concentration (1-4 % v/v referred to 35% w/w aq. solution), Novozym® 435 (1-2 g L^{-1}). The final reaction volume was 15 mL. All the 32 reactions were left in a thermoshaker at a certain temperature for 5 h. The reactions were quenched with a saturated solution of $NaHSO_3$, extracted with EtOAc and dried over Na_2SO_4. Conversion of oleic acid into the corresponding epoxide was analyzed as system response and was evaluated by GC/MS analysis after treating samples with MeOH and trimethylsilyldiazomethane.

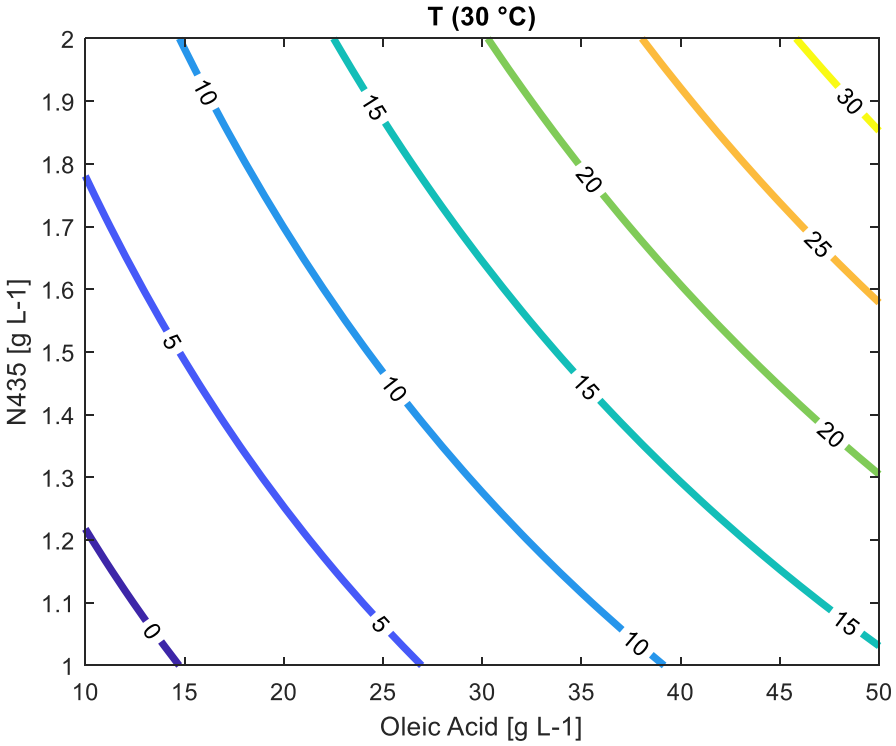

Figure S1. Contour plot of conversion [%] as a function of oleic acid and Novozym® 435 concentration [g L^{-1}] evaluated at a temperature of 30 °C. Lines refer to constant conversion, and the value is reported on the labels.

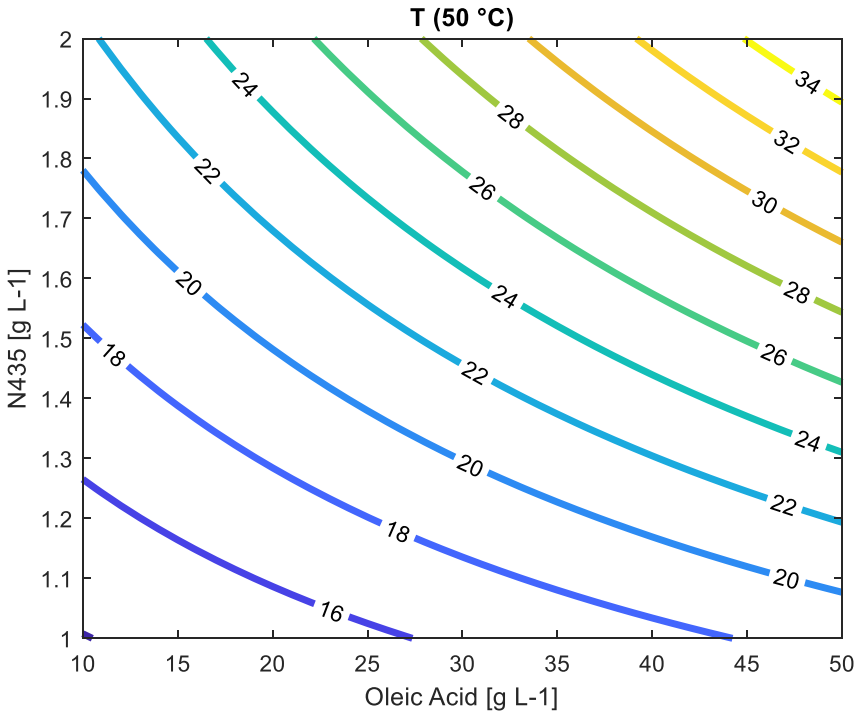

Figure S2. Contour plot of conversion [%] as a function of oleic acid and Novozym® 435 concentration [g L^{-1}] evaluated at a temperature of 50 °C. Lines refer to constant conversion, and the value is reported on the labels.

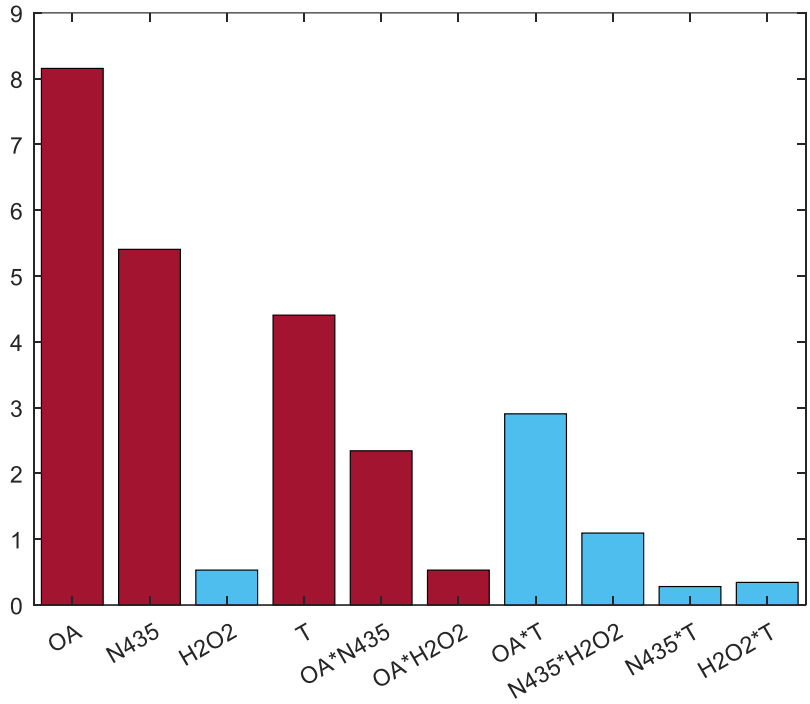

Figure S3. Coefficient plot of variable effects (first and second order); red=positive effect; light blue=negative effect.

Factorial design - Oxidative cleavage of oleic acid diol

[a] Conversion calculated on the basis of GC/MS analysis.

n° run	AcOEt [mL]	NaClO 10%[mL]	Hydroxy-oxo-stearic acid% [a]	Pelargonic Acid%[a]
1	13	10	8%	55%
2	5	4	5%	15%
3	13	4	6%	28%
4	5	10	6%	19%
5	13	10	7%	37%
6	5	4	6%	15%

7	13	4	3%	37%
8	5	10	3%	18%

Table S2. Factorial design for oxidative cleavage of oleic acid diol.

For all the experiments we submitted 50 mg of oleic acid diol and 1 mg of Triton-X. The reactions were run in duplicates. All the 8 reactions were left in a thermoshaker (170 rpm) at the controlled temperature of 45°C for 24 h.

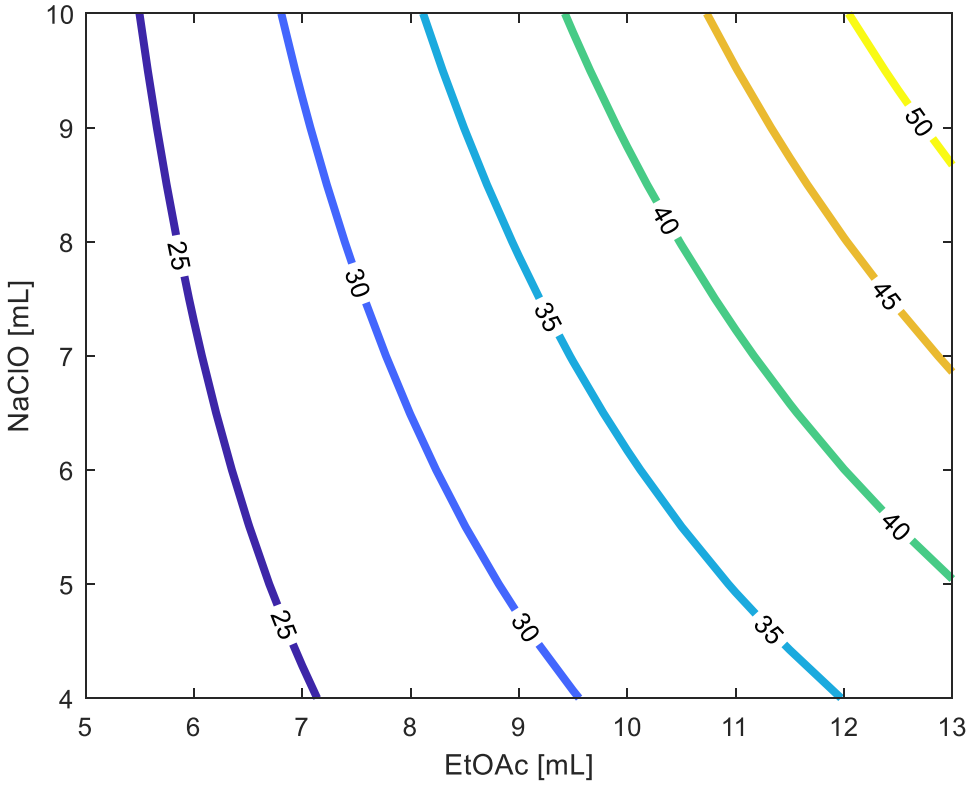

Figure S4. Contour plot of conversion [%] as a function of ethyl acetate and sodium hypochlorite volume [mL]. Lines refer to constant conversion, and the value is reported on the labels.

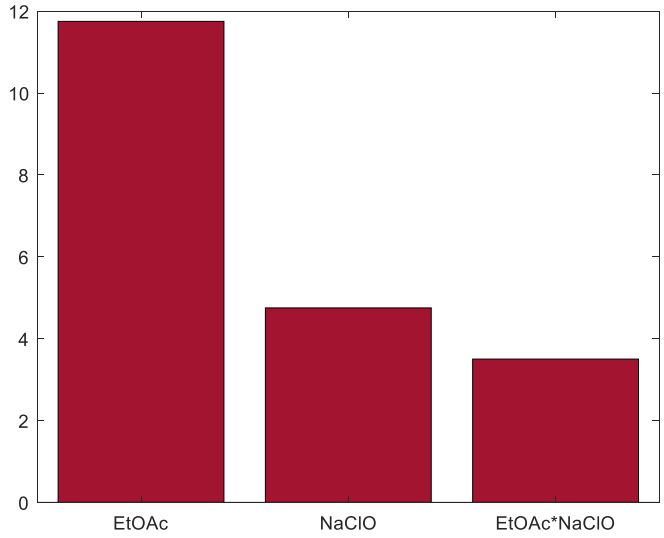

Figure S5. Coefficient plot of variable effects (first and second order); red=positive effect; light blue=negative effect.

Experimental Part

General analytical methods

^{1}H and ^{13}C NMR spectra were recorded on a 400 or 500 MHz spectrometer in $CDCl_3$ or CD_3OD solution at r.t.. The chemical shift scale was based on internal tetramethylsilane. GC/MS analyses were performed using an HP-5MS column (30 m × 0.25 mm × 0.25 µm, Agilent Technologies Italia Spa, Cernusco sul Naviglio, Italy). The following temperature program was employed: 50 °C/10 °C min^{-1} /250 °C (5 min)/50 °C min^{-1} /300 °C (10 min). The samples for GC/MS were treated with MeOH and trimethylsilyldiazomethane 10% in hexane, to derivatize carboxylic acids by transformation into the respective methyl esters.

General procedure for lipase-mediated hydrolysis of soapstock

Soapstock (10 g) was suspended in distilled water (30 mL). The initial pH was found to be 10.0. The lipase Eversa Transform 2.0, a liquid lipase from *Thermomyces lanuginosus* (100 mg, 1% w/w) was then added to the suspension. The reaction was kept under mechanical stirring for 12 h at r.t. in a two-neck round-bottom flask. Conversion was monitored by ^{1}H NMR. At the end of the reaction, the pH value was 8.0. A diluted solution of H_3PO_4 (8% v/v) was added to the suspension to a final pH 4.5-5.0. The organic phase was recovered by centrifugation (5000 rpm, 25°C, 20 min), yielding a mixture of free fatty acids (4.50 g, final yield 45% w/w), showing the following composition, obtained by ^{1}H NMR analysis and confirmed by GC/MS analysis of the corresponding methyl esters (see Supplementary Information, Appendix *Chapter 5*): 80-87% oleic acid, 9% linoleic acid, 4-11% saturated acids (mainly palmitic and stearic acids).

Epoxidation of hydrolyzed soapstock (factorial design analysis)

A 2^4 full factorial experimental design was applied to the epoxidation of the mixture of FFAs, containing 83% oleic acid derived from soapstock hydrolysis to study the influence of temperature, enzyme load, oleic acid and hydrogen peroxide concentration on final conversion. The conversion percentage of oleic acid into the corresponding epoxide (*Y*) was taken as response, while the four parameters (X_1-X_4) and their levels were: oleic acid concentration, X_1 (10-50 g L^{-1}, corresponding to 12-60 g L^{-1} of hydrolyzed mixture); Novozym® 435 load, X_2 (1-2 g L^{-1}); hydrogen peroxide 35% *w/w*

concentration, X_3 (1-4 % *v/v*), temperature X_4 (30-50°C). All the experiments were conducted in duplicates, for a total of 32 reactions. The final reaction volume was 15 mL. All the 32 reactions were left in a thermoshaker at the controlled temperature for 5 h. The reactions were quenched with a saturated solution of Na_2SO_3, extracted with EtOAc and dried over Na_2SO_4. Conversion of oleic acid into the corresponding epoxide was analyzed as system response and was evaluated by GC/MS analysis after treating samples with MeOH and trimethylsilyldiazomethane. Data were processed using Minitab and the following multivariate regression model was obtained: $Y = 21.7 + 8.2 \cdot X_1 + 5.4 \cdot X_2 - 0.53 \cdot X_3 + 4.4 \cdot X_4 + 2.34 \cdot X_1 \cdot X_2 - 0.15 \cdot X_2 \cdot X_3$. The table of factorial plan and response and the factorial design analysis graphs are reported in Supplementary Information, Appendix *Chapter 5*.

Epoxidation of hydrolyzed soapstock followed by diol isolation (batch conditions)

The mixture of fatty acids recovered from the enzymatic splitting of soapstock (0.9 g) was dispersed in acetonitrile (15 mL). Then, aq. H_2O_2 35% (150 μL, 1% v/v) and Novozym® 435 (30 mg, 2 g L^{-1}) were added. The reaction was left in a thermoshaker at 50 °C for 5 h. The enzyme was removed by filtration and the reaction quenched with a saturated solution of saturated Na_2SO_3 (1 mL), extracted with EtOAc and dried over Na_2SO_4. Conversion of oleic acid into the corresponding epoxide was analyzed as system response and was evaluated by GC/MS analysis after treating samples with MeOH and trimethylsilyldiazomethane. Oleic acid conversion to epoxide corresponded to 40%. A diluted solution of sulfuric acid 2 M (100 μL) was added to the mixture causing diol **4** precipitation as a white solid that was recovered by filtration (293 mg, yield 35%).

Epoxidation of hydrolyzed soapstock followed by diol isolation (continuous-flow conditions)

The mixture of fatty acids recovered from the enzymatic splitting of soapstock (9.6 g) was dispersed in acetonitrile (160 mL), stirred in a shaker overnight at 50 °C, then cooled. The insoluble residue was filtered (1.3 g) and the solution obtained had a final concentration of 52 g L^{-1}, corresponding to 43 g L^{-1} of oleic acid (83% of total FAAs). Aqueous H_2O_2 35% (1.6 mL, 1 % v/v) was added. A portion of this solution (45 mL) was introduced into a 50 mL jacketed stirred tank reactor, containing Novozym® 435 (90 mg, 2 g L^{-1}) and kept at the constant temperature (50°C) by means of a thermostat. The remaining solution was continuously pumped into the reactor at a constant flowrate (150 μL min^{-1}) by two peristaltic pumps, corresponding to a residence time of 5 h. A suction solvent filter for

HPLC was placed at the suction tube to avoid tube blocking caused by enzyme beads. The system continuously operated for 12 h, and the outlet composition was periodically sampled and analysed by GC/MS. The fractions corresponding to a conversion in the range of 40-60% (from 2 to 12 h, 100 mL) and the volume inside the reactor (44% conversion, 45 mL) were collected (total volume 145 mL) and quenched by adding a saturated solution of Na_2SO_3 (6 mL). A diluted solution of sulfuric acid 2 M (2.5 mL, 0.25 eq.) was added to the mixture causing diol **4** precipitation as a white solid that was recovered by filtration (3.3 g, yield 47%): ^{1}H NMR (CD_3OD, 400 MHz) [1]: δ = 3.45-3.35 (2H, m, 2*CH*OH), 2.29 (2H, t with J = 7.4 Hz, CH_2COOH), 1.70-1.15 (26H, m, 13 CH_2), 0.97-0.82 (3H, m, CH_3). ^{13}C NMR (CD_3OD, 100.6 MHz) [1]: δ = 177.6, 75.29, 75.26, 35.0, 34.0, 33.9, 33.0, 30.8, 30.7, 30.6, 30.42, 30.37, 30.2, 27.04, 26.96, 26.1, 23.7, 14.4. GC/MS (EI) as a methyl ester, obtained by treatment with MeOH and trimethylsilyldiazomethane 10% in hexane, t_r = 23.85 min: *m/z* (%) = 294 (M^+ – 36, 1), 187 (48), 155 (100), 138 (30).

Oxidative cleavage of threo-9,10-dihydroxystearic acid (4) to azelaic and pelargonic acid (factorial design)

Oxidative cleavage of diol **4** (50 mg) to azelaic and pelargonic acids was performed in a biphasic EtOAc/aq. NaClO solution using Triton X-100 (1 mg) as phase transfer catalyst. The influence of EtOAc and NaClO on the conversion was analyzed through a 2^2 full factorial experimental design. The amount of diol **4** converted into pelargonic acid, azelaic acid and hydroxy-oxostearic acid isomers was taken as system response (Y). The two factors (X_1, X_2) and their levels were: 5-13 mL for EtOAc (X_1) and 4-10 mL for NaClO (X_2). All the experiments were conducted in duplicates, for a total of 8 reactions. The reactions were kept at 45°C for 24 h. The organic layer was then quenched with a saturated solution of Na_2SO_3 and dried over Na_2SO_4. Conversion of diol **4** into converted into pelargonic acid, azelaic acid and hydroxy-oxostearic acid was analyzed by GC/MS after treating samples with MeOH and trimethylsilyldiazomethane. Data were processed using Minitab and the following multivariate regression model was obtained: $Y = 33.5 + 11.75 \cdot X_1 + 4.75 \cdot X_2 + 3.5 \cdot X_1 \cdot X_2$. The table of factorial plan and response and the factorial design analysis graphs are reported in Supplementary Information, Appendix *Chapter 5*.

Oxidative cleavage of threo-9,10-dihydroxystearic acid (4) to azelaic and pelargonic acid (continuous-flow conditions)

Diol **4** (50 mg; 0.16 mmol) and Triton-X 100 (1 mg) were added to EtOAc (13 mL). Diol solubilization was ensured by keeping the solution in a thermoshaker (170 rpm) at 50°C for 1 h. This organic solution was pumped at 120 μL min^{-1} and was mixed in a T-junction with a solution of NaClO 10% (10 mL) pumped at a flowrate of 100 μL min^{-1} for a total flowrate of 220 μL min^{-1} corresponding to a residence time of 45 min. The segmented biphasic flow entered a 10 mL heated tubular coil kept at 45°C. The mixture collected at the outlet was quenched by adding a sat. Na_2SO_3 aq. solution, and the composition of the organic phase was evaluated by GC/MS analysis after derivatization with MeOH and trimethylsilyldiazomethane: 80% of **6a**,**b** isomers, 10% dioxo derivative **5**, 10% diol **4**. The organic phase was flowed again through a 10 mL tubular coil at the same flowrate and temperature with fresh aq. NaClO 10% solution. The mixture at the outlet was recovered and the still warm organic phase was separated, cooled to r.t. washed first with aq. Na_2SO_3, then with water, dried (Na_2SO_4), and concentrated under reduced pressure to afford pelargonic acid (25 mg, 88%): ^{1}H NMR ($CDCl_3$, 400 MHz, ppm): [2] δ = 9.81 (1H, s, COOH), 2.37 (2H, t with J = 7.5 Hz, CH_2COOH), 1.75-1.2 (12H, m, 6CH_2), 0.80 - 0.95 (3H, m, CH_3). ^{13}C NMR ($CDCl_3$, 100.6 MHz, ppm):[2] δ = 180.3, 34.2, 31.9, 29.3, 29.23, 29.21, 24.8, 22.8, 14.2; GC/MS (EI) as a methyl ester, obtained by treatment with MeOH and trimethylsilyldiazomethane 10% in hexane, t_r = 9.33 min: m/z (%) = 172 (M^+, 0.5), 141 (15), 129 (18), 87 (45), 74 (100). The aqueous phase was treated with aq. Na_2SO_3, acidified with HCl 10% and extracted with EtOAc. The combined organic phases were dried (Na_2SO_4), and concentrated under reduced pressure, to obtain azelaic acid (23 mg, 76%): ^{1}H NMR (CD_3OD, 400 MHz, ppm): [3] δ = 2.28 (4H, t with J = 7.4 Hz, 2CH_2COOH), 1.75 - 1.55 (4H, m, 2CH_2), 1.4 -1.2 (6H, m, 3CH_2). ^{13}C NMR (CD_3OD, 100.6 MHz, ppm):[3] δ = 177.5, 34.9, 29.97, 29.93, 26.0. GC/MS (EI) as a methyl ester, obtained by treatment with MeOH and trimethylsilyldiazomethane 10% in hexane, t_r = 13.9 min: m/z (%) = 185 (M^+ – 31, 55), 152 (100), 143 (47), 111 (63).

References

[1] Awang, R.; Ahmad, S.; Kang, Y.B.; Ismail, R. Characterization of dihydroxystearic acid from palm oleic acid. *J. Am. Oil Chem. Soc.* **2001**, *78*, 1249-1252.

[2] Liu, Y.; Cornella, J.; Martin, R. Ni-catalyzed carboxylation of unactivated primary alkyl bromides and sulfonates with CO_2. *J. Am. Chem. Soc.* **2014**, *136*, 11212-11215.

[3] Schievano, E.; Morelato, E.; Facchin, C.; Mammi, S. Characterization of markers of botanical origin and other compounds extracted from unifloral honeys. *J. Agric. Food Chem.* **2013**, *61*, 1747-1755.